Big Brains and Small Teeth: a primate comparative approach to dental and mandibular reduction in hominins

Alessio Veneziano

A thesis submitted in partial fulfilment of the requirements of Liverpool John Moores University for the degree of Doctor of Philosophy.

June 2017

Abstract

Within the genus *Homo*, we observe a decrease in mandibular robusticity and in the size of anterior and postcanine dentition, a trend that is usually referred to as reduction or gracilisation. Factors linked to diet, food processing and encephalization have been suggested to be the main drivers of this trend. Stone tools and fire would have allowed Pleistocene hominins to reduce food toughness, thus relaxing the selective pressures on the masticatory apparatus. In the Holocene, the changes in human lifestyle triggered by agriculture would have determined the reduction in human tooth size. Brain expansion may have acted as a constraint on the development of the lower jaw. In this work, a primate perspective was adopted to clarify the relative influence of adaptive and non-adaptive factors on mandibular and dental reduction in the genus *Homo*. The effect of diet and structural constraints (allometry and encephalization) on dental and mandibular size and robusticity were analysed. The results show that incisor size and mandibular robusticity correlate significantly with diet proxies in non-human extant catarrhines and with neurocranium shape changes in the neurocranium in *Homo sapiens*. In non-human African apes, the elongation of the neurocranium influences postcanine tooth size. In *Homo*, body size plays an important part in tooth size allometry, but not in robusticity. These results suggest that improvements in tool-based food preparation may have been a leading factor in the reduction of incisor size in hominins. Molars and premolars were probably influenced by the expansion of the neurocranium during Pleistocene, and incisor size may be constrained by neurocranium shape changes in *H. sapiens*. This work confirmed the importance of food processing in the trend of reduction and produced convincing evidence for the significance of structural constraints in the evolution of the hominin anatomy. These findings contribute to explain the complex evolution of the human skull.

Acknowledgements

Several people contributed to the production of this work and I am very grateful to all of them. In particular, I want to thank all my colleagues of the Faculty of Science at Liverpool John Moores University, my friends and my family for the help and the attentions received during the fulfilment of my Ph. D. degree. Special thanks go to Federica Landi for her intellectual and personal support; to Antonio Profico for his availability to discuss the topic of this dissertation and clarifying my doubts; to Eleanor Dove and Ian Towle for all the things we shared during the last three years. I am grateful to my supervisors Isabelle De Groote, Joel D. Irish and Carlo Meloro for their advice and support, which made this dissertation possible. I want to thank Chris Stringer for the useful comments on my work. My gratitude goes to all the persons and institutions that made my thesis possible: Peter Brown, the Natural History Museum (NHM) in London, the Muséum National d'Histoire Naturelle in Paris, the National Museum of Kenya, the anthropological museum "G. Sergi" in Roma, the Smithsonian Institution the Museum of Comparative Zoology at Harvard and the Royal Museum for Central Africa in Tervuren. I want to thank the people curating the following online databases: the Primate Research Institute at Kyoto University database, the Africanfossils archive, the Digital Archive of fossil hominoids at the University of Vienna, the MorphoSource database at Duke University, the "Human Origins Database" and the "anthropological data free" database. Finally, I am grateful to John Moores University for funding my research during the past three years.

Contents

Chapter 1: Mandibular and dental reduction in the genus *Homo* 1

1.1 Overview 1

1.2 Human evolution and catarrhines 4

1.3 Functional meaning of mandibular shape in primates 8

1.4 Masticatory function of primate tooth size 12

1.5 The trend of mandibular and dental reduction 14

1.6 Hypotheses on dental and mandibular reduction in Pleistocene *Homo* 17

1.7 Hypotheses on dental reduction in *Homo sapiens* 20

1.8 Limitations of previous studies 21

1.8.1 Keeping dental and mandibular reduction up-to-date 21

1.8.2 The importance of body size and encephalization 22

1.8.3 Food mechanical properties and jaw adaptations: an untested assumption 23

1.9 Aims of this work 24

Chapter 2: Material and methods 25

2.1 The sample 25

2.2 The morphological data 26

2.3 Body weight, feeding and tool use variables 32

2.4 The use of CT and surface scans: comparability, rendering and accuracy 33

2.5 Alveolar length as a proxy for dental size 37

2.6 Accuracy of robusticity indices measured on virtual mandibles 37

2.7 Landmarking error and missing landmark estimation 39

2.8 The analytical approach: traditional and Geometric Morphometrics 41

2.9 Phylogenetic controlled analyses 43

2.10 The R analytical environment 45

Chapter 3: Mandibular and dental reduction in an updated archaeological and palaeontological context 47

3.1 Introduction 47

3.2 Material and methods 49

3.3 Results 51

3.3.1 Mandibular robusticity 51

3.3.2 Dental reduction during the Pleistocene 54

3.3.3 Dental reduction during the Holocene 59

3.4 Discussion 64

Chapter 4: Mandibular and dental reduction: insights from the masticatory scaling in hominins and other catarrines 68

4.1 Introduction 68

4.2 Material and methods 70

4.2.1 The sample and data collection 70

4.2.2 PGLS and ANCOVA 73

4.3 Results 75

4.3.1 Models of evolution and PGLS 75

4.3.2 Phylogenetic ANCOVA 77

4.4 Discussion 84

4.4.1 Phylogenetic signal 84

4.4.2 *Homo* and the catarrhine variability 85

Chapter 5: Size, robusticity and diet in catarrhines: a comparative look at dental and mandibular reduction in *Homo* 88

5.1 Introduction 88

5.2 Material and methods 90

5.2.1 The sample and the morphological data 90

5.2.2 Feeding and behavioural data 92

5.2.3 The correlation procedure 95

5.3 Results 97

5.4 Discussion 104

Chapter 6: Size, robusticity and diet in catarrhines: a comparative look at dental and mandibular reduction in *Homo* 107

6.1 Introduction 107

6.2 Material and methods 109

6.2.1 The sample 109

6.2.2 Quantifying neuro-mandibular integration 111

6.2.3 Redundancy analysis 112

6.3 Results 113

6.3.1 Shape allometry and sexual dimorphism 113

6.3.2 Shape integration 114

6.3.3 Variance explained by integration 118

6.4 Discussion 121

6.4.1 Neuro-mandibular integration 121

6.4.2 The neurocranium as a constraint 122

Chapter 7: Discussion and conclusions 124

7.1 Rethinking dental and mandibular reduction 124

7.2 The dietary component 126

7.3 The neurocranial constraint on the lower jaw 129

7.4 Final remarks 131

References 133

Appendix 1 154

Appendix 2 206

List of abbreviations and notations

α:	attraction parameter in the Ornstein-Uhlenbeck model of evolution
afa:	*Australopithecus afarensis*
Asfc:	microwear variable, Area-Scale Fractal Complexity
Aus:	australopithecines (including *Paranthropus* and *Australopithecus*)
BM:	Brownian Motion model of trait evolution
boi:	*Paranthropus boisei*
Cat:	non-hominin extant catarrhines
CCL:	Chewing Cycle Length, duration of the chewing cycle
CS:	Centroid Size
DF:	Degrees of Freedom
DH:	Diet Heterogeneity index
DQ:	Diet Quality index
EB:	Early-Burst model of trait evolution
EF:	Extractive Foraging index
EH:	early *Homo*
epLsar:	microwear variable, Length-scale anisotropy of relief
F:	value of the F-test, F statistics
flo:	*Homo floresiensis*
FT:	Feeding Time index
g:	grams, measure of weight
hab:	*Homo habilis*
HAsfc9:	microwear variable, Heterogeneity of Area-scale fractal complexity
I_1, I_2:	lower incisors
I_1-I_2:	the alveolar length of lower incisors
JT:	Jonckheere-Terpstra

KW:	Kruskal-Wallis
λ:	Pagel's λ model of trait evolution and its transformation parameter
LP:	Lower Palaeolithic
M_1, M_2, M_3:	lower molars
M_1-M_3:	the alveolar length of lower molars
MA:	Middle Ages
Me:	Mesolithic
MP:	Middle Palaeolithic
N-M:	variable of Neuromandibular integration pattern
Ne:	Neolithic
nea:	*Homo neanderthalensis*
OU:	Ornstein-Uhlenbeck model of trait evolution
P_3, P_4:	lower premolars
P_3-P_4:	the alveolar length of lower premolars
PCA:	Principal Component Analysis
PGLS:	Phylogenetic Generalized Least Squares
r:	acceleration/deceleration parameter of the Early-Burst model
R^2:	R squared, coefficient of determination
rob:	*Paranthropus robustus*
R pls:	estimate of covariation of the Singular Warp analysis
RDA:	Redundancy Analysis
Rob SY:	robusticity index measured at mandibular symphysis
Rob M_1, M_2, M_3:	robusticity index measured at first molar
rud:	*Homo rudolfensis*
sap:	*Homo sapiens*
spR^2:	semi-partial R^2
SW:	Singular Warp
SY:	mandibular symphysis
Tfv:	microwear variable, Textural Fill Volume

TU:	Tool Use, variable of tool use in non-hominin extant catarrhines
UP:	Upper Palaeolithic

Chapter 1

Introduction

1.1 Overview

Mandibles and teeth occupy a special place in the study of human evolution. Within the hominin clade, we not only find remarkable changes in mandibular and dental morphology, we also observe a trend toward small, gracile lower jaws that is evident in the genus *Homo* and reaches an extreme in *Homo sapiens* (Emes et al., 2011). The gracilisation, or reduction, of the lower jaw in modern humans is seen as the result of a within-species trend that occurred during the evolution of *Homo sapiens* from upper Palaeolithic to the Neolithic. To explain the peculiarly small and gracile lower jaw in humans, the attention focused on its possible functional meaning. Several factors have been claimed to have driven mandibular and dental reduction both in *Homo* and in anatomically modern humans: the use of lithic tools (Zink & Lieberman, 2016) and the adoption of fire for cooking (Wrangham & Carmody, 2010) have been (and are still) seen as the most plausible causes. Despite the efforts of decades of study, the truth about mandibular and dental reduction has not been revealed entirely, and the main questions regarding the peculiar evolution of the hominin lower jaw are still open.

Together with mandibular and dental reduction, the genus *Homo* has undergone other distinctive trends that transformed human anatomy. In particular, a net increase in body size is observed at the passage from early *Homo* to later Pleistocene species (Grabowski et al., 2015). In addition, the hominin brain enlarged considerably during the Pleistocene, with *H. neanderthalensis* and *H. sapiens* displaying an expansion of their braincase volume unparalleled among living and extinct primates (Rightmire, 2004). The increase in body size and brain volume may have modified the morphology of mandibles and teeth in hominins, including modern humans (Bastir et al., 2006). Therefore, the possibility that structural

constraints drove mandibular and dental reduction should not be overlooked, and integrating functional and structural factors may reveal the multifactorial nature of this trend.

Since the first official description of Neanderthal bones in 1864 (King, 1864), paleoanthropological excavations literally brought to light an ever increasing record of fossil evidence (Delisle, 2016). Hominin fossils open a window on our origins and help to explain our anatomy and behaviour. Nevertheless, the paleoanthropological record is intrinsically fragmentary and heterogeneously spread over time and space, which makes it difficult to reconstruct the past using fossils only. To overcome this drawback, the information available in extant mammals can be used to fill the intrinsic gaps of the fossil record. Primates are a particularly suitable group of comparison for hominins (Cachel, 2006). *Homo sapiens* is part of the primate clade and, therefore, it and its ancestors share part of their evolutionary history and numerous physical and behavioural features with monkeys and other apes.

The aim of this work is to clarify the significance of adaptive and non-adaptive factors on the trend of mandibular and dental reduction in hominins, including modern humans. The analyses are focused on testing the roles of food-processing, body size and neurocranium modifications on the gracilisation of the hominin lower jaw. The work is structured in seven chapters, which include the theoretical background as well as the methodological and analytical frameworks used. The analyses are reported in chapters 3 to 6, each one including a specific introduction that reports the literature review relevant to the aims of that chapter. Although these introductions overlap to the general literature review provided in chapter 1, they were conceived to embed each step of the analysis in a more specific background.

Chapter 1 describes the framework of ideas acting as the foundation of this work and it represents a report of the relevant literature on the subject of dental and mandibular reduction. In the first place, the choice of adopting a primate perspective for studying the trend of reduction is commented, and the reasons and benefits of using a comparative approach in human evolution are highlighted. The functional and biomechanical meaning of dental size and mandibular robusticity are emphasised. The trends of dental and mandibular reduction in hominins are described. The hypotheses put forward to explain the patterns of reduction are discussed, and their assumptions and limitations are highlighted. The aims and hypotheses of this work are stated.

Chapter 2 provides a comprehensive description of the methodological approach adopted in this work. The material, the morphometric data recorded and the techniques used to collect it are described. The statistical methods and approaches are reported and justified.

Chapter 3 is the first of the four chapters that constitute the analytical body of this work. Here the reduction trends in robusticity and dental size in Pleistocene and Holocene are tested by using a large dataset of metric data. The results and previous hypotheses are commented in the light of the current, updated knowledge about human evolution.

In **chapter 4**, the influence of body size on mandibular and dental size is examined by comparing hominins with other catarrhines. This comparison offers the chance to quantify the uniqueness of the hominin lower jaw. This chapter underlines the importance of considering body size variations to understand the constraint acting on the hominin lower jaw. In addition, it suggests that the small dental and mandibular size is distinctive in late hominins.

In **chapter 5** the attention is drawn to the relationship between the morphology of the lower jaw, diet and tool use in catarrhines. The analyses performed test the common assumption that differences in dental size and mandibular robusticity reflect differences in diet or biomechanical adaptations. The results are used to examine the trend of reduction from a primate perspective.

In **chapter 6**, the neurocranium and the lower jaw are analysed together to outline possible patterns of structural constraints on dental size and robusticity. A Geometric Morphometric approach is used to study the morphological integration between the mandible and the head. The hypothesis that encephalization drove the trend of reduction in hominins is tested. Multiple linear regression approaches are used to define the relevance of neuro-mandibular integration on the modifications in dental size and robusticity in extant African apes and modern humans.

In **chapter 7**, the results obtained in chapters 3 to 6 are discussed, and main conclusions are offered regarding the multifactorial nature of the trend of mandibular and dental reduction.

This work provides evidence that the evolution of the lower jaw in hominins was influenced by both dietary factors and structural constraints. The results suggest that food processing

played a crucial role in the onset of the trend of reduction in the Pleistocene, and that encephalization and neurocranium modifications contributed to the reduced postcanine dentition and robusticity in late Pleistocene and Holocene. The peculiar reorganisation in the brain volume in *H. sapiens* may have had a relevant effect on the unique mandibular robusticity in modern humans.

1.2 Human evolution and catarrhines

The study of human evolution is a practice asking one of the most meaningful questions for understanding our own existence: why are we what we are? Although the human anatomy bear signs of our evolutionary path (Aiello & Dean, 2000), it only represents the final step of our history. To understand the way that led to the present humanity, we can compare ourselves to other animals. The comparative approach is based on the logical idea that the biology of a species may be better understood when compared to the biology of other species (Harvey & Pagel, 1991). The list of intellectuals who used and fostered the comparative approach for studying humans includes famous names and dates far back in time. In his "Generation of animals", Aristoteles of Stagira (384-322 BC) wrote: "…the inner parts of man are to a very great extent unknown, and the consequence is that we must have recourse to an examination of the inner parts of other animals whose nature in any way resembles that of man" (Pellegrin, 1986: pp 196). The opinion that other animals could provide information transferable on the human anatomy was present among physicians during ancient times. In the Roman period, Galen (AD 129–200/216) performed several dissections on animals, in particular pigs, which he preferred for their similarities with the human body (Corner, 1927). The first example of a direct, complete evaluation of the anatomical differences and similarities between primates and humans is probably to be attributed to Andreas Vesalius (1514-1564). Indeed, in his *Fabrica*, Vesalius highlights the differences between the anatomy of humans, which he dissected, and the anatomy reported by Galen, who relied on pig and monkey dissections since he was not allowed to dissect humans during his times (Cosans & Frampton, 2009). Nevertheless, the real place of humans in the natural world was only disclosed by the work of Carl Linnaeus (1707-1778), who recognised *Homo sapiens* as

belonging to the order Primates, and of Charles Darwin (1809-1882), who suggested a common descent of humans and other apes (Cosans & Frampton, 2009).

Primates are the logical group of comparison for *Homo sapiens*. Many of the similarities between monkeys, apes and humans make sense only in the light of their close phylogenetic relationships (Wildman et al., 2003). Primates have been successfully used as a means of comparison in the study of human evolution, on several topics regarding hominin morphology. Copes & Kimbel (2016) questioned the cranial vault thickness as a hominin autapomorphy (derived trait) by comparing fossil hominins with a broad sample of primates. Their results helped clarify that the proportion of cortical bone over diploë, rather than the cranial vault thickness, can be considered as a distinctive trait of the hominin lineage. Steele et al. (2013) analyse the morphology of the hyoid bone in *Australopithecus*, *Homo*, *Gorilla* and *Pan*, interpreting the result for their implications on the evolution of the human speech. Hand and foot morphology in primates is usually compared to better understand the onset of bipedal locomotion (Zehr et al., 2009), and manual dexterity can be analysed in a comparative perspective to understand tool-making skills in hominins (Pouydebat et al., 2009). These and other examples show how primates represent a common element in the research on hominin variability and evolution, in particular when dealing with the major trends that occurred in the hominin lineage. For example, a comparative approach has been adopted to test if the peculiar encephalization observed in hominins is linked to social organisation (Schultz & Dunbar, 2010), tool use skills (Lefebvre, 2013) or to ecological factors acting on the energy requirements of the human brain (Snodgrass et al., 2009; Barrickman & Lin, 2010). Every possibility that human and primate brain evolution is driven by the same factors should be investigated before attempting to define lineage-specific explanations (Isler & Van Schaik, 2014). In these terms, hominin encephalization recalls some fundamental aspects of the trend in dental and mandibular reduction in *Homo*, which appears to be another unique feature among primate groups. Some of the major explanations proposed rely on the uniqueness of hominin behaviour, such as the use of fire and stone tools, as main drivers of change (Wrangham & Carmody, 2010; Zink & Lieberman, 2016). These hypotheses may be correct, but they need to be tested. Primates offer a good opportunity to look at the masticatory variability of hominins in terms of the ecological and structural factors that may influence it. A primate comparison may highlight the evolutionary background of hominin mandibular and

dental evolution, thus allowing a better understanding of the pattern of reduction, whether it has or does not have a connection with patterns observed in primates.

Although the primate clade exhibits many similarities with hominins, more shared features can be found by looking at the parvorder of Catarrhini. In fact, catarrhines share with us several anatomical, physiological, developmental and behavioural features, which make them particularly suitable for comparisons with humans and fossil hominins (Cachel, 2006). Cachel (2006) compiles a comprehensive list of twenty-nine features shared by hominins and non-hominin catarrhines. A summary of the most remarkable is here reported.

1. Catarrhines are diurnal. Concentrating their activity during light hours has important ecological consequences, which can be recognised in the cranial morphology. For example, nocturnal primates developed adaptations to poor conditions of light, such as large orbits (Ross et al., 2007), which in some cases are extremely enlarged if compared to cranial size, as in tarsiers (Castenholz, 1984). These morphological adaptations set strong constraints on the developing skull (Jeffery et al., 2007). Consequentially, being diurnal, humans and other catarrhines may share more similar constraints (or absence of) than humans and non-catarrhine primates.

2. Catarrhines have larger body size than platyrrhines (New World monkeys). Body size has implications on the ecology and morphology of primates and mammals in general. A large body size is associated with a high proportion of plant matter in the diet, thus with an herbivorous lifestyle, while small mammals usually rely on insects for their daily energy intake (Milton & May, 1976; Robinson & Redford, 1986). When size changes, a dietary shift is expected (Leonard & Robertson, 1984). The size of a species defines the biomechanical constraints of its masticatory system, since animals of different sizes would need to accommodate different stresses when chewing (Druzinsky, 1993). Although the catarrhine variability in body size overlaps with that of other primate groups, there are no catarrhine insectivores, though many species seem to integrate their diet with a certain amount of animal matter, insects or meat (National Research Council US, 2003). All catarrhines are mainly folivores or frugivores and, often, a mixture of the two (National Research Council US, 2003).

3. Several traits are highly sexually dimorphic in catarrhines (Dixson, 1998). Body size and canine size exemplify this statement and dimorphism in such traits is common in many catarrhine species (Leutenegger & Kelly, 1977; Leigh & Shea, 1995; Grueter & Van Schaik, 2009). According to the Rensch's rule (Rensch, 1950), size dimorphism among species of the same lineage will increase with increasing body size when the male is the larger sex, as in catarrhines. Although male and female humans differ in stature, other traits commonly dimorphic in catarrhines are missing. Human canines, for example, are less dimorphic than in other apes and the same is found in the genus *Australopithecus* (Leutenegger & Shell, 1987) and fossil *Homo* (Emes et al, 2011). The traits that hominins do not share with other catarrhines represent a good example of the advantages of using a comparative approach in human evolution. By differing from a common catarrhine trend for a trait, the hominin condition is likely to have occurred because the factors shaping the catarrhine variability were absent or overwhelmed by other processes. The reduction in the size of the hominin canines is often linked to changes in the social organization toward a system characterized by a low male-male competition or monogamy (Plavcan & Van Schaik, 1997; Smith, 1981). An alternative explanation suggests that the smaller canines in hominins are due to a structural constraint of tooth overcrowding in the jaws, because of changes in proportions between tooth types and of the reduction of face prognathism (Jungers, 1978). It is interesting to notice that while the first hypothesis is based on the observation of a primate condition, the second relies on trends that are not paralleled outside the hominin group.

One additional feature, not listed by Cachel (2006) and strictly related to the masticatory anatomy, makes catarrhines an excellent source for comparing the hominin lower jaw. Hominins and other catarrhines share the same number of teeth for each tooth type, meaning they have the same dental formula (Swindler, 2002). Platyrrhines, which shared a common ancestor with catarrhines around 40 My (Schrago et al., 2012), host three premolars in each side of both the upper and lower jaw, instead of the two premolars seen in catarrhines. This fact may underline the presence of common evolutionary and developmental drivers. The similarities in the dentition of hominins and other catarrhines are probably the result of their phylogenetic relatedness.

For the reasons so far expressed, catarrhines represent the best basis of comparison for understanding the evolution of hominins. Adopting a catarrhine comparative approach provides the unique chance of understanding the mandibular and dental reduction by defining the phylogenetic framework in which hominins arose.

1.3 Functional meaning of mandibular shape in primates

The lower jaw is the only movable bone element in the skull. Because of its role in mastication, the lower jaw and its variability across mammals follows dietary habits (Janis, 1990; Weijs, 1994; Boyer, 2008). To succeed in the task of mastication, the lower jaw and dentition involved in several activities and movements, like grinding, crushing, chewing and swallowing food (Crompton & Hiiemae, 1969). The morphology of the masticatory apparatus is thus the result of several forces acting simultaneously on the same bone for one purpose (Hylander, 1979; Ross et al., 2012). The picture is complicated by the fact that the mandibular morphology is linked to functions other than mastication (Ross et al., 2012; Emes et al. 2011). The mandible provides structure and protection to the oral cavity, it is involved in the production of sounds through the pharynx, and it hosts part of the muscles implicated in facial expression, at least in primates (Chevalier-Skolnikoff, 1973; Burrows et al., 2006). Although many factors contribute to shaping the primate lower jaw, masticatory efficiency have often been considered to be the main drivers of mandibular and dental evolution (Ross et al., 2012) and the size and robusticity of the lower jaw are important for meeting the biomechanical requirements of mastication (Hylander, 1979).

The catarrhine mandible is a bilaterally symmetric bone consisting of two main modules: a body, or corpus mandibulae, and two quadrilateral-shaped rami, which are in structural continuity with the corpus and project upward forming an obtuse angle with its main axis (White et al., 2011). The lower jaw articulates with the two temporal bones through the condylar processes on the rami, forming the temporomandibular joint, while the body supports the dentition. The masseter and temporalis muscles are the main actors involved in generating bite force (Van Spronsen et al., 1989). The masseter runs along the whole length of the zygomatic arch to the ramus of the mandible, occupying its concavity and inserts in the

gonial angle, the lowest part of the ramus (Standring & Gray, 2008). The function of the masseter when contracting is to elevate the mandible, thus closing the oral cavity (Hylander & Johnson, 1985). The temporalis originates from the upper lateral side of the cranium, from the temporal line or, if present, from the sagittal crest, and reaches the coronoid process of the mandible, situated on its upper anterior process (Standring & Gray, 2008). The temporalis generates the main force of bite closure and is involved in mandibular retraction (Latif, 1957). Catarrhines (including humans) exhibit the same number of teeth for each toot type for both maxillary and mandibular dentition. In each hemi-mandible, we observe one central and one lateral incisor (I_1 and I_2 respectively), followed by one canine (C_1), two premolars (P_3 and P_4) and three molars (M_1, M_2 and M_3)

The overall morphology of the lower jaw is thought to reflect the biting force generated and it is supposed to adapt to increase in efficiency by counteracting the stresses of mastication (Hylander, 1979; Raadsheer et al., 1999). To accommodate these requirements, there is remarkable variation in the proportions of the rami and corpus of the mandible (Smith, 1983; Weijs, 1988; Humphrey et al., 1999), which reflect the relative importance of the muscles in generating the forces acting during mastication. The lower jaw is often described as a lever system (Throckmorton et al., 1980). This model provides useful predictions about the functional morphology of the mandible (Hylander, 1975a; Smith, 1978; Spencer, 1998). In this model, the lower jaw acts as a 3rd class lever when biting by the anterior dentition (Westneat, 2003): the applied force (generated by the masticatory muscles) is placed between the fulcrum (the temporomandibular joint) and the load (the food item). When the food is processed through the posterior dentition, the mandible becomes a 2nd class lever, with the load closer to the fulcrum than the applied force (Westneat, 2003). As a lever, we recognise two arms in the lower jaw: the in-lever arm connecting the fulcrum to the point where the muscle force (F_i) is applied, and the out-lever arm, which connects the fulcrum to the point where the food applies a resisting force (F_o) to the lower jaw (Westneat, 2003). The ratio between the in-lever (L_i) and out-lever (L_o) arm lengths provides an index, or Mechanical Advantage (MA), of the bite force that a lower jaw is capable of generating (Westneat, 2003). Given the same out-lever arm length, increasing the in-lever arm gives a higher MA:

$$MA = \frac{F_o}{F_i} = \frac{L_i}{L_o}$$

In the primate mandible, both ramus breadth and corpus length contribute to the length of the out-lever arm, while the length of the in-lever arm is approximately linked to the height and breadth of the ramus, for the forces of the masseter and temporalis, respectively (Spencer, 1998). Therefore, if the out-lever arm is kept constant, we expect that taller rami are associated with bigger masseter forces (thus higher MA) than shorter rami. In the same way, broader rami in respect of corpus length indicate a higher MA. Longer mandibular corpora are instead associated with higher out-lever forces, thus leading to a lower MA.

Disproportional changes in mandibular ramus and corpus dimensions can have important effects on the lever action of the lower jaw (Throckmorton et al., 1980). In a comparative study of colobines and cercopithecines, Bouvier (1986) recognised different adaptations in the condyles and mandibular corpus of the two groups, clearly resulting from specific mandibular scaling patterns. Changes in the mandibular condyles may affect the biomechanical distribution of forces during the bite, as the condyle is the fulcrum of the lever system of the lower jaw (Hylander, 1975a). Other studies found that allometric scaling patterns occurred in the components of the lever system of the mandible; the arm describing the action of the temporalis muscle, for example, has been found to scale with positive allometry with mandibular length across anthropoid primates (Ross et al., 2009a). This implies a higher mechanical advantage in larger mandibles than in smaller ones, because of a more powerful action of the temporalis as an effect of scaling. The functional significance of the scaling of the mandibular lever system has been confirmed by comparative studies; by comparing African colobines, Koyabu & Endo (2008) found higher MA in the lower jaw of durophagous, seed-eater species than in young leaf-eater ones, suggesting an adaptive significance of the relative proportions of the rami and corpus of the mandible. Taylor (2002) examined the morphology of the lower jaw in African apes, concluding that the mechanical requirements of the diet of *Gorilla beringei* may explain its morphological differences from chimpanzees, such as a higher mandibular ramus, which can be important in defining the masseter lever arm. If we consider the mandible as a lever system, the dimensions of the masticatory muscles are important for the magnitude of the force produced along the in-lever

arm (Sasaki et al., 1989; Raadsheer et al., 1999). It is not clear how the masticatory muscles scale in respect of the entire masticatory apparatus and skull size, and different studies report discordant results. Cachel (1984) observed isometric scaling of the dry weight of masticatory muscles over body size and skull size measurements in anthropoid primates. Anapol et al. (2008) found isometry between masseter/temporalis muscle cross-sectional area and body weight in platyrrhines only, while the same muscles in catarrhines seem to scale with positive allometry when compared to cranial measurements.

The act of masticating produces mechanical stress on the mandible. The mandibular corpus is subject to sagittal bending, twisting and torsional forces generated during the power stroke of mastication (Demes et al. 1984; Tams et al., 1997; Van Eijden, 2000). These forces result in compressive and tensile stresses along the lower and alveolar border of the corpus, respectively (Hylander, 1979). The bone reacts by changing its trabecular distribution along the mandibular corpus (Daegling & Hylander, 1997; Van Ruijven et al., 2002). The shape is also important in resisting the strains caused by chewing; in particular, Hylander (1979) highlighted the importance of the major axis of the mandibular corpus at the level of molars in counteracting masticatory stresses, and suggested that increasing the corpus height by keeping width constant results in an efficient way of withstanding simultaneous torsion and sagittal bending. Cross-sectional height and width are the major axes defining mandibular robusticity, which is considered of biomechanical relevance in primate mastication (Hylander, 1979; Daegling, 1989).

The same stress resistance applies to the mandibular symphysis, the structure generated by the fusion of the two halves of the mandible along the sagittal plane. The symphysis is a compact structure whose resistance is achieved by modifications of the inferior and superior transverse tori (Hylander, 1985; Daegling, 2001), shelf-like bony elements extending internally (or lingually) to the mandible and transversally to the symphysis itself, and projecting posteriorly (White et al., 2011). In catarrhines, the relative size of the inferior and superior tori are variable (Hylander 1979; Daegling, 1989; Daegling & Jungers, 2000); in modern humans, the tori are often faint, sometimes only perceivable as irregularities of the surface, and the superior and inferior mental spines are visible in the same area (Guy et al., 2008). As for the tori, the cortical thickness of the bone at the symphyseal midline of the catarrhine mandible seems involved in stress resistance (Demes et al., 1984; Hylander, 1985).

The symphyseal depth and oblique inclination of the symphysis are also involved in strain dispersion during incisal biting (Begun et al., 2013). For example, gorillas and chimpanzees exhibit a robust superior torus and a thinner inferior one, the latter extending more posteriorly than the former (Begun et al., 2013). Humans exhibit a peculiar symphyseal morphology usually referred to as chin, which is unique among primates (Schwartz & Tattersall, 2000). The chin is a forward protrusion of the area surrounding the mandibular symphysis, also known as the mental eminence, and it contributes to the flattened appearance of the human face. This unique feature has been traditionally considered a biomechanical adaptation of the human lower jaw (Daegling, 1993; Ichim et al., 2006), mainly because of the important role of the anthropoid mandibular symphysis in resisting bending and shearing stresses during mastication (Hylander, 1984; Hylander et al., 2000). Nevertheless, some early studies have proposed non-mechanical explanations to the emergence of the chin in anatomically modern humans (Weidenreich, 1941; Riesenfeld, 1969) and more evidence has been produced (Schwartz & Tattersall, 2000).

1.4 Masticatory function of primate tooth size

Tooth size is useful in describing the adaptation to different types of foods. For example, at equal body size, monkeys with smaller incisors are associated with a more folivorous dietary regime than monkeys bearing bigger incisors (Hylander, 1975b). As observed by Hylander (1975b), the colobines are well adapted to a leaf-eating strategy and developed incisors that are comparatively smaller than those of cercopithecines, who forage mostly on fruit (National Research Council US, 2003). Nevertheless, diet composition in catarrhines is not very strict and every species is able to eat varying amounts of secondary food sources (National Research Council US, 2003; Doran-Sheehy et al., 2009). For example, despite their large incisors, cercopithecines of the genus *Papio* are reported to include high amounts of leaves and grasses in their diet (Norton et al., 1987). This plasticity in the use of incisors probably results from the adaptation to food mechanical properties. When switching to a more folivorous regime, papionins use their front teeth for food preparation and manipulation (Hylander, 1975b). In addition, the fruit generally eaten by papionins need extensive incisal

preparation (Whitehead & Jolly, 2000). Other adaptations can reduce the need for incisal preparation by folivorous primates, such as the physiological adaptation of colobines to the consumption of plant material (Kirkpatrick, 2007; Koyabu & Endo, 2009). Indeed, all colobines are foregut fermenters, *i.e.* their foregut microbial environment breaks down cellulose, making it available for further digestion (Lambert, 1998). Therefore, colobines are physiologically equipped to extract higher amounts of energy from the plants than the non-foregut fermenters. Without similar adaptations, papionins switching to plant material may have to spend more time to prepare their food, making it more easily digestible (Hylander, 1975b). Indeed, colobines make infrequent use of incisors for food preparation (Jolly, 1970).

Folivorous catarrhines exhibit a larger postcanine dentition than frugivorous species (Kay, 1975), as an adaptation to breaking down the tough plant material thanks to higher food processing rates (DeGusta et al., 2003). By studying wild populations of howler monkeys (*Alouatta palliata*), a folivorous species (Glander, 1981), DeGusta et al. (2003) found a correlation between individual fitness and molar size, suggesting that large molars may be advantageous in prevalently folivorous species. Nevertheless, postcanine megadontia has been described in several primate species known to feed on hard objects (durophagy) (Daegling et al., 2011). In particular, durophagous primates exhibit enlargement of the second premolar (P_4) relative to the molars (Daegling et al., 2011). In the West African sooty mangabey (*Cercocebus atys*), the megadont P_4 is considered an adaptation to the consumption of hard seeds (Fleagle & McGraw, 1999; Swindler, 2002), which account for a large amount of the dietary intake (Daegling et al., 2011). An enlarged P_4 relative to the molars is present in other species known to feed on hard objects, such as *Pongo pygmaeus*, although it consumes such foods infrequently (Taylor, 2006b). Although an enlarged P_4 may provide adaptive advantages, other known durophagous species do not exhibit postcanine megadontia and species with an enlarged P_4 relative to the molars do not feed on hard objects (Daegling et al., 2011). Therefore, factors other than diet may influence postcanine tooth size. Wood (1979) reports molar crown area to scale isometrically with body size in *Homo*, *Gorilla*, *Pan*, *Papio* and *Colobus*. Willis & Swindler (2004) suggest that molar size differences across colobines may reflect phylogeny and variation in body size.

The dietary plasticity of catarrhines undermines the use of dental size as a proxy for diet. First, most catarrhine species adjust their diet depending on the seasonal availability of food

(Chapman & Chapman, 1990; Hill, 1997; Wrangham et al., 1998; Brockman & Van Schaik, 2005; Doran-Sheehy et al., 2009), thus demonstrating that primates have quite varied diets and can eat other foods despite the apparent masticatory adaptations. In addition, the similarities in diet between different species are dependent on their phylogenetic relatedness (Kamilar & Cooper, 2013). When a species diverges from another, the traits of the new forming species are not fully free to change in respect of the new environmental conditions. The new species retains several features belonging to its closest living relative, since they have shared a recent evolutionary history; this constraint is known as phylogenetic inertia (Blomberg & Garland, 2002), and it has been described for several morphological, behavioural and ecological features (Cheverud et al., 1985; Kappeler, 1990; Chapman & Rothman, 2009). In the case of diet and morphological traits, the patterns shared by catarrhine species are at least in part the result of phylogenetic inertia (Blomberg et al., 2003; Kamilar & Cooper, 2013).

1.5 The trend of mandibular and dental reduction

The skull reflects many aspects of the life history of a species and it hosts most of the sensory organs and the brain (Standring & Gray, 2008). The brain, in particular, played an important role in the evolution of hominins because of its remarkable increase in volume, or encephalization (Rightmire, 2004; Wittman & Wall, 2007; Shultz et al., 2012). Nevertheless, other skull elements bear signs of human uniqueness. The cranial base modified under the influence of locomotion and integrated with the vertebral column to fit the requirements of bipedalism (Lieberman et al., 2000; Russo & Kirk, 2013). The hominin face underwent progressive flattening during Pleistocene (Trinkaus, 2003; Pearson, 2008; Holton et al., 2011). Although less iconic in palaeoanthropology, the changes in the hominin lower jaw represent one of the major trends that occurred in hominins and contributed to human uniqueness (McHenry, 1982). Being primarily involved in food processing, few anatomical elements are as informative as jaws and teeth. They encompass information about the ecological niche of hominins (Hutchinson & MacArthur, 1959; Cachel, 1996). Understanding the evolution of the hominin lower jaw may help to clarify the way our ancestors interacted with their environment.

The genus *Australopithecus* thrived in eastern and southern Africa in a variety of species currently recognised in the hominin fossil record of Plio-Pleistocene (Aiello & Andrews, 2000). Their lower jaws were less robust than what is observed in extant African apes, chimpanzees and gorillas (Kustaloglu, 1961; Emes et al., 2011), at the same time bearing larger postcanine teeth (McHenry, 1984). Their canines reduced in size over time, as testified by the large, highly dimorphic canines exhibited by the fossil of earlier hominins (Wood & Stack, 1980; Haile-Selassie, 2001). Nevertheless, their lower jaw was robust and their dentition large compared to the gracile appearance of the mandibles and teeth of modern humans (Lieberman, 1992, Wood & Aiello, 1998; Emes et al., 2011). Around 2.7 My, the genus *Paranthropus* arose from *Australopithecus* (Suwa et al., 1996), evolving toward a massive implementation of the masticatory apparatus. Sometimes referred to as megadont (Wood & Constantino, 2007; Emes et al., 2011), these hominins exhibited a uniquely developed postcanine dentition, with molarised premolars and large molars (Wood & Stack, 1980; Grine & Martin, 1988; Delezene & Kimbel, 2011), accompanied by an enlarged mandible with a robust mandibular corpus and tall ramus (McCollum, 1999; Rak & Hylander, 2008). Although the anterior dentition (incisors and canines) is on average smaller than in *Australopithecus*, the appearance of their lower jaw has often been thought to be the result of dietary specialisation (Demes & Creel, 1988; Teaford & Ungar, 2000). Because of its hyper-robust masticatory anatomy, *P. boisei* was nicknamed the “Nutcracker man” (Lee-Thorp, 2011), and it exhibited the thickest enamel ever observed in the hominin clade (Olejniczak et al., 2008). A different group developed, presumably from *Australopithecus*, around 2.4 My (Prat et al., 2005) and gave rise to the genus *Homo*. Because of the remarkable jaw changes that resulted from this event, the dimensions of mandible and teeth are usually diagnostic for the attribution of early forms of *Homo* instead of late australopithecines (Guy et al., 2008; Lague et al., 2008).

The evolutionary trends observed in the masticatory apparatus of the genus *Homo* are referred to as reduction and/or gracilisation (Robinson, 1954; Carlson & Van Gerven, 1977; Bastir et al., 2004). Several traits, and in particular dental size and mandibular robusticity, are involved in this trend (Chamberlain & Wood, 1985; Emes et al., 2011). The genus *Homo* exhibits a smaller mandible compared to extant non-human apes and australopithecines, in terms of corpus length and ramus height, (Lieberman 1992, Wood & Aiello 1998, Emes et al. 2011). The mandible of *H. sapiens* is shorter and wider at the condyles than that of the

chimpanzee, *Pan troglodytes*, although they share features such as the reduced height of the mandibular corpus and ramus, the latter being shorter than in *Gorilla* (Humphrey et al., 1999). The reduced size is accompanied by changes in robusticity both from *Australopithecus* to *Homo* as well as within the genus *Homo* (Chamberlain & Wood, 1985). The robusticity index is calculated as the ratio between mandibular corpus width and height, usually measured below the first molar (Daegling, 1989). *Homo* has a lower robusticity index than australopithecines, and a more gracile mandible is observed more in middle to late Pleistocene *Homo* than in the earlier species (Chamberlain & Wood, 1985). The modern human symphysis represents another peculiarity when considered within primate variability. In fact, *H. sapiens* is the only of the hominin species exhibiting a chin (Schwartz & Tattersall, 2000), formed as the forward extrusion of the symphyseal region. The modern human symphysis presents a less complex anatomy than that observed in previous hominin species and other primates, and often lacks a well-developed superior transverse torus, and shows a reduced cross-sectional width in respect of australopithecines and early *Homo* (Guy et al., 2008).

The genus *Homo* exhibits a high variability in dental size and the reduction took place principally in the postcanine dental area (McHenry, 1982; Emes et al. 2011). Changes are already evident in early *Homo*, which possesses smaller premolars and molars than extant non-human apes and australopithecines (Sofaer et al., 1971; Pilbeam & Gould, 1974; Andrews et al., 1991; Macho & Moggi-Cecchi, 1992; Wood, 1992; McHenry & Coffing, 2000). Nevertheless, postcanine size in *H. habilis* and *H. rudolfensis* (habilines) was still large and australopith-like if compared to later *Homo* species, and signs of reduction in the lower jaw started only from *H. ergaster* (Wood, 1999). Nevertheless, the dental similarities between australopithecines and habilines may reflect both masticatory adaptation and/or shared ancestry. Postcanine size is reduced considerably in *H. ergaster*, a species that first developed anatomical similarities to later *Homo* species (Wood, 1999), and in middle Pleistocene (Rightmire, 2008), and this reduction continued throughout the Pleistocene (Brace et al., 1987; De Castro & Nicolas, 1995; Franciscus & Trinkaus, 1995). Incisors/molar size ratios in early *Homo* are larger than in australopithecines, which in turn show smaller front dentition than extant non-human apes (Ungar, 2012). A decrease in incisor dimensions has been suggested in *H. ergaster* and later hominins, continuing throughout the Pleistocene and in *H.*

sapiens (Bailit & Fieadlaender, 1966; Ungar, 2012). Some studies support the possibility of a relative increase of incisor size during middle Palaeolithic, followed by a decrease (Brace, 1967).

Further reduction in the human jaw and dentition took place from the late Pleistocene and throughout the Holocene (Brace, 1967; Brace and Mahler, 1971; Brose and Wolpoff, 1971; Brace, 1976; Frayer, 1977; Smith, 1977; Brace, 1979; Chamla, 1980; Brace et al., 1987; Calcagno and Gibson, 1988; Y'Edynak, 1989; Pinhasi et al., 2008). This trend involves changes in both the jaw morphology and in dental crown dimensions, and it has been observed mainly in human populations from the archaeological records of Europe, North Africa and the near East, from upper Palaeolithic/early Holocene to Neolithic (Pinhasi & Meiklejohn, 2011). In the mandible, the trend of reduction affected anterior symphyseal height and ramus breadth (Pinhasi et al., 2008), and Coon (1955) reports a shortening of the mandibular ramus in post-Mesolithic humans. A number of studies reports cases of dental reduction in other parts of the world, including Asia (Brace, 1976), Australia (Brace et al., 1980; St Hoyme & Turner, 1980) and North America (Sciulli et al., 1979; Hinton et al., 1980; Larsen, 1981). Although populations distant from each other may have undergone dental reduction in response to different factors, the worldwide trend makes it a feature characteristic of modern humans' recent evolution. Gradual changes in dental crown dimensions have been observed in each tooth type, with particular attention to incisors and postcanine teeth (Calcagno and Gibson, 1988), and a recent study (Pinhasi & Meiklejohn, 2011) suggested that the Bucco-Lingual (BL) dimensions are more affected than the Mesio-Distal (MD) diameter. According to Brace et al. (1987) and as confirmed by other studies (Pinhasi et al., 2008; Pinhasi & Meiklejohn, 2011), the rate of reduction in dental dimensions during the Holocene was higher than in the late Pleistocene.

1.6 Hypotheses on dental and mandibular reduction in Pleistocene Homo

The genus *Homo* underwent remarkable changes in diet, subsistence and cranial anatomy, all factors that may have influenced the mandible and teeth directly or indirectly, by modifying food mechanical properties (slicing with stone tools, fire) or acting as a constraint on the

development of the lower jaw (e.g., encephalization). Since jaws and teeth are involved primarily in mastication, it is not surprising that the main hypotheses on dental and mandibular reduction in hominins deal with changes in diet and subsistence strategies.

With the forest gradually transforming into grassland and savannah (Kingston et al., 1994; WoldeGabriel, 1994), australopithecines faced the necessity to switch from their previous food supply, likely mostly made up of fruit, to a new niche constituted by the resources available in an open habitat (Lee-Thorpe et al., 2010; Grine et al., 2012). Herbaceous vegetation and vegetal underground storage organs became central in the diet of australopithecines (Laden & Wrangham, 2005). As a result, *Australopithecus* and *Paranthropus* exhibit relatively large chewing surfaces and thick enamel (Teaford and Ungar, 2000; Wood and Strait, 2004). The genus *Homo* may have incorporated higher amounts of meat into the diet (Speth, 1989; Stanford & Bunn, 2001). Equipped with stone tools, early *Homo* were able to obtain a high-quality food (meat and marrow) from carcasses left behind by large predators (Lupo, 1998). Although meat is a good source of energy, it is difficult to chew, as reported by studies on meat consumption in chimpanzees (Wrangham, 2009; Tennie et al., 2014). These findings suggest that the consumption of meat may not have been directly responsible for dental and mandibular changes. Nevertheless, the availability of stone tools may have allowed improvements in processing meat before consumption. In fact, Zink & Lieberman (2016) tested the efficacy of slicing in reducing the time and force of chewing meat and their results suggest that the use of lithic tools would have allowed hominins to modify the biomechanical properties of meat enough to allow a reduction in the chewing cycle and bite force.

Some authors (Brace, 1987; Wrangham and Conklin-Brittain, 2003; Wrangham, 2009; Wrangham & Carmody, 2010) emphasise the role of fire in human evolution. In particular, the practice of cooking, made possible by the use of fire, may have enhanced the energy income in the hominin diet. Indeed, compared to raw food, cooked food is more easily digestible and nutrients can be extracted with higher efficiency (Wrangham, 2009). In addition, cooking would have modified the food's mechanical properties, softening the tissues formerly tough to chew (Bouton & Harris, 1972; Christensen et al., 2000). The capability of the masticatory apparatus to counteract high stresses during mastication would have been reduced, with the consequent dental and mandibular reduction. Although plausible, it is not clear at what time

of the Pleistocene hominins started having a deliberate control on fire (Rolland, 2004). There are indications of fire use in African paleoanthropological sites known for the presence of *H. ergaster* and dated 1.6 My (Rowlett, 2000), while it is suggested that the habitual use of fire in Europe is detectable in the archaeological record only from 300-400 ky (Roebroeks & Villa, 2011; Shimelmitz et al., 2014). Nevertheless, it is difficult to discriminate between intentional and unintentional use of fire (Gregg & Grybush, 1976; Scherjon et al., 2015). This hypothesis links hominin anatomy to one of the most peculiar behaviour of our species. The adoption of cooking as a regular practice would have provided hominins with a surplus of energy (Wrangham, 2009), that was easier to chew, thus reducing mastication force and chewing time (Bouton & Harris, 1972). Nevertheless, to demonstrate that fire contributed to the reduction in mandible and teeth, it should have been used on a regular basis, a practice uncertain in early *Homo* as much as in later hominins, such as *H. neanderthalensis* (Henry, 2017). Future discoveries will clarify the relationship between fire and the trend of reduction.

The idea behind the main hypotheses on mandibular and dental reduction in hominins is that chewing foods that are intrinsically softer or that are made softer by processing would result in a relaxation of the selective pressures on mastication (Calcagno & Gibson, 1988; Wrangham & Carmody, 2010). Therefore, lowered biomechanical requirements would not need robust lower jaws and large dental crowns. Although plausible, other major anatomical changes that occurred in the hominin skull may have had an influence on the onset of the trend of reduction (Arsuaga et al., 2014; Spoor et al., 2015). In particular, encephalization accounts for most of the variability in the skull of *Homo* during the entire Pleistocene (Ruff et al., 1997; Rightmire, 2004). Expanding brain volume altered the morphology of the hominin neurocranium, which kept an overall ape-like elongated shape pattern during the entire Pleistocene and became globular in anatomically modern *H. sapiens* because of a reorganisation of the entire cranial vault (Lieberman et al., 2002). Spoor et al. (2015) observed that brain enlargement in early *Homo* preceded postcanine reduction, while in Neanderthals dental reduction started earlier than brain expansion (Arsuaga et al., 2014). These findings suggest that the relationship between encephalization and dental reduction is complex. Despite this complexity, a mutual relationship between the lower jaw and the neurocranium appears plausible. The anatomical regions of the skull are tightly connected to each other and the remarkable changes that took place in the neurocranium might have had structural

consequences on the contiguous bones. Indeed, it has been shown that skeletal elements that are in physical association are prone to influence each other's development (Klingenberg et al., 2003; Klingenberg, 2008) and evolution (Porto et al., 2009). When this occurs, the elements are said to be morphologically integrated (Olson & Miller, 1999). Previous studies found morphological integration between mandible, temporal bone and basicranium in humans (Bastir & Rosas, 2005; 2006), indicating that the lower jaw is associated with modifications of the rest of the skull.

1.7 Hypotheses on dental reduction in Homo sapiens

The post-Pleistocene reduction of the masticatory apparatus was at the centre of a heated debate during the 1960s and '70s, when C. L. Brace (1963) proposed that the elaboration of new food practices may have caused the observed pattern of tooth size decrease. In particular, he recognised two events as crucial for this trend: first, the adoption of cookery in late Pleistocene would have triggered dental reduction in both Neanderthals and *H. sapiens* (Brace et al., 1987). Second, the introduction of pottery in the Holocene, associated with the first forms of agricultural subsistence, would have caused a second acceleration of tooth size decrease in *Homo sapiens* (Brace, 1979; Brace et al., 1987). Brace argued that these changes in tooth size have to be regarded as the result of the *Probable Mutation Effect* (PME) (Brace, 1963). The PME model suggests that in the absence of natural selection, mutations would act as the main force of change on the genetic mechanisms of development, disrupting them and so determining a decrease in size and complexity of anatomical structures (Brace and Mahler, 1971). In this regard, the reduction in the masticatory apparatus may be seen as the result of the relaxation of selective pressures because of lowered functional requirements.

Other models have been proposed that explain the observed patterns of dentognathic reduction in post-Pleistocene *Homo sapiens*, all linked to the idea that dramatic changes in mandible and teeth must have been triggered by changes in the subsistence patterns. The *Increasing Population Density Effect* (IPDE) sees the key to understand tooth crown reduction in the changes of population densities due to the shift to a sedentary lifestyle (Macchiarelli & Bondioli, 1986). Higher population densities resulted in a selection toward the reduction of

nutritional and metabolic requirements, eventually leading to the reduction in body size; the masticatory apparatus reduced as a by-product (Macchiarelli & Bondioli, 1986). The *Selective Compromise Effect* (SCE) proposes instead that the transition to agriculture, with the consequent increase in the consumption of abrasive foods, determined the tooth reduction in post-Pleistocene *Homo sapiens* (Calcagno, 1986; 1989). Smaller and less complex crowns were positively selected because they reduce the chances of developing caries, and thicker enamel was positively selected to counteract occlusal wear (Calcagno & Gibson, 1988). Despite these models provide plausible explanations for the observed trends, they have never been validated and only the SCE proved to be in partial accordance with dental metric data (Pinhasi et al., 2008). Nevertheless, this may be specific to Middle-East rather than a general trend.

1.8 Limitations of previous studies

Dental and mandibular reduction in *Homo* has been thoroughly analysed both quantitatively and qualitatively. Nevertheless, as common in science, those studies are not free from errors. Most of the limitations are not specific to some of those works, but involve assumptions widespread among scholars and never tested, or not in accordance with the theory (Calcagno & Gibson, 1988). In other cases, some aspects of the trend just need to be updated. Here, the major limitations of the previous studies on dental and mandibular reduction are discussed. These limitations have been rarely highlighted in literature and represent an obstacle to the possibility of validating the major hypotheses on dental and mandibular reduction.

1.8.1 Keeping dental and mandibular reduction up-to-date

A vast literature on dental and mandibular reduction has been produced from the 1950s to '80s (Coon, 1955; Brace, 1967; Brose and Wolpoff, 1971; Chamla, 1980; Chamberlain & Wood, 1985; Brace et al., 1987; Calcagno and Gibson, 1988), and includes the first attempts to quantify and explain the trend of dentognathic reduction in the genus *Homo*, in particular within *H. sapiens* (Brace, 1967, 1979). Those works had a large influence on later research, as

shown by the fact that the hypotheses proposed in those studies have been central in recent papers (Pinhasi et al., 2008; Pinhasi & Meiklejohn, 2011). An obvious limitation of those studies is that the trends they described are based on just a part of the data available today. The palaeoanthropological and archaeological data have been updated in the last decades; the amount of dental material increased and data have been made freely available through online databases (Gordon & Wood, 2007; Voisin et al., 2012). Therefore, the trends of dental and mandibular reduction can now be updated. In addition, the hypotheses proposed in those studies need to be reconsidered in the light of up-to-date knowledge in palaeoanthropology, evolution and genetics. The Probable Mutation Effect (PME) (Brace, 1963) represents one clear example. This hypothesis embodies the general view that the dentognathic reduction in *H. sapiens* (and in hominins in general) is the result of relaxation of selective pressures (or selective neutrality) because of lowered functional requirements. This view may not hold in the light of some recent fact about the genetics of development. Although experimental evidence suggest that some metric traits in the mandible of laboratory mice are dependent on alterations of single genes (Cheverud et al., 1997), the majority of genes is involved in several pathways (pleiotropy) (Wagner & Zhang, 2011): disrupting one signalling pathway may disrupt many others, producing detrimental effects to the development of the entire organism (Calcagno and Gibson, 1988). In addition, Calcagno & Gibson (1988) suggest that the progressive reduction of tooth size may be indicative of positive selection rather than selective neutrality.

1.8.2 The importance of body size and encephalization

Previous studies interpreted dental and mandibular reduction as independent from other important events in human evolution. Changes in the masticatory apparatus of hominins took place at the same time as several ecological, cultural and anatomical modifications (McHenry, 1994; Schick & Toth, 1994; McHenry & Coffing, 2000; Ambrose, 2001). In *Homo*, dental and mandibular reduction occurred contemporarily to the shift toward the consumption of larger quantities of meat (Speth, 1989; Stanford & Bunn, 2001); the improvements in tool use for food processing (Domínguez-Rodrigo et al., 2005); the control of fire (Goren-Inbar et al., 2004; Roebroeks & Villa, 2011; Gowlett & Wrangham, 2013); the development of agriculture (Larsen, 1995; Winterhalder & Kennett, 2006). In addition, body size (Grabowski et al., 2015)

and brain size (Rightmire, 2004) increased in the genus *Homo* and throughout the Pleistocene, and are of particular importance for the study of dental and mandibular reduction.

Structural body changes can drive alterations in the size and shape of the masticatory apparatus (Cachel, 1984). Changes in body size can affect tooth size, by modifying the patterns of dental allometry (Gingerich et al., 1982). Previous studies acknowledged the remarkable changes in body size in hominins, but the effect of these changes on the overall differences in tooth size across hominins is rarely addressed (Chamberlain & Wood, 1985; Brace et al., 1987). In addition, recent updates (Grabowski et al., 2015) in the estimates of hominin body size allow a better understanding of the role of tooth allometry in the trend of reduction.

A link between encephalization and dentognathic reduction has been hypothesized (Jiménez-Arenas et al., 2014). Previous studies addressed this hypothesis by looking exclusively at postcanine dentition (Jiménez-Arenas et al., 2014) and tempo of evolution of postcanine size and brain size (Gómez-Robles et al., 2017). Nevertheless, incisor size and mandibular robusticity are just as much important. In addition, the covariation between brain and lower jaw has to be studied. The neurocranium, which expanded accordingly with the increase in brain size, is in physical connection with the lower jaw through the temporomandibular joint (White et al., 2011). Therefore, the study of morphological integration between the neurocranium and the lower jaw can provide useful information on their mutual interactions. Few works focused on the patterns of morphological integration between the mandible and the cranium (Bastir et al., 2004), although not explicitly testing the link between dentognathic reduction and encephalization.

1.8.3 Food mechanical properties and jaw adaptations: an untested assumption

The main hypothesis on dental and mandibular reduction in hominins looks at improvements in tool use for food processing (Zink et al., 2014). This hypothesis suggests that to eat foods that are softened by pounding, slicing or cooking, a hominin individual does not need large, robust jaws (Zink & Lieberman, 2016). As a result, the hominin masticatory apparatus reduced through time because the selective pressures for keeping robust jaws mitigated when hominins were capable of modifying the mechanical properties of foods. This view is based

on the assumption that differences in size and robustness in the hominin mandibles and teeth reflect adaptive dissimilarities. Studies on primate feeding adaptations (Ross et al., 2012) highlighted the multifactorial nature of the morphological variability in mandibles and teeth. Factors other than diet or food mechanical properties (*e.g.*, behavioural and dietary plasticity, phylogeny) can be important in shaping the primate lower jaw (Ross et al., 2012; Meloro et al., 2015). It is necessary to test the assumption that differences in mandibular robusticity and tooth size among hominins represent functional differences.

1.9 Aims of this work

The hypotheses that try to explain dentognathic reduction as a result of dietary shifts, improvements in food processing or as a structural by-product of encephalization put the emphasis on two types of evolutionary factors: adaptive and non-adaptive. The directional selection toward smaller teeth and gracile jaws indicates adaptation (Calcagno & Gibson, 1988). Structural reduction in response to relaxation of selective pressures, as advocated by the PME hypothesis (Brace, 1963), or neurocranium expansion indicates a non-adaptive event in the evolution of the human masticatory apparatus (Smith et al., 1985). In this work, the lower jaw is analysed by looking at correlations between masticatory anatomy, dietary/functional factors (adaptive) and structural constraints (non-adaptive). The main aim of this work is to test the roles of food-processing, body size and neurocranium modifications on the gracilisation of the hominin lower jaw. A primate comparative approach is adopted by analysing hominins as part of the variability of Catarrhini, to define the morphological, phylogenetic and evolutionary boundaries set by belonging to the order Primates. The limitations of previous studies (discussed above) are addressed. Body size and encephalization are taken into account in terms of their structural influence on tooth size and mandibular robusticity. The assumption that differences in mandibular robusticity and tooth size among hominins represent functional differences is tested in catarrhines. The hypothesis that mandibular and dental reduction in the genus *Homo* is structurally constrained, rather than functionally driven, is tested.

Chapter 2

Material and methods

2.1 The sample

The morphological data analysed in this work were recorded on mandible, teeth and neurocrania of primate and hominin skulls from different sources and in different formats. In absolute numbers, the sample consists of measurements recorded on 63 species of non-hominin catarrhines and 13 hominin species, including 12 fossil taxa and *Homo sapiens*. The primate sample includes 9 Colobinae (25 specimens), 39 Cercopithecinae (116 specimens), 9 Hylobatidae (36 specimens) and 6 Hominidae (106 specimens), for a total 283 individuals. Each group includes only individuals of known sex, producing subsamples of females (56 species) and males (55 species). To avoid ontogenetic biases, only adult individuals were included in the sample. A fully erupted third molar was used to determine the adult age-class. The hominin sample includes specimens belonging to the genera *Australopithecus* (3 species), *Paranthropus* (2 species) and *Homo* (7 species). Part of the fossil dataset consists of dental and mandibular measurements from Plio-Pleistocene to recent hominins, and includes measurements on 5161 individual mandibular lower teeth, and on 111 mandibular corpora. Sex information was obtained from Wolpoff (1971; 1979), Wood (2001) and Schwartz & Tattersall (2005), but it is not known for all of the fossil hominins included. Modern *H. sapiens* is represented by 20 mandibles from mixed non-European individuals of known sex. Additional 3D data was collected on the neurocranium of 20 modern *H. sapiens* and 5 other species of Hominidae (105 specimens).

Some specimens in the sample were available as three-dimensional (3D) surface scans of real specimens and casts or in Computed Tomography (CT) format, and some of the hominin data are recorded on the actual fossil specimens. The primate specimens were available from the

online and museum databases of the Primate Research Institute at Kyoto University (KUPRI, http://dmm.pri.kyoto-u.ac.jp), the primate collection of the Smithsonian Institution (www.humanorigins.si.edu), from the MorphoSource database at Duke University (www.morphosource.org), from the Museum of Comparative Zoology at Harvard (via MorphoSource) and from the Royal Museum for Central Africa in Tervuren, Belgium (via http://www.metafro.be/). Part of the fossil hominin sample was obtained from the collections housed at the Natural History Museum (NHM) in London, the Muséum National d'Histoire Naturelle (MNHN) in Paris and the National Museum of Kenya (NMK) in Nairobi. Another part of the hominin sample was available from the online databases MorphoSource, NESPOS (www.nespos.org), the Africanfossils archive (www.africanfossils.org) and from the Digital Archive of fossil hominoids (www.virtual-anthropology.com) at the University of Vienna. Other hominins were digitally acquired from the cast collections of Liverpool John Moores University and the anthropological museum "G. Sergi" (Roma). These specimens were obtained by digital reconstruction using photogrammetry, following the procedure described in Falkingham (2012). A DSLR Nikon D3300 with a 60mm macro lens was used to collect pictures of the specimens, which were then processed in Agisoft Photoscan 1.2.4 to build a three-dimensional surface model. Peter Brown (www.peterbrown-palaeoanthropology.net) kindly provided a CT-scan of *Homo floresiensis* LB1. The specimens belonging to modern human populations come from the human skeletal collection at the Smithsonian Institution, and were made available by Copes (2012). Dental and mandibular measurements of fossil hominins and modern humans were available on the online databases "anthropological data free" (Voisin et al., 2012) and the "Human Origins Database" (Gordon & Wood, 2007). Exhaustive information about the catarrhine and hominin samples are reported in Appendix 1, and are simplified in Table 2.1.

2.2 The morphological data

The morphological data used include several types of measurements and recordings, and it is principally meant to represent mandibular robusticity and size, dental dimensions and shape of the cranium and lower jaw. Part of the analyses relied on the use of traditional hominin

dental and mandibular metrics. Bucco-Lingual (BL) and Mesio-Distal (MD) maximal diameters were used to approximate tooth size and to calculate dental area (BL x MD). For fossil hominins, alveolar lengths were used as proxies of the size of each tooth type. In particular, the alveolar lengths of incisors (I_1-I_2), premolars (P_3-P_4) and molars (M_1-M_3) were included in the analyses. Dental and alveolar measurements are shown in Figure 2.1. Canines were excluded because of the effect of changes in sexual dimorphism that occurred during human evolution (Brace, 1967; Jungers, 1978), which were not the focus of the analyses in which the dental metric data were used. In addition, the studies on dental and mandibular reduction focused largely on incisors and the postcanine dentition (McHenry, 1984; Emes et al. 2011). For mandibular robusticity, mandibular corpus height (H) and width (W) at the symphysis (SY) and at each molar (M_1, M_2 and M_3) are used to calculate the robusticity index (W/H x 100).

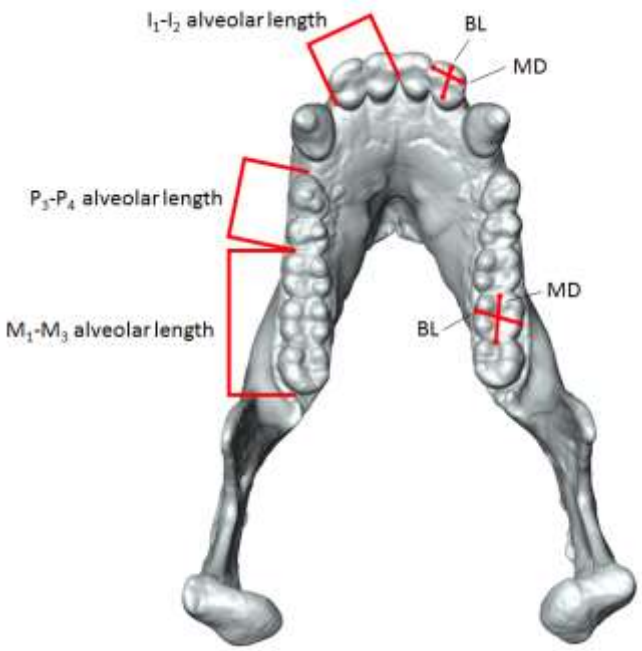

Figure 2.1 Dental and alveolar measurements shown on the mandible and teeth of a *Pan troglodytes* from the collection of the Kyoto University Primate Research Institute (KUPRI), specimen 505 of the KUPRI database. (**MD**: Mesio-Distal diameter; **BL**: Bucco-Lingual diameter). For further details, see Section 2.2.

Table 2.1 The catarrhine sample (including hominins) at the taxonomical scale of genus. The number of species, number of female and male individuals per genus are reported for catarrhines. Sex information for individual hominin specimens is available in Appendix 1.

	Genus	N Species	N Females	N Males
Colobinae	*Colobus*	2	3	1
	Nasalis	1	0	1
	Piliocolobus	1	1	2
	Presbytis	1	2	2
	Procolobus	1	2	1
	Pygathrix	1	0	1
	Trachypithecus	2	6	3
Cercopithecinae	*Allenopithecus*	1	1	0
	Cercocebus	4	4	5
	Cercopithecus	7	8	9
	Chlorocebus	2	1	3
	Erythrocebus	1	1	1
	Lophocebus	2	2	1
	Macaca	16	31	28
	Mandrillus	2	2	4
	Papio	3	4	6
	Theropithecus	1	2	3
Hylobatidae	*Bunopithecus*	1	2	1
	Hylobates	4	8	5
	Nomascus	3	5	4
	Symphalangus	1	6	5
Hominidae	*Gorilla*	2	15	26
	Pan	2	16	15
	Pongo	2	15	19
Hominini	*Paranthropus*	2	-	-
	Australopithecus	3	-	-
	Homo	7	-	-

Three-dimensional (3D) landmarks were used to describe both shape and size of teeth, mandible and neurocrania. The landmarks were collected on only one-half of the aforementioned anatomical regions (hemi-mandibles and hemi-crania). Use of half of the mandible was necessitated by the state of preservation of the fossil specimens, and this approach allowed for an increased sample size and reduced the need for missing data to be estimated. A series of 28 3D landmarks was recorded on the mandibles and 15 landmarks on the neurocrania of all catarrhines, including fossil hominins and modern humans. The landmarks were recorded on surface models obtained from CT-scans or photogrammetry, by using the software Amira (version 5.4.5, FEI Visualization, Berlin). The landmark configurations are displayed in Figure 2.2 and are defined in Appendix 1. Size information was extrapolated by calculating the centroid size (CS) of the landmark configuration, defined as the square root of the sum of squared distances of each landmark from the centroid of the configuration (Dryden & Mardia, 1998). In addition, a Generalised Procrustes Analysis (GPA) was performed to obtain shape coordinates of mandibles and neurocrania. The alignment and calculation of CS were performed in the R package "Morpho" (Schlager, 2013).

To obtain traditional metric data for the species not available in online databases, 3D virtual models were used to extract alveolar lengths and robusticity indices. Alveolar lengths were measured as the minimum chord distances between midpoints of the interalveolar septa for incisors, premolars and molars. To extract the robusticity index from the 3D surfaces, the action of Vernier callipers was simulated by using a geometric procedure developed in R for the purpose of this work. 3D alveolar landmarks were collected and then used to estimate the plane orthogonal to the M_1 alveolar plane and intersecting the mandible. The plane was translated to meet the midpoint between the alveolar plane at M_2 and M_3, thus intersecting the mandible at these positions. For the symphyseal robusticity, three points were recorded that define the sagittal plane. The intersections between these planes and the mandible were used to extrapolate the width and height of the mandible at symphysis and molars. The procedure is shown in Figure 2.3. Table 2.2 shows the number of data entries for dental dimensions, alveolar lengths, mandibular CS, mandibular robusticity, mandibular shape and neurocranium shape.

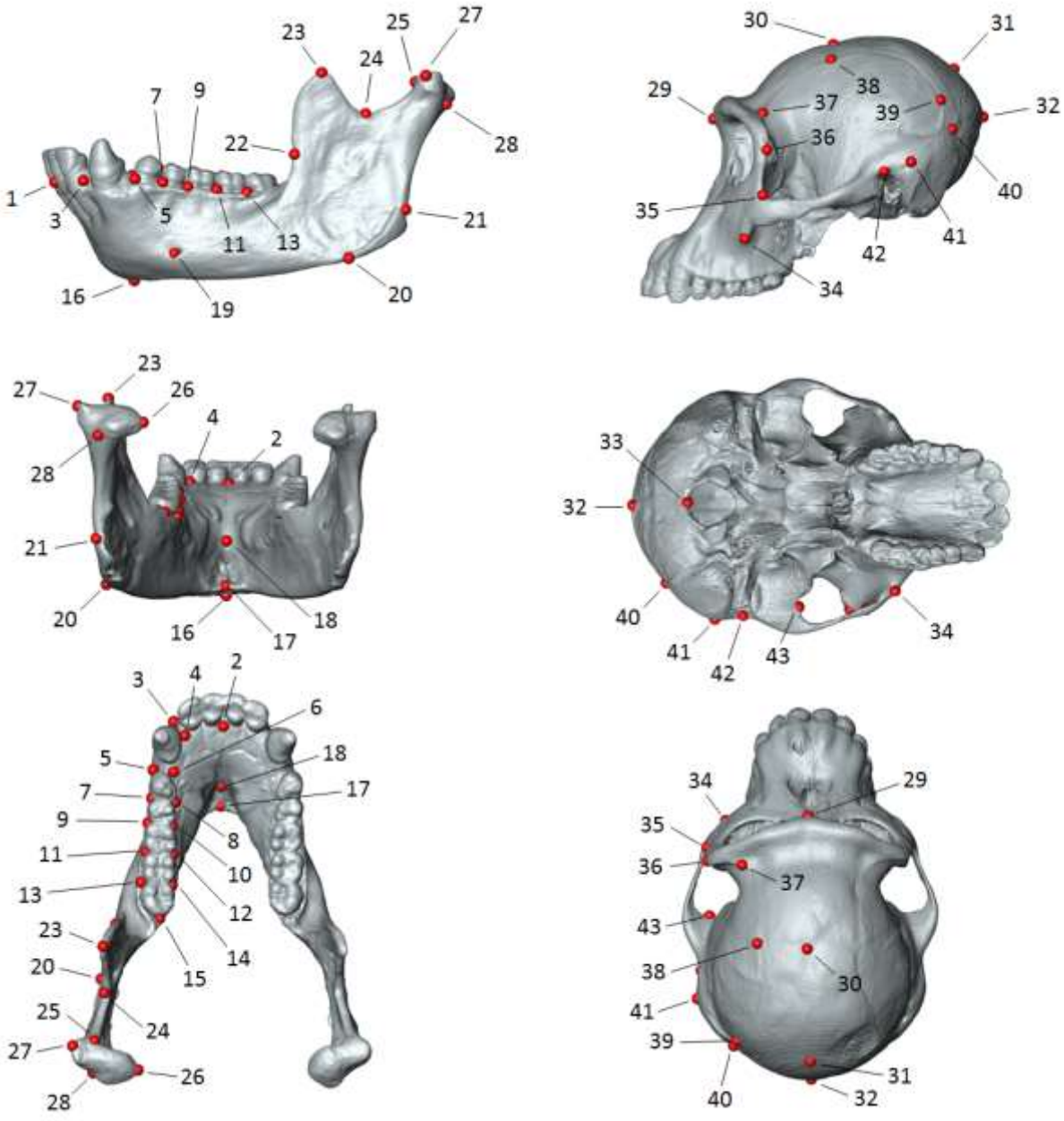

Figure 2.2 Landmark configurations on the mandible (left, 1-28) and the neurocranium (right, 29-43), shown on the mandible and neurocranium of a *Pan troglodytes* from the collection of the Kyoto University Primate Research Institute (KUPRI), specimen 505 of the KUPRI database. The landmarks are defined in Appendix 1. The enumeration follows the table of definitions.

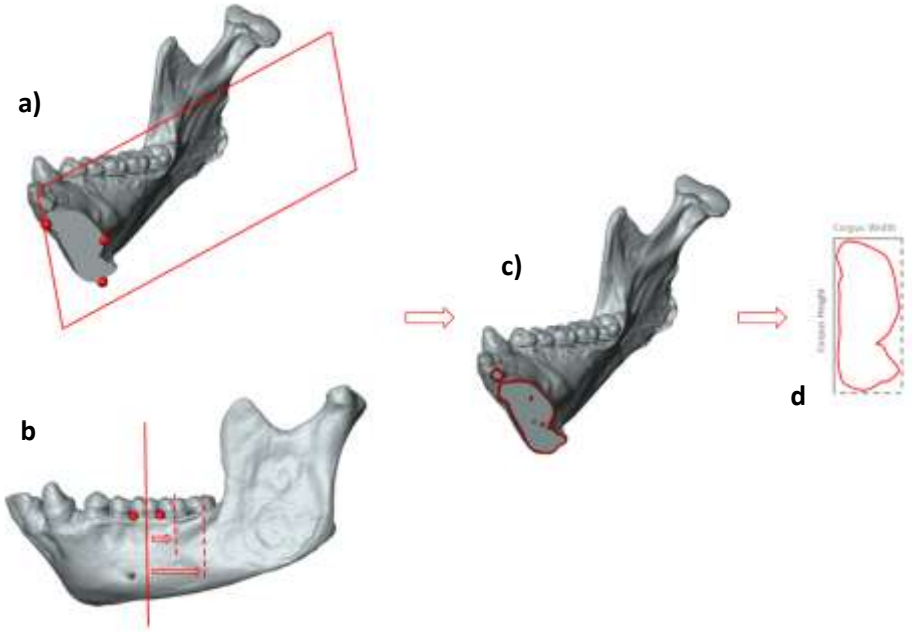

Figure 2.3 Computational procedure for the extrapolation of Robusticity indices shown on the mandible of a *Pan troglodytes* from the collection of the Kyoto University Primate Research Institute (KUPRI), specimen 505 of the KUPRI database. Three landmarks are used to define **(a)** the sagittal plane for intersecting the symphysis and **(b)** a plane orthogonal to the alveolar plane to intersect the mandible at the M_1 level. The plane at M_1 is translated toward the second and third molars. The intersection **(c)** provides a bi-dimensional profile of the mandible **(d)**, whose main axes represent mandibular corpus height and width.

Table 2.2 *Sample size for the morphological traits analysed. The number of data entries are reported for individual specimens in the catarrhine and hominin samples. The hominin sample includes modern humans.*

	Individuals	**non-hominin Catarrhines**	**Hominins**
Mesio-Distal diameter	4276	-	4276
Bucco-Lingual diameter	4508	-	4508
Dental Area	4062	-	4062
Alveolar length I_1-I_2	342	279	63
Alveolar length P_3-P_4	355	279	76
Alveolar length M_1-M_3	351	279	72
Robusticity at Symphysis	342	282	60
Robusticity at M_1	372	282	90
Robusticity at M_2	361	282	79
Robusticity at M_3	334	282	52
Mandibular Centroid Size	321	283	38
Mandibular Shape	125	105	20
Neurocranium shape	125	105	20

2.3 Body weight, feeding and tool use variables

Body weight information was incorporated in the analyses. For non-human primates, values of body weight averaged by species and sex were retrieved in the literature (Smith & Jungers, 1997; National Research Council US, 2003). Data collected on both wild and captive individuals were included. For hominin body weight, the most updated estimations from the literature were adopted, averaged by species and sex, when available (McHenry & Berger, 1998; Jiménez-Arenas et al., 2014; Grabowski et al., 2015). Body weight information was retrieved for 63 species of non-hominin catarrhines and 11 hominin species. A table of body weight values for hominins and other catarrhines is reported in Appendix 1.

Data were obtained from several sources, focusing on aspects of diet, subsistence strategies and tool use in catarrhines, recorded on both captive and wild individuals. In particular, four different categories of data were collected: diet percentages, dental microwear, feeding duration and feeding behaviour. Diet percentages refer to the relative amount of certain food type categories that are present in the diet of a species. Fruit/seed, plant soft materials, plant fibrous materials, tree gum, fungi and animal matter were considered as food categories, assuming these groups account for the complete (100%) diet for each species. Diet percentage data include information about 63 species (National Research Council US, 2003).

Dental microwear analysis is commonly performed to infer aspects of diet in mammals and it has been extensively applied to primates, including hominins (Scott et al., 2012; Ungar et al., 2012; DeSantis et al., 2013). It relies on the inspection of the patterns of scratches and pits left on tooth enamel after the contact with food during mastication (Scott et al., 2006). The microwear data here collected include variables describing surface roughness (Area-Scale Fractal Complexity, or Asfc), the anisotropy of surface properties (Length-scale anisotropy of relief, or epLsar), heterogeneity of surface properties (Heterogeneity of Area-scale fractal complexity, or HAsfc9) and textural volume patterns (Textural fill volume, or Tfv). Further details on these measurements can be found in Scott et al. (2006). Microwear was available for 19 species, including 12 extant non-human catarrhines and 7 fossil hominins, in Grine et al. (2006), Scott et al. (2012) and Ungar et al. (2012).

Data on feeding time (FT) and chewing cycle duration (CCL) were collected from Ross et al. (2009a, b). Feeding time is the proportion of time spent by a species on feeding activities.

Here this variable does not account for foraging activities other than moving food into the mouth, chewing and swallowing, and derives from observations performed on wild animals (Ross et al., 2009b). The duration of the chewing cycle refers to the length of time between successive maximum jaw gapes and was measured on animals in captivity (Ross et al., 2009b). Feeding time and chewing cycle duration are available for 24 and 12 species of catarrhines, respectively.

The behavioural data is based on evidence of tool use (TU) or extractive foraging practices (EF) in non-human catarrhines gathered by Reader et al. (2011) as part of a study on primate general intelligence. The data consist of frequencies of observations of tool use and extractive foraging behaviours available in about 4000 articles. The data are expressed as the total number of reported examples and a protocol was used to correct for the differential research effort on species. The research effort was measured as the total number of papers in behavioural research that have been published about each species in a specified time span in a number of international journals (Reader et al., 2011). Tool use and extractive foraging data were available for 54 catarrhine species.

2.4 The use of CT and surface scans: comparability, rendering and accuracy

The use of virtual imaging in physical anthropology has become part of the standard procedures adopted to study skeletal morphology, in particular when dealing with fragile fossil specimens (Mafart et al., 2004). The availability of museum collections in digital formats facilitated the access to archaeological and fossil material, thus increasing the opportunity of gathering large datasets. Nevertheless, the application of 3D acquisition techniques in anthropology and the consequent distribution of digital specimens has not followed specific criteria (Johnson, 2016). One of the main concerns has been to determine if virtual specimens accurately reproduce the topological appearance of the real object. Also, it is important to test if CT and surface scans can coexist in the same sample without producing any bias. Several authors have attempted to answer this question, and evidence supports the accuracy and comparability of CT and surface scanning (Lam et al., 2003; Ramsthaler et al., 2010; Sholts et al., 2010). Fourie et al. (2011) found consistent results when testing the reliability of CT, laser

scanning and photogrammetry in an anthropometric context. All the three methods could virtually replicate the measurement produced on the real specimens, with little difference between the methods themselves. Other authors have tested the validity of photogrammetry in physical anthropology (Aldridge et al., 2005; Weinberg et al., 2006) and report low levels of errors associated with anthropometric measurements. These studies support the use of surface scanning for the construction of large anthropological databases (Majid et al., 2005).

CT scanning techniques are widely used in physical anthropology because of the possibility to extract density information and internal features of skeletal elements (Weber, 2001). As for photogrammetry, the reproducibility of anthropometric measurements from CT-scans has been confirmed in several works (Fajardo et al., 2002; Kim et al., 2005; Kubo et al., 2008; Stull et al., 2014), but the rendering of CT data by extrapolation of a 3D surface can introduce topological artefacts in the surface used for data collection, hence error (Raman & Wenger, 2008). CT data consist of a range of grey-scale values representing the densities of the object scanned (Herman, 2009). Figure 2.4 shows the density values (grey) extracted from the CT-scan of a *P. troglodytes* (specimen 505 of the KUPRI database) and the bone densities are highlighted (red stripes). The extraction and graphical representation were performed in R by using the package “oro.dicom” (Whitcher et al., 2011).

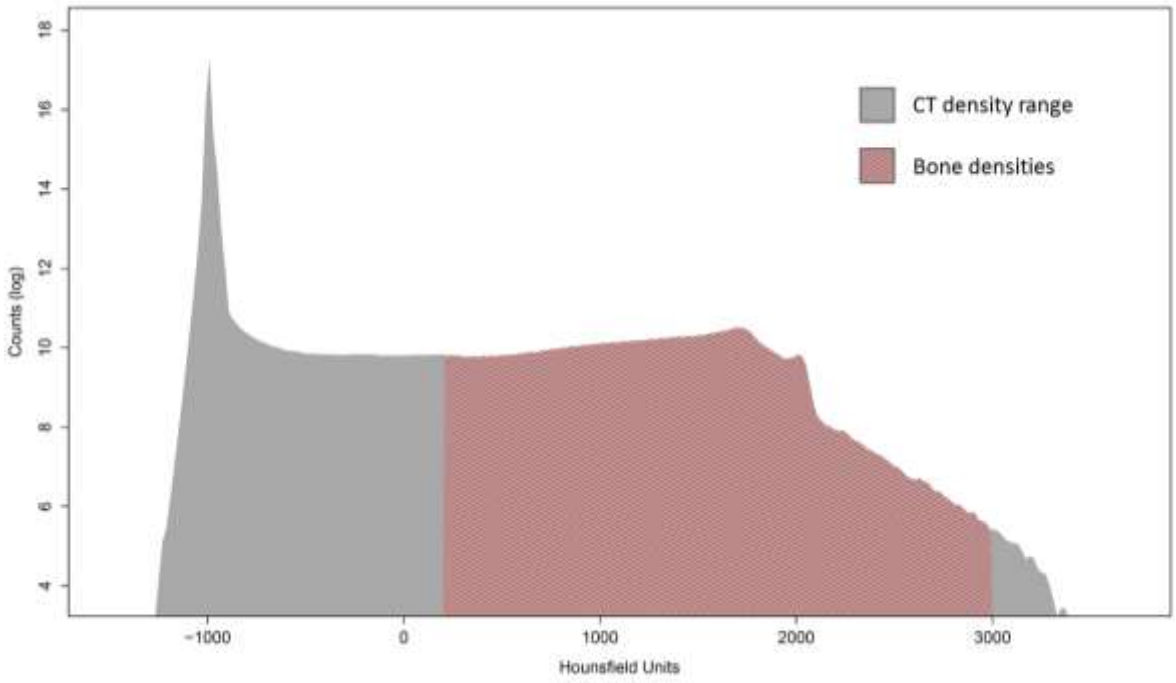

Figure 2.4 Range of densities in a Computed Tomography (CT) scan. In a medical CT scan, the densities are expressed in Hounsfield Units (HU) and each material covers a specific range. The bone material (red stripes) starts from 200 HU. The high peak on the left is air.

To isolate and distinguish a particular region of the object, a threshold in the grey-scale values can be set. A fully automatic selection of the threshold is difficult to develop since the densities of different materials of an object overlap one another (Herman, 2009). When the scan is in DICOM (Digital Imaging and COmmunication in Medicine) format, the position of the different materials along the density histogram is known and it is expressed in Hounsfield units (HU) (Mah et al., 2014). Nevertheless, their boundaries are not neat. In Figure 2.4, bone material is found above 200 HU (De Oliveira et al., 2008), and a threshold of 200 selects all the densities major and equal to 200 HU (Herman, 2009). The data provided in online databases may consist of the CT data itself or its rendered surfaces, without proper specifications of the threshold values used, although they are usually chosen to include bone and enamel. The topological differences associated with differential thresholding can be kept low if caution is applied. The CT-scan model of a *Pan troglodytes* mandible was rendered at 0 and 400 HU (Figure 2.5), crossing the optimal value for bone rendering. The topological differences between the surfaces generated were estimated by calculating the Mesh

Distance, which is the euclidean distance between each vertex of one surface and the closest point on the other surface (Bærentzen & Aanæs, 2002). Figure 2.5 shows that different thresholds produce small differences between the relative interpolated surfaces, lower than 1 mm over the entire surface, when the threshold is set in the region of expectation of the bone material.

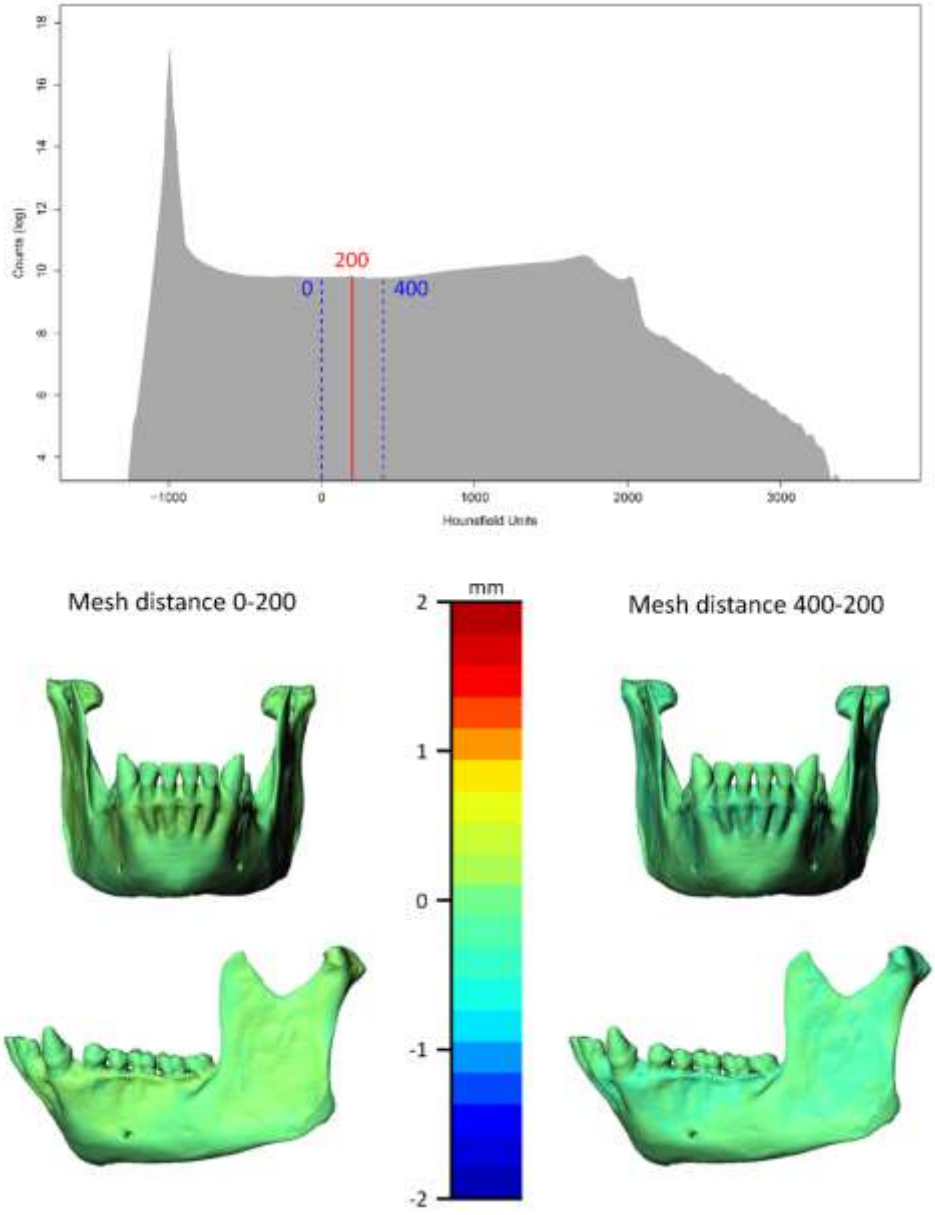

Figure 2.5 Distances between surfaces extracted from a CT scan of the mandible of a *Pan troglodytes* using non-optimal values of threshold (shown above). Each vertex of the surface is coloured proportionally to the distance between the surfaces generated at optimal and sub-optimal values of threshold. The green-yellow patterns indicate distances in the range of less than 1 mm, as reported by the colour map.

2.5 Alveolar length as a proxy for dental size

This work relied on the availability of dental size data of fossil hominins from online databases. When only hominins were analysed, the use of Mesio-Distal (MD) and Bucco-Lingual (BL) diameters measured on teeth was possible, thanks to the availability of data in online databases. These measurements have been widely used in previous studies on dental reduction (Brace, 1979; Pinhasi et al., 2008). MD and BL measurements on catarrhine teeth are not available in online databases for a sufficiently large number of species. In addition, although 3D virtual models of primate mandibles are available, the dentition is rarely well preserved. For these reasons, the measurement of alveolar length for each tooth type was adopted when comparing hominins to catarrhines. Alveolar length is measured along the alveoli to obtain information about the space occupied by each tooth type along the tooth row. The use of alveolar length as a proxy for tooth size allowed a sample size suitable to the application of comparative methods.

2.6 Accuracy of robusticity indices measured on virtual mandibles

The height and width of mandibular corpus were used to calculate the robusticity index. These measurements were available for hominins in the Human Origins Database (Gordon & Wood, 2007), but not for other catarrhines. To solve this issue, a virtual protocol was generated to extract height and width information from virtual 3D models of primate mandibles, using a series of landmarks located on the mandibular symphysis and on the alveoli of the first molar (for full description, see Section 2.2). An assessment was performed to demonstrate that this method produces results comparable to the direct measurement of mandibular corpus height and width, at least on virtual specimens. Corpus height and width at M_1 were directly measured on the 3D models of 30 catarrhine mandibles in the software Amira (version 5.4.5, FEI Visualization, Berlin). The virtual protocol was used to extract corpus height and width of the same 30 specimens. Corpus height and width (both measured and extracted by means of the virtual method developed here) were used to calculate robusticity index. For each of the 30 specimens, the robusticity index obtained from direct measurements was compared to the one extracted by using the virtual protocol. The results are shown in Figure 2.6. The

comparison between measured and extrapolated indices yielded a small standard error of 0.012 and a slope of 1±0.024 at 95% of confidence, indicating that the protocol is reliable. Also, the percent error for each observation was always lower than 5%. These results demonstrate that the virtual protocol for calculating the robusticity index can be reliably used along with measurements on real specimens.

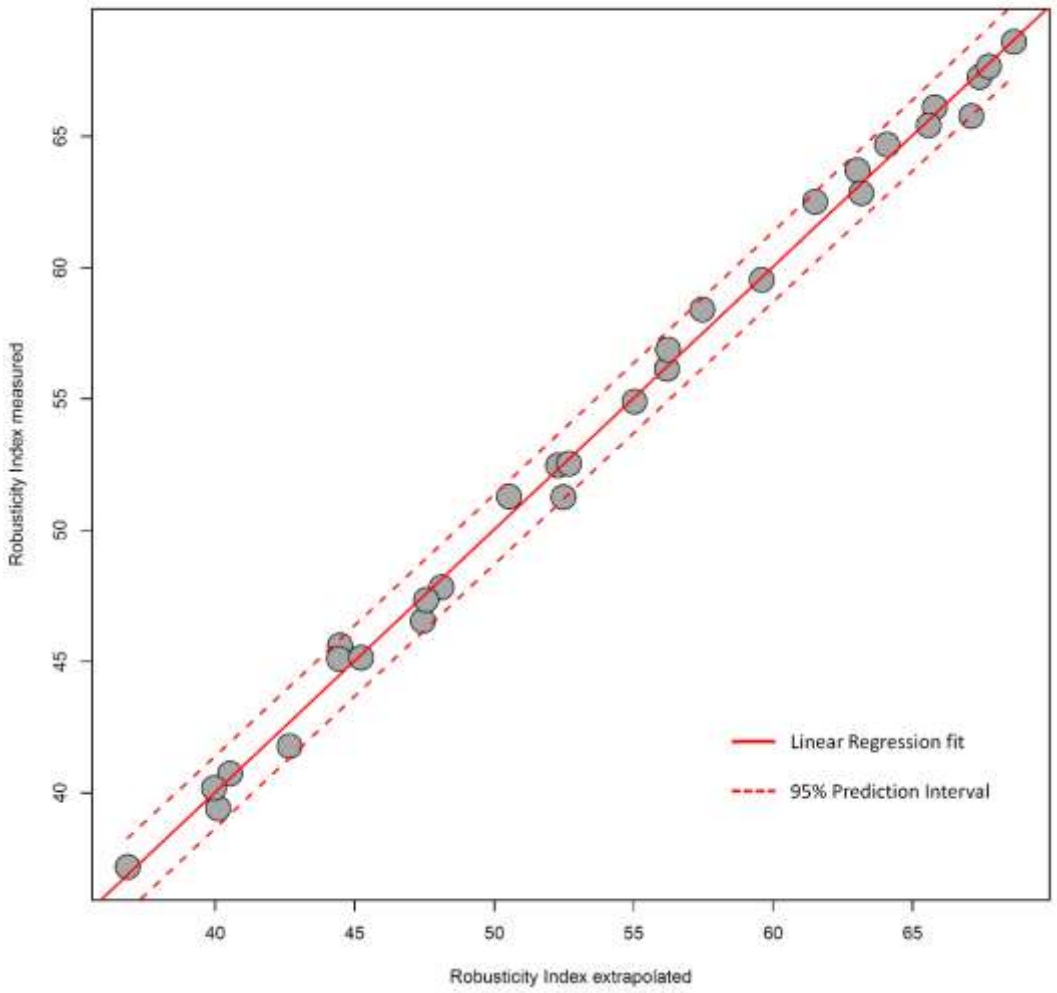

Figure 2.6 Comparison between robusticity index measured on the 3D models of primate mandibles and the same index extracted by means of a virtual protocol generated in R (see Section 2.2). The regression yielded a standard error of 0.012, indicating a good fit between the two methods. The protocol for virtual extrapolation of robusticity indices is described in Section 2.2.

2.7 Landmarking error and missing landmark estimation

Recording landmarks on 3D surfaces is a procedure prone to both inter- and intra-observer errors. Since a single observer collected the entire landmark sample in this work, only the second source of error might have affected the data. The amount of error produced during the landmarking procedure was quantified by collecting 10 repeats of the landmark configuration (Figure 2.2, Section 2.2) of 3 mandibles of female *P. troglodytes*. The landmark configurations were aligned by Procrustes superimposition and a Principal Components Analysis (PCA) was performed to visually appreciate the intra- and inter-specimen differences (Figure 2.7). A Procrustes ANOVA (Klingenberg & McIntyre, 1998) was performed to infer the statistical significance of the intra- and inter-specimen differences. This method quantifies the amount of shape variation attributable to one or multiple factors (grouping variables) in a linear model, by working with multivariate response variables. This analysis tests the null hypothesis of independence between the response variable and the factor. An implementation of Procrustes ANOVA was used, and it is embedded in the R package "geomorph" (Adams & Otárola-Castillo, 2013). A significant difference is present between specimens but not between replicates, indicating that the landmarking procedure did not produce biologically relevant errors. The results are presented in Table 2.3.

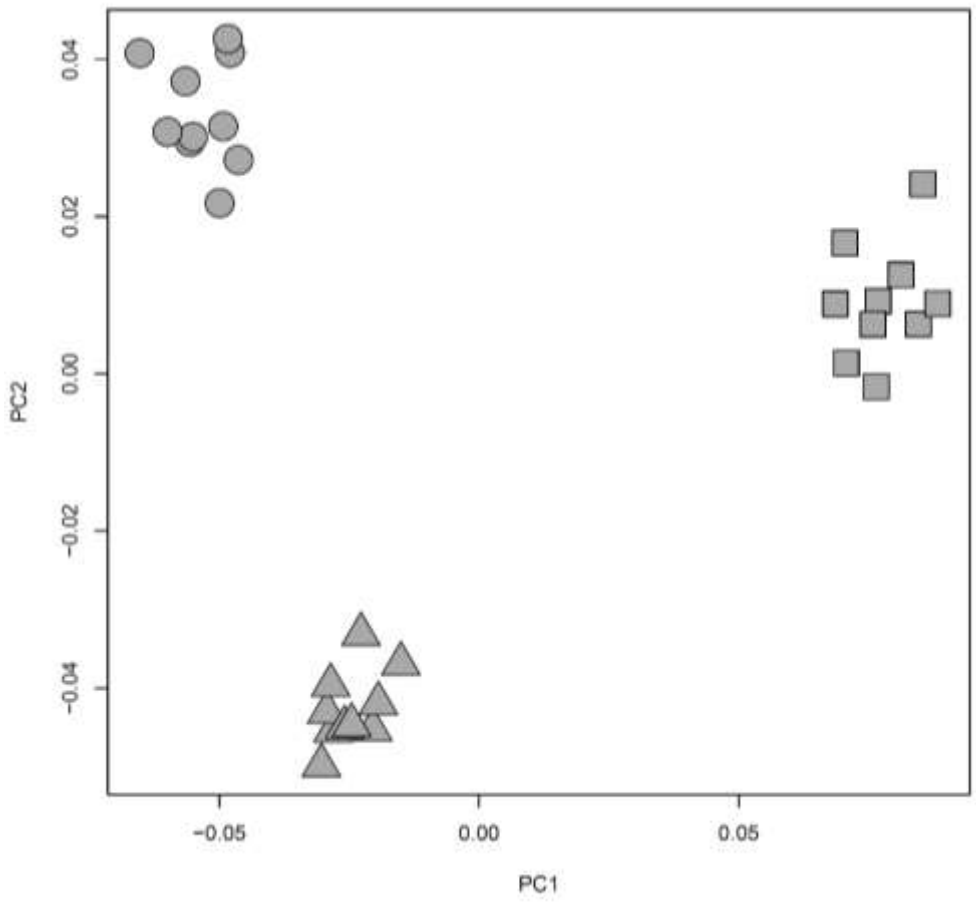

Figure 2.7 Principal Component Analysis (PCA) for landmark accuracy. The three groups (designated by circles, squares and triangles) represent 10 replicas of the landmark configurations of three *P. troglodytes* mandibles.

Table 2.3 Results of the Procrustes ANOVA on the replicas of the landmark configurations of the mandible. The results indicate significant differences between the three individuals and their relative replicas.

	DF	Sum of Squares	Mean of Squares	F	p-value
1 vs 2	18:19	0.054	0.003	29.4	0.001
1 vs 3	18:19	0.054	0.003	21.84	0.001
2 vs 3	18:19	0.006	0.003	9.37	0.001

Fossil and archaeological specimens are often fragmentary or incomplete, depending on the taphonomic events that may have occurred after death (Behrensmeyer, 1988). According to Arbour & Brown (2014), these specimens should not be removed from the sample, unless inadequate to record a sufficient amount of landmarks. In fact, removal of incomplete specimens for the presence of missing landmarks is not justified, because their exclusion can alter the effect of the analysis more than happens when missing data are estimated (Arbour & Brown, 2014). In this work, the missing landmarks were estimated by means of a Thin Plate Spline (TPS) procedure implemented in the R package "Morpho" (Schlager, 2013). The TPS was used because it has been demonstrated to be a reliable method for missing landmark estimation in biological specimens (Arbour & Brown, 2014). TPS is an interpolation method that uses a deformation grid to map the position of landmarks onto a reference configuration (Bookstein, 1997a). TPS can be used to estimate the missing landmarks by deforming the incomplete configuration onto the mean shape (consensus) of the complete configurations. TPS estimation performs best when only one or few landmarks are missing from one configuration. Only specimens with a maximum of 14.3% of missing data (4 on 28 landmarks) were included in the sample, and, in most cases, fewer than four landmarks were missing. All the incomplete specimens belonged to the fossil hominin sample. A list of the incomplete specimens and the amount of missing data estimated is presented in Appendix 1.

2.8 The analytical approach: traditional and Geometric Morphometrics

Morphometrics is the use of standardised measurements to extract quantitative information that can be used to describe organisms and compare them mathematically and statistically. Since biological objects are usually complex in their appearance, it is not surprising that the morphometric approach flourished in the study of the living things. Being based on measurements, the data, the analyses and the results of morphometrics are written in numbers, which acquire a biological meaning only if associated by univocal definitions (Zelditch et al., 2012). To compare similar objects, the measurements used to describe their shape have to be homologous, this meaning that those descriptors must correspond to

structures or positions that have the same biological, developmental or evolutionary meaning in different organisms or species (Bookstein, 1997a).

Traditional morphometrics relies on linear measurements of length, height and depth to quantify shape, which makes it simple to perform and almost costless, but these advantages come with major drawbacks. One of these issues is the interdependence of measurements: measurements sharing the same or similar directions describe part of the same variation, and it is difficult to isolate their single contributions (Zelditch et al., 2012). This issue has been overcome by the advent of Geometric Morphometrics (GM), that uses homologous coordinates (or landmarks) and their mutual relationships to approximate the geometry of an object and describe its shape (Zelditch et al., 2012). GM is a set of methods to produce quantitative comparisons of shapes. These methods derive from the necessity of accurately describe objects (in the present case, skeletal elements) whose topology is too complex to be approximated by polygons and polyhedrons. When homologous points are scarce, curves of landmarks and patches of semi-landmarks (Bookstein, 1997b; Mitteroecker & Gunz, 2009) can be applied, as long as enough homologous landmarks can be used to reference the curves and patches. GM relies on a set of methods that solve the inter-correlation between measurements and remove size (Bookstein, 1997a). Statistical ordination methods, like Principal Component Analysis (PCA), are used to decompose the shape in a series of variables sorted by their decreasing variance (Zelditch et al., 2012). This procedure is conceived to keep each variable orthogonal to the others, thus cancelling the mutual correlation between them (Wold et al., 1987). Size is removed by aligning different shapes by Procrustes superimposition (Bookstein, 1997a), which scales each shape to a unit Centroid Size (the square root of the sum of squared distances of a set of landmarks from their centroid, the standard size proxy in GM) after translating and rotating them to reduce the distance between homologous landmarks. After alignment, the square root of the sum of squared differences between the positions of the landmarks, or Procrustes distance (Bookstein, 1997b), represents the shape differences between objects, free from the effects of size and spatial location.

The subject of dental and mandibular reduction is linked to certain morphological traits, such as dental size and mandibular robusticity, that have been studied using linear measurements (Wolpoff, 1971; Brace, 1979; Chamberlain & Wood, 1985). Their advantage is the simplicity and the opportunity to use univariate statistics, which makes the results easy to interpret. In

addition, certain features are evaluated on regions of the mandible that lack homologous landmarks. As an example, the mandibular corpus has few anatomical landmarks, and the robusticity at the level of molars can be more easily extrapolated by measuring width and height, rather than constructing a curve of landmarks across the section of the mandible. Other aspects of the evolution of the human mandible are better exemplified by studying the shape of the lower jaw and the skull using Geometric Morphometrics. In fact, GM can be used to approximate the entire shape of the mandible in a multivariate statistical framework and produces an intuitive and compelling visualization of the results.

In this work, a mixed approach of traditional and Geometric morphometrics was used, taking advantage of the benefits provided by the two sets of methods. The traditional approach was used for studying dental size and robusticity, to align with the measurements employed by the majority of studies on dental and mandibular reduction. GM was adopted for evaluating mandibular size and to study the patterns of covariation between the lower jaw and the neurocranium, which make sense only in a multivariate statistical framework.

2.9 Phylogenetic controlled analyses

A primate comparative approach has been extensively adopted in the study of human evolution (Cachel, 2006). Using a broad taxonomic sample is a valuable way to reveal functional and ecological aspects in hominin evolution, but such an approach can be misleading because of the phylogenetic relationships among taxa (Freckleton et al., 2002). Every taxon shares a common ancestor with others because they diverged from the same species at some point during evolution. The diverging species accumulate modifications with respect to the common ancestor. Nevertheless, they retain common traits because of their shared ancestry (Blomberg & Garland, 2002). In summary, species that are more closely related tend to share more traits than species that separated formerly. Significant phylogenetic signals have been found in the mandibular size and shape of primates (Plavcan & Daegling, 2006; Meloro et al., 2015). Comparative studies can rely on the availability of phylogenetic data that account for the relatedness between species in the sample investigated.

In this work, a phylogenetic tree built from genetic data of non-hominin catarrhines was used. This primate molecular phylogeny is available from the online database 10ktrees (Arnold et al., 2010), and is part of a larger project on mammalian phylogeny. The data were used to build a phylogenetic tree representative of relatedness between the non-hominin catarrhine species in the sample. For the hominin phylogeny, the topology published by Dembo et al. (2015), based on a Bayesian statistical approach applied on a matrix of morphological traits of hominins, was used. Palaeontological data of First and Last Appearance Datum (FAD and LAD) of fossil hominins was used to reconstruct plausible times of divergence between taxa. Potts (2013) provides a list of FAD and LAD data from several literature sources. Branch lengths were scaled to fit the time of divergence between *P. troglodytes* and *H. sapiens* in the non-hominin catarrhine phylogenetic tree, by using the R package "ape" (Paradis et al., 2004). The catarrhine and hominin trees were then merged. Figure 2.8 shows the hominin phylogeny as adopted in this work. The primate tree is displayed in Appendix 1.

Several methods have been developed to account for phylogeny in comparative analyses. The principal approaches to test for phylogenetic independence in the structure of a correlation between two variables are Phylogenetic Independent Contrasts (PIC; Felsenstein, 1985) and Phylogenetic Generalized Least Squares (PGLS; Grafen, 1989). The two methods produce identical results when the regression is fitted assuming a Brownian Motion (BM) model of evolution. The BM model represents the null model of trait evolution: it assumes that the evolutionary change is neutral. Brownian Motion has proven to be satisfactory to express the phylogenetic correlation among species (Felsenstein, 1985). Blomberg et al. (2012) proved the equivalency of PIC and PGLS when BM is assumed. Nevertheless, evolutionary change is often non-neutral and the adaptation of a trait is better described by using models of evolution that require alterations of the branch lengths of the phylogenetic tree (Harmon et al., 2010). In this work, PGLS methods were applied to account for phylogeny in correlations. Brownian Motion and other models of trait evolution were used to describe the phylogenetic structure of the correlation. In these cases, PGLS is much more versatile than PIC, and several PGLS methods have been developed to fit linear and non-linear regressions, also allowing an estimation of evolutionary parameters.

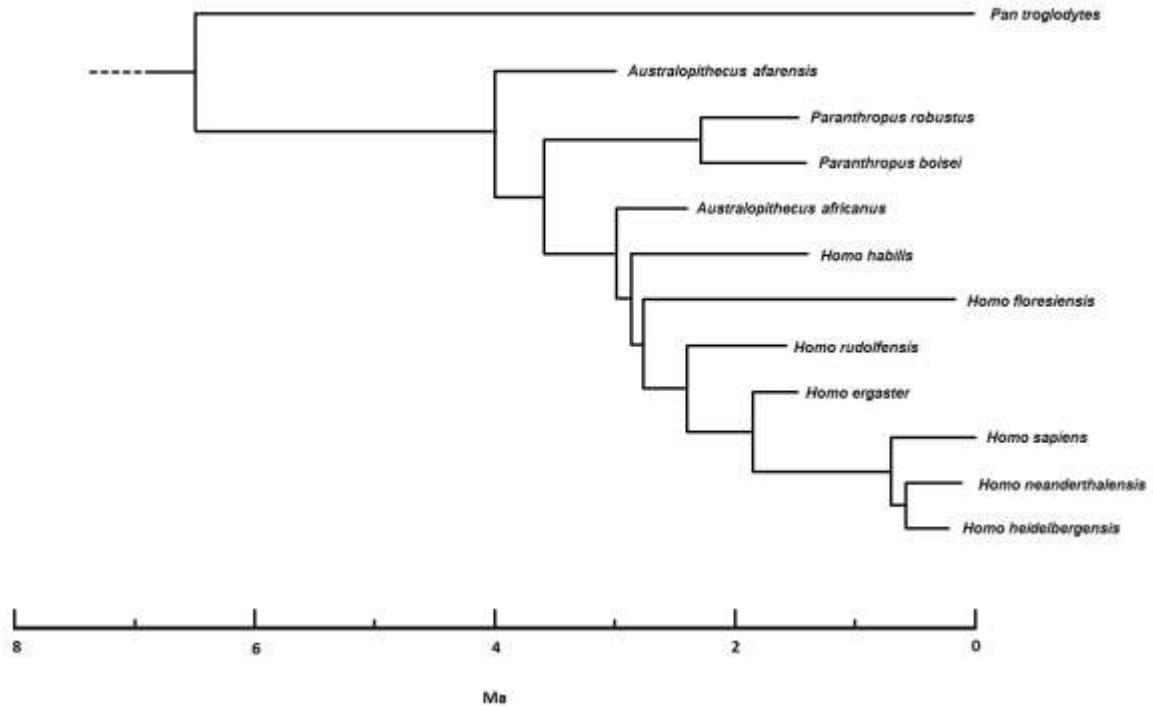

Figure 2.8 The hominin phylogeny adopted in this work. The hominin tree was merged with the catarrhine molecular phylogeny. The catarrhine tree is shown in Appendix 1. The topology of the hominin tree was taken from Dembo et al. (2015)

2.10 The R analytical environment

R is an open-source programming language designed for object-oriented coding (R Core Team, 2015). Although renowned for its reliability in statistical analyses, R is a highly versatile graphic tool and a powerful computational environment. In addition, R is free, unlike other software commonly used in science, and is supported by a vast community of users networked via numerous platforms online. These attributes allow the user to approach problems in a more effective way, by coordinating with a vast network of scientists worldwide. From a user's perspective, the use of R is unlimited: having access to its source code, any method can be modified or implemented, and it is possible to generate methods not available in proprietary software packages. Also, R promotes the automation of analytical methods and procedures, thus making the application of research methods faster. A great amount of biological analytical methods are embedded in R packages that can be freely

downloaded via internet. Several packages embed phylogenetic methods (Paradis et al., 2004; Revell, 2012; Adams & Otárola-Castillo, 2013; Orme et al., 2013), morphometrics tools for analysis and visualization (Adams & Otárola-Castillo, 2013; Schlager, 2013), and multivariate statistics (Dixon, 2003; Venables & Ripley, 2013).

The analyses carried out in this work were performed in R, mostly using packages provided by the Comprehensive R Archive Network (R Core Team, 2015). This was possible because of the effort of several researchers and R users who developed the methods applied here and provided them in packages made freely available. Thanks to their work, morphometric analyses, graphic tools, phylogenetic methods and updated statistical approaches are available.

Chapter 3

Mandibular and dental reduction in an updated archaeological and palaeontological context

3.1 Introduction

In the decades of the 1950s and '60s, anthropologists started highlighting the gracile appearance of living humans' masticatory apparatus, by comparing it to the archaeological record and to the hominin fossils available back then (Coon, 1955; Brace, 1963). The lower jaw was particularly useful in discerning such a pattern of reduction through time. Coon (1955) reported a shorter mandibular ramus and a less strongly developed temporalis muscle in post-Mesolithic humans compared to pre-Mesolithic humans, *H. neanderthalensis* and "*H. rhodesiensis*" (today known as *H. heidelbergensis*). He suggested that major modifications to the human facial complex might be the result of the amount of chewing needed to process food. A robust mandibular corpus was commonly interpreted as indicating strong biomechanical requirements (Jolly, 1970; Daegling, 1989), therefore relating the morphology of the lower jaw to food-linked selective pressures on mastication. Brace (1963, 1967; Brace & Mahler, 1971) was one of the first authors to bring the structural reduction of the human masticatory apparatus to the attention of the scientific community. In his perspective, the small size of the human dentition was due to changes in food processing practices, and he reserved a special importance to the invention of pottery in the Holocene (Brace et al. 1987). The use of pottery for crushing and grinding hard foods would have modified their texture, which is believed to influence the biomechanics of mastication (Peyron et al., 1997; Mioche et al., 1999; Lucas et al., 2004; Norconk et al., 2009). Brace (1979) and other authors also suggested that fire might have played a role in the evolution of human dentition (Coon, 1962; Wrangham & Conklin-Brittain, 2003), by softening food and consequently reducing

masticatory effort, while others have attributed this role to tool manufacturing (Frayer, 1977; Zink et al., 2014). Many of these hypotheses look at food processing and jaw biomechanics as crucial in the onset of lower jaw reduction in *Homo*, and are supported by archaeological and experimental evidence (Zink & Lieberman, 2016).

Previous studies provided detailed descriptions of the trends and hypotheses to explain them, but they often overlooked the importance of body size (Ruff, 2002). Body size changes might have had a remarkable influence on the allometric patterns of tooth size. Indeed, body size is known to influence tooth size in primates (Wood, 1979; Gingerich et al., 1982). In particular, some author (Gingerich, 1977) argue that molar size can be used for estimating body size in fossil hominoids. Within *Homo*, body size changed considerably during the Pleistocene (Grabowski et al., 2015). A decline in the body size of *H. sapiens* from 50 kyr to the Neolithic has been described (Ruff, 2002), and this seems to be a general trend, not geographically limited. Because of the changes in body size, differences in tooth size may be the effect of allometry. Recent body size estimates in hominins have been produced (McHenry & Berger, 1998; Jiménez-Arenas et al., 2014; Grabowski et al., 2015), allowing a better understanding of the real differences between tooth size among hominins. In addition, the palaeontological and archaeological record available today sheds light on the variability of our ancestors and can improve our understanding of the evolutionary paths that led to our modern anatomy. More data are now available also because of online data sharing and the creation of easily accessible databases. These online archives literally bring the work of many generations of scholars in the hands of today researchers and represent a unique opportunity of gathering large amounts of information to answer questions in the light of modern Palaeoanthropology.

Metric data were gathered from online databases to test if the patterns of dental and mandibular reduction in *Homo* are in accordance with the trends described in previous literature. The results are discussed in the light of the knowledge of modern palaeoanthropology and taking into account up-to-date body size estimates. The conclusions may help to interpret the trends of dental and mandibular reduction in the context of an updated paleoanthropological and archaeological framework.

3.2 Material and methods

The sample includes hominin species ranging from lower Palaeolithic to modern humans of mixed non-Europeans populations, and the data consist of measurements on lower dentition and mandibles. Information on sample size for robusticity index and dental measurements are reported in Table 3.1 and 3.2 respectively. The dental metric data include 5161 individual teeth divided into seven hominin and time groups: early *Homo*, lower, middle and upper Palaeolithic, Mesolithic, Neolithic and Middle Ages. Only measurements on permanent lower dentition were collected, and canines were excluded, because of the effect of sexual dimorphism during human evolution (Brace, 1967; Jungers, 1978) and the concomitant lack of exhaustive sex information for fossil and archaeological specimens (see Chapter 2 for further details). Bucco-Lingual (BL) and Mesio-Distal (MD) maximal diameters were used to approximate dental size and to calculate dental area (BL x MD). A graphical representation of the dental measurements is shown in Chapter 2, Figure 2.1. The dental metric data is available in the "Human Origins Database" and in the "anthropological data free" database.

Measurements of mandibular corpus height (H) and width (W) at the symphysis (SY) and at each molar (M_1, M_2 and M_3) were used to calculate the robusticity index (W/H x 100). To include a broader hominin variability, the robusticity index of modern humans and additional fossil hominins was measured from 3D scans. The entire procedure is described in Chapter 2, Section 2.2, and is represented in Figure 2.3. In addition, Section 2.2 includes an estimate of the error of the procedure, which indicates a good reliability for this protocol. The mandibular measurements used for robusticity are available in the "Human Origins Database". The sample used for extracting the robusticity index includes CT scans, micro CT scans and surface models digitalized by using photogrammetry. The 3D models of hominin specimens were collected from online databases (MorphoSource, NESPOS, the Africanfossils archive and the Digital Archive of Fossil Hominoids), museums (Natural History Museum in London, the Muséum National d'Histoire Naturelle in Paris and the National Museum of Kenya in Nairobi), or from the cast collections of Liverpool John Moores University and the anthropological museum "G. Sergi" (Roma). Peter Brown kindly provided the CT-scan of *Homo floresiensis* LB1 (www.peterbrown-palaeoanthropology.net). For further details, see Chapter 2 and Appendix 1.

Table 3.1 Sample size for the robusticity indices used in the analyses. A full list of information about individual specimens is reported in Appendix 1.

	Sample size of robusticity indices			
	M_1	**M_2**	**M_3**	**SY**
Paranthropus aethiopicus	2	2	-	2
Paranthropus boisei	25	23	10	12
Paranthropus robustus	4	4	3	-
Australopithecus afarensis	11	7	-	4
Australopithecus africanus	4	3	1	2
Homo habilis	5	3	2	2
Homo rudolfensis	5	3	1	3
Homo ergaster	7	6	5	7
Homo erectus	4	3	2	4
Homo floresiensis	1	1	1	1
Homo heidelbergensis	3	3	3	3
Homo neanderthalensis	7	8	8	8
Upper Palaeolithic *Homo sapiens*	4	4	4	4
Modern *Homo sapiens*	18	18	18	18
Total	100	88	58	70

Table 3.2 Sample size for Mesio-Distal and Bucco-Lingual dental diameters. A full list of information about individual specimens is reported in Appendix 1.

	Sample size of dental diameters							
	I_1	**I_2**	**P_3**	**P_4**	**M_1**	**M_2**	**M_3**	**Total**
Early *Homo*	2	2	4	6	7	9	5	35
Lower Palaeolithic	36	43	55	49	66	57	52	358
Middle Palaeolithic	21	30	35	37	43	40	33	239
Upper Palaeolithic	46	56	54	50	73	74	49	402
Mesolithic	238	261	279	277	274	278	260	1867
Neolithic	142	167	175	172	197	176	123	1152
Middle Ages	89	127	186	185	185	189	147	1108
Total	574	686	788	776	845	823	669	5161

To test for differences in dental size and mandibular robusticity during Pleistocene and Holocene, Kruskal-Wallis rank sum test (Hollander et al., 2013) was performed. The Pleistocene trend is an inter-species pattern, while the Holocene reduction involves only the species *H. sapiens*. For this reason, the analyses for the Pleistocene and Holocene trends were performed separately. The Robusticity data was grouped in the categories australopithecines (*Australopithecus* and *Paranthropus*), early *Homo* (*H. habilis*, *H. rudolfensis*, *H.ergaster*, *H. erectus* and *H. floresiensis*) and later *Homo* (*H. heidelbergensis*, *H. neanderthalensis* and *H. sapiens*). The dental data for Pleistocene hominins was divided in the groups early *Homo*, lower, middle and upper Palaeolithic, and the species included in these categories are included in Appendix 1. The Holocene sample was divided in Upper Palaeolithic, Mesolithic, Neolithic and Middle Ages, and each group was compared to the others. The Jonckheere-Terpstra test for ordered differences among classes (Jonckheere, 1954) was performed to check for the statistical significance of a decreasing trend in the samples analysed. The statistical level of significance accepted in the analyses was set at 0.05 (95% of confidence).

3.3 Results

3.3.1 Mandibular robusticity

For mandibular robusticity, there was a pattern separating early *Homo* from later species (Figure 3.1). Early *Homo* falls within the australopithecine variability. For each of the robusticity indices analysed, there were significant differences between the group means of australopithecines, early and later *Homo*, as indicated by the results of the Kruskal-Wallis test (Table 3.3). A pairwise comparison showed that early and later *Homo* differ in all the indices analysed, while early *Homo* differs from australopithecines for the M_2 robusticity only (Table 3.4). The Jonckheere-Terpstra test confirmed a pattern of reduction in mean robusticity between early and later *Homo*, and in the mean M_2 robusticity between australopithecines and early *Homo*. The results of the Jonckheere-Terpstra test are shown in Table 3.3.

Table 3.3 Results and statistics of the Kruskal-Wallis (KW) and Jonckheere-Terpstra (JT) tests for differences between robusticity indices of the groups australopithecines, early *Homo* and late *Homo*. The p-values achieving statistical significance are shown in bold.

	DF	KW Chi^2	KW p-value	JT (decreasing mean)	JT p-value
Robusticity M_1	2	35.98	**< 0.001**	689.5	**< 0.001**
Robusticity M_2	2	44.58	**< 0.001**	332.5	**< 0.001**
Robusticity M_3	2	29.04	**< 0.001**	122	**< 0.001**
Robusticity SY	2	13.58	**0.001**	554.5	**0.006**

Table 3.4 Results of the Kruskal-Wallis pairwise comparisons between robusticity indices of the groups australopithecines, early *Homo* and late *Homo*. Significant comparisons are labelled "S". The level of significance was set at 0.05 (95% confidence).

	Australopith - early *Homo*	Australopith - Late *Homo*	early *Homo* - Late *Homo*
Robusticity M_1	-	S	S
Robusticity M_2	S	S	S
Robusticity M_3	-	S	S
Robusticity SY	-	-	S

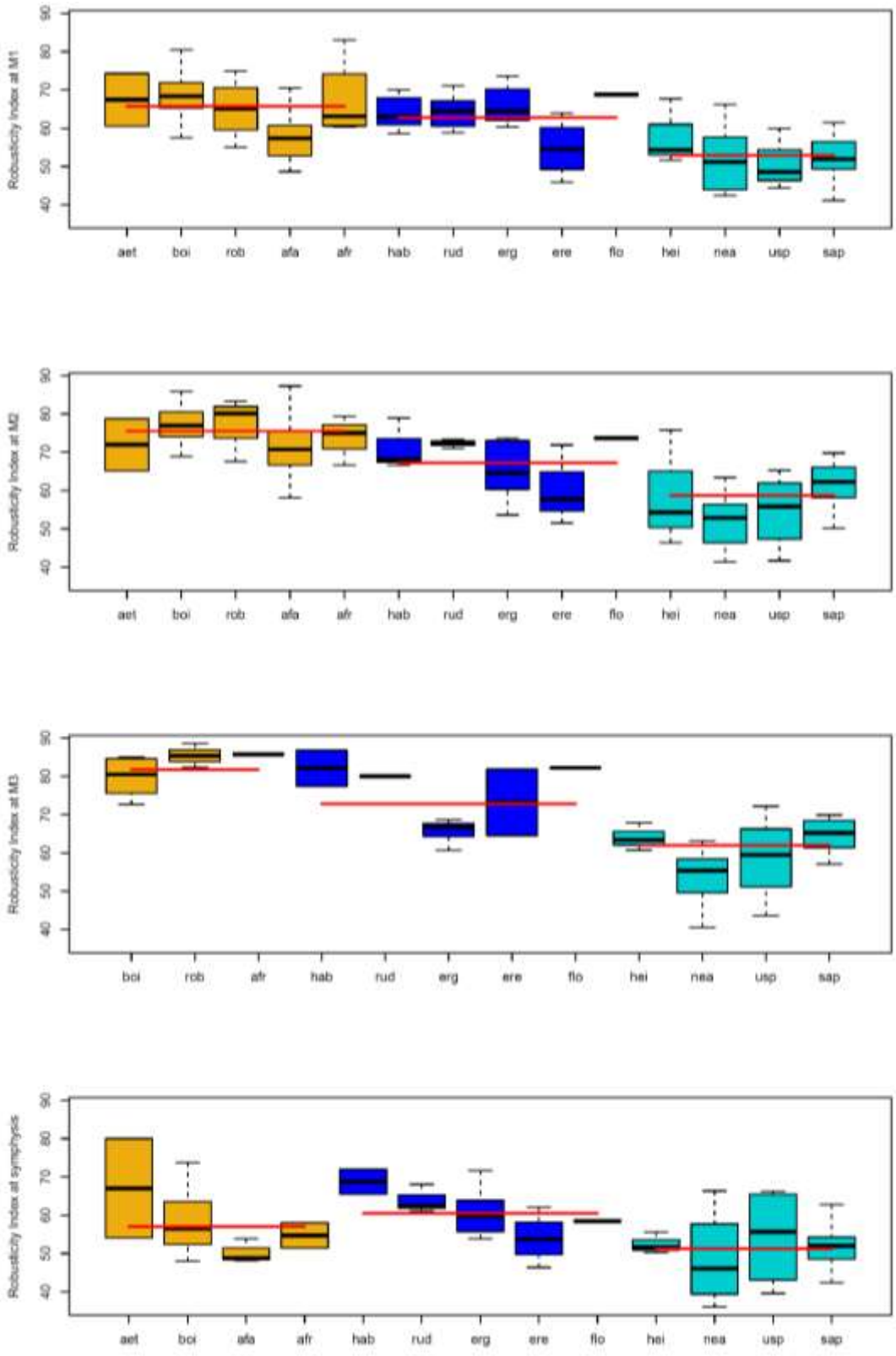

Figure 3.1 Robusticity index calculated at first, second, third molar and mandibular symphysis of australopiths (gold), early *Homo* (blue) and late species of *Homo* (cyan). The red lines indicate the mean robusticity for each group. **aet**: *P. aethiopicus*; **boi**: *P. boisei*; **rob**: *P. robustus*; **afa**: *A. afarensis*; **afr**: *A. africanus*; **hab**: *H. habilis*; **rud**: *H. rudolfensis*; **erg**: *H. ergaster*; **ere**: *H. erectus*; **flo**: *H. floresiensis*; **hei**: *H. heidelbergensis*; **nea**: *H. neanderthalensis*; **usp**: upper Palaeolithic *H. sapiens*; **sap**: modern *H. sapiens*.

3.3.2 Dental reduction during the Pleistocene

The two incisors (I_1 and I_2) shared a common pattern of variation throughout the Pleistocene. The Kruskal-Wallis and Jonckheere-Terpstra tests confirmed the presence of an overall trend of decrease in the BL dimension for I_1 (JT p: 0.004) and in both MD and BL diameters for I_2 (JT $p < 0.001$), from lower to upper Palaeolithic, although a significant increase is present for I_1 BL diameters and area from middle to upper Palaeolithic. Significant changes occurred in the I_1 and I_2 area from lower to upper Palaeolithic, but the hypothesis of a decreasing pattern is not supported for the first incisor (JT p: 0.182). MD and BL of P_3 decreased from middle to upper Palaeolithic (JT $p < 0.001$), while P_4 underwent a significant reduction in both the diameters from early *Homo* to lower Palaeolithic and from middle to upper Palaeolithic. Based on the Jonckheere-Terpstra test, these changes account for a reduction in both MD (JT $p < 0.001$) and BL (JT p: 0.014) diameters. The results for premolar area recall the trends observed for the dental diameters. There was a significant reduction of MD in M_1 (JT $p < 0.001$), with remarkable changes from early *Homo* to lower Palaeolithic, and in M_2 and M_3 (JT $p < 0.001$) from middle to upper Palaeolithic. M_1 and M_3 do not exhibit an overall reduction in BL (JT p: 0.1 and 0.438 respectively), but lower Palaeolithic and later hominins display a significantly smaller BL diameter in all molars. During Pleistocene, M_1, M_2 and M_3 areas reduced significantly from early *Homo* to lower Palaeolithic and from middle to upper Palaeolithic for M_2 and M_3 only. The Palaeolithic trends in dental size are shown in Figures 3.2 and 3.3, and the results of the analyses are presented in Tables 3.5 and 3.6.

Table 3.5 Results and statistics of the Kruskal-Wallis (KW) and Jonckheere-Terpstra (JT) tests for differences between dental measurements of the groups early *Homo*, lower, middle and upper Palaeolithic. The p-values achieving statistical significance are shown in bold.

	DF	KW Chi^2	KW p-value	JT (decreasing mean)	JT p-value
Mesio-Distal I_1	3	5.00	0.172	1043.5	0.114
Mesio-Distal I_2	3	21.05	**< 0.001**	1375.5	**< 0.001**
Mesio-Distal P_3	3	72.14	**< 0.001**	1196	**< 0.001**
Mesio-Distal P_4	3	26.53	**< 0.001**	2402	**< 0.001**
Mesio-Distal M_1	3	22.64	**< 0.001**	4065	**< 0.001**
Mesio-Distal M_2	3	43.66	**< 0.001**	3093.5	**< 0.001**
Mesio-Distal M_3	3	37.10	**< 0.001**	1893	**< 0.001**
Bucco-Lingual I_1	3	41.97	**< 0.001**	1303.5	**0.004**
Bucco-Lingual I_2	3	37.47	**< 0.001**	1869	**< 0.001**
Bucco-Lingual P_3	3	48.48	**< 0.001**	1599.5	**< 0.001**
Bucco-Lingual P_4	3	20.40	**< 0.001**	2762.5	**0.014**
Bucco-Lingual M_1	3	11.97	**0.007**	5272	0.100
Bucco-Lingual M_2	3	24.50	**< 0.001**	4207.5	**0.004**
Bucco-Lingual M_3	3	19.79	**< 0.001**	3178.5	0.438
Area I_1	3	22.82	**< 0.001**	1053.5	0.182
Area I_2	3	27.30	**< 0.001**	1414	**< 0.001**
Area P_3	3	65.71	**< 0.001**	1184.5	**< 0.001**
Area P_4	3	24.08	**< 0.001**	2421.5	**0.001**
Area M_1	3	17.58	**< 0.001**	4326	**0.004**
Area M_2	3	29.00	**< 0.001**	3484	**< 0.001**
Area M_3	3	24.43	**< 0.001**	2404.5	**0.006**

Table 3.6 Results of the Kruskal-Wallis pairwise comparisons between dental measurements of the groups early *Homo* (**EH**), lower (**LP**), middle (**MP**) and upper Palaeolithic (**UP**). Significant comparisons are labelled "S". The level of significance was set at 0.05 (95% confidence).

	EH - LP	**EH - MP**	**EH - UP**	**LP - MP**	**LP - UP**	**MP - UP**
Mesio-Distal I_1	-	-	-	-	-	-
Mesio-Distal I_2	-	-	S	-	S	S
Mesio-Distal P_3	-	S	S	-	S	S
Mesio-Distal P_4	S	S	S	-	-	S
Mesio-Distal M_1	S	S	S	-	-	-
Mesio-Distal M_2	S	S	S	-	S	S
Mesio-Distal M_3	S	-	S	-	S	S
Bucco-Lingual I_1	-	-	-	S	-	S
Bucco-Lingual I_2	-	-	-	-	S	S
Bucco-Lingual P_3	-	-	S	-	S	S
Bucco-Lingual P_4	S		S	-	-	S
Bucco-Lingual M_1	S	S	S	-	-	-
Bucco-Lingual M_2	S	S	S	-	-	-
Bucco-Lingual M_3	S	-	S	S	-	-
Area I_1	-	-	-	S	-	S
Area I_2	-	-	S	-	S	S
Area P_3	-	-	S	-	S	S
Area P_4	S	S	S	-	-	S
Area M_1	S	S	S	-	-	-
Area M_2	S	S	S	-	-	S
Area M_3	S	-	S	-	-	S

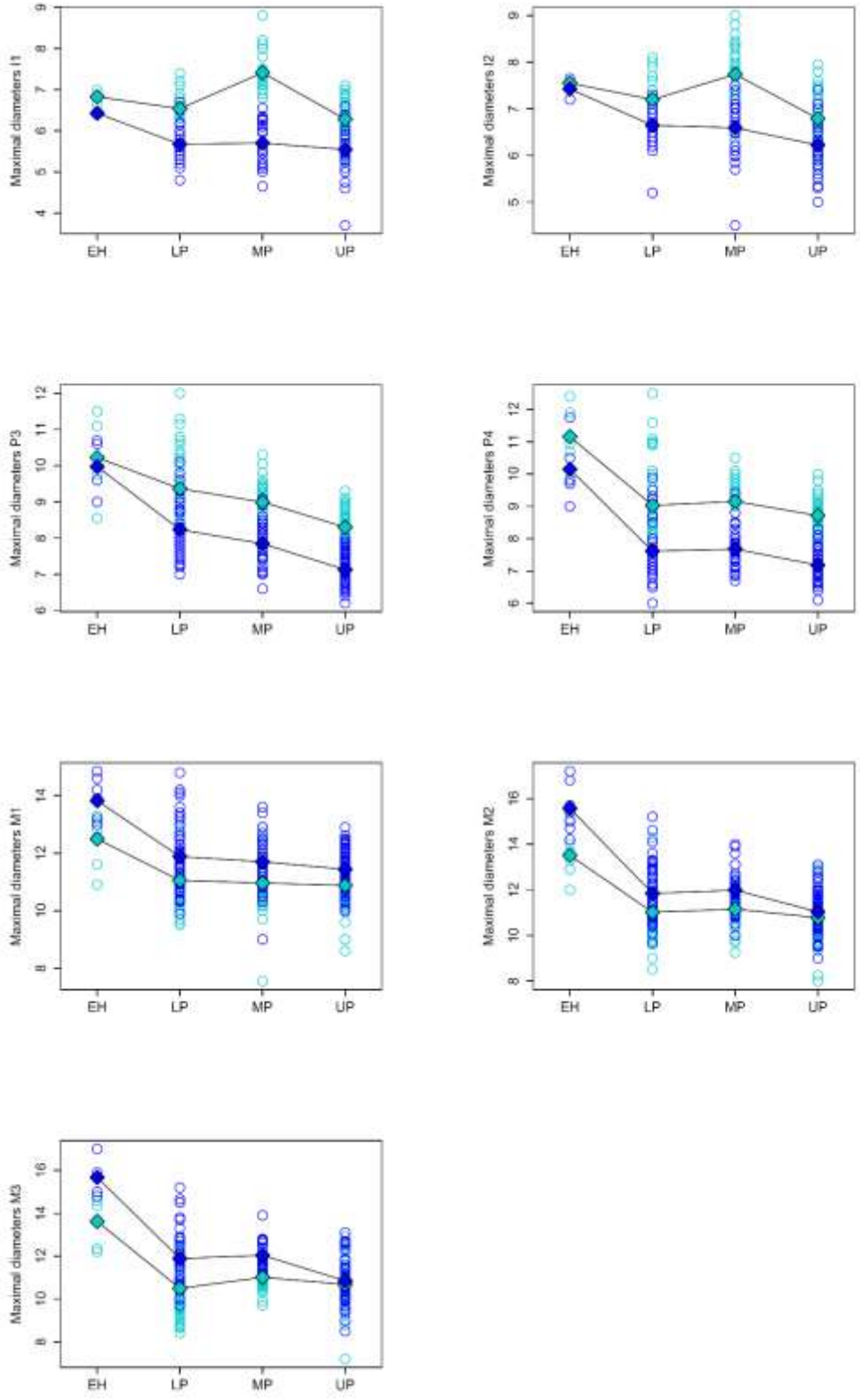

Figure 3.2 Mesio-Distal (blue circles) and Bucco-Lingual (cyan circles) diameters of the mandibular dentition of Early *Homo* (**EH**), lower (**LP**), middle (**MP**) and Upper Palaeolithic (**UP**) humans. The mean diameters for each period are shown as diamonds.

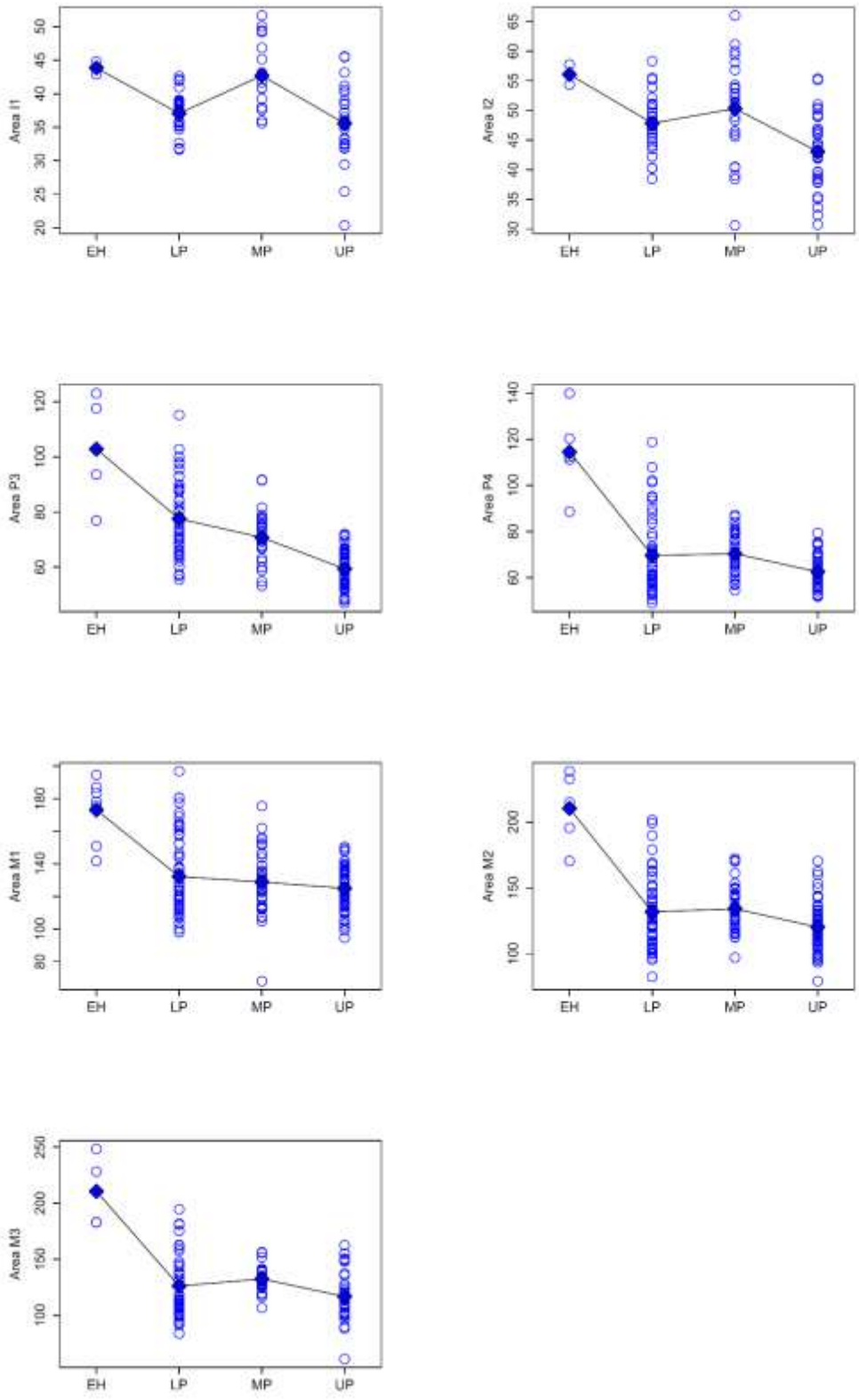

Figure 3.3 Dental area of the mandibular dentition of Early Homo (**EH**), lower (**LP**), middle (**MP**) and Upper Palaeolithic (**UP**) humans. The mean areas for each period are shown as diamonds.

3.3.3 Dental reduction during the Holocene

The Jonckheere-Terpstra test applied on the Holocene trends reported significance in dental size reduction in all teeth and variables analysed (JT $p < 0.001$ in all the cases), although size increase occurred after Neolithic in some cases. In I_1, MD and BL diameter decreased after Mesolithic and upper Palaeolithic respectively, and both increased significantly from Mesolithic to Neolithic. I_2 dental diameters decreased after Mesolithic. In addition, the results highlighted a trend of reduction in the area of both incisors from upper Palaeolithic to Neolithic and a significant increase from Neolithic to Middle Ages in I_1. Similar patterns were observed for the variation in P_3 and P_4. In both teeth, a reduction in MD occurred from Mesolithic to Neolithic and in BL from upper Palaeolithic to Mesolithic. P_3 and P_4 area decreased significantly from upper Palaeolithic and Mesolithic respectively, and stabilised after Neolithic in both cases. The MD diameter of M_1 decreased from upper Palaeolithic to Neolithic and experienced a statistically significant increase after Neolithic, and its BL dimension decreased from Mesolithic to Neolithic. The area of the first molar reduced from Mesolithic to Neolithic and increased again after Neolithic. In the second molar, there was a continuous reduction of MD diameter from upper Palaeolithic to Neolithic, and a reduction of BL and molar area from Mesolithic to Neolithic. In M_3, there were significant differences in all the dental variables considered, which highlighted an overall decrease from Mesolithic to Neolithic. Figure 3.4 and 3.5 report the trends of MD, BL and dental area in *Homo sapiens* from upper Palaeolithic to middle ages. The results are shown in Tables 3.7 and 3.8.

Table 3.7 Results and statistics of the Kruskal-Wallis (KW) and Jonckheere-Terpstra (JT) tests for differences between dental measurements of the groups Upper Palaeolithic (**UP**), Mesolithic (**Me**), Neolithic (**Ne**) and Middle Ages (**MA**). The p-values achieving statistical significance are shown in bold.

	DF	KW Chi^2	KW p-value	JT (decreasing mean)	JT p-value
Mesio-Distal I_1	3	112.51	**< 0.001**	8222.5	**< 0.001**
Mesio-Distal I_2	3	111.18	**< 0.001**	17915	**< 0.001**
Mesio-Distal P_3	3	209.50	**< 0.001**	37160	**< 0.001**
Mesio-Distal P_4	3	159.48	**< 0.001**	37526.5	**< 0.001**
Mesio-Distal M_1	3	122.94	**< 0.001**	52714	**< 0.001**
Mesio-Distal M_2	3	118.00	**< 0.001**	49731.5	**< 0.001**
Mesio-Distal M_3	3	48.73	**< 0.001**	34985	**< 0.001**
Bucco-Lingual I_1	3	50.67	**< 0.001**	20087.5	**< 0.001**
Bucco-Lingual I_2	3	60.02	**< 0.001**	31531.5	**< 0.001**
Bucco-Lingual P_3	3	79.86	**< 0.001**	52203.5	**< 0.001**
Bucco-Lingual P_4	3	52.40	**< 0.001**	58406.5	**< 0.001**
Bucco-Lingual M_1	3	245.35	**< 0.001**	37303.5	**< 0.001**
Bucco-Lingual M_2	3	201.58	**< 0.001**	42923	**< 0.001**
Bucco-Lingual M_3	3	161.98	**< 0.001**	24785.5	**< 0.001**
Area I_1	3	57.0755	**< 0.001**	7084	**< 0.001**
Area I_2	3	86.7732	**< 0.001**	13930.5	**< 0.001**
Area P_3	3	160.8016	**< 0.001**	35691	**< 0.001**
Area P_4	3	102.643	**< 0.001**	38946	**< 0.001**
Area M_1	3	190.86	**< 0.001**	35382.5	**< 0.001**
Area M_2	3	177.3682	**< 0.001**	41579	**< 0.001**
Area M_3	3	111.5112	**< 0.001**	27134	**< 0.001**

Table 3.8 Results of the Kruskal-Wallis pairwise comparisons between dental measurements of the groups Upper Palaeolithic (**UP**), Mesolithic (**Me**), Neolithic (**Ne**) and Middle Ages (**MA**). Significant comparisons are labelled "S". The level of significance was set at 0.05 (95% confidence).

	UP - Me	**UP - Ne**	**UP - MA**	**Me - Ne**	**Me - MA**	**Ne - MA**
Mesio-Distal I_1	-	S	-	S	S	S
Mesio-Distal I_2	-	S	S	S	S	-
Mesio-Distal P_3	-	S	S	S	S	-
Mesio-Distal P_4	-	S	S	S	S	-
Mesio-Distal M_1	S	S	S	S	S	S
Mesio-Distal M_2	S	S	S	S	S	-
Mesio-Distal M_3	-	S	S	S	S	-
Bucco-Lingual I_1	-	S	S	S	-	-
Bucco-Lingual I_2	S	S	S	S	S	-
Bucco-Lingual P_3	S	S	S	-	-	-
Bucco-Lingual P_4	S	S	S	-	-	-
Bucco-Lingual M_1	-	S	S	S	S	-
Bucco-Lingual M_2	-	S	S	S	S	-
Bucco-Lingual M_3	-	S	S	S	S	-
Area I_1	-	S	S	S	-	S
Area I_2	S	S	S	S	S	-
Area P_3	S	S	S	S	S	-
Area P_4	-	S	S	S	S	-
Area M_1	-	S	S	S	S	S
Area M_2	-	S	S	S	S	-
Area M_3	-	S	S	S	S	-

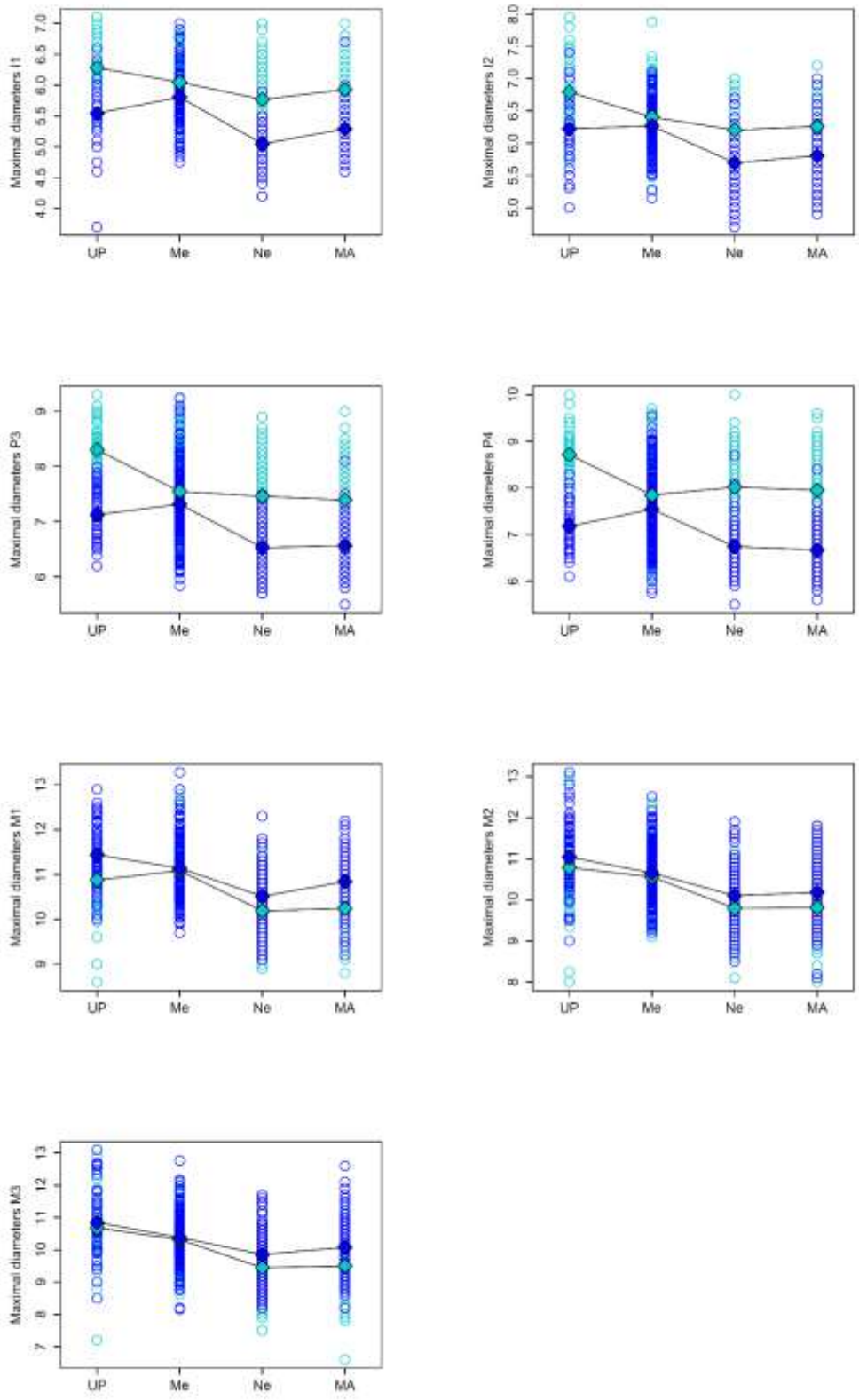

Figure 3.4 Mesio-Distal (blue circles) and Bucco-Lingual (cyan circles) diameters of the mandibular dentition of Upper Palaeolithic (**UP**), Mesolithic (**Me**), Neolithic (**Ne**) and Middle Ages (**MA**) humans. The mean diameters for each period are shown as diamonds.

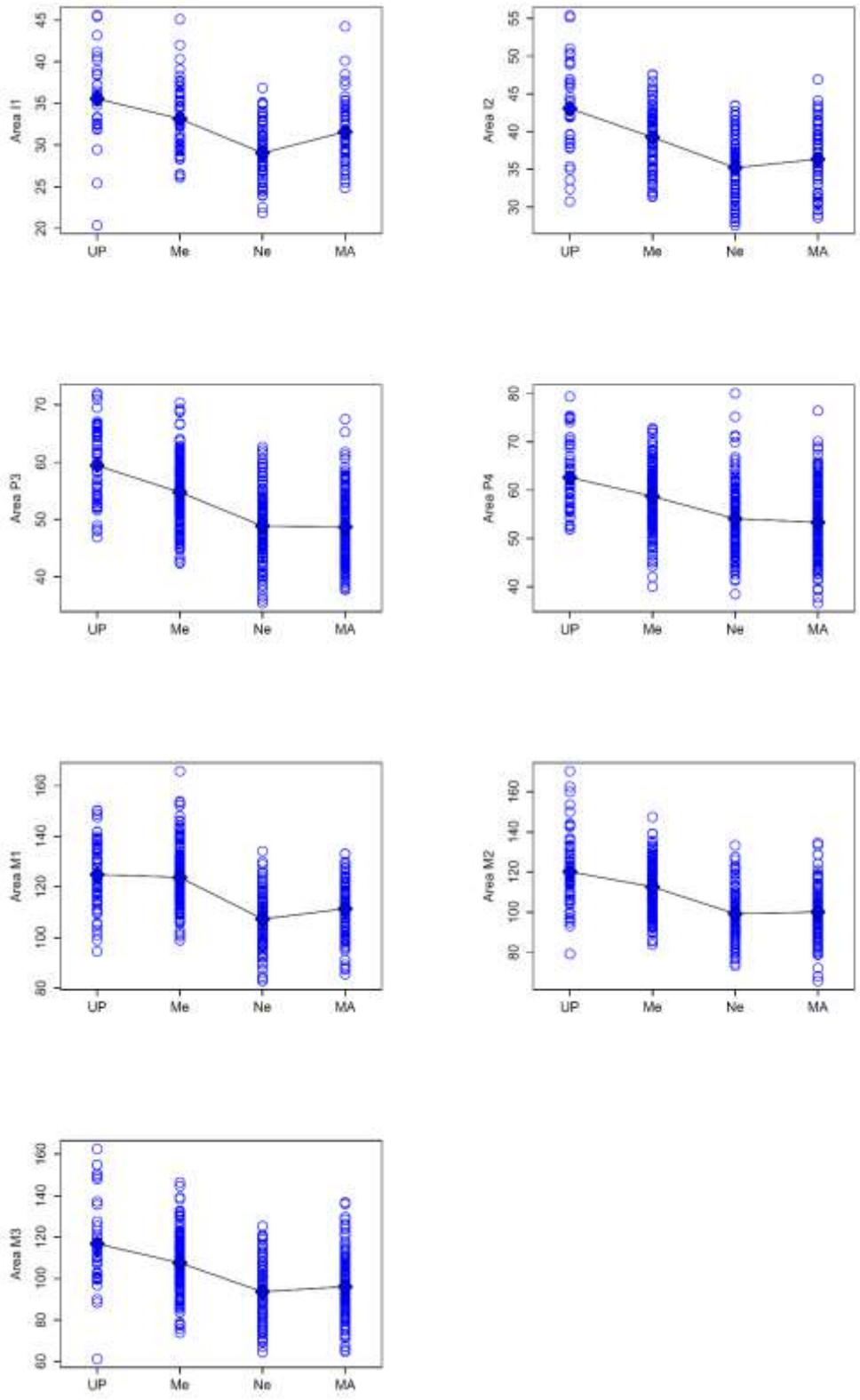

Figure 3.5 Dental area of the mandibular dentition of Upper Palaeolithic (**UP**), Mesolithic (**Me**), Neolithic (**Ne**) and Middle Ages (**MA**) humans. The mean areas for each period are shown as diamonds.

3.4 Discussion

The study of mandibular and dental reduction traditionally focused on two main aspects of lower jaw morphology, which varied the most during human evolution: robusticity and tooth size (Brace, 1979; Chamberlain & Wood, 1985). Several scholars joined the study of these features in hominins and modern humans, and few authors (Coon, 1955; 1962; Brace, 1967; Brace & Mahler, 1971; Brace et al., 1987) are still influential about the subject of dental and mandibular reduction. Nevertheless, our interpretations of human evolution have changed in the last few decades, thanks to larger fossil and archaeological records. The analysis performed here, which is based on large datasets made available in online databases, confirmed the patterns previously described for both robusticity and dental size.

Chamberlain & Wood (1985) noticed marked variations in robusticity within the genus *Homo*, with early *Homo* exhibiting larger indices than later species. Their findings are based on robusticity at the level of the first molar, whose importance has been well recognised in the study of human bite biomechanics (Ferrario et al., 2004). The results described above confirmed this pattern and extended it to M_2, M_3 and symphyseal robusticity. The differences between early (*H. habilis, H. rudolfensis, H. ergaster, H. erectus* and *H. floresiensis*) and later species of *Homo* (*H. heidelbergensis, H. neanderthalensis* and *H. sapiens*) were larger than those between early *Homo* and australopithecines (Figure 3.1, Table 3.4), suggesting that the most profound changes occurred within the genus *Homo*. If we consider the inclusion of the genus *Paranthropus* in the group of australopithecines, this result is noteworthy. Indeed, a link has been suggested between the robust masticatory apparatus of *Paranthropus* and a diet based on tough foods (Wood & Constantino, 2007). Nevertheless, by considering the dietary breadth and habitat preference in living species and in fossil hominins, Wood & Strait (2004) proposed a common generalist strategy for *Paranthropus* and early *Homo*, which is in contrast with the findings based on the study of morphological traits. Accordingly, Ungar et al. (2006) suggested that early *Homo* might have adopted a flexible subsistence strategy, rather than having undergone a full transition from closed-forest to open-habitat foods. Chamberlain & Wood (1985) underlined that the differences in robusticity between australopithecines are not necessarily dependent on diet, but rather a by-product of scaling with body size. In the genus *Homo*, robusticity does not scale with size (Chamberlain & Wood, 1985). Therefore, the australopith mandibular robusticity might have been retained in early

Homo as a result of the close shared ancestry between the two groups. Nevertheless, it is still possible that the differences in robusticity within the genus *Homo* were generated by biomechanical requirements. As highlighted by studies on primate jaw biomechanics (Hylander, 1979; Smith, 1983), the cross-sectional shape of the mandibular corpus acts to resist vertical, horizontal and torsional forces during mastication. This role of the corpus and symphyseal shape has been confirmed in African apes (Taylor, 2006a) and in humans (Daegling & Hylander, 1998).

Previous studies indicated a middle Palaeolithic increase in incisor dimensions, which, in turn, dropped again during the upper Palaeolithic (Brace, 1967). The present results statistically confirm an increase in the I_1 area during middle Palaeolithic, mostly as a result of bucco-lingual variations (Figure 3.2 and 3.3). If hominin body size estimates are correct, the differences between lower, middle and upper Palaeolithic (mainly represented by *H. heidelbergensis*, *H. neanderthalensis* and *H. sapiens*, respectively, in this analysis) are less marked than observed. In fact, Neanderthals exhibit a larger body size than *H. heidelbergensis* and *H. sapiens*. Therefore, the middle Palaeolithic increase in incisor size may be due to allometry. This view has been highlighted by Brace et al. (1987), who suggest that tooth size differences between Neanderthals and modern humans may represent an allometric effect of changes in body size.

A significant reduction in postcanine dimensions is observed throughout the Pleistocene, with steeper decreases from early *Homo* to lower Palaeolithic and from middle to upper Palaeolithic (Figure 3.2 and 3.3). Dental size differences within *Homo* appear remarkable when we consider the changes in body size from habilines to later species. For early *Homo*, body size estimates report smaller values than in *H. heidelbergensis* and *H. neanderthalensis* (Jiménez-Arenas et al., 2014; Grabowski et al., 2015). This would indicate that dental reduction following early *Homo* might be even steeper when accounting for body size. From the traditional perspective on dental and mandibular reduction, such strong modification derived from changes in dietary habits or food processing, but decades of studies have emphasised the importance of non-adaptive factors in phenotypic evolution (Weber, 2011). Phylogenetic constraints and behaviour do influence the dietary habits of primate species (Silver & Marsh, 2003; Kamilar & Cooper, 2013). *Homo* most likely had access to a large variety of foods, which can be modified in their texture and properties thanks to improved food

processing skills (Zink et al., 2014). Foods made softer by slicing or cooking, hence behavioural factors, do not necessitate the same biomechanical resistance required by tough food items (Zink & Lieberman, 2016). These lowered requirements may be a cause of dental and mandibular diversification within the genus *Homo*, but it is not clear if hominin behaviour drove the evolution of masticatory apparatus, and such a link may be difficult to establish. While few hominin species may have been able to control fire, it is not sure if they could start one at will (Roebroeks & Villa, 2011; Sandgathe et al., 2011; Shimelmitz et al., 2014). Nevertheless, experimental evidence (Zink & Lieberman, 2016) suggests that slicing and pounding modify the biomechanical properties of meat enough to allow a reduced chewing cycle and bite force.

According to Brace (1967), dental size reduction accelerated at the end of Pleistocene, showing an unprecedented rate during the Holocene. The results presented above highlight a drop in dental size following the upper Palaeolithic, consistently with Brace's work. In addition to that trend, an increase in incisor size during Neolithic was found. It is possible that differences in the sample affect the results, with the medieval sample generating from only a few populations from one European region. Nevertheless, the results showed a common trend in both incisors and postcanine dentition during the Holocene, with major changes in post-Mesolithic horizons. Dental size variations during the Holocene have been commonly attributed to changes in subsistence patterns related to the onset of agriculture (Larsen, 1995; Pinhasi & Meiklejohn, 2011). The post-Mesolithic trend in dental reduction could be the result of changes in subsistence, considered the most fundamental innovations that agriculture imposed on the human lifestyles (Larsen, 1981; 1995). Nevertheless, Pinhasi et al. (2008) noticed that the reduction in both upper and lower dentition preceded crop domestication in a temporal sequence of southern Levant populations. Indeed, the results presented above suggest that the decrease in dental size occurred earlier, in correspondence with the upper Palaeolithic-Holocene boundary (Figure 3.5 and Table 3.8). These results suggest that dental reduction may have preceded the onset of agriculture, even if the trend may have accelerated during and after the transition. Food processing also may have played a role in the Holocene trend. As pointed out by Brace et al. (1987), the invention of pottery during the Neolithic may have been a crucial step, for the possibility of reducing food to liquid or semi-solid consistency. In support of this idea, Brace et al. (1987) claimed the fact that no edentulous

individuals are present in the archaeological record before the appearance of pottery. The hominin fossil record, however, now falsifies this point of view: the hominin remains of *H. georgicus*, dated around 1.8 Ma, include the earliest case of completely edentulous individuals in the hominin lineage (Martinón-Torres et al., 2008). This fact raises several questions about the importance of social structure and behaviour over adaptation.

Although the drop in dental size from upper Palaeolithic to the Neolithic runs parallel with changes in subsistence, the possibility that this trend of reduction is the effect of changes in body size should not be overlooked. Indeed, a general trend of reduction in human body size from 50 kyr to the Neolithic has been documented (Ruff, 2002). The Holocene reduction in tooth size may be at least in part the allometric by-product of body size reduction. This view would support the results of Pinhasi et al. (2008), who noticed that dental reduction preceded crop domestication in southern Levant populations. Whether dental reduction was caused by the food processing innovations linked to agriculture or by changes in body size, it may have had a positive impact on dental health (Calcagno & Gibson, 1988). Calcagno (1986; 1989) suggested that the dental crown evolution in humans could be constrained by the advantage of reducing enamel surface for avoiding caries and the necessity of large crown areas to process abrasive foods efficiently, a point of view also known as the "Selective Compromise Effect" hypothesis. Pinhasi et al. (2008) analysed time-series dental data from the Levant and found results that supported this hypothesis.

In the light of the results presented above and the larger palaeoanthropological and archaeological evidence, we can no longer be sure about certain assumptions in the subject of dental and mandibular reduction. Technological achievements during human evolution provided a good explanation for the morphological changes in teeth and mandible during the early stages of the genus *Homo* and later during the Holocene. Nevertheless, body size is likely to have driven major allometric changes in the hominin and human dentition. The major obstacle to the interpretation of the trend of reduction is the contemporaneity of the events occurred during the Pleistocene and Holocene, which may confound the relationships of causality. Understanding the timing of these events accurately will clarify the actual relationships between the improvements in food processing and morphological variations in the hominin and human masticatory apparatus.

Chapter 4

Mandibular and dental reduction: insigths from the masticatory scaling in hominins and other catarrhines

4.1 Introduction

A reduction in the masticatory apparatus is regarded as a major trend in human evolution. The genus *Homo* exhibits a reduced size of the mandible relative to other African apes and australopithecines (Lieberman, 1992; Wood & Aiello, 1998; Emes et al., 2011) and we observe a reduction in mandibular robusticity, or the corpus width/corpus height ratio, from early *Homo* to later species (Chamberlain & Wood, 1985). In addition, *Homo* has smaller molars and premolars than australopithecines (Sofaer et al., 1971; Pilbeam & Gould, 1974; Macho & Moggi-Cecchi, 1992; Wood, 1992; McHenry & Coffing, 2000) and other great apes (Andrews et al., 1991), and the postcanine dentition has reduced within the genus (McHenry, 1982); a drop in postcanine size has been observed within the genus *Homo* during the Pleistocene (Brace et al., 1987; De Castro & Nicolas, 1995; Franciscus & Trinkaus, 1995) and Holocene (Pinhasi et al., 2008), while incisors increased during the middle Pleistocene and reduced again after the late Pleistocene (Brace, 1967). Concerning *Homo sapiens*, it has been argued that a specific trend in postcanine reduction occurred during the last 100 ka (Fitzgerald & Hillson, 2005), with an acceleration over the last 10 ka of evolution (Brace et al., 1987; Quam et al., 2009; Pinhasi & Meiklejohn, 2011).

The trend of reduction has been traditionally considered the result of a dietary shift or improvements in food processing techniques, such as progress in lithic tool manufacturing and/or the adoption of fire for cooking (Wrangham & Conklin-Brittain, 2003; Wrangham, 2009; Zink & Lieberman, 2016). These events would have led to the consumption of softer

foods and, as suggested, a relaxation of selective pressures on the masticatory apparatus (Calcagno & Gibson, 1988; Wrangham & Carmody, 2010). From this perspective, morphological changes that occurred in the hominin masticatory apparatus are of greatest importance to define how culture may have affected biological evolution, if it did.

Size is particularly relevant in the study of mandibular and dental reduction in hominins. Variations in size are commonly accompanied by morphological changes affecting the general proportions of skeletal parts, a phenomenon known as allometry (Mosimann, 1970). When allometry operates on a certain skeletal region, the morphology of that region changes as a by-product of size variations. The robusticity of the australopithecine mandible, for example, is reported to increase with mandibular corpus size (Chamberlain & Wood, 1985). In addition, the size of teeth and mandibles is influenced by changes in body size, which in turn can be driven by ecological factors, such as diet (Gingerich et al., 1982; Jiménez-Arenas et al., 2014; Meloro et al. 2015).

Although morphological variations due to the trend of reduction are well-studied, a relative quantification of its effects in hominins is missing. The reduction took place at different stages during hominin evolution (Brace, 1979; McHenry & Coffing, 2000; Emes et al., 2011; Pinhasi & Meiklejohn, 2011). The relative proportions of the reduction elicited by each of these events are of utmost importance in understanding the factors behind them. In addition, the possibility that the trend of reduction may have produced "extreme" or "unique" phenotypes has never been addressed in the study of dental and mandibular reduction. A species exhibiting an extreme variant of a trait (*i.e.*, lying well out of its own group variability), for example, may indicate that the trait has undergone selection (Price et al., 2003; Rueffler et al., 2006). Quantifying the levels of reduction in dental and mandibular size could lead to a better understanding of hominin lower jaw variability and its evolution.

To define the mandibular and dental size of the hominin species as "extreme", a comparative approach is needed, focusing on the relationship between hominins and their closest living clade, the other catarrhine primates. A primate comparative approach has been extensively and successfully applied in the study of human evolution, for example in studies about encephalization (Leonard et al., 2003), cranial thickness (Copes & Kimbel, 2016), hominin diet (Ungar et al., 2006) and dental morphology (Jiménez-Arenas et al., 2014).

In this work, a comparative approach is used to quantify the differences in mandibular and dental size variability between hominins and other catarrhines. The scaling patterns of dental and mandibular size are analysed with respect to body size, and phylogenetic comparative methods are adopted. The hypothesis that the trend of mandibular and dental reduction in *Homo* has been driven by variations of the allometric scaling of the lower jaw or by changes in the overall mandibular and dental size is tested. The main aim was to determine if the reduction produced hominin species bearing mandibles and teeth whose size lies outside the non-hominin catarrhine variability. The results of this study are of great importance to understand the variability of dental and mandibular size in hominins, especially for modern humans, whose lower jaw appears particularly gracile as an effect of the trend of reduction.

4.2 Material and methods

4.2.1 The sample and data collection

The sample is composed of mandibles and associated tooth rows of 63 species of primates belonging to the Catarrhini. The non-human primate sample includes Cercopithecoidea and Hominoidea, comprising Colobinae (9 species), Cercopithecinae (39 species), Hylobatidae (9 species) and non-hominin Hominidae (6 species). Only adult individuals from both sexes were selected. A fully erupted third molar was used to determine the adult age-class. The hominin sample includes 84 adult individuals from the genera *Australopithecus* (2 species), *Paranthropus* (2 species) and *Homo* (7 species), for a total of 11 species. Sex information was obtained from Wolpoff (1971; 1979), Wood (2011) and Schwartz & Tattersall (2005), but it is not known for all of the fossil hominins included. *Homo sapiens* is represented by 20 mandibles from mixed non-European populations, belonging to both sexes. Full information about the primate and hominin sample are reported in Appendix 1. A summary of the sample is shown in Table 4.1 and 4.2.

The material in this study consists of linear measurements and virtual specimens available in CT-scan and micro CT scan format, or acquired through photogrammetry. The data are available from online databases and from museums (see Chapter 2 and Appendix 1 for further

details). Peter Brown kindly provided the CT-scan of *Homo floresiensis* LB1 (www.peterbrown-palaeoanthropology.net). The hominin linear measurements were collected from the Human Origins Database onine (www.humanoriginsdatabase.org) and correspond to the measurements in Wood (1991). For further details, refer to Chapter 2.

Table 4.1 The catarrhine sample size divided into four taxonomic groups. Numbers of species, individual, female and male specimens included in the sample are reported. A complete list is available in Appendix 1.

	Individuals	**Females**	**Males**	**Species**
Colobinae	25	14	11	9
Cercopithecinae	115	55	60	39
Hylobatidae	36	21	15	9
non-hominin Hominidae	106	46	60	6

Table 4.2 The hominin sample size divided into species. Numbers of individual, female, male specimens and specimens of unknown sex are reported.

	Individuals	**Females**	**Males**	**Unknown sex**
Australopithecus afarensis	1	1	-	-
Australopithecus africanus	4	3	1	-
Paranthropus boisei	22	-	-	22
Paranthropus robustus	2	2	-	-
Homo ergaster	7	-	-	7
Homo habilis	4	-	-	4
Homo rudolfensis	6	-	-	6
Homo floresiensis	1	1	-	-
Homo heidelbergensis	3	1	1	1
Homo neanderthalensis	14	4	4	6
Homo sapiens	20	10	10	-

A series of 28 three-dimensional landmarks was recorded on the surface models of hemi-mandibles using the Amira software package (version 5.4.5, FEI Visualization, Berlin). The configuration of landmarks and a graphical representation of the measurements are shown in Figure 2.2, and their definitions are presented in Appendix 1. The landmark configurations of the specimens in the sample were aligned using Procrustes superimposition, and centroid size (CS) was calculated as a proxy for mandibular size. The alignment and calculation of CS were performed in the R package "Morpho" (Schlager, 2013). Due to the fragmentary nature of the fossil specimens, missing 3D landmarks were estimated. Estimation was performed by a Thin Plate Spline (TPS) procedure implemented in the R package "Morpho" (Schlager, 2013). For further details about the procedure, refer to Chapter 2. Full information on the amount of landmarks estimated are reported in Appendix 1. Alveolar length was used as a proxy for dental size. It was measured by recording the minimum chord distance between midpoints of the interalveolar septa for each tooth type, and it will be indicated as I_1-I_2, P_3-P_4 and M_1-M_3. Canines were not included because their variability is highly linked to sexual dimorphism among primates (Plavcan, 2001; 2004) and no complete sex information was available for most of the hominin sample. Further considerations about the reliability and the use of these data is available in Chapter 2.

Body weight information was incorporated in the analyses. For non-human primates, values of body weight were averaged by species and sex (Smith & Jungers, 1997; National Research Council US, 2003). For hominin body size, the most updated estimates were used (McHenry & Berger, 1998; Jiménez-Arenas et al., 2014; Grabowski et al., 2015). Body weight values for catarrhines (including hominins) are reported in Appendix 1. As a preliminary step, CS, alveolar length and body weight were averaged by species and sex, and were log-transformed, to obtain separate datasets for males and females. Because of incomplete sex estimation for the fossil hominin sample, specimens of undetermined sex were included in both the male and female subsamples to increase sample size. All the analyses were run separately on each subsample.

To account for phylogenetic relatedness in the sample, a primate molecular phylogeny available from the online database 10ktrees was used (Arnold et al., 2010). For the hominin sample, a phylogeny was built following the topology published by Dembo et al. (2015). Branch lengths were scaled to fit the time of divergence between *P. troglodytes* and *H.*

sapiens in the primate phylogenetic tree. The extant catarrhine and fossil hominin trees were then merged. The fossil hominin tree is shown in Figure 2.8, Chapter 2, and the extant catarrhine phylogeny is displayed in Appendix 1.

4.2.2 PGLS and ANCOVA

Species exhibit phenotypic similarities as an effect of their shared ancestry and phylogenetic information can be used to account and correct for this effect (Diaz-Uriarte & Garland, 1996; Freckleton et al., 2002; Blomberg et al., 2003). Phenotypic traits can evolve by following different patterns and more than one evolutionary model can be tested when applying a phylogenetic correction. To determine the model of evolution to be used for the phylogenetic correction of our data, the fits of four models were compared: Brownian Motion (BM), Pagel's Lambda (λ), Ornstein-Uhlenbeck (OU) and Early Burst (EB). Under a BM model of evolution, traits evolve following a random walk after each event of speciation, and phenotypic difference between taxa is proportional to the time of divergence from their common ancestor (Felsenstein, 1973). The λ model is a transformation of the BM where the tree internal branch lengths are multiplied by the factor λ, specifying the degree of phylogenetic signal in the data (Pagel, 1999). If λ equals 0, data are independent on phylogeny, whereas if it is 1 it then corresponds to a BM model. The OU model describes the evolution of traits under stabilizing selection (Butler & King, 2004). It corresponds to a random walk attracted by an optimum, with the attraction proportional to a parameter α (Butler & King, 2004). When α is 0, the OU matches a BM model. In EB, trait evolution accelerates or decelerates depending on a rate parameter *r* (Harmon et al., 2010). When *r* is 0, the EB reduces to a BM model. Phylogenetic Generalized Least Squares (PGLS) regressions were fitted assuming each of the four evolutionary models, by using mandibular CS and alveolar lengths (dependent variables) and weight (independent variable). For the λ, OU and EB models, the parameters λ, α and *r* were estimated. The log-likelihood of each PGLS regression was calculated and a log-Likelihood ratio test was applied for assessing statistical differences between each model and the null model (BM). The models that resulted statistically more accurate than BM were compared against each other to define the best fitting model. The resulting evolutionary models and relative parameters that best fit the data were used for phylogenetic corrections in the later steps of analysis. To account for the presence of fossil species in the phylogenetic

tree, the PGLS regression was weighted on the diagonal of the phylogenetic variance-covariance matrix, using the R package “ape” (Paradis et al., 2004). The PGLS was performed using the R package “phylolm” (Ho & Ané, 2014). The analyses were performed separately on females and males.

The null hypothesis tested is that *Homo* does not differ from other extant catarrhines in mandibular and dental size and scaling, when body size is considered. Analysis of Covariance (ANCOVA) was performed on mandibular CS and alveolar lengths (dependent variables) and body weight (independent variable) to analyse the differences in slope and intercept among groups, by following the phylogenetic ANCOVA method proposed by Smaers & Rohlf (2016) and embedded in the R package “evomap” (Smaers, 2014). The phylogenetic tree used in the ANCOVA was scaled accordingly to the results obtained in the previous step of the analysis, by using the R package “geiger” (Harmon et al., 2008). To determine the differences in slope, two phylogenetic ANCOVA were performed, one including all hominins and another including only *Homo*. For testing differences in intercepts, four tests were used by holding the slope constant: (1) differences among australopithecines, *Homo* and other extant catarrhines, (2) *Homo* versus australopithecines, while controlling for differences with other extant catarrhines, (3) *Homo* versus other extant catarrhines, while controlling for differences with australopithecines and (4) australopithecines versus other extant catarrhines, while controlling for differences with *Homo*.

To determine if mandibular and dental reduction produced unique phenotypes in the genus *Homo*, hominin species deviations from the size scaling pattern of the catarrhine mandible and teeth was tested. Again, the phylogenetic ANCOVA method developed by Smaers & Rohlf (2016) was applied, this time on each hominin species in the sample, every time controlling for differences with the other hominin species. The analyses of phylogenetic ANCOVA were performed on male and female subsamples separately.

4.3 Results

4.3.1 Models of evolution and PGLS

The PGLS analysis indicated that mandibular and dental scaling with body size does not evolve in line with the EB model. The rate parameter *r* was 0 in both females and males, for mandibular CS and the alveolar length of all tooth types. Therefore, the EB models calculated here fully corresponded to BM models and were excluded from the analyses. The Pagel's λ model fitted the data variably, with the λ parameter ranging from 0 (premolars) to 0.684 (incisors) in females and 0.647 (molars) to 0.762 (incisors) in males. The OU model fitted the data with values of α ranging from 0.14 (molars) to 0.745 (premolars) in females and 0.085 (mandible) to 0.154 (incisors) in males. Table 4.3 reports information relative to the evolutionary model fits and their log-likelihood values. For both λ and OU, the log-likelihood was always greater than the values of the BM models, in both females and males. The log-likelihood ratio test favoured the λ and OU models over BM, indicating a better fit of the former than the null model of trait evolution (Table 4.4). Comparing log-likelihood for λ and OU suggested that the OU model should be preferred for premolars and molars in the female subsample, and for molars only in the male subsample. Nevertheless, Cooper et al. (2015) showed that, in simulated phylogenies, the OU models are often favoured over BM in log-likelihood ratio tests, even when the phylogeny itself is generated by assuming a BM model of evolution. This is particularly common when sample size (number of tips in the tree) includes fewer than 100 species (Cooper et al., 2015). Unless otherwise specified, in the following analyses the results obtained considering the λ model are reported. The results of the OU model are also discussed in those cases where log-likelihood was higher than in the λ model. Nevertheless, results relative to the OU model should be interpreted with caution because the sample includes fewer than 100 species. The results of the PGLS regressions are reported in Table 4.5, and Figure 4.1 shows the scatterplot of tooth type size and mandible size versus body size. The results of the PGLS regressions adopting the OU model are provided in Appendix 2. All regressions were statistically significant for both λ and OU models, and showed a negative allometric pattern. Isometry is expected at a slope of 0.33, since body weight varies volumetrically (three dimensions, Wakat et al. 1971) while CS and alveolar length act as linear measurements (one dimension).

Table 4.3 Phylogenetic Generalized Least Squares fits between mandibular Centroid Size (CS), incisal (I_1-I_2), premolar (P_3-P_4) and molar (M_1-M_3) versus body weight, under different evolutionary models. λ, α and *r* specify the amount of phylogenetic signal, the attraction parameter and the rate of evolutionary acceleration-deceleration in Pagel's Lambda, Ornstein-Uhlenbeck and Early Burst models respectively.

	Brownian Motion	Pagel's Lambda		Ornstein-Uhlenbeck		Early Burst	
Females	**logLik**	**logLik**	**λ**	**logLik**	**α**	**logLik**	***r***
CS	45.49	62.23	0.649	56.19	0.179	45.49	0
I_1-I_2	14.94	30.88	0.684	26.7	0.467	14.94	0
P_3-P_4	10.64	34.41	0	34.83	0.745	10.64	0
M_1-M_3	31.46	34.37	0.51	39.93	0.14	31.46	0

	Brownian Motion	Pagel's Lambda		Ornstein-Uhlenbeck		Early Burst	
Males	**logLik**	**logLik**	**λ**	**logLik**	**α**	**logLik**	***r***
CS	42.05	50.77	0.685	46.36	0.085	42.05	0
I_1-I_2	7.58	23.43	0.762	15.54	0.154	7.58	0
P_3-P_4	4.1	9.1	0.749	8.87	0.088	4.1	0
M_1-M_3	30.15	33.59	0.647	34.81	0.099	30.15	0

Table 4.4 Likelihood ratio tests for goodness of fit under Pagel's Lambda and Ornstein-Uhlenbeck models. The two models were tested against the Brownian Motion null model of trait evolution. All comparisons resulted significant, indicating that both Pagel's Lambda and Ornstein-Uhlenbeck models fit the data better than the simple Brownian Motion model.

	Brownian Motion vs Pagel's Lambda			Brownian Motion vs Ornstein-Uhlenbeck		
Females	**DF**	**LikRatio**	**p-value**	**DF**	**LikRatio**	**p-value**
CS	3 4	33.49	< 0.001	3 4	21.41	< 0.001
I_1-I_2	3 4	31.89	< 0.001	3 4	23.52	< 0.001
P_3-P_4	3 4	47.54	< 0.001	3 4	48.39	< 0.001
M_1-M_3	3 4	5.82	0.016	3 4	16.94	< 0.001

	Brownian Motion vs Pagel's Lambda			Brownian Motion vs Ornstein-Uhlenbeck		
Males	**DF**	**LikRatio**	**p-value**	**DF**	**LikRatio**	**p-value**
CS	3 4	17.45	< 0.001	3 4	8.63	0.003
I_1-I_2	3 4	31.34	< 0.001	3 4	15.57	< 0.001
P_3-P_4	3 4	9.99	0.002	3 4	9.52	0.002
M_1-M_3	3 4	6.89	0.009	3 4	9.33	0.002

Table 4.5 Results of the Phylogenetic Generalized Least Squares regressions between mandibular Centroid Size (CS), incisal (I_1-I_2), premolar (P_3-P_4) and molar (M_1-M_3) versus body weight, under Pagel's Lambda model of evolution. The results obtained assuming an Ornstein-Uhlenbeck model of trait evolution are presented in Appendix 2.

Females	**intercept**	**slope**	**R^2**	**λ**	**p-value**
CS	2.405	0.289	0.83	0.649	< 0.001
I_1-I_2	0.042	0.216	0.65	0.684	< 0.001
P_3-P_4	0.595	0.215	0.65	0	< 0.001
M_1-M_3	0.465	0.301	0.72	0.51	< 0.001

Males	**intercept**	**slope**	**R^2**	**λ**	**p-value**
CS	2.26	0.306	0.74	0.685	< 0.001
I_1-I_2	-0.155	0.243	0.55	0.762	< 0.001
P_3-P_4	0.788	0.208	0.18	0.749	< 0.001
M_1-M_3	0.52	0.299	0.67	0.647	< 0.001

4.3.2 Phylogenetic ANCOVA

The phylogenetic ANCOVA using the λ model yielded the results in Tables 4.6 and 4.7. Results of the phylogenetic ANCOVA using the OU model are shown in Appendix 2. The genus *Homo* did not depart significantly from the slope of other extant catarrhines in mandible size, a result repeated in both sexes (p-values 0.863 and 0.17 for females and males respectively). The opposite result was observed for premolars (p-values 0.021 and 0.01 for females and males respectively) and molars (p-values 0.011 and < 0.001 for females and males respectively), indicating a different scaling of postcanine dentition in respect to body size in *Homo* and other extant catarrhines. The scaling of incisor size in *Homo* differed from the other extant catarrhine pattern in males (p-value 0.112), but not in females (p-value 0.019). Australopithecines seem to influence the results related to the mandible, while it did not considerably affect the rest of the lower jaw (Table 4.6). The phylogenetic correction based on the OU model produced the same result for *Homo*, in those cases for which it was relevant (female premolars and molars, male molars).

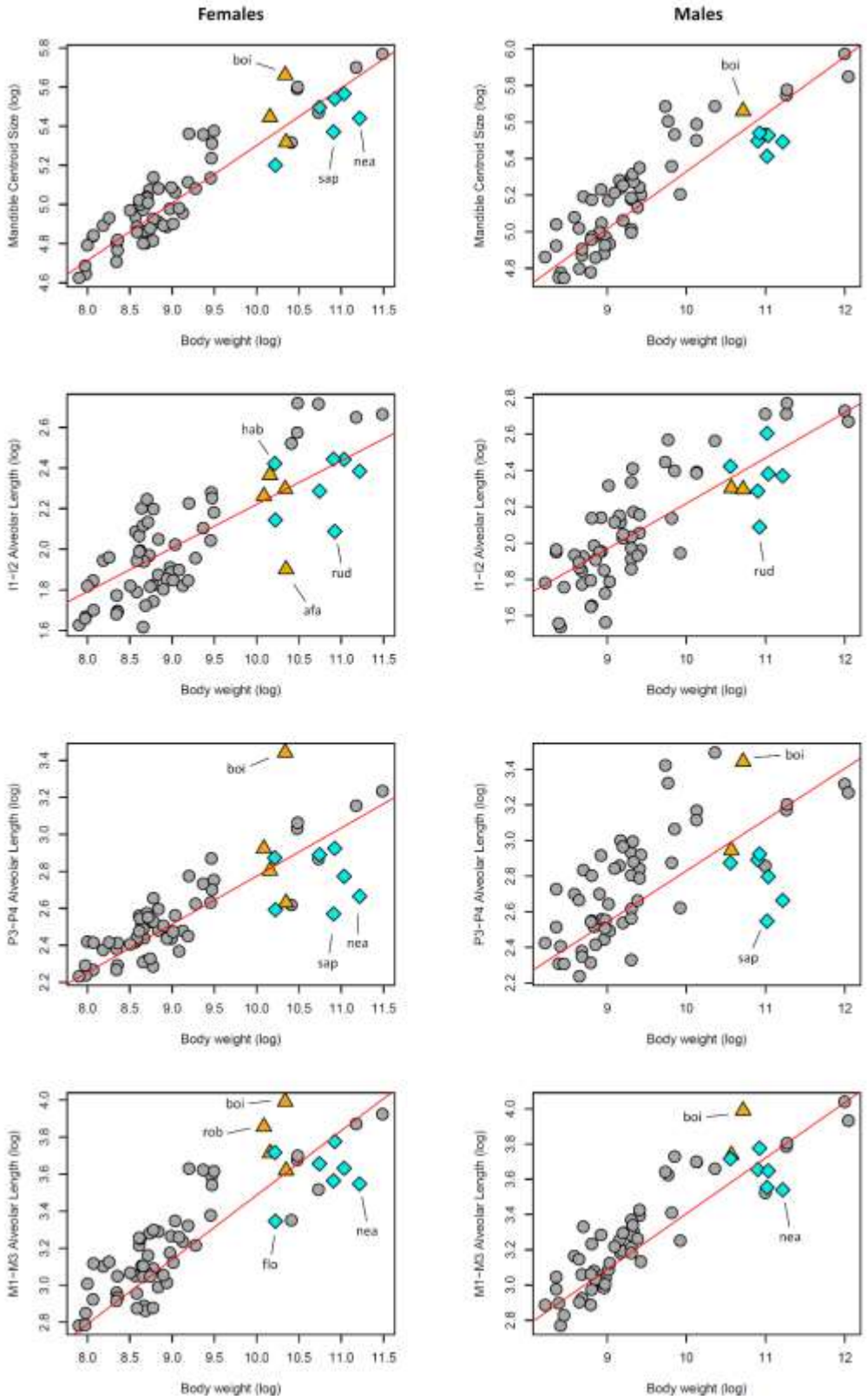

Figure 4.1 Regressions between mandibular Centroid Size (CS) and alveolar lengths versus body weight. The predicted trend (red) was calculated for non-hminin extant catarrhines (grey circles), excluding hominins (australopiths: golden triangles, *Homo*: cyan diamonds). The species diverging from the regression line are labelled. (**afa**: *A. afarensis*; **boi**: *P. boisei*; **rob**: *P. robustus*; **hab**: *H. habilis*; **rud**: *H. rudolfensis*; **flo**: *H. floresiensis*; **nea**: *H. neanderthalensis*; **sap**: *H. sapiens*).

Table 4.6 Results of the Phylogenetic ANCOVA for slope differences between the groups of fossil hominins, *Homo* and other extant catarrhines, assuming a Pagel's Lambda model of evolution. Here "Catarrhines" refers to non-hominin extant catarrhines. Significant p-values are shown in bold.

	Catarrhines vs Hominins			**Catarrhines vs *Homo***		
Females	**DF**	**F**	**p-value**	**DF**	**F**	**p-value**
CS	61 62	7.6	**0.008**	58 59	0.03	0.863
I_1-I_2	62 63	2.929	0.092	58 59	2.604	0.112
P_3-P_4	62 63	14	**< 0.001**	58 59	5.655	**0.021**
M_1-M_3	62 63	25.693	**< 0.001**	58 59	6.820	**0.011**

	Catarrhines vs Hominins			**Catarrhines vs *Homo***		
Males	**DF**	**F**	**p-value**	**DF**	**F**	**p-value**
CS	57 58	9.793	**0.003**	56 57	1.928	0.17
I_1-I_2	59 60	6.626	**0.013**	57 58	5.820	**0.019**
P_3-P_4	59 60	17.891	**< 0.001**	57 58	7.133	**0.01**
M_1-M_3	59 60	36.843	**< 0.001**	57 58	17.963	**< 0.001**

The null hypothesis of non-difference in size between *Homo* and other extant catarrhines when body size wass taken into account was not rejected for the mandible and molars in females (p-values 0.072 and 0.816 respectively) and for the mandible, premolars and molars in males (p-values 0.18, p-value 0.1 and 0.416 respectively). When corrected for phylogeny by considering an OU model, results for the molars did not change, and *Homo* and other extant catarrhines did not differ for female premolars (p-value 0.892). There was no significant difference in *Homo* and australopithecines in incisor alveolar length for males and females (p-values 0.899 and 0.332 respectively). When OU was considered instead of the λ model, australopithecines and *Homo* were not statistically different for female premolar size (p-value 0.679). Australopithecines and other extant catarrhines showed significant differences in the size of female incisors (p-value 0.018), and female and male molars (p-values < 0.001 and 0.003 respectively) when using the λ models; considering the OU model left the results unaltered.

Table 4.7 Results of the Phylogenetic ANCOVA for differences in intercepts between the groups of *Homo*, australopithecines and catarrhines, assuming a Pagel's Lambda model of evolution. Significant p-values are shown in bold. (**Aus**: australopithecines; **Cat**: non-hominin extant catarrhines).

	***Homo* vs Aus vs Cat**			***Homo* vs Aus | Cat**		
Females	**DF**	**F**	**p-value**	**DF**	**F**	**p-value**
CS	61 63	8.202	**< 0.001**	61 62	16.328	**< 0.001**
I_1-I_2	62 64	3.688	**0.031**	62 63	0.016	0.899
P_3-P_4	62 64	8.053	**< 0.001**	62 63	14.213	**< 0.001**
M_1-M_3	62 64	15.151	**< 0.001**	62 63	26.329	**< 0.001**

	***Homo* vs Cat | Aus**			**Aus vs Cat | *Homo***		
Females	**DF**	**F**	**p-value**	**DF**	**F**	**p-value**
CS	61 62	3.344	0.072	61 62	2.596	0.112
I_1-I_2	62 63	6.603	**0.013**	62 63	5.949	**0.018**
P_3-P_4	62 63	10.161	**0.002**	62 63	1.68	0.2
M_1-M_3	62 63	0.054	0.816	62 63	17.452	**< 0.001**

	***Homo* vs Aus vs Cat**			***Homo* vs Aus | Cat**		
Males	**DF**	**F**	**p-value**	**DF**	**F**	**p-value**
CS	57 59	4.648	**0.013**	57 58	8.964	**0.004**
I_1-I_2	59 61	2.704	0.075	59 60	0.956	0.332
P_3-P_4	59 61	9.447	**< 0.001**	59 60	18.731	**< 0.001**
M_1-M_3	59 61	11.004	**< 0.001**	59 60	21.553	**< 0.001**

	***Homo* vs Cat | Aus**			**Aus vs Cat | *Homo***		
Males	**DF**	**F**	**p-value**	**DF**	**F**	**p-value**
CS	57 58	1.815	0.183	57 58	2.62	0.111
I_1-I_2	59 60	5.311	**0.025**	59 60	1.885	0.175
P_3-P_4	59 60	2.792	0.1	59 60	3.184	0.079
M_1-M_3	59 60	0.672	0.416	59 60	9.698	**0.003**

Tables 4.8 and 4.9 list the results of the phylogenetic ANCOVA applied to the divergence of each species from the scaling pattern of non-hominin extant catarrhines using the λ models. Results obtained by using the OU model are available in Appendix 2. The hominin samples were different for mandible and teeth and between sexes (Table 4.2). Therefore, the fact that one species was an outlier for teeth but not for mandible, or for one sex only, makes sense only if that species was present for both variables. Regarding the CS of the mandible, *P. boisei*, *H. neanderthalensis* and *H. sapiens* diverged significantly from the scaling patterns of female other extant catarrhines (p-values < 0.001, 0.027 and 0.04 respectively), and only *P. boisei* was confirmed as an outlier in the male subsample (p-value 0.004). For incisor alveolar length, *A. afarensis* (absent in the male subsample), *H. habilis* and *H. rudolfensis* significantly diverged from female other extant catarrhines (p-values 0.001, 0.03 and 0.009 respectively), and *H. rudolfensis* was outside the variability of male other extant catarrhines (p-value 0.002). Although for the postcanine dentition there were cases where the OU-based phylogenetic correction performed better than the λ model, issues have been raised about the good fit of this model (Cooper et al. 2015). The results relative to the λ and, where relevant, the OU models are here reported. The premolar size of *P. boisei*, *H. neanderthalensis* and *H. sapiens* was outside the variability of female other extant catarrhines (p-values < 0.001, 0.016 and 0.023), but when the OU model was used for phylogenetic correction, only *P. boisei* was confirmed as an outlier. For male premolars, the divergent hominin species are *P. boisei* and *H. sapiens* (p-values < 0.001 and 0.024).

Paranthropus boisei, *P. robustus*, *H. floresiensis* and *H. neanderthalensis* departed significantly from the female other extant catarrhine pattern of molar size scaling (p-values 0.001, 0.008, 0.045 and 0.008 respectively), but *P. robustus* was within the other extant catarrhine molar size variability when switching from the λ to the OU model. Finally, *P. boisei* and *H. neanderthalensis* diverge from other extant catarrhines for male molar size (p-values < 0.001 and 0.005), and this result does not change under OU phylogenetic correction.

Table 4.8 Results of the Phylogenetic ANCOVA performed on the female sample. Test for fossil hominin species divergence from the scaling trajectory of other extant catarrhines, assuming a Pagel's Lambda model of evolution. Significant p-values are shown in bold.

	CS			**I_1-I_2**		
	DF	**F**	**p-value**	**DF**	**F**	**p-value**
A. afarensis	61 62	0.951	0.333	62 63	11.573	**0.001**
A. africanus	61 62	3.715	0.059	62 63	3.266	0.076
H. ergaster	61 62	0.087	0.769	62 63	0.068	0.795
H. floresiensis	61 62	3.369	0.0713	62 63	0.238	0.6271
H. habilis	-	-	-	62 63	4.915	**0.03**
H. heidelbergensis	61 62	0.138	0.711	62 63	0.332	0.567
H. neanderthalensis	61 62	5.164	**0.027**	62 63	0.149	0.7
H. rudolfensis	61 62	0.009	0.926	62 63	7.274	**0.009**
H. sapiens	61 62	4.386	**0.04**	62 63	0.668	0.417
P. boisei	61 62	23.461	**< 0.001**	62 63	0.432	0.513
P. robustus	-	-	-	62 63	0.784	0.379

	P_3-P_4			**M_1-M_3**		
	DF	**F**	**p-value**	**DF**	**F**	**p-value**
A. afarensis	62 63	1.219	0.274	62 63	0.031	0.862
A. africanus	62 63	0.24	0.626	62 63	1.595	0.211
H. ergaster	62 63	0.014	0.907	62 63	0.397	0.531
H. floresiensis	62 63	1.237	0.27	62 63	4.169	**0.045**
H. habilis	62 63	0.798	0.375	62 63	1.474	0.229
H. heidelbergensis	62 63	1.44	0.235	62 63	1.874	0.176
H. neanderthalensis	62 63	5.441	**0.023**	62 63	7.466	**0.008**
H. rudolfensis	62 63	0.003	0.96	62 63	0.01	0.919
H. sapiens	62 63	6.162	**0.016**	62 63	2.738	0.103
P. boisei	62 63	35.529	**< 0.001**	62 63	11.177	**0.001**
P. robustus	62 63	2.267	0.137	62 63	7.6	**0.008**

Table 4.9 Results of the Phylogenetic ANCOVA performed on the male sample. Test for fossil hominin species divergence from the scaling trajectory of other extant catarrhines, assuming a Pagel's Lambda model of evolution. Significant p-values are shown in bold.

	CS			**I_1-I_2**		
	DF	**F**	**p-value**	**DF**	**F**	**p-value**
A. afarensis	-	-	-	-	-	-
A. africanus	-	-	-	59 60	0.754	0.389
H. ergaster	57 58	0.011	0.917	59 60	0.367	0.547
H. floresiensis	-	-	-	-	-	-
H. habilis	-	-	-	59 60	3.762	0.057
H. heidelbergensis	57 58	0.001	0.973	59 60	0.149	0.701
H. neanderthalensis	57 58	2.089	0.154	59 60	0.86	0.358
H. rudolfensis	57 58	0.121	0.729	59 60	10.024	**0.002**
H. sapiens	57 58	2.695	0.106	59 60	3.806	0.056
P. boisei	57 58	8.964	**0.004**	59 60	0.108	0.743
P. robustus	-	-	-	-	-	-

	P_3-P_4			**M_1-M_3**		
	DF	**F**	**p-value**	**DF**	**F**	**p-value**
A. afarensis	-	-	-	-	-	-
A. africanus	59 60	0.646	0.425	59 60	2.681	0.107
H. ergaster	59 60	0.009	0.924	59 60	0.454	0.503
H. floresiensis	-	-	-	-	-	-
H. habilis	59 60	0.128	0.721	59 60	1.747	0.191
H. heidelbergensis	59 60	0.4	0.529	59 60	1.327	0.254
H. neanderthalensis	59 60	3.769	0.057	59 60	8.552	**0.005**
H. rudolfensis	59 60	0.077	0.783	59 60	0.02	0.889
H. sapiens	59 60	5.392	**0.024**	59 60	3.082	0.084
P. boisei	59 60	21.017	**< 0.001**	59 60	14.575	**< 0.001**
P. robustus	-	-	-	-	-	-

4.4 Discussion

The genus *Homo* underwent important transitions characterized by cultural and technological developments, events that had a remarkable impact on the hominin lifestyle and are assumed responsible for making us "human" by affecting both our sociality and anatomy (Wrangham, 2009; Pinhasi & Meiklejohn, 2011; Zink & Lieberman, 2016). A particularly small and gracile lower jaw is part of this human anatomical uniqueness and, although the factors that drove the trend of reduction have never been fully demonstrated, differences in the masticatory apparatus within hominins are undeniable. Understanding the place of hominins in the natural variability of the lower jaw can help in understanding the traits that were modified most in response to the trend of reduction. In addition, it is important to understand the mechanisms that allowed the changes observed in the morphology of the masticatory apparatus in *Homo*.

4.4.1 Phylogenetic signal

The results stress the importance of using phylogenetic methods to study human morphological evolution. In fact, the scaling patterns of mandibular and dental size were variably influenced by the phylogenetic relationships among the taxa analysed here. The phylogenetic signal λ indicated that, for most cases, phenotypic differences in mandible and tooth size increased with the time of divergence, thus likely being subject to neutral drift after speciation. Interestingly, the phylogenetic signal for the postcanine dentition diverged between sexes and the difference was remarkable in the size of premolars. Phylogenetic dependence was absent from premolar size in females ($\lambda = 0$), but not in males ($\lambda = 0.749$). This result suggests that changes in premolar size may follow an evolutionary pattern that is different from the other tooth types. In addition, there were sex differences in the scaling patterns of incisors, despite no remarkable results about the phylogenetic dependence were found in this case. Pragmatically, these findings highlight the need to consider sexual dimorphism as an influential element in the interpretation of dental reduction, in particular for what concerns incisors and premolars.

4.4.2 Homo *and the catarrhine variability*

When considered in relation to body size, the mandibular and dental size of *H. sapiens* appeared unusual. If we consider the trend toward a larger body size that characterized the evolution of *Homo* (Ruff, 2002; Grabowski et al., 2015), we would expect this to have at least partially counterbalanced the reduction in the masticatory apparatus. Indeed, the results indicated that the size of the catarrhine lower jaw grows with body size and an increase in body size in *Homo* would have driven an increase in mandibular and dental size. An overall decrease in the mandibular and dental size at the dawn of the genus *Homo* would be a plausible explanation for the unexpectedly small size of the human lower jaw. The results on slopes differences reject this possibility: for postcanine size, the genus *Homo* did not depart substantially from the observed extant catarrhine variability. Based on these results, changes in the allometric scaling pattern in hominins would provide a more solid mechanism for the onset of the reduction, at least for what concerns postcanine dentition. In fact, the genus *Homo* diverged significantly from the slope of the extant catarrhine sample for postcanine size, and no differences in intercepts were present. This shows that, in the genus *Homo*, some event occurred that modified its catarrhine-like scaling trajectory, rather than the dimensions of it. Furthermore, the results obtained for the single hominin species divergence indicated *H. sapiens* and *H. neanderthalensis* as outside the across-catarrhine variability for postcanine size. These findings suggest that changes in the allometric scaling of premolars and molars may have been stronger in the upper Palaeolithic and Holocene than earlier in the evolution of the genus *Homo*. Sex differences seemed to confound this result in premolars, which are known to be highly sexually dimorphic in certain groups of primates (Harvey et al., 1978; Fleagle et al., 1980). Nonetheless, when the data was phylogenetically corrected by using the OU instead of the λ model, this sex difference did not hold, indicating a possible adaptive significance of the premolars, as supported by the OU model. Concerns have been raised, however, over the use of OU in phylogenies of low species counts (Cooper et al., 2015).

Mandibular scaling with body size in the genus *Homo* shares both similar slope and intercepts with the across-catarrhine trajectory. These results suggest that the factors driving dental reduction may have not caused modifications in mandibular size, although other morphological features could have been affected, such as mandibular robusticity (Chamberlain & Wood, 1985). *H. sapiens* and *H. neanderthalensis* appeared somewhat

peculiar in these respects, with results outside the across-catarrhine variability for mandibular size. As for the postcanine dentition, this may be seen as the effect of a more pronounced reduction occurred in the late Pleistocene and Holocene than in the lower and middle Palaeolithic. In this perspective, the modifications of the lower jaw that took place in Neanderthals and humans would be unique in considerably affecting the size of the mandible, and not just the postcanine dentition.

For mandibular and postcanine size, few species of *Homo* diverged from the other extant catarrhine variability: *H. neanderthalensis* and *H. sapiens* departed from the allometric pattern across catarrhines because of their smaller dental size, and this was particularly evident for Neanderthal molars. An opposite pattern was observed in *P. boisei*, whose mandible and postcanine teeth resulted larger than expected from its body size. The "hyper-robust" skull morphology of *P. boisei* (Walker et al., 1986; Walker & Leakey 1988; Wood & Costantino, 2007) has been usually ascribed to its masticatory adaptations, and its large mandible, premolars and molars are part of this robusticity. This suggests that dietary and biomechanical factors may have played an important role in the trends of mandibular and postcanine reduction during upper Palaeolithic and Holocene.

The literature about dental reduction describes a size increase in incisors during the middle Pleistocene followed by a size reduction (Brace, 1967). Our results confirmed those differences between early *Homo* and later species. Indeed, *H. habilis* and *H. rudolfensis* were the only species departing from the across-catarrhine variability after phylogenetic correction. Nevertheless, the results for incisors seemed to be influenced by sexual dimorphism in the catarrhine sample. In the female sample, *Homo* and other extant catarrhines shared the same incisor size scaling slope while differing in the intercept. This would indicate that, for incisors, the hypothesis of a net decrease of dental size in the genus *Homo* should be preferred over the possibility of a change of allometric trajectory. Nevertheless, in the male sample, an opposite result for the slope was found. It is also possible that the sex differences in body size have influenced the result.

The results suggest that for early *Homo* and middle Pleistocene hominins, body size changes can explain a large part of mandibular and postcanine size variability. The drop in dental size following early *Homo* may not have been as dramatic as the reduction seen from the Upper Palaeolithic to recent times, as highlighted above. *H. neanderthalensis* and *H. sapiens*

experienced stronger mandibular and postcanine size variations than in earlier *Homo* species, reaching a phenotype that is unique in size within the across-catarrhine variability. The hard object feeding habit of *P. boisei* (Smith et al., 2015) and its concomitant extremal position in primate mandibular and postcanine size variability may suggest a role of biomechanical and dietary factors in the postcanine reduction during Upper Palaeolithic and Holocene. A net size decrease at the dawn of the genus *Homo* does not seem a plausible explanation for the gracile appearance of the modern human mandible and teeth, for which alterations in the allometric rates of change between the lower jaw and the body size are more likely to explain the observed patterns of reduction (Pilbeam & Gould, 1974).

These results suggest that the direction and mode of dental and mandibular reduction is not homogeneous within hominins, and different causes should be investigated to explain the trends that occurred at different times during human evolution. In addition, the results confirmed that mandibular and dental size are distinctive features of late Pleistocene and modern humans.

Chapter 5

Size, robusticity and diet in catarrhines: a comparative look at dental and mandibular reduction in *Homo*

5.1 Introduction

Dental size and mandibular robusticity reduced during the evolution of the genus *Homo* and these changes may have had a major influence on several aspects of hominin life history (Brace, 1963; Chamberlain & Wood, 1985; McHenry & Coffing, 2000; Bastir et al., 2004; Emes et al., 2011). The hypotheses put forward to explain the trends of dental and mandibular reduction in the genus *Homo* (including modern humans) depict the mandible and teeth as conforming to changes in subsistence strategies (Wrangham, 2009; Zink et al., 2014). Dental and mandibular differences among hominins have been ascribed to dietary shifts or food processing. The big chewing surfaces, thick enamel and the molar-like premolars of australopithecines, in particular *Paranthropus* (Teaford and Ungar, 2000; Wood and Strait, 2004), are hypothesized to be the result of the consumption of herbaceous vegetation and vegetal underground storage organs, following the transformation of forests into grasslands and savannahs (Kingston et al., 1994; WoldeGabriel, 1994). With the genus *Homo*, a change in ecological niche probably started: the consumption of more meat (Speth, 1989; Stanford and Bunn, 2001). It has been proposed that increased exploitation of this resource was made easier by improvements in food processing skills, such as the use of stone tools for slicing meat and the ability to control fire for cooking, and some experimental evidence support this view (Wrangham, 2009; Zink & Lieberman, 2016). As a result, the ecological niche adopted by early *Homo* and its food processing skills have been considered responsible for the mandibular and postcanine size reduction (Brace, 1963; Calcagno & Gibson, 1988; Wrangham & Carmody, 2010; Zink & Lieberman, 2016). Dental and mandibular variations during the

Holocene were thoroughly debated during the 1960s and ‘70s, and the development of agricultural subsistence strategies has been considered the reason for tooth size decrease in *Homo sapiens* (Pinhasi & Meiklejohn, 2011).

From this perspective, mandibular and dental reduction in both early hominins and anatomically modern humans could be seen as the result of the relaxation of selective pressures because of lowered functional requirements (Brace, 1963). Therefore, we should expect smaller, more gracile lower jaws in hominins adapted to consume foods that are intrinsically softer or that are made softer because of processing, such as slicing or cooking. Although this view may sound convincing, it is based on the (untested) assumption that differences in size and robustness in mandible and teeth reflect functional dissimilarities, thus adaptation. Every species, including humans, is adapted to its environment, but evolution follows a tortuous way and two facts may overpower the role of adaptation. First, species share ancestry because of their common evolutionary history, thus displaying traits appearing similar simply as a result of “phylogenetic inertia” (Blomberg & Garland, 2002). Second, a single species may appear or behave differently in different environments, or different species may respond similarly in the same environment, regardless of their adaptations, because of phenotypic and behavioural plasticity (Chapman & Chapman, 1990; Brockman & Van Schaik, 2005).

The phenomena of phylogenetic inertia and plasticity are well described in primates. Phylogenetic constraints have been found to influence body size (Cheverud et al., 1985) and patterns of sexual dimorphism (Leigh, 1992) in a broad range of primates. All primates, from Strepsirrhini to great apes, exhibit different levels of plasticity in morphology, probably as an adaptation to survive on fall-back foods when the main resource is not available, and this plasticity also has been observed in the masticatory apparatus (Lambert, 2009).

Primates have been divided into four main feeding categories (frugivores, folivores, gummivores and insectivores), depending on the main source of food each species relies on (Nunn & Van Schaik, 2002). Meloro et al. (2015) have shown that primate mandibular morphology shows distinguishable adaptations in terms of feeding when a large sample of non-human primates is analysed. Nonetheless, at smaller taxonomical scales, differences between species appear unclear, in part because of plasticity and phylogenetic inertia. Among catarrhines, where we observe mainly frugivorous and folivorous primates, many species do

not fall into one diet category, being somewhere between them (National Research Council US, 2003). Therefore, categorisation may not be sufficient to define dietary patterns, and the use of less strict criteria is prudent. In addition, several primates, including many species of catarrhines, developed tool use skills to access sources of food otherwise difficult to exploit (Van Schaik et al., 1999). Although for many species tool use is occasional, others exhibit this behaviour on a regular basis (Reader et al., 2011). Few authors (Teleki, 1974; Parker & Gibson, 1977) have addressed the role of tool use on primate subsistence, but an association between tool use, subsistence and masticatory anatomy in non-hominin primates has never been claimed, as it has been proposed for hominins (Bailit & Firedlaender, 1966). To state that the differences in mandibular and dental robustness in hominins have a functional meaning, we should test this assumption in catarrhines, both focusing on diet and food processing.

To address the issue of dental and mandibular reduction in *Homo*, here we use a primate comparative framework. In particular, the aim is to test the assumption of dependence between size, robusticity and function in the masticatory apparatus of catarrhines, to make inferences on the patterns of reduction observed in hominins (including *H. sapiens*). A phylogenetic comparative method was applied to study morphometric descriptors of mandible and teeth, by comparing them to feeding and tool use variables. This work highlights the difficulties in relating anatomy, diet and behaviour, and suggests that certain changes in the hominin lower jaw may have been triggered by dietary factors.

5.2 Material and methods

5.2.1 The sample and the morphological data

The sample included Colobinae (9 species), Cercopithecinae (39 species), Hylobatidae (9 species), and Hominidae (6 species) for a total of 63 species. Only adult individuals of both sexes were included in the sample, and a fully erupted third molar was used to determine the adult age-class. The sample was divided in female and male subsamples. Further specifications for the catarrhine sample are reported in Table 2.1, Chapter 2, and in Appendix 1. Few fossil hominin species were included in the sample, split in 6 species and belonging to

the genera *Australopithecus* (2 species), *Paranthropus* (2 species) and *Homo* (2 species). Sex information was obtained from Wolpoff (1971; 1979), Wood (2011) and Schwartz & Tattersall (2005). Individuals of unknown sex were included in both the female and male subsamples. Modern humans were included in the sample by collecting data on 20 mandibles from individuals of mixed non-European populations of known sex. A summary of the primate and hominin samples is shown in Table 5.1. Complete information about the sample are available in Appendix 1. The material in this study consisted of measurements collected on real specimens, casts and virtual specimens. The virtual sample was available in CT, micro CT scan and photogrammetry formats. The data was available from online databases (KUPRI, NESPOS, MorphoSource, the Africanfossils archive and the digital archive of fossil hominoids) and from museums (Natural History Museum in London, the Muséum National d'Histoire Naturelle in Paris, the National Museum of Kenya in Nairobi, the Museum of Comparative Zoology at Harvard, the Royal Museum for Central Africa in Tervuren, the cast collections of Liverpool John Moores University and the anthropological museum "G. Sergi" in Roma). The modern human sample belong to the skeletal collection of the Smithsonian Institution, and was made available by Copes in CT format (2012). For further details, refer to Chapter 2. The linear measurements for the hominin sample were collected from the Human Origins Database (www.humanoriginsdatabase.org) and correspond to the measurements in Wood (1991).

The morphological data analysed included mandibular size, robusticity and dental size. Mandibular size was estimated as the Centroid Size (CS) of a configuration of 28 landmarks recorded on hemi-mandible 3D surfaces. The landmarks were collected using the Amira software package (version 5.4.5, FEI Visualization, Berlin), and the configuration is displayed in Figure 2.2, Chapter 2. The definitions for the landmarks are reported in Appendix 1. Dental size for each tooth type was approximated by the alveolar length of incisors, premolars and molars. Alveolar lengths were measured as the minimum chord distance between midpoints of the inter-alveolar septa for each tooth type. Since teeth are frequently missing *postmortem* in mandibles of museum specimens and fossils, alveolar length was used as a proxy for tooth size to maximize sample size. For part of the fossil specimens, measurements were collected from the online "Human Origins Database". Alveolar lengths are presented in Figure 2.1, Chapter 2. Robusticity was measured on the mandibular corpus at the level of the symphysis (SY), first (M_1), second (M_2) and third molars (M_3). It was calculated as a ratio between width

(W) and height (H), providing the robusticity index (W/H x 100) (Daegling, 1989). Height and width of fossil hominin mandibles were available in the "Human Origins Database". For other specimens, the robusticity index was measured on virtual specimens by simulating the action of Vernier callipers. The virtual protocol used to extract robusticity in catarrhine mandibles is discussed in Chapter 2 and displayed in Figure 2.3. Further considerations on the use of alveolar length and the error of virtually extracted robusticity indices can be found in Chapter 2.

Body size information for each primate and fossil hominin was included. For non-human primates, body weight averaged by species and sex was available from the literature (Smith and Jungers, 1997; National Research Council US, 2003). For hominin body size values, the best estimations from studies of relevant, complete fossils were used (McHenry and Berger, 1998; Jiménez-Arenas et al., 2014; Grabowski et al., 2015). Further information about body size is provided in Appendix 1.

5.2.2 Feeding and behavioural data

Data from several sources was gathered, focusing on aspects of diet, subsistence strategies and tool use in catarrhines. In particular, four different types of data related to ecology and behaviour were collected: diet percentages, dental microwear, feeding duration and feeding behaviour. These variables are intrinsically affected by high levels of measurement error (Freckleton, 2011). Except microwear, they rely on field observations of populations or captive animals. Microwear patterns refer to the last meal of an individual (Teaford & Oyen, 1989), thus reducing the dietary spectrum observable. Despite their limited accuracy, these data have been successfully used in other studies (Ross et al., 2009a; Reader et al., 2011; Scott et al., 2012; Jiménez-Arenas et al., 2014), and are well suited to test hypotheses about mandibular and dental reduction.

Diet percentages refer to the relative amount of certain food type categories in the diet of a species (National Research Council US, 2003). Fruit/seed, plant soft materials, plant fibrous materials, tree gum, fungi and animal matter were used as food categories, assuming these groups account for the complete (100%) diet for each species. These percentages were used to calculate the diet quality index (DQ) and an index of diet evenness (DH, or diet

heterogeneity). DQ was calculated following the equation in Sailer et al. (1985), previously applied in other works focusing on primate morphology (Allen & Kay, 2011):

$$DQ = 1s + 2r + 3.5a$$

where *s* represents the percentage of structural plant parts, *r* is the percentage of reproductive plant parts, *a* is the percentage of animal matter in the diet, and the constants 1, 2 and 3.5 account for the relative energetic values per unit mass of *s*, *r* and *a* respectively. DH was calculated as the Simpson's diversity index (1-D.), common in ecological studies (Pielou, 1969):

$$DH = 1 - \Sigma (n / N)^2$$

Here n / N is the proportion of each food category in the diet. The Simpson's diversity index was used to account for the prevalence of certain food types in the diet, so that DH becomes a measure of dietary specialisation. Diet percentages of 56 species were included in the female sample and 55 species for the male sample (National Research Council US, 2003).

Dental microwear analysis is commonly performed to infer aspects of diet in mammals and it has been extensively applied to primates and hominins (Scott et al., 2012; Ungar et al., 2012; DeSantis et al., 2013). It relies on the inspection of the patterns of scratches and pits left on tooth enamel after the contact with food during mastication (Scott et al., 2006). Through time, microwear data have proven successful in discriminating between different diets (Scott et al., 2006). Microwear data included variables describing dental surface roughness (Area-Scale Fractal Complexity, or *Asfc*), the anisotropy of surface properties (Length-scale anisotropy of relief, or *epLsar*), heterogeneity of surface properties (heterogeneity of Area-scale fractal complexity, or *HAsfc9*) and textural volume patterns (Textural fill volume, or *Tfv*). Further details on these measurements can be found in Scott et al. (2006). Dental microwear data was retrieved for 18 species (female) and 17 species (male) from Grine et al. (2006), Scott

et al. (2012) and Ungar et al. (2012b), and include 6 fossil hominin species. The data were produced using the same parameters and, therefore, were comparable.

Data on feeding time (FT) and chewing cycle length (CCL) was obtained from Ross et al. (2009a, b). Feeding time is the proportion of time spent by a species on feeding activities. This variable does not account for foraging activities other than moving food into the mouth, chewing and swallowing (Ross et al., 2009a). Feeding time, as used here, derives from observations performed on wild animals (Ross et al., 2009b). The duration of the chewing cycle refers to the length of time between successive maximum jaw gapes. Ross et al. (2009b) found that food physical properties have little impact on the chewing cycle duration, although such a correlation would be expected. Nonetheless, this variable was included since information about the relationship between lower jaw morphology and chewing cycle may provide useful insights on the evolution of the primate mandible. The values for chewing cycle duration were measured on animals in captivity (Ross et al., 2009b). Feeding time was collected for 22 species (female) and 23 species (male). Chewing cycle length information was available for 9 and 10 species for females and males, respectively.

The behavioural data is based on evidence of tool use (TU) or extractive foraging practices (EF) in catarrhines in Reader et al. (2011). The data consist of frequencies of observations of tool use and extractive foraging behaviours available from about 4000 scientific articles (Reader et al., 2011). The data are expressed as the total number of reported examples and a protocol was used to correct for the differential research effort on species. The research effort was measured as the total number of papers in behavioural research that were published about each species in a specified time span in a number of international journals (Reader et al., 2011). The correction was performed by modifying the protocol provided in the reference paper. The authors (Readers et al., 2011) extracted the orthogonal residuals from Ordinary Least Squares (OLS) regression lines forced through the origin between the reported examples of behaviour and the total number of behavioural studies per species. This correction presents two major drawbacks. First, despite the causality between the two factors, there is a mutual influence and OLS does not account for it (Markovsky & Van Huffel, 2007). Second, forcing the regression through the origin means assuming that, for any amount of papers published about any behaviour of a species, there must be some paper published about extractive foraging or tool use, which is not necessarily true. To solve these

issues, the data was corrected by applying Total Least Squares (TLS) not forced through the origin. Following Reader et al. (2011), orthogonal residuals were calculated. The behavioural data include 47 species.

To account for phylogenetic relatedness in the sample, a primate molecular phylogeny was obtained from the online database 10ktrees (Arnold et al., 2010). For the hominin sample, a phylogeny was built following the topology published by Dembo et al. (2015), as shown in Figure 2.8. Branch lengths in the hominin phylogeny were scaled to fit the time of divergence between *P. troglodytes* and *H. sapiens* in the primate tree. The extant catarrhine and fossil hominin trees were then merged. Further details are provided in Chapter 2.

5.2.3 The correlation procedure

The analyses were performed for females and males separately. In each correlation, each subsample was reduced to include only the species available for the morphological trait, the phylogenetic tree and the independent variable. The number of species included in each correlation is reported in Table 5.1. To test for the dependence between morphological, ecological and behavioural proxies in primates, Phylogenetic Generalized Least Squares was performed (PGLS) assuming a Pagel's Lambda (λ) model of evolution. In the λ model of trait evolution, the branch lengths of the tree are multiplied by the factor λ, specifying the degree of phylogenetic signal in the data (Pagel, 1999). If λ equals 0, data are independent on phylogeny. The parameter λ was estimated for each correlation by using the R package "phylolm" (Ho & Ané, 2014). Mandibular Centroid Size (CS, log-transformed), alveolar lengths (log-transformed) and the robusticity indices were used as dependent variables, the ecological and behavioural proxies were considered as independent ones. To account for the effect of body size on the other variables, body weight was included as a covariate (Christians, 1999). To improve interpretability and avoid over-parametrization and multicollinearity (Lehmann & Dunbar, 2009), each independent variable was analysed separately. Each correlation was tested by 2nd degree orthogonal polynomial fitting; thus, each regression consisted of an intercept and three additional terms: 1st degree term (slope) and 2nd degree term (curvature) for the independent variable and a 1st degree term for the covariate (slope

for body weight). These terms are indicated as X, X^2 and B, and the full model is described by the following equation:

$$y = \beta_0 + \beta_1 X + \beta_2 X^2 + \beta_3 B$$

where β_0 is the intercept and $\beta_{1\text{-}3}$ are the coefficients of the equation terms. Regressions were not performed to find a predictor model for the mandibular and dental variables in relation to dietary and tool use proxies, but to detect the presence of a significant statistical effect of the independent variables on the dependent ones. Therefore, testing multiple equation terms is useful to isolate the effects, reducing the error. The significance of each term was tested adopting a level of 95% of confidence (α: 0.05). For the regression exhibiting a significant effect of X or X^2, a semi-partial R^2 was calculated as an indication of the variance explained by the sole independent variable ($X+X^2$). The semi-partial R^2 was calculated as the difference between the total R^2 (from the regression including X, X^2 and B) and the R^2 calculated by excluding the variables X and X^2 (Kutner et al., 2005). The regressions were performed by using the R-packages “ape” (Paradis et al., 2004), “nlme” (Pinheiro et al., 2015) and “phylolm” (Ho & Ané, 2014).

Table 5.1 Sample size. The number of species included in each correlation is reported. For the meaning of tags, refer to the main text, paragraph 5.2.

Female	DQ	DH	Asfc	epLsar	Tfv	HAsfc9	CCL	FT	TU	EF
CS	56	56	16	16	16	16	9	22	47	47
I_1-I_2	55	55	13	13	13	13	9	22	46	46
P_3-P_4	55	55	15	15	15	15	9	22	46	46
M_1-M_3	55	55	14	14	14	14	9	22	46	46
Rob SY	56	56	17	17	17	17	9	22	47	47
Rob M_1	56	56	18	18	18	18	9	22	47	47
Rob M_2	56	56	18	18	18	18	9	22	47	47
Rob M_3	56	56	17	17	17	17	9	22	47	47

Male	DQ	DH	Asfc	epLsar	Tfv	HAsfc9	CCL	FT	TU	EF
CS	55	55	13	13	13	13	10	23	47	47
I_1-I_2	55	55	12	12	12	12	10	23	47	47
P_3-P_4	55	55	13	13	13	13	10	23	47	47
M_1-M_3	55	55	12	12	12	12	10	23	47	47
Rob SY	55	55	16	16	16	16	10	23	47	47
Rob M_1	55	55	17	17	17	17	10	23	47	47
Rob M_2	55	55	17	17	17	17	10	23	47	47
Rob M_3	55	55	16	16	16	16	10	23	47	47

5.3 Results

There were significant regressions for several dependent variables in both females and males, but not necessarily for every term of the correlation. In many cases, only the body weight (covariate) achieved significance over 95% of confidence, and these results are not discussed here. In addition, several regressions displayed negative adjusted R^2, meaning the absence of correlation because of poor statistical power, and these, too, were not considered. The significant regressions displayed various levels of phylogenetic dependence, as indicated by the lambda values ranging from 0 to 1 and in most cases very close to the two extremes. The

values of semi-partial R^2 calculated on each significant regression are shown in Table 5.2. The regression terms and adjusted R^2 for each regression are reported in Table 5.3 and 5.4. The p-values are available in Appendix 2.

Table 5.2 Semi-partial R^2 of the independent variables calculated for the significant regressions. The semi-partial R^2 for X ($X+X^2$) is the difference between the R^2 of the full regression (including all the independent variables and covariates) and the R^2 of the regression performed excluding $X+X^2$. For the meaning of tags, refer to the main text, paragraph 5.2.

Female	Partial R^2 ($X+X_2$)	Total R^2	Male	Partial R^2 ($X+X_2$)	Total R^2
I_1-I_2 - DQ	0.13	0.778	**CS - Tfv**	0.05	0.925
I_1-I_2 - Asfc	0.05	0.652	**I_1-I_2 - Asfc**	0.09	0.794
I_1-I_2 - Tfv	0.12	0.724	**I_1-I_2 - epLsar**	0.02	0.723
I_1-I_2 - HAsfc9	0.15	0.756	**P_3-P_4 - HAsfc9**	≈ 0	0.635
P_3-P_4 - Tfv	0.03	0.874	**P_3-P_4 - TU**	0.02	0.382
P_3-P_4 - HAsfc9	0.01	0.854	**M_1-M_3 - DH**	0.02	0.765
M_1-M_3 - Asfc	0.07	0.849	**M_1-M_3 - HAsfc9**	0.09	0.937
M_1-M_3 - epLsar	0.07	0.854	**Rob M_3 - Tfv**	0.51	0.51
Rob M_1 - epLsar	0.5	0.599	**Rob M_3 - CCL**	0.5	0.575

In females, diet quality (DQ) and microwear variables showed a significant effect on incisal alveolar length (I_1-I_2), with the X term reaching over 95% confidence in each case. DQ (p X: 0.02) accounted for a positive linear effect on I_1-I_2, with a coefficient (β_1) of 0.501 and a semi-partial R^2 (spR^2) of 13.5% of the total variance (Table 5.2). Similarly, increases in *Asfc* (p X: 0.012), *Tfv* (p X: 0.025) and *HAsfc9* (p X < 0.001) accounted for rises in I_1-I_2 (β_1: 0.46, 0.57 and 0.62 respectively). In addition, the three variables explain 5%, 12.2% and 15.4% of the total variance in I_1-I_2. Microwear variables were found to influence alveolar premolar length (P_3-P_4) in females, although explaining a relatively small variance (Table N). *Tfv* (p X < 0.001) and *HAsfc9* (p X^2: 0.045) showed significant effects of X (β_1: 0.28) and X^2 (β_2: -0.23) terms respectively. There was a significant effect of *Asfc* (p X^2: 0.025) and *epLsar* (p X^2: 0.02) on

female molar alveolar length (M_1-M_3), relating to the X^2 term (β_2: 0.33 and 0.34 respectively), although these variables account for a small part of the variance in M_1-M_3 (spR^2: 7%). The variable *epLsar* (p X: 0.019) accounts for a negative effect (β_1: -18.52) on M_1 robusticity in females, with a large amount of variance explained (50%), although the contribution of X^2 is not relevant and may determine an overestimation of the spR^2. In each case, a significant effect of body size explained variations in the dependent variables (Figure 5.2, Figure 5.1).

There were significant effects of microwear on several morphological traits in the male subsample. Mandibular Centroid Size (CS) was positively correlated with *Tfv* (p X^2: 0.035, β_2: 0.24). I_1-I_2 was associated to *Asfc* (p: 0.033, β_1: 0.3) and *epLsar* (p: 0.035, β_1: -0.34), while P_3-P_4 and M_1-M_3 were significantly influenced by *HAsfc9* (p X^2: 0.047, β_2: -0.17 and p X: 0.005, β_1: -0.35 respectively). M_3 robusticity was found in a positive correlation with *Tfv* (p X: 0.047, β_1: 25.06 and p X^2: 0.012, β_2: 33.21). Beside microwear, other independent variables produced significant effects on the morphological traits analysed. P_3-P_4 (p X^2: 0.002, β_2: -0.51) was significantly correlated with Tool Use (TU). The effect of Diet Evenness (DH) on M_1-M_3 reached 95% significance (p X^2: 0.03, β_2: 0.21). Finally, there was a significant effect of Chewing Cycle Length (CCL) on M_3 robusticity (p X: 0.046, β_1: -16.31 and p X^2: 0.014, β_2: 15.52). The effect of body size on the correlation was high in most cases, as shown in Figure 5.2. The variance explained by the independent variables was small in many cases, but high for M_3 robusticity (Table 5.2).

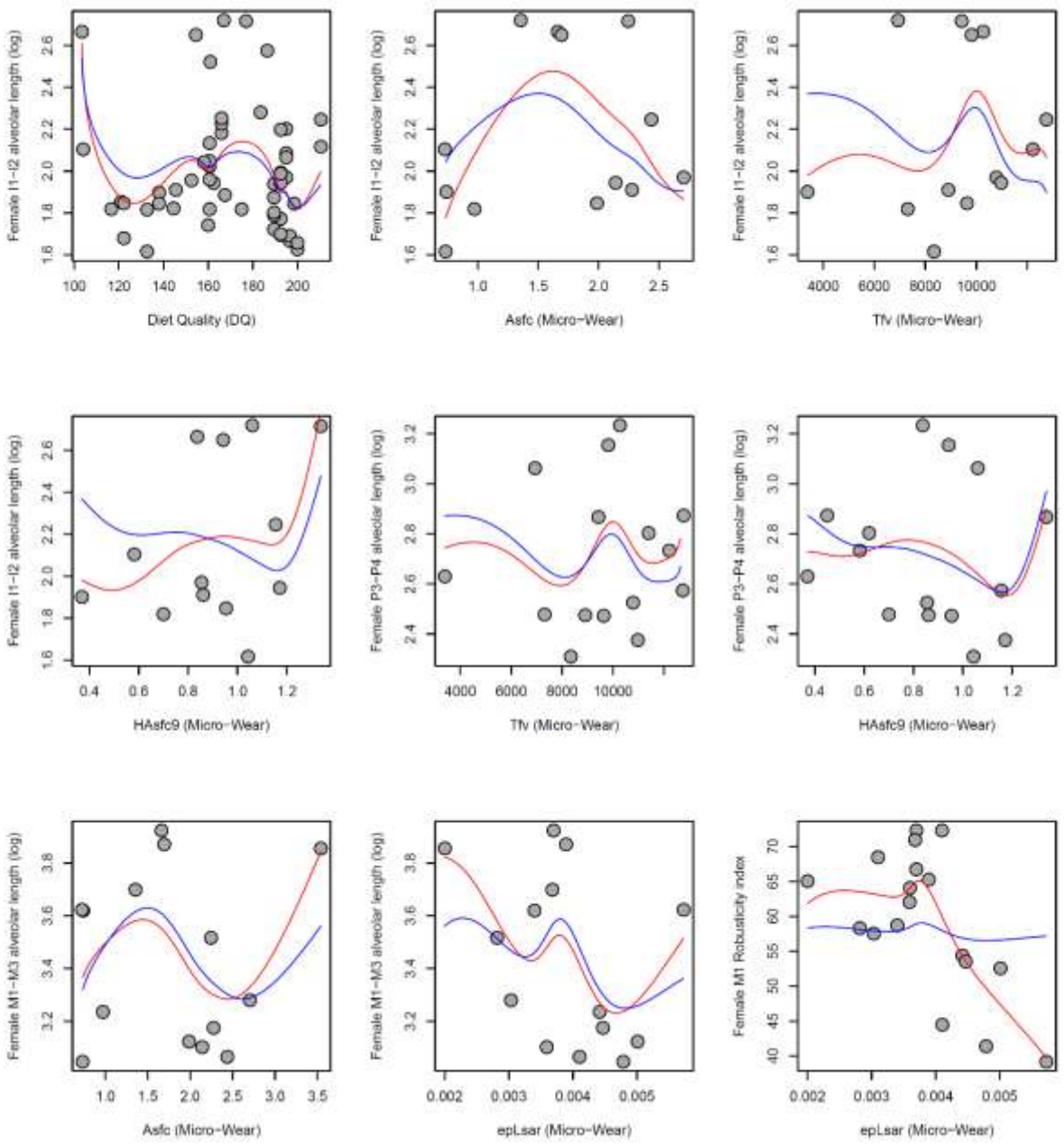

Figure 5.1 Scatterplots of the significant correlations for the female subsample. The red line represents the predictions based on the full model ($X+X^2+B$) between dependent and independent variables. The blue line represents the predictions based on body size only. The prediction lines are approximated by a Beziér polynomial curve. A marked overlap of the lines indicates that body size accounts for a large part of the variance explained by the full model.

Table 5.3 Terms and adjusted R^2 for the regressions performed using the female sample. The significant terms are shown in bold, except for regressions with poor statistical power, indicated by a negative adjusted R^2. The p-values for each term are available in Appendix 2.

		DQ	DH	Asfc	epLsar	Tfv	HAsfc9	CCL	FT	TU	EF
CS	**X**	0.039	0.023	0.003	-0.06	0.19	-0.058	0.287	0.043	0.011	-0.025
	X^2	-0.011	0.02	0.173	0.165	0.11	-0.088	-0.067	0.025	-0.042	0.029
	B	**0.299**	**0.292**	**0.317**	**0.289**	**0.313**	**0.285**	**0.209**	**0.322**	**0.309**	**0.299**
	R^2	0.81	0.82	0.85	0.85	0.86	0.82	0.84	0.77	0.75	0.76
I_1-I_2	**X**	**0.501**	0.188	**0.459**	-0.247	**0.565**	**0.623**	0.4	0.283	0.269	0.042
	X^2	-0.006	-0.01	-0.395	0.094	-0.053	-0.092	-0.053	-0.214	0.042	0.138
	B	**0.31**	**0.211**	**0.306**	**0.261**	**0.33**	**0.349**	**0.239**	**0.314**	**0.247**	**0.224**
	R^2	0.78	0.63	0.65	0.56	0.72	0.76	0.81	0.72	0.65	0.62
P_3-P_4	**X**	0.186	0.008	0.07	0.058	**0.275**	0.099	0.132	0.043	0.022	-0.12
	X^2	0.055	0.035	-0.183	-0.069	0.008	**-0.225**	0.105	0.109	-0.169	0.034
	B	**0.287**	**0.257**	**0.269**	**0.285**	**0.295**	**0.273**	0.222	**0.249**	**0.284**	**0.262**
	R^2	0.78	0.76	0.81	0.8	0.87	0.85	0.56	0.8	0.69	0.69
M_1-M_3	**X**	-0.002	-0.066	0.1	-0.093	0.234	-0.155	0.248	0.032	-0.086	-0.148
	X^2	0.013	-0.048	**0.327**	**0.338**	0.253	-0.122	-0.123	0.217	-0.059	0.033
	B	**0.347**	**0.352**	**0.283**	**0.273**	**0.285**	**0.28**	**0.198**	**0.341**	**0.367**	**0.363**
	R^2	0.59	0.56	0.85	0.85	0.85	0.78	0.79	0.58	0.57	0.56
Rob SY	**X**	-5.352	-4.339	-4.984	-2.091	17.354	-14.19	1.706	-1.945	-6.198	-16.01
	X^2	-0.474	0.22	-6.969	-9.051	1.316	-3.769	-1.513	3.959	-0.196	-1.041
	B	4.409	4.797	2.154	3.097	0.166	2.455	0.251	0.822	4.158	4.924
	R^2	-0.04	-0.05	-0.07	-0.04	-0.26	0.05	-0.54	-0.13	-0.04	-0.06
Rob M_1	**X**	24.189	-9.293	5.837	**-18.52**	1.162	-0.466	11.644	-3.627	4.74	1.29
	X^2	6.771	-8.546	-10.09	-13.02	-14.88	-10.44	5.802	2.751	3.091	-1.581
	B	2.12	0.003	0.614	**4.712**	-0.955	1.504	2.191	0.798	-1.342	-1.312
	R^2	-0.05	-0.05	-0.13	0.6	-0.65	-0.17	0.19	-0.22	-0.13	-0.2
Rob M_2	**X**	4.716	-11.98	-0.159	-4.596	3.366	-5.841	-5.862	-13.54	-6.756	-13.4
	X^2	9.606	0.591	3.851	0.569	2.238	-15.25	9.736	-4.735	1.995	9.336
	B	-0.103	-0.81	-4.697	-4.259	-4.177	-7.861	4.782	-0.697	-1.781	-1.651
	R^2	-0.2	-0.06	-1.11	-0.87	-1.02	-2.19	0.07	-0.34	-0.27	-0.16
Rob M_3	**X**	6.75	-4.948	-1.699	-7.752	11.911	-7.294	-4.985	-1.89	-5.114	-7.622
	X^2	3.508	-3.098	9.005	3.614	7.687	-16.36	4.923	-2.523	6.543	4.299
	B	0.401	-0.191	-4.968	-3.295	-1.954	-9.839	3.861	-1.949	-1.759	-0.988
	R^2	-0.08	-0.06	-0.99	-0.52	-0.37	-2.4	-0.19	-0.42	-0.12	-0.08

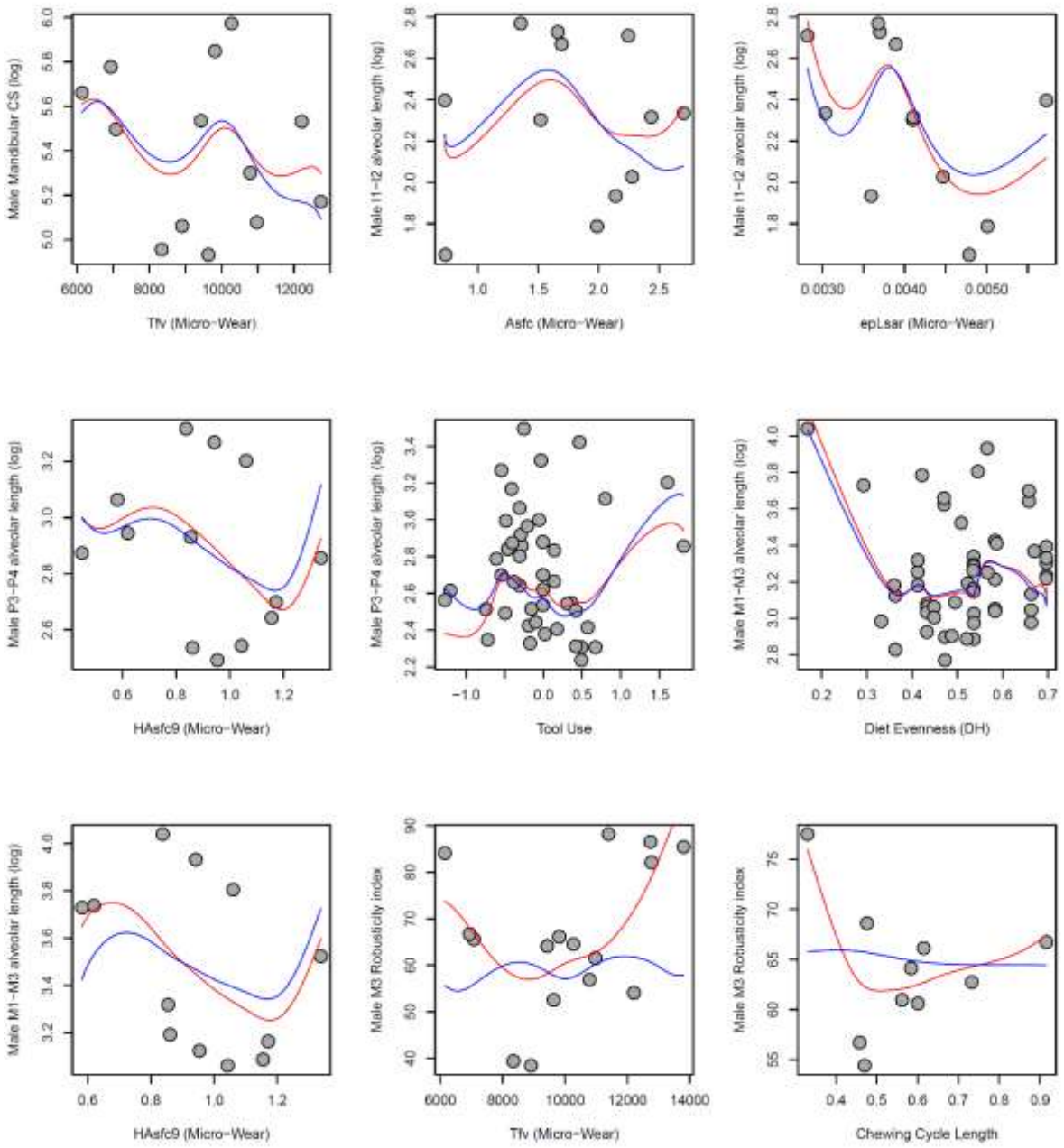

Figure 5.2 Scatterplots of the significant correlations for the male subsample. The red line represents the predictions based on the full model ($X+X^2+B$) between dependent and independent variables. The blue line represents the predictions based on body size only. The prediction lines are approximated by a Beziér polynomial curve. A marked overlap of the lines indicates that body size accounts for a large part of the variance explained by the full model.

Table 5.4 Terms and adjusted R^2 for the regressions performed using the male sample. The significant terms are shown in bold, except for regressions with poor statistical power, indicated by a negative adjusted R^2. Information about intercepts, standard errors and p-values for each term are available in Appendix 2.

		DQ	DH	Asfc	epLsar	Tfv	HAsfc9	CCL	FT	TU	EF
CS	**X**	0.03	0.096	-0.129	-0.024	0.168	-0.097	0.356	-0.167	0.012	-0.09
	X^2	-0.022	0.173	0.186	0.126	**0.238**	-0.032	-0.178	0.091	-0.22	-0.001
	B	**0.315**	**0.303**	**0.308**	**0.28**	**0.284**	**0.278**	**0.186**	**0.324**	**0.326**	**0.318**
	R^2	0.73	0.76	0.88	0.87	0.92	0.86	0.79	0.71	0.69	0.68
I_1-I_2	**X**	0.226	0.079	**0.303**	**-0.338**	0.244	0.208	0.502	-0.262	0.209	0.074
	X^2	0.003	0.003	0.301	0.139	0.327	0.141	-0.211	-0.07	0.031	0.156
	B	**0.272**	**0.248**	**0.321**	**0.276**	**0.279**	**0.305**	**0.159**	**0.247**	**0.265**	**0.269**
	R^2	0.68	0.65	0.79	0.72	0.78	0.66	0.86	0.58	0.62	0.64
P_3-P_4	**X**	0.119	0.155	-0.123	0.19	0.036	-0.16	0.346	-0.231	0.073	-0.122
	X^2	-0.115	0.145	0.033	0.014	-0.101	**-0.167**	-0.226	0.303	**-0.515**	-0.141
	B	**0.292**	**0.278**	**0.255**	**0.256**	**0.274**	**0.248**	0.086	**0.292**	**0.325**	**0.302**
	R^2	0.38	0.42	0.6	0.6	0.51	0.63	0.15	0.4	0.38	0.37
M_1-M_3	**X**	-0.19	0.013	-0.203	0.212	0.195	**-0.345**	0.157	0.086	-0.029	-0.116
	X^2	0.008	**0.21**	0.066	0.113	0.078	0.108	-0.056	0.1	-0.159	-0.067
	B	**0.301**	**0.305**	**0.264**	**0.281**	**0.276**	**0.252**	**0.302**	**0.3**	**0.325**	**0.32**
	R^2	0.72	0.76	0.85	0.86	0.85	0.94	0.67	0.71	0.69	0.7
Rob SY	**X**	-3.035	2.897	-12.04	-3.004	17.414	-21.45	4.585	-2.72	9.347	5.901
	X^2	-4.376	-0.325	-17.37	-15.77	7.432	-1.669	-11.21	7.434	-0.749	1.49
	B	-1.43	-1.128	0.565	2.898	4.462	1.887	-0.146	0.003	-0.367	0.862
	R^2	-0.15	-0.19	-0.10	-0.11	-0.09	-0.05	0.47	-0.1	-0.03	-0.02
Rob M_1	**X**	0.202	-10.77	11.595	-7.306	4.558	5.058	-15.53	9.627	1.84	-2.715
	X^2	6.494	-9.15	-7.834	-2.938	-9.133	-8.172	26.482	0.185	2.362	6.915
	B	0.667	1.023	2.942	**4.271**	1.371	2.316	6.605	1.212	0.201	0.348
	R^2	-0.13	-0.01	0.26	0.25	-0.19	-0.09	0.22	-0.02	-0.16	-0.16
Rob M_2	**X**	-0.649	-5.932	1.219	-8.241	4.481	4.144	-4.091	-5.487	-1.773	-5.719
	X^2	3.324	-1.405	8.006	2.601	4.947	-7.028	11.072	13.746	14.044	6.351
	B	-1.258	-1.218	-6.176	-6.4	-5.221	-6.743	1.339	-2.307	-2.625	-1.647
	R^2	-0.33	-0.26	-1.42	-1.25	-1.22	-1.89	-0.23	-0.22	-0.17	-0.23
Rob M_3	**X**	20.529	-10.79	4.294	-15.10	**25.06**	3.512	**-16.31**	17.953	-3.946	-8.008
	X^2	17.706	-9.007	4.8	-6.381	**33.21**	-9.174	**15.52**	-5.642	4.482	1.321
	B	-0.436	-1.929	-4.353	-4.351	5.559	-8.803	**5.22**	-4.109	-2.557	-2.057
	R^2	-0.13	-0.11	-0.81	-0.5	0.51	-1.93	0.58	-0.03	-0.17	-0.17

5.4 Discussion

Being primarily involved in processing food, the lower jaw is clearly adapted to resist the stresses of mastication, and evidence has been gathered to support the biomechanical interpretation of mandibular shape in primates (Hylander, 1979, 1985; Humphrey et al., 1999). In conformity with the assumption that differences in tooth size and mandibular robusticity account for differences in biomechanical profiles of the lower jaw, the trend of mandibular and dental reduction in *Homo* (including modern humans) has been considered to be the effect of food texture alterations in the diet of our ancestors (Wrangham and Carmody, 2010; Zink & Lieberman, 2016). By means of its improved food processing skills, the genus *Homo* had the chance of modifying the mechanical properties of its food, thus releasing the selective pressures on its own mastication. This hypothesis assumes a close link between feeding habits and masticatory anatomy, in particular concerning dental size and mandibular robusticity.

Across catarrhines, the link between the anatomy of the lower jaw and dietary adaptations seems elusive, at least concerning dental size and mandibular robusticity. Among the independent variables tested, most failed to predict size and robusticity (Tables 5.3 and 5.4). In a number of cases, significant effects of dietary and behavioural proxies were observed, although these accounted only for small amounts of the total variance of the morphological traits analysed (less than 10%, Table 5.2). It is possible that changes in dental size and mandibular robusticity occur as a "threshold response" to modifications in diet or feeding regime (Roff, 1996), rather than following a continuous variability. This would explain the absence of strong and consistent correlations in the data. Nevertheless, a dietary component is undeniably affecting the variability of dental size and mandibular robusticity.

Microwear was found to correlate with dental size, and its effects explained around 10% or more of the variance of the dependent variables, although only in few instances. Variations in the size of incisors were associated with changes in microwear patterns when *Asfc*, *Tfv* and *HAsfc9* were used as predictors. These variables record the patterns of dental wear due to contact with food and abrasion; they can reveal the types of foods consumed and their toughness (Scott et al., 2005; 2006). *Asfc* and *Tfv* are higher in primates eating seeds and fruit, and lower in species consuming leaves, while high values of *epLsar* indicate a diet made of tough food. Therefore, they are representative of food textural properties. As reported

above, the size of the incisors increases with *Asfc* and *Tfv* but drops when *epLsar* increases. These results indicate that smaller incisors are characteristic of species with a diet based on tough foods. Hylander (1975b) observed that colobines are well adapted to a leaf-eating strategy and bear incisors that are comparatively smaller than cercopithecines, which forage mostly on fruit. Furthermore, when papionins switch to a more folivorous diet following environmental changes, they make extensive use of front dentition (Jolly, 1970; Hylander, 1975b), supporting a possible evolutionary meaning of small incisors in the consumption of leaves. A similar pattern is suggested by the correlation between incisal alveolar length and diet quality (DQ), which revealed a significant effect of the latter on the former, with small DQ indices (typical of folivorous primates) associated to smaller incisors.

The regressions on mandibular robusticity produced the highest associations between morphological traits and dietary proxies, although only a few correlations were significant (Tables 5.3 and 5.4). Surprisingly, symphyseal robusticity is not significantly influenced by any of the independent variables, a fact that contradicts the usual predictions about this mandibular region. Indeed, the symphysis has often been considered as shaped to support the biomechanical stresses of incisal biting in primates (Hylander, 1975b; 1985; Daegling, 2001). Nevertheless, the robusticity index may not be enough to justify such a role: other factors may be dominant, such as its three-dimensional shape and orientation. Microwear (*epLsar* and *Tfv*) and Chewing Cycle Length (CCL) displayed relatively high power in predicting robusticity at the level of first and third molar, explaining about 50% of their variances (Table 5.2). Studies on the morphology of the mandibular corpus in primates suggested that robusticity may be involved in counteracting torsional and bending stresses during mastication (Hylander, 1979) and, in general, it is believed to resist masticatory strains. The results described here confirm that robusticity has a biomechanical meaning in the mandible. Indeed, M_3 robusticity changes positively with *Tfv* and negatively with CCL, indicating that less robust mandibular corpora are required when chewing hard, brittle foods, which require shorter chewing cycles than tough food, but higher forces applied (Ross et al., 2009b). Nevertheless, a contradictory result is found for M_1 robusticity in females, which decrease when *epLsar* increases.

In the light of what was observed across catarrhines, links between diet and anatomy are difficult to find and trying to estimate the diet of a fossil hominin based on its masticatory

morphology may be misleading and inaccurate. Nevertheless, certain features seem to be correlated with food properties rather than diet itself. According to the results described here, we should expect a trend of stasis or increase with time for incisal size in *Homo*, which has actually occurred. Indeed, while the size of postcanine dentition reduced during the Pleistocene, incisors underwent more complex modifications and increased in size during middle Palaeolithic (McHenry, 1984). Thanks to advanced food processing skills, the genus *Homo* could modify the mechanical properties of foods making them softer to chew. Food softening would result in a reduction of the time needed for chewing and to more gracile corpora. In this case, the changes in feeding habits in *Homo* would have probably released its masticatory apparatus from the need to perform long chewing, thereby reducing the selective pressures for maintaining a robust mandible. Therefore, the gracilisation of the mandibular corpus by relaxation of selective pressures on mastication (Calcagno & Gibson, 1988; Wrangham & Carmody, 2010) is in line with the current results.

The patterns observed for incisors and robusticity may not necessarily result from changes in diet or feeding habits, but they could be a by-product of other major structural changes in mandible and cranium. This would be consistent with the fact that different results are obtained using the female and male subsamples. This may be due to sexual distinction in the diet. Although differences in feeding habits between males and females of the same species have been reported (Harrison, 1983; Rose, 1994), this is not a common situation and it is difficult to believe that it could have produced differential masticatory adaptations in the two sexes of one species. However, sexual dimorphism accounts for major variations in the morphology of the catarrhine cranium (Plavcan, 2001).

The patterns observed across catarrhines support the hypotheses that look at food processing and the consequent food softening to explain the onset of mandibular and dental reduction in the genus *Homo*. Nevertheless, the relationship between anatomy and dietary proxies was not consistent among morphological traits and sexes, suggesting that these factors may have had a limited role in the trend of reduction, confined to the major dietary leaps faced by our ancestors. Considering the major modifications occurred in the hominin skull, it is necessary to check if allometry and encephalization may have had a major part in determining the variance in dental size and mandibular robusticity.

Chapter 6

Neuro-mandibular integration in humans and other African apes

6.1 Introduction

The human skull is the result of millions of years of morphological evolution that involved all its parts. The cranial base modified to fit the anatomical requirements of bipedal locomotion (Lieberman et al., 2000; Russo & Kirk, 2013). The hominin face underwent a progressive flattening (orthognathism) from the condition of marked prognathism in australopithecines (Trinkaus, 2003; Pearson, 2008; Holton et al., 2011). The neurocranium expanded to fit the extreme enlargement of the brain (Rightmire, 2004). Finally, the lower jaw reduced in size and robusticity, and appears to be particularly gracile in modern humans (Chamberlain & Wood, 1985; Emes et al., 2011). Although each skull region evolved under the influence of different factors, some of these changes occurred simultaneously and may be inter-related (Lieberman, 1995; Bilsborough & Rae, 2015). Since the skull regions are anatomically connected to each other, it is plausible to assume a reciprocal influence between them. Indeed, structural modifications in one skeletal region may produce changes in other regions, a phenomenon that goes under the name of morphological integration (Cheverud, 1982; Klingenberg, 2008). When integration occurs, the evolutionary meaning of morphological variability is difficult to assess; the changes in one region may be simple by-products of changes in a contiguous region, and a trend that appears to be adaptive is a side effect of structural modifications on adjacent regions (Klingenberg, 2008). The increase in brain size, or encephalization, and the consequent changes in the size and shape of the neurocranium are the most prominent transformations in the hominin skull. *Homo sapiens* exhibits a brain size to body size ratio that is unparalleled among mammals (Leutenegger, 1982; Herculano-

Houzel, 2009). In addition, a morphological reorganisation from the elongated appearance of the brain in primates and Pleistocene hominins to a more globular shape has occurred in *H. sapiens* (Lieberman et al., 2002). This reorganisation is believed to be one of the main factors contributing to the cognitive distinctiveness of modern humans (Bruner, 2004; Roth & Dicke, 2005; Holloway et al., 2009), and some authors argued that encephalization may have severely constrained the evolution of the skull (Lieberman, 1995; Bruner & Ripani, 2008; Bastir et al., 2010).

Besides encephalization, other trends in the evolution of the skull contributed to human uniqueness. The reduction in dental and mandibular dimensions and robusticity (Brace, 1963; McHenry, 1982; Chamberlain & Wood, 1985; Emes et al., 2011) is of particular importance for understanding hominin interactions with their environment. Food processing skills and changes in subsistence strategies have been proposed as pivotal to the onset of the trend of reduction (Wrangham & Carmody, 2010; Zink & Lieberman, 2016). Since the main role of the masticatory apparatus is food processing, it is not surprising that the main hypotheses about the trend of dental and mandibular reduction are linked to diet. Nevertheless, the lower jaw is connected to the cranium by the temporomandibular joint; therefore, mandible and teeth are potentially prone to the structural changes caused by encephalization (Bookstein et al., 2003; Bastir et al., 2005). The idea of mandibular and dental reduction as a by-product of brain evolution is supported from a developmental point of view. Indeed, in ontogeny, the mandible is the last region of the skull to finish morphological development, following the cranial base, neurocranium and face respectively (Bastir et al., 2006). Therefore, the neurocranium may substantially constrain the development of the mandible.

To determine if the trend of reduction is affected by encephalization, it is necessary to quantify the level of integration between the lower jaw and the neurocranium and to test for dependence between neurocranium morphology and lower jaw shape, size and robusticity. Analysing the patterns of neuro-mandibular integration only in *H. sapiens* would not be sufficient to infer the causal relationship between dental/mandibular reduction and encephalization. A comparison between humans and related species is fundamental to reject the possibility that the reduction in jaw robusticity and dental size is the structural effect of neuro-mandibular integration in all hominoids. African apes are the closest living relatives of humans (Wildman et al., 2003; Mikkelsen et al., 2005) and have been previously used in

studies of human skull integration (Bastir & Rosas, 2004; Bastir et al., 2005; Singh et al., 2012). Although *H. sapiens* and *P. troglodytes* are genetically more similar to each other than the latter is to gorillas (Ruvolo, 1997), there are more craniofacial similarities among non-human African apes than between those and humans (Mitteroecker et al., 2004). This is mostly due to differences in cranial ontogeny between *H. sapiens* and other African apes (Mitteroecker et al., 2004). Nevertheless, differences in ontogeny, allometry and sexual dimorphism (Shea, 1983; Leigh & Shea, 1995, 1996) exist among non-human African apes. Therefore, the use of both gorillas and chimpanzees can help to clarify the influence of allometry and sexual dimorphism on the pattern of neuro-mandibular integration.

In this work, the patterns of morphological integration between the neurocranium and the lower jaw are analysed by adopting a Geometric Morphometric approach. The hypothesis of interdependence between neurocranium and mandibular shape is tested on a sample of *Pan*, *Gorilla* and *H. sapiens*, to determine if the covariation between the two skull regions is shared among African apes. The relative influence that neurocranium, sex and allometry have on the morphological variability of the lower jaw is assessed. In addition, the correlations between the mandibular integration pattern, robusticity and dental size are analysed to evaluate the level of dependence between the neurocranium and traits associated with mandibular and dental reduction. The results suggest that the neurocranium significantly affects the evolution of mandibular morphology in African apes, and suggest that the globular reorganisation of the brain may have been important in shaping the gracile morphology of the lower jaw in *H. sapiens*, but not in fossil hominins.

6.2 Material and methods

6.2.1 The sample

The sample used in this study consists of 64 mandibles and matching crania belonging to the species *Gorilla gorilla* (22 individuals, 8 females and 14 males), *Pan troglodytes* (22 individuals, 13 females and 9 males) and *Homo sapiens* (20 individuals, 10 females and 10 males). The specimens used belong to adult individuals of known sex. A complete summary of the sample

is presented in Table 6.1. The eruption of the third molar is used to estimate adulthood. The specimens are available from the online database of the Primate Research Institute at Kyoto University (KUPRI) and the primate and human skeletal collections hosted at the Smithsonian Institution. Further details about the sample are provided in Chapter 2 and in Appendix 1. All the specimens were available in CT-scan format.

Table 6.1 Sample size divided per species and sex. The specimens were available in CT-scan format.

	Individuals	**Females**	**Males**
Gorilla gorilla	22	8	14
Pan troglodytes	22	13	9
Homo sapiens	20	10	10
Total	64	31	33

The data used consists of 3D coordinates, linear measurements and metric indices measured on the virtual reconstructions. A series of 28 landmarks was recorded on the virtual 3D surfaces of the mandibles and 15 landmarks were collected on the neurocranium. The 3D landmark configurations were recorded using the software Amira (version 5.4.5, FEI Visualization, Berlin), and were chosen to describe the overall morphology of the anatomical regions analysed. A graphical representation of the landmarks is shown in Figure 2.2, in Chapter 2, and their definition is provided in Appendix 1. The landmarks of both configurations were aligned through a Generalised Procrustes Analysis (GPA) using Procrustes superimposition (Zelditch et al., 2012), thus minimising the effect of size and spatial orientation. The resulting aligned configurations were used to extract size and shape information for mandibles and neurocrania of each individual in the sample. Centroid Size (CS) was used as a proxy for mandible and neurocranium size (Dryden & Mardia, 1998), and shape was approximated by the aligned 3D coordinates. Alveolar length and indices of mandibular robusticity were measured on the virtual reconstructions following the

procedures described in Chapter 2. Alveolar length was used to approximate dental size of incisors (I_1-I_2), premolars (P_3-P_4) and molars (M_1-M_3), and robusticity indices were measured at the symphysis (Rob SY), and below each molar (Rob M_1, M_2 and M_3).

6.2.2 Quantifying neuro-mandibular integration

The aligned 3D landmarks of the mandible and neurocranium are used to analyse the main pattern of morphological integration between the two anatomical regions. As a preliminary step, the effects of size (allometry) and sex (dimorphism) on the morphological variability of each species are assessed. The aligned coordinates are tested for allometry, sex-related differences and sex-allometry interaction by means of Procrustes ANOVA (Klingenberg & McIntyre, 1998). This method fits a linear model to quantify the amount of shape variation that can be attributed to one or more independent variables (categorical or continuous). Statistical significance is calculated by randomization of residuals (Collyer et al. 2015). When a significant effect of sex or size is found, the shape data are corrected accordingly, by extracting the residuals of the linear model fitted by the Procrustes ANOVA. The corrected and raw data are used in the following integration analysis to define if sex and size are significant in determining the pattern of neuro-mandibular integration. The Procrustes ANOVA method applied here is embedded in the R package “geomorph” (Adams & Otárola-Castillo, 2013).

Singular Warp (SW) analysis was performed to quantify the morphological integration between neurocranium and mandible. SW is a Partial Least Squares performed within a morphometric context (Bookstein et al., 2003). It computes the linear combinations of two sets of variables (two landmark sets) that have the highest mutual predictive power. SW produces vectors of shape variations and individual scores that maximise covariation between the two sets of landmarks analysed, and provides an estimate of covariation (here referred to as Rpls) based on Pearson’s correlation test (Hollander et al., 2013). To calculate the significance of the integration test, the estimated value of integration is compared to the distribution of values obtained by randomly permuting (1000 times) the individuals. When the estimated covariation is larger than the permuted distribution, integration is significant (Bookstein et al. 2003). The first singular warp is used to visualize the major shape covariation

patterns between neurocranium and mandible. For each species, the mandible landmarks were aligned by Procrustes superimposition: the individuals showing the smaller Procrustes distance from the mean shape of their species were chosen for the visualization. The 3D surfaces of these individuals are warped to fit the landmark configuration of the mandible and neurocranium mean shape by using Thin Plate Spline (TPS; Bookstein, 1989). The warped surfaces (now representing the species mean shapes) are warped along the first singular warp using TPS. The resulting surfaces represent the shape covariation of mandible and neurocranium along the first singular warp. The Singular Warps analysis and the TPS warping are performed in the R packages "geomorph" (Adams & Otárola-Castillo, 2013) and "Morpho" (Schlager, 2013) respectively.

6.2.3 Redundancy analysis

Redundancy Analysis (RDA) (Legendre & Legendre, 2012) is a statistical ordination method used to extract the relative and joined contributions of a set of independent variables (explanatory) on a set of dependent variables (response). It uses multiple linear regressions to extrapolate a matrix of predicted values that are then ordinated by Principal Component Analysis (Legendre & Legendre, 2012). RDA provides the joined and unique contributions of the independent on the dependent variables as values of adjusted R^2 (Palmer, 1993). RDA is performed on each species to determine the relative influence of sex, size and the neuro-mandibular covariation pattern to the variance of mandibular shape. The shape of the mandible consists of a matrix of individual PC scores extracted from the PCA performed on the mandibular landmarks aligned by Procrustes superimposition. The mandible SW scores of the first singular warp are used to describe the pattern of neuro-mandibular covariation. Sex and mandibular size are used as additional independent variables. The statistical significance of the neuro-mandibular integration pattern is assessed by applying random permutations of the dependent variables. To understand if the integration between mandible and neurocranium could affect mandibular and dental reduction, RDA is performed on alveolar lengths and robusticity indices (dependent variables). Sex and mandibular size are used as additional independent variables. The RDA is performed by using the R package "vegan" (Dixon, 2003).

6.3 Results

6.3.1 Shape allometry and sexual dimorphism

G. gorilla and *H. sapiens* show a significant correlation between shape and size in both mandible and neurocranium. In *Gorilla*, Procrustes ANOVA between shape and size yields a R^2 of 0.15 (p: 0.001) for the mandible and a R^2 of 0.25 (p: 0.001) for the neurocranium. In *H. sapiens*, size is significantly correlated with mandibular (p: 0.002) and neurocranial (p: 0.022) shape, but it does not explain a large amount of the total variance (R^2: 0.12 and 0.1 respectively). Sex-related differences are found in the mandibular shape of *G. gorilla* (R^2: 0.09, p: 0.013) and *H. sapiens* (R^2: 0.09, p: 0.015), but not in the neurocranium. Mandibular shape differences between the sexes are not the result of sexual dimorphism in size, as indicated by the non-significant sex-size interaction terms in the models tested in the Procrustes ANOVA. No significant allometric signal or sex-related differences are found in the mandible and neurocranium of *P. troglodytes*. Tables 6.2 and 6.3 reports the results of the Procrustes ANOVA for the three species.

Table 6.2 Results of the Procrustes ANOVA for the shape of the mandible. The relationship between shape, size (Centroid Size of the landmark configuration), sex and their interaction (Size + Sex) is reported. Significant p-values are shown in bold.

Gorilla gorilla	**DF**	**F**	**R^2**	**p-value**
Size	1	3.841	0.15	**0.001**
Sex	1	2.239	0.09	**0.013**
Size + Sex	1	0.803	0.03	0.564
Pan troglodytes	**DF**	**F**	**R^2**	**p-value**
Size	1	1.091	0.05	0.356
Sex	1	0.904	0.04	0.442
Size + Sex	1	0.852	0.04	0.456
Homo sapiens	**DF**	**F**	**R^2**	**p-value**
Size	1	2.458	0.12	**0.002**
Sex	1	1.893	0.09	**0.015**
Size + Sex	1	0.621	0.03	0.765

Table 6.3 Results of the Procrustes ANOVA for the shape of the neurocranium. The relationship between shape, size (Centroid Size of the landmark configuration), sex and their interaction (Size + Sex) is reported. Significant p-values are shown in bold.

Gorilla gorilla	**DF**	**F**	**R^2**	**p-value**
Size	1	7.14	0.25	**0.001**
Sex	1	1.481	0.05	0.111
Size + Sex	1	1.339	0.05	0.130
Pan troglodytes	**DF**	**F**	**R^2**	**p-value**
Size	1	2.042	0.09	0.071
Sex	1	1.667	0.07	0.087
Size + Sex	1	0.724	0.03	0.544
Homo sapiens	**DF**	**F**	**R^2**	**p-value**
Size	1	2.09	0.11	**0.022**
Sex	1	0.824	0.04	0.532
Size + Sex	1	0.618	0.03	0.748

6.3.2 Shape integration

Singular Warp analysis reveals a significant pattern of integration between mandible and neurocranium in all the species here tested. The results of the analysis are reported in Table 6.4. The shape variations associated with the first singular warp are shown in Figures 6.1, 6.2 and 6.3. The Partial Least Squares performed on the aligned landmarks of *G. gorilla* returned an Rpls of 0.88 (p: 0.005). The reduction of parietal breadth and cranial length, as well as the shortening of the zygomatic arch in the neurocranium of *G. gorilla*, are associated with the decrease of ramus breadth and corpus height in the mandible, with a sizeable reduction in the bucco-lingual dimension of the molar row (Figure 6.1). In *P. troglodytes*, the integration between the mandible and neurocranium (Rpls: 0.80, p: 0.021) is explained by the covariation between the major axes of the cranial vault (length and breadth) and changes in corpus height, ramus breadth and the condyles in the mandible. In particular, a narrower vault and shorter zygomatic arch are accompanied by an increase in mandibular corpus height, a narrower ramus displaying a reduced gonial angle and a less robust appearance of the condyles (Figure 6.2). In *H. sapiens*, mandibular corpus and ramus height are associated with

modifications in the overall geometry of the neurocranium (Rpls: 0.88, p: 0.011), in particular in the shape of the lambdoid region. Lambdoid flattening, resulting in a lowered position of the opisthocranion, is associated with reduced height for both corpus and ramus of the mandible. In the ramus, this pattern is determined by a less upward projecting coronoid process, which is instead more developed in cranial vaults with rounded appearance and less elongated (Figure 6.3). When corrected for the effect of size, the covariation between mandible and neurocranium shape in both *G. gorilla* and *H. sapiens* stays significant (p:0.025 and p: 0.039 respectively). This integration was found to be non-significant in *G. gorilla* when the data are corrected for the effect of sex.

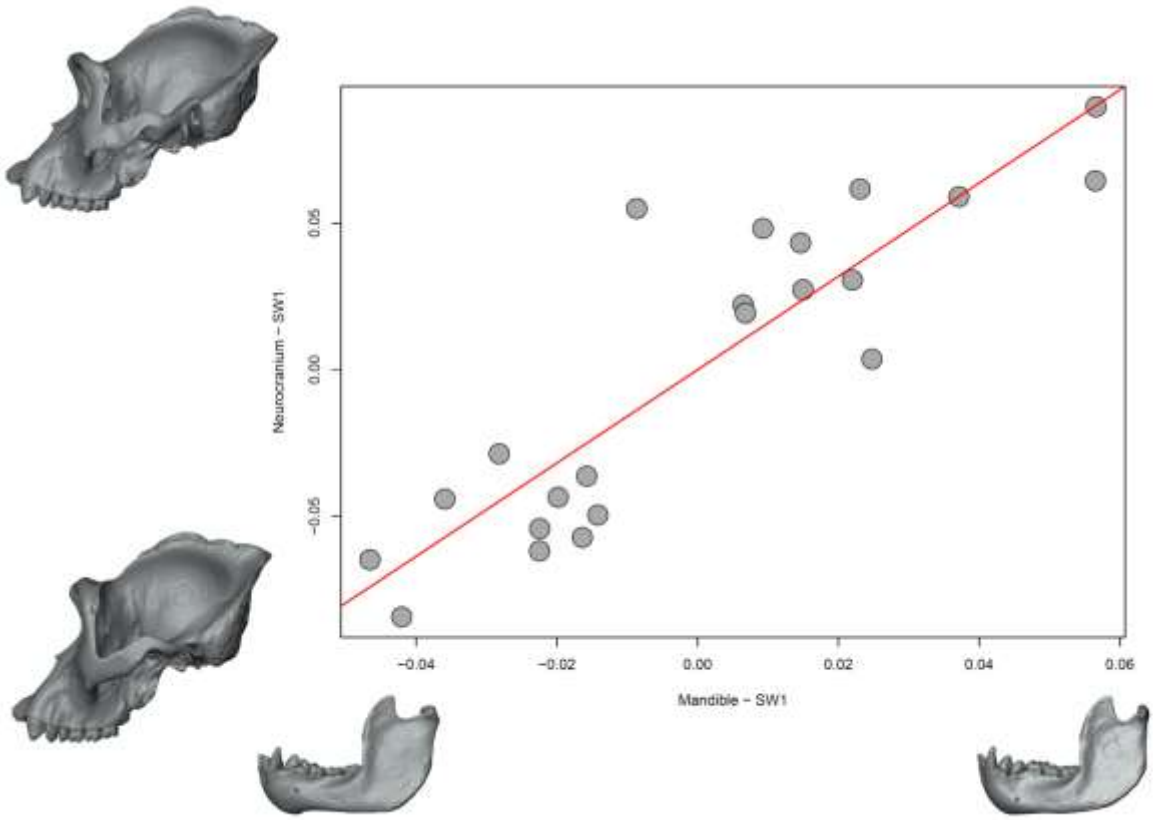

Figure 6.1 First Singular Warp maximising the covariation between neurocranium (Y axis) and mandibular (X axis) shapes in *Gorilla gorilla*. The shape variations of mandible and neurocranium along the first singular warp (SW1) are shown as Thin-Plate-Spline warped surfaces, and are displayed along the respective axes. The shape differences along one axis represent the shape variations associated with the changes in shape along the other axis. Each surface corresponds to the shape at minimum and maximum of its axis. The warped surfaces show how changes in the neurocranium influence the shape of the mandible. See Section 6.3.2 for further descriptions of the shape variations. Variations are meaningful only for neurocranium and mandible, not for face. See Figure 2.2, Chapter 2, for landmark configurations.

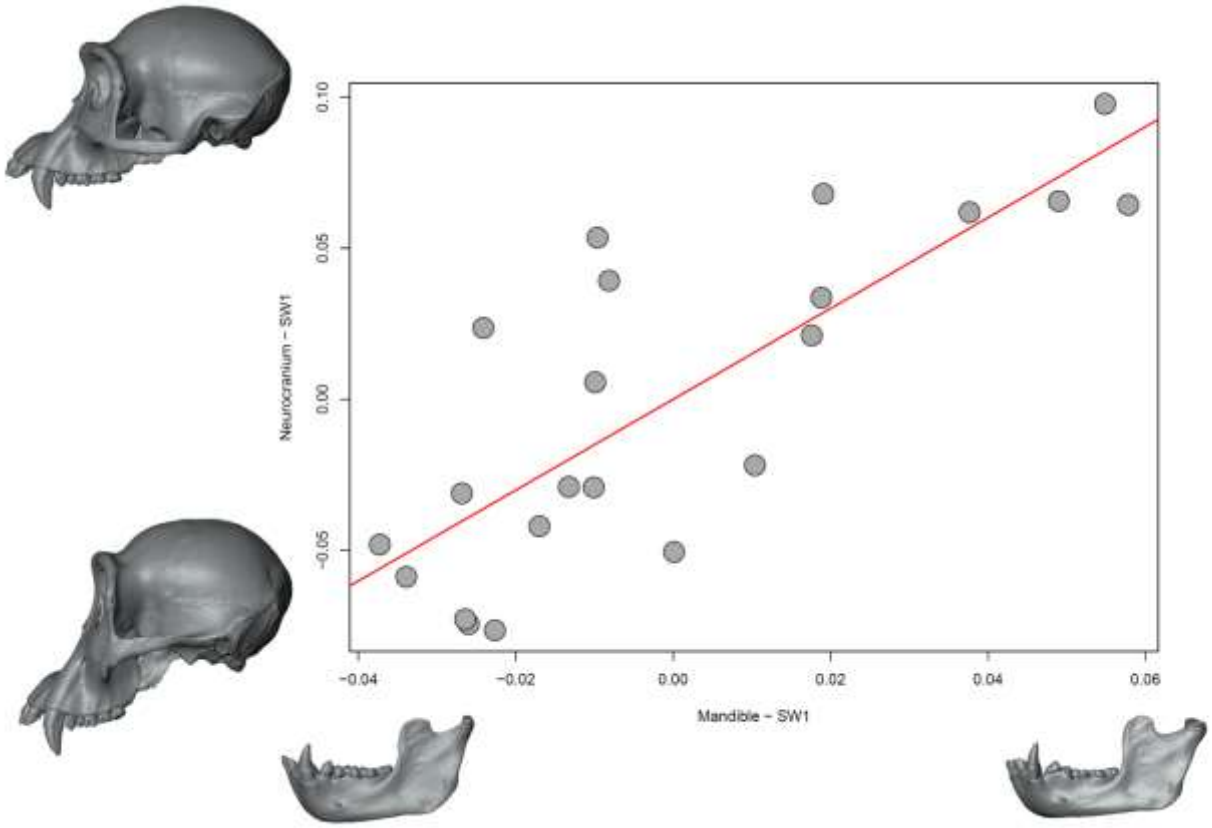

Figure 6.2 *First Singular Warp maximising the covariation between neurocranium (Y axis) and mandibular (X axis) shapes in* Pan troglodytes*. The shape variations of mandible and neurocranium along the first singular warp (SW1) are shown as Thin-Plate-Spline warped surfaces, and are displayed along the respective axes. The shape differences along one axis represent the shape variations associated with the changes in shape along the other axis. Each surface corresponds to the shape at minimum and maximum of its axis. The warped surfaces show how changes in the neurocranium influence the shape of the mandible. See Section 6.3.2 for further descriptions of the shape variations. Variations are meaningful only for neurocranium and mandible, not for face. See Figure 2.2, Chapter 2, for landmark configurations.*

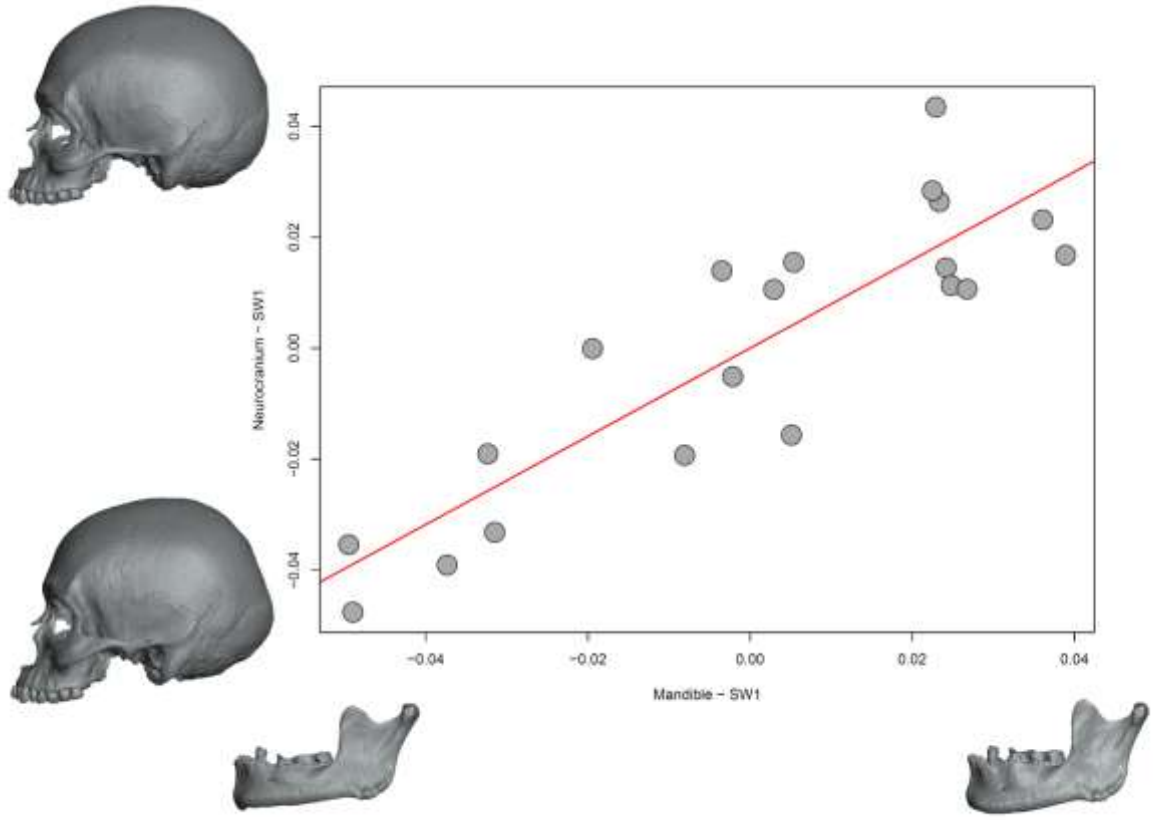

Figure 6.3 First Singular Warp maximising the covariation between neurocranium (Y axis) and mandibular (X axis) shapes in *Homo sapiens*. The shape variations of mandible and neurocranium along the first singular warp (SW1) are shown as Thin-Plate-Spline warped surfaces, and are displayed along the respective axes. The shape differences along one axis represent the shape variations associated with the changes in shape along the other axis. Each surface corresponds to the shape at minimum and maximum of its axis. The warped surfaces show how changes in the neurocranium influence the shape of the mandible. See Section 6.3.2 for further descriptions of the shape variations. Variations are meaningful only for neurocranium and mandible, not for face. See Figure 2.2, Chapter 2, for landmark configurations.

Table 6.4 Singular Warps results showing the estimate of morphological integration (R pls) between mandible and neurocranium shape, and relative p-values. Size- and sex-corrected singular warps were not calculated for *P. troglodytes* because, in this species, mandible and neurocranium shape are not significantly correlated with size and sex (see Table 6.3). For further detail on the method and calculations, see main text of this chapter. Significant p-values are shown in bold.

	Procrustes aligned coordinates	
	R pls	**p-value**
Gorilla gorilla	0.88	**0.005**
Pan troglodytes	0.8	**0.021**
Homo sapiens	0.88	**0.011**

	Coordinates size corrected (Residuals)	
	R pls	**R pls**
Gorilla gorilla	0.83	**0.025**
Pan troglodytes	-	-
Homo sapiens	0.86	**0.039**

	Coordinates sex corrected (Residuals)	
	R pls	**R pls**
Gorilla gorilla	0.74	0.226
Pan troglodytes	-	-
Homo sapiens	0.9	**0.002**

6.3.3 Variance explained by integration

The redundancy analysis shows that the pattern of neuro-mandibular covariation explains significant fractions of the overall mandibular shape variation in each species. The results of the redundancy analysis are shown in Table 6.5. In *G. gorilla*, the neuro-mandibular shape covariation accounts for a 16% of the mandibular shape variance, but 7% comes from joined contributions of sex and size effects. The resulting unique 9% of contribution from the neuro-mandibular covariation is statistically significant (p: 0.001). In *P. troglodytes*, the covariation pattern shows a unique contribution of 20% (p: 0.001) of the total shape variance of the mandible, and no joined contribution of sex or size is found. In *H. sapiens*, 14% of the

mandibular shape variance is affected by the pattern of neuro-mandibular integration (p: 0.001); sex and size do not contribute to that percentage.

Metric data of alveolar lengths and robusticity are used to determine the effect of neurocranium shape on the measurements traditionally linked to dental and mandibular reduction. A significant correlation exists between the neuro-mandibular pattern of covariation and molar alveolar length in *G. gorilla* (Variance: 45%, p: 0.001), and allometry and sexual dimorphism do not contribute to this pattern. No other metric variables are significantly affected by neuro-mandibuarl integration in *G. gorilla* (Table 6.5). In *P. troglodytes*, premolar (Variance: 32%, p: 0.006) and molar alveolar lengths (Variance: 41%, p: 0.003) are subject to the effects of neurocranium shape variations; sex and size explain 7% of the neuro-mandibular contribution to the variance of premolar alveolar length (Table 6.5), therefore, the unique contribution of the neurocranial shape changes is 25%. The neuro-mandibular integration in *H. sapiens* produces a significant effect on incisor alveolar length (Variance: 51%, p: 0.003) and robusticity measured below M_1 (Variance: 38%, p: 0.012), with minor effects of sex and size.

Table 6.5 Results of the Redundancy Analysis to assess the contributions of neuro-mandibular integration to the variance of mandibular shape (PC scores), alveolar lengths (I_1-I_2, P_3-P_4 and M_1-M_3) and robusticity indices (Rob SY, M_1, M_2 and M_3). The joined contribution of sex, size and neuro-mandibular integration (**N-M** x **Sex** x **Size**) and the unique contribution of neuro-mandibular integration (**N-M | Sex** x **Size**) are reported. In addition, the table reports the contribution of sex and size to the variance explained by neuro-mandibular integration (**Sex** x **Size | N-M**). The contributions are expressed as percentage of the total variance. Significant p-values are shown in bold.

	Gorilla gorilla			
	N-M x **Sex** x **Size**	**N-M | Sex** x **Size**	**Sex** x **Size | N-M**	**p-value**
Mandible shape	16 %	9 %	7 %	**0.004**
I_1-I_2	27 %	6 %	21 %	0.144
P_3-P_4	12 %	0 %	12 %	0.43
M_1-M_3	45 %	45 %	0 %	**0.001**
Rob SY	3 %	0 %	3 %	0.308
Rob M_1	6 %	0 %	6 %	0.47
Rob M_2	1 %	0 %	1 %	0.593
Rob M_3	29 %	16 %	13 %	0.053
	Pan troglodytes			
	N-M x **Sex** x **Size**	**N-M | Sex** x **Size**	**Sex** x **Size | N-M**	**p-value**
Mandible shape	20 %	20 %	0 %	**0.001**
I_1-I_2	4 %	0 %	4 %	0.352
P_3-P_4	32 %	25 %	7 %	**0.005**
M_1-M_3	41 %	41 %	0 %	**0.002**
Rob SY	2 %	0 %	2 %	0.647
Rob M_1	1 %	0 %	1 %	0.893
Rob M_2	0 %	0 %	0 %	0.712
Rob M_3	0 %	0 %	0 %	0.928
	Homo sapiens			
	N-M x **Sex** x **Size**	**N-M | Sex** x **Size**	**Sex** x **Size | N-M**	**p-value**
Mandible shape	14 %	14 %	0 %	**0.001**
I_1-I_2	51 %	51 %	0 %	**0.003**
P_3-P_4	1 %	0 %	1 %	0.361
M_1-M_3	14 %	14 %	0 %	0.077
Rob SY	2 %	2 %	0 %	0.253
Rob M_1	38 %	37 %	1 %	**0.008**
Rob M_2	0 %	0 %	0 %	0.52
Rob M_3	6 %	3 %	3 %	0.226

6.4 Discussion

6.4.1 Neuro-mandibular integration

The physical connection between the different skull regions implies a certain level of mutual influence on their development and evolution (Klingenberg, 2008; Bastir et al., 2010). Therefore, it is not surprising that the neurocranium and mandible display significant morphological integration in humans and other African apes in the analysis here. Nevertheless, this pattern has never received explicit consideration, although other authors recognise the presence of morphological integration between the mandibular ramus and the temporal bone (Bastir et al., 2004). The findings that mandible and neurocranium changes accordingly in different species (Figure 6.2) are unexpected. Certain mandibular features appear associated with similar neurocranium variations in both *H. sapiens* and other African apes. In *G. gorilla*, integration is influenced by sexual dimorphism, and the patterns observed are not in accordance with the other species in the sample, but homologous structures are involved. In the three species, the shortening of neurocranial length is associated with changes in the breadth of the mandibular ramus (Figure 6.1, 6.2 and 6.3), although ramus breadth increases in *G. gorilla* and decreases in *P. troglodytes* and *H. sapiens*. In *P. troglodytes* and *H. sapiens*, the height of the mandibular corpus increases while the neurocranium shortens and becomes more globular. These results suggest that the neurocranium may act as a structural constraint in the development of the lower jaw. Part of the mandibular shape variance (see Table 6.5) is indeed explained by the pattern of neuro-mandibular covariation; therefore, the evolution of the neurocranium may help to unravel the modifications that took place during the evolution of the mandible in the genus *Homo*. The development of the neurocranium constrains that of the mandible, rather than vice versa, and this observation is supported by the temporal sequence of morphological development in the human skull. The shape of the lower jaw ends its development as the last of the skull regions in modern humans (Bastir et al., 2006). Although a reciprocal effect is possible during the early stages of development, the changes imposed on the adult form of the lower jaw may be controlled by the spatial demands of the neurocranium, the size of which modified considerably during human evolution (Leutenegger, 1982; Rightmire, 2004).

6.4.2 The neurocranium as a constraint

The covariation between neurocranium shape and mandibular corpus height has important implications for the evolution of the lower jaw. Mandibular "gracilisation" and tooth size reduction are considered among the major trends in the evolution of the hominin skull (McHenry, 1982; Emes et al., 2011). Robusticity is approximated by the width to height ratio of mandibular corpus, usually measured below the first molar, and it is known for its role in counteracting torsional and bending forces during mastication in primates (Hylander, 1979; 1985). Increases in corpus height result in a reduction of mandibular robusticity, as observed in the evolution of the genus *Homo* (Chamberlain & Wood, 1985). The results of the Redundancy Analysis support the idea that variations in robusticity are subject to changes in the shape of the neurocranium in *H. sapiens* (Table 6.5). Incisor size seems to increase when the neurocranium is more rounded and brachycephalic, probably because the mandible is less constrained along the coronal plane (Figure 6.3). These effects are linked to occipital alterations that are typical of modern human variability, such as the position of the opisthocranion (Figure 6.2), which encompasses the variation from brachycephalic to dolichocephalic skulls (Lahr, 1996). The descriptions of early upper Palaeolithic human skulls include dolichocephaly as a distinctive trait of this group (Lieberman, 1995). The results gathered here suggest that certain aspects of mandibular and dental reduction in *H. sapiens* may have been driven by structural changes elsewhere, rather than biomechanical requirements of the lower jaw. As highlighted by the Redundancy Analysis, neurocranium shortening has the potential to affect negatively the dimensions of molars and premolars in African apes (Table 6.5), but this is not the case for modern humans. Postcanine dentition is not significantly altered by the pattern of neuro-mandibular integration in *H. sapiens*, thus indicating that the Holocene trend of reduction in postcanine tooth size (Brace, 1979; Pinhasi & Meiklejohn, 2011) cannot be credited to shape changes in the neurocranium. These considerations may not be applicable to the trend of mandibular and dental reduction observed in Pleistocene *Homo*. In fact, the neuro-mandibular integration in *H. sapiens* involves shape variations that are unparalleled in other hominins, whose neurocranium developed along the anteroposterior axis, a pattern shared by Pleistocene hominins and other extant primates (Lieberman et al., 2002).

The results presented above support the hypothesis that the trend of mandibular and dental reduction is under the influence of neurocranium shape changes, at least in *H. sapiens*. The marked restructuring that occurred in the human skull can partially explain the low mandibular robusticity observed in this species, but not the differences observed in postcanine dentition. These findings highlight the importance of postulating multifactorial hypotheses to explain human evolutionary trends, and suggest that structural, non-adaptive factors had a larger influence on human morphological evolution than previously thought.

Chapter 7

Discussion and conclusions

7.1 Rethinking dental and mandibular reduction

Human evolution is an ever-changing field. The studies on the Denisovan genome (Gibbons, 2011; Stringer & Barnes, 2015) and the recent discovery of *Homo naledi* in South Africa (Stringer, 2015; Schroeder et al., 2017) are examples of how new discoveries can affect well-established opinions in human evolutionary studies. In addition, several branches of biology provide palaeoanthropologists with the raw theoretical material to test their hypotheses in the light of new knowledge on primate and human behaviour, ecology and evolution. Therefore, advancements in many disciplines can modify our perception of human evolution. These are the main reasons why the ideas and concepts about the biological history of our ancestors are so mutable. Nevertheless, certain hominin evolutionary trends seem to be quite stable, despite the many discoveries that have followed since the time they were first described. The trends of dental reduction and gracilisation of the lower jaw in the Pleistocene and Holocene has received remarkable attention by the scientific community, and the reduction in postcanine teeth, incisors and mandibular robusticity have been confirmed in the work of several authors (Coon, 1955; Calcagno, 1986; Chamberlain & Wood, 1985; Brace et al., 1987; Humphrey et al., 1999; Pinhasi & Meiklejohn, 2011).

The results presented above describe the same morphological variations highlighted by previous studies (Chapter 3). These findings represent an additional validation of the descriptions reported previously, thus indicating that the gracile mandibles and small teeth of modern humans represent a well-established feature of the evolution of our species and its ancestors. Nevertheless, the claim that a gracile mandible and reduced dental dimensions are peculiar to the genus *Homo* needs revision. Based on the present results, the genus *Homo*

is clearly clustered in two main groups in terms of robusticity and dental size: early *Homo* (corresponding to species of the lower Pleistocene) and later species (from middle to late Pleistocene and Holocene). Early *Homo* exhibits a lower jaw as robust as those of the australopithecines (Chapter 3), and its postcanine dentition is not smaller than expected when one considers across-catarrhine variability (Chapter 4). Instead, a unique lower jaw is found in later species, in particular in the late Pleistocene. Therefore, a gracile lower jaw is not a unique trait of the genus *Homo*. The dawn of the genus may not correspond to the most influential event that would have caused the onset of the reduction in the hominin mandible and teeth, although there may have been a delay between certain innovations (such as improvements in stone tool use) and the appearance of certain anatomical features. Nevertheless, only the postcanine and mandibular size of *H. sapiens* and *H. neanderthalensis* are outside across-catarrhine variability, indicating that the reduction produced extreme phenotypes only in these late hominins. The results of this work suggest that the drivers of dental and mandibular reduction should not be looked for among early *Homo* species, but among the hominins alive during the middle Pleistocene and later time periods.

Another consideration concerns the role of adaptive versus non-adaptive factors in the evolution of the hominin lower jaw. The main hypotheses on the trend of reduction assume that differences in dental size and mandibular robusticity reflect functional differences. The mandible and teeth are involved in mastication, and, in primates, the form of the lower jaw determines a specific biomechanical profile (Hylander, 1979; Daegling, 1989; Humphrey et al., 1999). Nevertheless, several factors other than biomechanics and diet are involved in the development of the masticatory apparatus. In catarrhines, for example, phylogenetic inertia (Cheverud et al., 1985; Kappeler, 1990; Chapman & Rothman, 2009) and behavioural plasticity (Hylander, 1975b; Chapman & Chapman, 1990; Brockman & Van Schaik, 2005) can override the importance of biomechanics. This work provides evidence that structural modifications of the skull (non-adaptive) can have remarkable effects on the lower jaw (Chapter 3, 4 and 6). Major anatomical modifications occurred following early *Homo*, such as an increase in body size (Ruff, 2002; Grabowski et al., 2015) and encephalization (Rightmire, 2004). Postcanine and mandibular size reduction likely occurred as a result of allometric rate variations (Chapter 4), and the anatomical transformations following early *Homo* may be explained by the alteration of allometric patterns in the lower jaw by changes in growth rhythms (Vrba, 1996;

Mitteroecker et al., 2004). Body size might have played a major role in postcanine tooth size variations among Pleistocene hominins and Holocene *H. sapiens* (Chapter 3). Both mandibular robusticity and incisor size can be significantly influenced by shape changes in the neurocranium (Chapter 6). Instead, dietary proxies explained only small parts of dental size variances (Chapter 5), and the effects were significant only in few cases. As indicated by research on mandible biomechanics in catarrhines (Hylander, 1979; Daegling & Hylander, 1998), robusticity plays an important part in resisting the masticatory stresses, and the above results are in accordance with this point of view. Robusticity is better suited to explain differences in diet and food properties than postcanine dentition (Chapter 5), indicating that mandibular corpus shape in hominins may have modified in response to changes in food toughness.

7.2 The dietary component

Diet is a fundamental factor in hypotheses on dental and mandibular reduction, although these are more concerned with food mechanical properties than with food itself (Zink et al., 2014). The ability to process food using stone tools (Zink & Lieberman, 2016) or by cooking (Christensen et al., 2000) is at the core of the hypothesis that cultural development in hominins may have relaxed the selective pressures on the masticatory apparatus, eventually allowing mandible and dentition to reduce in size and robusticity. Although non-hominin extant catarrhines do not use fire, many species are able to use tools to break hard foods and soften their texture (Van Schaik et al., 1999). Therefore, non-hominin catarrhines can be used to test the link between lower jaw anatomy, diet and tool use. The above results highlighted the difficulties in relating anatomy, diet and behaviour. Body size has a remarkable influence on dental size and mandibular robusticity (Chapter 5), suggesting that changes in body size may override the adaptive modifications of the masticatory apparatus in response to dietary factors. Nevertheless, there is a diet-linked component in the variability of dental size and mandibular robusticity.

The presence of small incisors in catarrhines was found to be an indicator of low diet quality, consumption of tough foods and long chewing cycles, three factors that are correlated with

each other. Hylander (1975b) suggested that a correlation exists between incisal size in anthropoid primates and the size of the food items eaten by the species. Large food items need extensive preparation before entering the mouth, while small fruits, seeds and leaves can be chewed without pre-processing. As an example, papionins include both large food items and leaves in their diets, which they process by means of their front teeth (Hylander, 1975b; Whitehead & Jolly, 2000). Papionins make large use of incisal preparation thanks to a thick enamel that counteracts the effect of dental wear (Jolly, 1970; Hylander, 1975b). Colobines, which rely on smaller food items than papionins, have smaller teeth in respect of their body size because their incisors do not undergo massive dental wear. The same mechanism is plausible for explaining the incisal reduction in hominins. In the genus *Homo*, incisors reduced in their dimensions from lower Pleistocene to Neolithic (Chapter 3), along with improvements in tool manufacturing and food processing techniques. The use of lithic tools in the Pleistocene reduced the size and toughness of food items by slicing, crushing and pounding (Zink & Lieberman, 2016), thus assigning to the hands the job previously accomplished by incisors. Although incisal reduction can be due to the relaxation of selective pressures in both colobines and hominins, this explanation does not account for incisal size variability. The relative size increase of the anterior teeth during middle Palaeolithic (Chapter 3) and the fact that incisor size in late hominins adhered to the expectations of catarrhines of similar body size (Chapter 4) suggests that other factors might counteract the functional incisal interpretation. The increase in body size that characterized hominins during the Pleistocene (Grabowski et al., 2015) is a valid candidate to explain incisor size variability, indicating again that factors other than biomechanics may have been important in the evolution of the hominin lower jaw.

Late hominin species were found out of the across-catarrhine variability for postcanine size (Chapter 4), because of their smaller premolars (*H. sapiens*) and molars (*H. neanderthalensis*) than were expected from their body size. At the same time, *P. boisei* and *P. robustus* exhibited the opposite condition. The large teeth and robust mandibles of the genus *Paranthropus* have been suggested as adaptations to hard foods (Walker et al., 1986; Walker & Leakey, 1988; Wood & Costantino, 2007). Recent studies found evidence that *Paranthropus* relied on a generalist diet, and so did early *Homo* (Ungar, 2004). Nevertheless, an increasing amount of studies indicate that the primate masticatory anatomy may be adapted to fall-back foods,

rather than to the foods usually exploited (Lambert, 2009). This would allow a species to survive when their main alimentary source is scarce or absent, and this may have been the case in the savannah-like landscape in which Plio-Pleistocene hominins lived (Kingston et al., 1994; WoldeGabriel, 1994). By analogy, the small premolars and molars in Neanderthals and modern humans could be explained as the effect of relaxed selective pressures. Starting from the late Pleistocene, hominins likely had deliberate control of fire (Roebroeks & Villa, 2011), improved manufacturing skills than in earlier species and could rely on hunting strategies and harvesting, made possible by more complex societies (Powell et al., 2009). These factors would have released hominins from both tough diets and fluctuations in food availability. Nevertheless, the results presented in Chapter 5 provide little support that dietary or subsistence factors drove postcanine reduction in hominins. Few correlations were found between dietary proxies, premolar and molar size across catarrhines, and even those limited cases did not account for large variances. One possibility is that variations in body size account for the majority of the postcanine size variability, a relationship that was emphasised by previous studies on postcanine allometry in primates (Wood, 1979; Gingerich et al., 1982). Nevertheless, premolar and molar size cannot be entirely attributed to changes in body size, and a certain amount of dietary specialisation was found in previous studies that took allometry into account (Kay, 1975).

Mandibular robusticity is largely recognised for its involvement in masticatory stress resistance in primates (Hylander, 1975b). Oval-shaped cross-sections of the mandibular corpus below the molars are known to oppose bending and torsional forces more efficiently than rounded sections (Hylander, 1975b). This polarised morphology reflects the biomechanical differences of a diet based on tough foods (long chewing, prolonged stress) or hard, brittle foods (Ross et al., 2009b). Tough food eaters are associated with a high robusticity index (rounded shape of corpus section), an adaptation to prolonged stress (Hylander, 1975b). The height of mandibular corpus increases (oval-shaped section) in primates that chew hard foods (Hylander, 1975b), as an adaptation to strong but not prolonged stress. The results reported in Chapter 5 support these differences, and indicate that food textural properties have high impact on the morphology of the catarrhine mandibular corpus. In hominins, remarkable modifications in robusticity are observed following early *Homo* species, which instead share a morphological pattern similar to

australopithecines (Chapter 3). These results agree with the hypothesis of mandibular gracilisation triggered by food processing advancements. In hominins, the reduction in the molar robusticity index would not indicate an adaptation to the consumption of hard foods, but rather the result of a loss of function determined by lower biomechanical requirements. Indeed, robusticity was found to decrease with shorter chewing cycles in non-hominin extant catarrhines (Chapter 5). A possible cause for this apparent convergence between hominins and hard-object feeders could be the loss of genetic and physiologic control over mandibular development (Calcagno & Gibson, 1988). This mechanism seems to agree with the *Probable Mutation Effect* model (PME, see Chapter 1 for further details), proposed by Brace for the Holocene trend of reduction (Brace, 1963; Brace and Mahler, 1971). Although this model has been criticised for over-simplifying the genetics of development and the effects of pleiotropy (Calcagno & Gibson, 1988), it is possible that certain aspects of it can be explained in a more modern perspective. In the case of robusticity, for example, it is plausible that the genetic pathways controlling mandibular shape could relax, although not be completely disrupted as suggested by PME, because of reduced gene expression following a decrease in selective pressures. As a result, it is possible to hypothesise that a structure out of a strict developmental control would be more likely affected by the growth of contiguous anatomical elements, which is indicated by studies on morphological integration in the skull (Lieberman, 1995; Bastir et al., 2010).

7.3 The neurocranial constraint on the lower jaw

The trend of encephalization in hominins developed along with mandibular and dental reduction, and the idea that brain expansion controlled the morphological evolution of the lower jaw is supported by several studies (Lieberman et al., 2002; Bastir et al., 2006; Bastir, 2008; Spoor et al., 2015). Nevertheless, the role of encephalization on mandibular and dental reduction did not receive as much attention as food processing hypotheses. Skull morphology could be highly affected by the levels of mutual influence between its elements (Klingenberg, 2008). The idea itself is intuitive: changes in one bone can modify a contiguous bone because the final anatomical ensemble needs to adhere to an expected form. The findings of this work

suggest that the neurocranium did structurally constrain the lower jaw during Pleistocene and that this may have overridden the effect of food processing advancements. Nevertheless, it has to be underlined that the relationship between encephalization and the trend of reduction is complex, and that brain expansion preceded postcanine reduction in early *Homo* (Spoor et al., 2015), and followed it in Neanderthals (Arsuaga et al., 2014). Therefore, it is unlikely that the expanding neurocranium was the factor triggering dental and mandibular reduction in hominins.

Hominins represent an oddity in the catarrhine skull variability. Their neurocranium enlarged conspicuously to fit an increasing brain size (Leutenegger, 1982; Herculano-Houzel, 2009), a pattern that has no parallel in primate evolution. *Homo sapiens* is even more peculiar, since its cranium reorganised to become a globular structure, whose growth differs from the ones of other primates, including other hominins. Indeed, the neurocranium in other hominins developed in a lengthwise direction, while modern humans exhibit a rounded, more spherical appearance of the head (Lieberman et al., 2002). In this work, it was found that changes in the neurocranium in humans and other African apes are likely to affect both dental size and mandibular robusticity (Chapter 6). In particular, the shortening of the neurocranium had a remarkable influence on postcanine size in *Pan troglodytes*, but not in *H. sapiens*. This result suggests that a shortened neurocranium produces a mesio-distal constraint on molars and premolars. It is possible that the postcanine dentition of Pleistocene *Homo* was constrained by the neurocranium, which may have had an influence in the dental reduction of particularly encephalized species, as in Neanderthals (Ruff et al., 1997). Indeed, the results above highlight the particularly small molar size in *H. neanderthalensis* (Chapter 5), which could be explained by the large expansion of its neurocranium. In addition, the low levels of correlation between dietary proxies and postcanine tooth size observed in Chapter 4 could be explained by the fact that major reduction in molars and premolars is guided by non-adaptive factors, like structural constraints.

The neurocranial constraint on the postcanine dentition found in *H. sapiens* is in accord with the fact that human premolars, but not molars, are found outside of the across-catarrhine scaling pattern (Chapter 5). A remarkable effect of neuro-mandibular integration was instead found on corpus robusticity (Chapter 6). Interestingly, neurocranium shape had an influence on mandibular corpus height in both humans and chimpanzees, but it does not seem to affect

robusticity in the latter. These results suggest a complex scenario for the evolution of mandibular robusticity, because of the concomitant influences of structural and dietary factors (Chapter 4). The results reported above seems to suggest that neurocranium reorganisation is a possible cause of the further reduction in robusticity in the slender mandible of *H. sapiens*, although the same effect may not necessarily explain the robusticity reduction in previous hominins.

7.4 Final remarks

This work aimed to clarify the reasons behind one of the major trend in the evolution of our ancestors. The trends of mandibular and dental reduction were analysed by looking at tooth size and lower jaw robusticity in fossil hominins, modern humans and other extant catarrhines. The analyses were designed to elucidate the role of adaptive and non-adaptive factors in the onset of the trend of reduction. The results obtained here highlight the complexity of hominin skull evolution, suggesting that a multifactorial perspective is necessary to explain the gracile appearance of the lower jaw in modern humans. Previous literature focused on single aspects of dental and mandibular reduction, generating a dual framework of ideas that favoured either food processing or encephalization as the main driver of the observed trend in hominins. The concomitant occurrence of these two events has always made it difficult to discern their unique contributions. The findings described here suggest abandoning the strict dualism between encephalization and food processing hypotheses, since both concur to explain the morphological variation that characterized the evolution of the hominin lower jaw. Based on the results above, low robusticity and the small postcanine dentition represent unique traits of late hominins, and this peculiar condition may be the result of both biomechanics and morphological integration between the lower jaw and the neurocranium. The size of incisors likely reduced because of the improvements in tool-based food preparation in hominins, thus relaxing the selection for a large front dentition. Molars and premolars were probably influenced by the expansion of the neurocranium during Pleistocene, although other factors might have been crucial in *H. sapiens*. This work provides support for the hypothesis that the gracile mandibular corpus of middle to late Pleistocene

Homo was the result of the relaxation of selective pressures on mastication with simultaneous passive variations generated by the development of contiguous cranial elements. In addition, the low robusticity exhibited by *H. sapiens* may reflect its peculiar pattern of encephalization. Thus, convincing evidence in support of a complex, multifactorial explanation for the trend of dental and mandibular reduction in hominins and humans has been provided.

References

Adams, D. C., & Otárola-Castillo, E. (2013). geomorph: an R package for the collection and analysis of geometric morphometric shape data. *Methods in Ecology and Evolution*, 4(4), 393-399.

Aiello, L. C., & Andrews, P. (2000). The australopithecines in review. *Human Evolution*, 15(1-2), 17-38.

Aiello, L. C., & Dean, C. (2000). *An introduction to human evolutionary anatomy*, Academic Press, London.

Aldridge, K., Boyadjiev, S. A., Capone, G. T., DeLeon, V. B., & Richtsmeier, J. T. (2005). Precision and error of three-dimensional phenotypic measures acquired from 3dMD photogrammetric images. *American Journal of Medical Genetics* Part A, 138(3), 247-253.

Allen, K. L., & Kay, R. F. (2012). Dietary quality and encephalization in platyrrhine primates. *Proceedings of the Royal Society of London B: Biological Sciences*, 279(1729), 715-721.

Ambrose, S. H. (2001). Paleolithic technology and human evolution. *Science*, 291(5509), 1748-1753.

Anapol, F., Shahnoor, N., & Ross, C. F. (2008). Scaling of reduced physiologic cross-sectional area in primate muscles of mastication. In Vinyard, C. J., Ravosa, M. J., & Wall, C. E. (Eds.), *Primate craniofacial function and biology*. Springer Science & Business Media, New York.

Andrews, P., Martin, L., Aiello, L., & Scandrett, A.E., (1991). Hominoid dietary evolution. *Philosophical Transactions of the Royal Society B: Biological Sciences*. 334, 199-209.

Arbour, J. H., & Brown, C. M. (2014). Incomplete specimens in geometric morphometric analyses. *Methods in Ecology and Evolution*, 5(1), 16-26.

Arnold, C., Matthews, L. J., & Nunn, C. L. (2010). The 10kTrees website: a new online resource for primate phylogeny. *Evolutionary Anthropology*, 19(3), 114-118.

Arsuaga, J. L., Martínez, I., Arnold, L. J., Aranburu, A., Gracia-Téllez, A., Sharp, W. D., Quam, R. M., Falguères, C., Pantoja-Pérez, A., Bischoff, J., Poza-Rey, E., Parés, J. M., Carretero, J. M., Demuro, M., Lorenzo, C., Sala, N., Martinòn-Torres, M., Garcìa, N., Alcàzar de Velasco, A., Cuenca-Bescos, G., Gòmez-Olivencia, A., Moreno, D., Pablos, A., Shen, C. C., Rodriguez, L., Ortega, A. I., Garcìa, R., Bonmatì, A., Bermudéz de Castro, J. M., & Carbonell, E. (2014). Neandertal roots: Cranial and chronological evidence from Sima de los Huesos. *Science*, 344(6190), 1358-1363.

Bærentzen, J. A., & Aanæs, H. (2002). Generating signed distance fields from triangle meshes. Tech. Rep. IMM-TR-2002-21, *Informatics and Mathematical Modelling*, Technical University of Denmark, Lyngby, Denmark.

Bailit, H. L., & Friedlaender, J. S. (1966). Tooth size reduction: A hominid trend. *American Anthropologist*, 68(3), 665-672.

Barrickman, N. L., & Lin, M. J. (2010). Encephalization, expensive tissues, and energetics: an examination of the relative costs of brain size in strepsirrhines. *American Journal of Physical Anthropology*, 143(4), 579-590.

Bastir, M. (2008). A systems-model for the morphological analysis of integration and modularity in human craniofacial evolution. *Journal of Anthropological Sciences*, 86, 37-58.

Bastir, M., & Rosas, A. (2004). Facial heights: evolutionary relevance of postnatal ontogeny for facial orientation and skull morphology in humans and chimpanzees. *Journal of Human Evolution*, 47(5), 359-381.

Bastir, M., & Rosas, A. (2005). Hierarchical nature of morphological integration and modularity in the human posterior face. *American Journal of Physical Anthropology*, 128(1), 26-34.

Bastir, M., & Rosas, A. (2006). Correlated variation between the lateral basicranium and the face: a geometric morphometric study in different human groups. *Archives of Oral Biology*, 51(9), 814-824.

Bastir, M., Rosas, A., & Kuroe, K. (2004). Petrosal orientation and mandibular ramus breadth: Evidence for an integrated petroso-mandibular developmental unit. *American Journal of Physical Anthropology*, 123(4), 340-350.

Bastir, M., Rosas, A., & O'Higgins, P. (2006). Craniofacial levels and the morphological maturation of the human skull. *Journal of Anatomy*, 209(5), 637-654.

Bastir, M., Rosas, A., & Sheets, H. D. (2005). The morphological integration of the hominoid skull: a partial least squares and PC analysis with implications for European Middle Pleistocene mandibular variation. In Slice, E. D. (Ed.), *Modern morphometrics in physical anthropology*. Kluwer Academic/Plenum Publishers, New York.

Bastir, M., Rosas, A., Stringer, C., Cuétara, J. M., Kruszynski, R., Weber, G. W., Ross, C. F., & Ravosa, M. J. (2010). Effects of brain and facial size on basicranial form in human and primate evolution. *Journal of Human Evolution*, 58(5), 424-431.

Begun, D. R., Ward, C. V., & Rose, M. D. (2013). *Function, phylogeny, and fossils: Miocene hominoid evolution and adaptations*. Springer Science & Business Media, New York.

Behrensmeyer, A. K. (1988). *Fossils in the making: vertebrate taphonomy and paleoecology*. University of Chicago Press, Chicago.

Bilsborough, A., & Rae, T. C. (2015). Hominoid cranial diversity and adaptation. In Henke, W., & Tattersall, I. (Eds.), *Handbook of paleoanthropology*. Springer, Berlin.

Blomberg, S. P., & Garland, T. (2002). Tempo and mode in evolution: phylogenetic inertia, adaptation and comparative methods. *Journal of Evolutionary Biology*, 15(6), 899-910.

Blomberg, S. P., Garland Jr, T., & Ives, A. R. (2003). Testing for phylogenetic signal in comparative data: behavioral traits are more labile. *Evolution*, 57(4), 717-745.

Blomberg, S. P., Lefevre, J. G., Wells, J. A., & Waterhouse, M. (2012). Independent contrasts and PGLS regression estimators are equivalent. *Systematic Biology*, syr118.

Bookstein, F. L. (1989). Principal warps: Thin-plate splines and the decomposition of deformations. IEEE *Transactions on pattern analysis and machine intelligence*, 11(6), 567-585.

Bookstein, F. L. (1997a). *Morphometric tools for landmark data: geometry and biology*. Cambridge University Press, New York.

Bookstein, F. L. (1997b). Landmark methods for forms without landmarks: morphometrics of group differences in outline shape. *Medical Image Analysis*, 1(3), 225-243.

Bookstein, F. L., Gunz, P., Mitterœcker, P., Prossinger, H., Schæfer, K., & Seidler, H. (2003). Cranial integration in *Homo*: singular warps analysis of the midsagittal plane in ontogeny and evolution. *Journal of Human Evolution*, 44(2), 167-187.

Bouton, P. E., & Harris, P. V. (1972). The effects of cooking temperature and time on some mechanical properties of meat. *Journal of Food Science*, 37(1), 140-144.

Bouvier, M. (1986). A biomechanical analysis of mandibular scaling in Old World monkeys. *American Journal of Physical Anthropology*, 69(4), 473-482.

Boyer, D. M. (2008). Relief index of second mandibular molars is a correlate of diet among prosimian primates and other euarchontan mammals. *Journal of Human Evolution*, 55(6), 1118-1137.

Brace, C. L. (1963). Structural reduction in evolution. *The American Naturalist*, 97(892), 39-49.

Brace, C. L. (1967). Environment, tooth form, and size in the Pleistocene. *Journal of Dental Research*, 46(5), 809-816.

Brace, C. L. (1976). Tooth reduction in the Orient. *Asian Perspectives*, 19(2), 203-219.

Brace, C. L. (1979). Krapina, "Classic" Neanderthals, and the evolution of the European face. *Journal of Human Evolution*, 8(5), 527-550.

Brace, C. L., Brown, T., Townsend, G. C., Harris, E. F., Howells, W. W., Huizinga, J., Constandse-Westermann, T. S., Hunt, E. E., Koritzer, R. T., Lombardi, A. V., Meiklejohn, C., Pietrusewsky, M., Preston, C. B., Roydhouse, R. H., Brace, C. L., Rosenberg, K. R., & Hunt, K. D. (1987). Gradual change in human tooth size in the late Pleistocene and post-Pleistocene. *Evolution*, 41(4), 705-720.

Brace, C. L., & Mahler, P. E. (1971). Post-Pleistocene changes in the human dentition. *American Journal of Physical Anthropology*, 34(2), 191-203.

Brockman, D. K., & Van Schaik, C. P. (2005). *Seasonality in primates: studies of living and extinct human and non-human primates*. Cambridge University Press, New York.

Brose, D. S., & Wolpoff, M. H. (1971). Early upper Paleolithic man and late middle Paleolithic tools. *American Anthropologist*, 73(5), 1156-1194.

Bruner, E. (2004). Geometric morphometrics and paleoneurology: brain shape evolution in the genus Homo. *Journal of Human Evolution*, 47(5), 279-303.

Bruner, E., & Ripani, M. (2008). A quantitative and descriptive approach to morphological variation of the endocranial base in modern humans. *American Journal of Physical Anthropology*, 137(1), 30-40.

Burrows, A. M., Waller, B. M., Parr, L. A., & Bonar, C. J. (2006). Muscles of facial expression in the chimpanzee (*Pan troglodytes*): descriptive, comparative and phylogenetic contexts. *Journal of Anatomy*, 208(2), 153-167.

Butler, M. A., & King, A. A. (2004). Phylogenetic comparative analysis: a modeling approach for adaptive evolution. *The American Naturalist*, 164(6), 683-695.

Cachel, S. (1984). Growth and allometry in primate masticatory muscles. *Archives of Oral Biology*, 29(4), 287-293.

Cachel, S. (1996). Megadontia in the teeth of early hominids. *Kaupia. Darmstadter Beitrage zur Naturgeschichte*, 6, 119-128.

Cachel, S. (2006). *Primate and human evolution*. Cambridge University Press, New York.

Calcagno, J. M. (1986). Dental reduction in post-Pleistocene Nubia. *American Journal of Physical Anthropology*, 70(3), 349-363.

Calcagno, J. M., & Gibson, K. R. (1988). Human dental reduction: Natural selection or the probable mutation effect. *American Journal of Physical Anthropology*, 77(4), 505-517.

Calcagno, J. M. (1989). *Mechanisms of Human Dental Reduction: A Case Study From Post-Pleistocene Nubia*. University of Kansas Publications in Anthropology, Lawrence.

Carlson, D. S., & Van Gerven, D. P. (1977). Masticatory function and post-Pleistocene evolution in Nubia. *American Journal of Physical Anthropology*, 46(3), 495-506.

Castenholz, A. (1984). The eye of *Tarsius*. In Niemitz, C. (Ed.), *Biology of tarsiers*. Gustav Fischer Verlag, Stuttgart.

Chamberlain, A. T., & Wood, B. A. (1985). A reappraisal of variation in hominid mandibular corpus dimensions. *American Journal of Physical Anthropology*, 66(4), 399-405.

Chamla, M. C. (1980). Etude des variations métriques des couronnes dentaires des Nord-Africains, de l'Epipaléolithique à l'époque actuelle. *L' Anthropologie*, 84(2), 254-271.

Chapman, C. A., & Chapman, L. J. (1990). Dietary variability in primate populations. *Primates*, 31(1), 121-128.

Chapman, C. A., & Rothman, J. M. (2009). Within-species differences in primate social structure: Evolution of plasticity and phylogenetic constraints. *Primates*, 50(1), 12.

Chevalier-Skolnikoff, S. (1973). Facial expression of emotion in nonhuman primates. In Ekman, P. (Ed.), *Darwin and facial expression: A century of research in review*. Academic Press, New York.

Cheverud, J. M. (1982). Phenotypic, genetic, and environmental morphological integration in the cranium. *Evolution*, 36(3), 499-516.

Cheverud, J. M., Dow, M. M., & Leutenegger, W. (1985). The quantitative assessment of phylogenetic constraints in comparative analyses: sexual dimorphism in body weight among primates. *Evolution*, 39(6), 1335-1351.

Cheverud, J. M., Routman, E. J., & Irschick, D. J. (1997). Pleiotropic effects of individual gene loci on mandibular morphology. *Evolution*, 51(6), 2006-2016.

Chivers, D. J. (1991). Species differences in tolerance to environmental change. In Box, H. O. (Ed.), *Primate responses to environmental change* (5-37). Chapman & Hall, London.

Christensen, M., Purslow, P. P., & Larsen, L. M. (2000). The effect of cooking temperature on mechanical properties of whole meat, single muscle fibres and perimysial connective tissue. *Meat Science*, 55(3), 301-307.

Christians, J. K. (1999). Controlling for body mass effects: Is part-whole correlation important? *Physiological and Biochemical Zoology*, 72(2), 250-253.

Collyer, M. L., Sekora, D. J., & Adams, D. C. (2015). A method for analysis of phenotypic change for phenotypes described by high-dimensional data. *Heredity*, 115(4), 357-365.

Coon, C. S. (1955). Some problems of human variability and natural selection in climate and culture. *The American Naturalist*, 89(848), 257-279.

Coon, C. S. (1962). *The History of Man: From the First Human to Primitive Culture and Beyond*. 2nd Ed., Jonathan Cape, London.

Cooper, N., Thomas, G. H., Venditti, C., Meade, A., & Freckleton, R. P. (2016). A cautionary note on the use of Ornstein Uhlenbeck models in macroevolutionary studies. *Biological Journal of the Linnean Society*, 118(1), 64-77.

Copes, L. (2012). *Comparative and experimental investigations of cranial robusticity in mid-Pleistocene hominins*. Ph.D. Dissertation, Anthropology, Arizona State University.

Copes, L. E., & Kimbel, W. H. (2016). Cranial vault thickness in primates: *Homo erectus* does not have uniquely thick vault bones. *Journal of Human Evolution*, 90, 120-134.

Corner, G. W. (1927). *Anatomical texts of the earlier Middle Ages: a study in the transmission of culture, with a revised Latin text of Anatomia Cophonis and translations of four texts*. Carnegie Institution, Washington.

Cosans, C. E., & Frampton, M. (2009). *History of Comparative Anatomy*. eLS. Wiley Online Library, http://www.els.net/WileyCDA/ElsArticle/refId-a0003085.html.

Crompton, A. W., & Hiiemae, K. (1969). How mammalian molar teeth work. *Discovery*, 5(1), 23-34.

Daegling, D. J. (1989). Biomechanics of cross-sectional size and shape in the hominoid mandibular corpus. *American Journal of Physical Anthropology*, 80(1), 91-106.

Daegling, D. J. (1993). Functional morphology of the human chin. *Evolutionary Anthropology*, 1(5), 170-177.

Daegling, D. J. (2001). Biomechanical scaling of the hominoid mandibular symphysis. *Journal of Morphology*, 250(1), 12-23.

Daegling, D. J., & Hylander, W. L. (1997). Occlusal forces and mandibular bone strain: Is the primate jaw "overdesigned"? *Journal of Human Evolution*, 33(6), 705-717.

Daegling, D. J., & Hylander, W. L. (1998). Biomechanics of torsion in the human mandible. *American Journal of Physical Anthropology*, 105(1), 73-88.

Daegling, D. J., & Jungers, W. L. (2000). Elliptical Fourier analysis of symphyseal shape in great ape mandibles. *Journal of Human Evolution*, 39(1), 107-122.

Daegling, D. J., McGraw, W. S., Ungar, P. S., Pampush, J. D., Vick, A. E., & Bitty, E. A. (2011). Hard-object feeding in sooty mangabeys (*Cercocebus atys*) and interpretation of early hominin feeding ecology. PLoS One, 6(8), e23095.

De Castro, J. M. B., & Nicolas, M. E. (1995). Posterior dental size reduction in hominids: the Atapuerca evidence. *American Journal of Physical Anthropology*, 96(4), 335-356.

DeGusta, D., Everett, M. A., & Milton, K. (2003). Natural selection on molar size in a wild population of howler monkeys (*Alouatta palliata*). *Proceedings of the Royal Society of London B: Biological Sciences*, 270(Supplement 1), S15-S17.

Delezene, L. K., & Kimbel, W. H. (2011). Evolution of the mandibular third premolar crown in early *Australopithecus*. *Journal of Human Evolution*, 60(6), 711-730.

Delisle, R. (2016). *Debating Humankind's Place in Nature, 1860-2000*: The Nature of Paleoanthropology. Routledge, New York.

Dembo, M., Matzke, N. J., Mooers, A. Ø., & Collard, M. (2015). Bayesian analysis of a morphological supermatrix sheds light on controversial fossil hominin relationships. *Proceedings of the Royal Society of London B: Biological Sciences*, 282(1812), 20150943.

Demes, B., & Creel, N. (1988). Bite force, diet, and cranial morphology of fossil hominids. *Journal of Human Evolution*, 17(7), 657-670.

Demes, B., Preuschoft, H., & Wolff, J. E. A. (1984). Stress-strength relationships in the mandibles of hominoids. In Chivers, D. J., Wood, B. A., & Bilsborough, A. (Eds.), *Food acquisition and processing in primates*. Springer Science & Business Media, New York.

De Oliveira, R. C. G., Leles, C. R., Normanha, L. M., Lindh, C., & Ribeiro-Rotta, R. F. (2008). Assessments of trabecular bone density at implant sites on CT images. *Oral Surgery, Oral Medicine, Oral Pathology, Oral Radiology and Endodontology*, 105(2), 231-238.

DeSantis, L. R., Scott, J. R., Schubert, B. W., Donohue, S. L., McCray, B. M., Van Stolk, C. A., Winburn, A. A., Greshko, M. A., & O'Hara, M. C. (2013). Direct comparisons of 2D and 3D dental microwear proxies in extant herbivorous and carnivorous mammals. *PLoS One*, 8(8), e71428.

Diaz-Uriarte, R., & Garland, T. (1996). Testing hypotheses of correlated evolution using phylogenetically independent contrasts: Sensitivity to deviations from Brownian motion. *Systematic Biology*, 45(1), 27-47.

Dixon, P. (2003). VEGAN, a package of R functions for community ecology. *Journal of Vegetation Science*, 14(6), 927-930.

Dixson, A. (1998). Primate sexuality. In Whelehan, P., & Bolin, A. (Eds.), *The International Encyclopedia of Human Sexuality*, John Wiley & Sons, Hoboken.

Domínguez-Rodrigo, M., Pickering, T. R., Semaw, S., & Rogers, M. J. (2005). Cutmarked bones from Pliocene archaeological sites at Gona, Afar, Ethiopia: Implications for the function of the world's oldest stone tools. *Journal of Human Evolution*, 48(2), 109-121.

Dominy, N. J., Lucas, P. W., Osorio, D., & Yamashita, N. (2001). The sensory ecology of primate food perception. *Evolutionary Anthropology*, 10(5), 171-186.

Doran-Sheehy, D., Mongo, P., Lodwick, J., & Conklin-Brittain, N. L. (2009). Male and female western gorilla diet: preferred foods, use of fallback resources, and implications for ape versus Old World monkey foraging strategies. *American Journal of Physical Anthropology*, 140(4), 727-738.

Druzinsky, R. E. (1993). The time allometry of mammalian chewing movements: Chewing frequency scales with body mass in mammals. *Journal of Theoretical Biology*, 160(4), 427-440.

Dryden, I. L., & Mardia, K. V. (1998). *Statistical analysis of shape*. John Wiley & Sons, Hoboken.

Emes, Y., Aybar, B., & Yalcin, S. (2011). On the evolution of human jaws and teeth: A review. *Bulletin of the International Association for Paleodontology*, 5(1), 37-47.

Fajardo, R. J., Ryan, T. M., & Kappelman, J. (2002). Assessing the accuracy of high-resolution X-ray computed tomography of primate trabecular bone by comparisons with histological sections. *American Journal of Physical Anthropology*, 118(1), 1-10.

Falkingham, P. L. (2012). Acquisition of high resolution three-dimensional models using free, open-source, photogrammetric software. *Palaeontologia Electronica*, 15(1), 15.

Felsenstein, J. (1973). Maximum-likelihood estimation of evolutionary trees from continuous characters. *American Journal of Human Genetics*, 25(5), 471.

Felsenstein, J. (1985). Phylogenies and the comparative method. *The American Naturalist*, 125(1), 1-15.

Ferrario, V. F., Sforza, C., Serrao, G., Dellavia, C., & Tartaglia, G. M. (2004). Single tooth bite forces in healthy young adults. *Journal of Oral Rehabilitation*, 31(1), 18-22.

FitzGerald, C., & Hillson, S. (2005). Dental reduction in late Pleistocene and early Holocene hominids: alternative approaches to assessing tooth size. *American Journal of Physical Anthropology*, 102-102.

Fleagle, J. G., Kay, R. F., & Simons, E. L. (1980). Sexual dimorphism in early anthropoids. *Nature*, 287(5780), 328-330.

Fleagle, J. G., & McGraw, W. S. (1999). Skeletal and dental morphology supports diphyletic origin of baboons and mandrills. *Proceedings of the National Academy of Sciences of the United States of America*, 96(3), 1157-1161.

Fourie, Z., Damstra, J., Gerrits, P. O., & Ren, Y. (2011). Evaluation of anthropometric accuracy and reliability using different three-dimensional scanning systems. *Forensic Science International*, 207(1), 127-134.

Franciscus, R. G., & Trinkaus, E. (1995). Determinants of retromolar space presence in Pleistocene *Homo* mandibles. *Journal of Human Evolution*, 28(6), 577-595.

Frayer, D. W. (1977). Metric dental change in the European Upper Paleolithic and Mesolithic. *American Journal of Physical Anthropology*, 46(1), 109-120.

Freckleton, R. P. (2011). Dealing with collinearity in behavioural and ecological data: Model averaging and the problems of measurement error. *Behavioral Ecology and Sociobiology*, 65(1), 91-101.

Freckleton, R. P., Harvey, P. H., & Pagel, M. (2002). Phylogenetic analysis and comparative data: a test and review of evidence. *The American Naturalist*, 160(6), 712-726.

Gibbons, A. (2011). Who were the Denisovans? *Science*, 333(6046), 1084-1087.

Gingerich, P. D. (1977). Correlation of tooth size and body size in living hominoid primates, with a note on relative brain size in Aegyptopithecus and Proconsul. *American Journal of Physical Anthropology*, 47(3), 395-398.

Gingerich, P. D., Smith, B. H., & Rosenberg, K. (1982). Allometric scaling in the dentition of primates and prediction of body weight from tooth size in fossils. *American Journal of Physical Anthropology*, 58(1), 81-100.

Glander, K. E. (1981). The foraging strategy of howler monkeys: A study in primate economics. *International Journal of Primatology*, 2(4), 381-382.

Gómez-Robles, A., Smaers, J. B., Holloway, R. L., Polly, P. D., & Wood, B. A. (2017). Brain enlargement and dental reduction were not linked in hominin evolution. *Proceedings of the National Academy of Sciences of the United States of America*, 114(3), 468-473.

Gordon A. D., Wood B. (2007). Human Origins Database (HOD): Managing published data and specimen information for fossil and comparative collections. *American Journal of Physical Anthropology*, Supplement. 44:117.

Goren-Inbar, N., Alperson, N., Kislev, M. E., Simchoni, O., Melamed, Y., Ben-Nun, A., & Werker, E. (2004). Evidence of hominin control of fire at Gesher Benot Yaaqov, Israel. *Science*, 304(5671), 725-727.

Gowlett, J. A., & Wrangham, R. W. (2013). Earliest fire in Africa: Towards the convergence of archaeological evidence and the cooking hypothesis. *Azania: Archaeological Research in Africa*, 48(1), 5-30.

Grabowski, M., Hatala, K.G., Jungers, W.L., Richmond, B.G., (2015). Body mass estimates of hominin fossils and the evolution of human body size. *Journal of Human Evolution*. 85, 75-93.

Grafen, A. (1989). The phylogenetic regression. *Philosophical Transactions of the Royal Society of London. Series B, Biological Sciences*, 326(1233), 119-157.

Gregg, M. L., & Grybush, R. J. (1976). Thermally altered siliceous stone from prehistoric contexts: intentional versus unintentional alteration. *American Antiquity*, 41(2), 189-192.

Grine, F. E., & Martin, L. B. (1988). Enamel thickness and development in *Australopithecus* and *Paranthropus*. In Grine, F. E. (Ed.), *The Evolutionary History of the Robust Australopithecines*, Transaction Publishers, New Brunswick.

Grine, F. E., Sponheimer, M., Ungar, P. S., Lee-Thorp, J., & Teaford, M. F. (2012). Dental microwear and stable isotopes inform the paleoecology of extinct hominins. *American Journal of Physical Anthropology*, 148(2), 285-317.

Grine, F. E., Ungar, P. S., & Teaford, M. F. (2006). Was the Early Pliocene hominin *'Australopithecus' anamensis* a hard object feeder? *South African Journal of Science*, 102(7-8), 301-310.

Grueter, C. C., & Van Schaik, C. P. (2009). Sexual size dimorphism in Asian colobines revisited. *American Journal of Primatology*, 71(7), 609-616.

Guy, F., Mackaye, H. T., Likius, A., Vignaud, P., Schmittbuhl, M., & Brunet, M. (2008). Symphyseal shape variation in extant and fossil hominoids, and the symphysis of *Australopithecus bahrelghazali*. *Journal of Human Evolution*, 55(1), 37-47.

Haile-Selassie, Y. (2001). Late Miocene hominids from the middle Awash, Ethiopia. *Nature*, 412(6843), 178-181.

Harmon, L. J., Losos, J. B., Jonathan Davies, T., Gillespie, R. G., Gittleman, J. L., Jennings, B., Kozak, K. H., McPeek, M. A., Moreno-Roark, F., Near, T. J., Purvis, A., Ricklefs, R. E., Schluter, D., Schulte II, J. A., Seehausen, O., Sidlauskas, B. L.,Torres-Carvajal, O., Weir, J. T., & Mooers, A. Ø. (2010). Early bursts of body size and shape evolution are rare in comparative data. *Evolution*, 64(8), 2385-2396.

Harmon, L. J., Weir, J. T., Brock, C. D., Glor, R. E., & Challenger, W. (2008). GEIGER: investigating evolutionary radiations. *Bioinformatics*, 24(1), 129-131

Harrison, M. J. (1983). Age and sex differences in the diet and feeding strategies of the green monkey, *Cercopithecus sabaeus*. *Animal Behaviour*, 31(4), 969-977.

Harvey, P. H., Kavanagh, M., & Clutton-Brock, T. H. (1978). Sexual dimorphism in primate teeth. *Journal of Zoology*, 186(4), 475-485.

Harvey, P. H., & Pagel, M. D. (1991). *The comparative method in evolutionary biology*. Oxford university press, Oxford.

Henry, A. G. (2017). Neanderthal cooking and the costs of fire. *Current Anthropology*, 58(S16), 329-336.

Herculano-Houzel, S. (2009). The human brain in numbers: A linearly scaled-up primate brain. *Frontiers in Human Neuroscience*, 3, 1-11.

Herman, G. T. (2009). *Fundamentals of computerized tomography: image reconstruction from projections*. Springer Science & Business Media, New York.

Hill, D. A. (1997). Seasonal variation in the feeding behavior and diet of Japanese macaques (*Macaca fuscata yakui*) in lowland forest of Yakushima. *American Journal of Primatology*, 43(4), 305-320.

Hinton, R. J., Smith, M. O., & Smith, F. H. (1980). Tooth size changes in prehistoric Tennessee Indians. *Human Biology*, 52(2), 229-245.

Ho, T., & Ané, C. (2014). A linear-time algorithm for Gaussian and non-Gaussian trait evolution models. *Systematic Biology*, 63(3), 397-408.

Hollander, M., Wolfe, D. A., & Chicken, E. (2013). *Nonparametric statistical methods*. John Wiley & Sons, Hoboken.

Holloway, R. L., Sherwood, C. C., Hof, P. R., & Rilling, J. K. (2009). Evolution of the brain in humans: Paleoneurology. In Binder, M. D., Hirokawa, N., & Windhorst, U. (Eds.), *Encyclopedia of neuroscience*. Springer, Berlin.

Holton, N. E., Franciscus, R. G., Marshall, S. D., Southard, T. E., & Nieves, M. A. (2011). Nasal septal and premaxillary developmental integration: Implications for facial reduction in *Homo*. *The Anatomical Record*, 294(1), 68-78.

Humphrey, L. T., Dean, M. C., & Stringer, C. B. (1999). Morphological variation in great ape and modern human mandibles. *Journal of Anatomy*, 195(4), 491-513.

Hutchinson, G. E., & MacArthur, R. H. (1959). A theoretical ecological model of size distributions among species of animals. *The American Naturalist*, 93(869), 117-125.

Hylander, W. L. (1975a). The human mandible: lever or link? *American Journal of Physical Anthropology*, 43(2), 227-242.

Hylander, W. L. (1975b). Incisor size and diet in anthropoids with special reference to Cercopithecidae. *Science*, 808855(1095), 189.

Hylander, W. L. (1979). The functional significance of primate mandibular form. *Journal of Morphology*, 160(2), 223-239.

Hylander, W. L. (1984). Stress and strain in the mandibular symphysis of primates: a test of competing hypotheses. *American Journal of Physical Anthropology*, 64(1), 1-46.

Hylander, W. L. (1985). Mandibular function and biomechanical stress and scaling. *American Zoologist*, 25(2), 315-330.

Hylander, W. L., & Johnson, K. R. (1985). Temporalis and masseter muscle function during incision in macaques and humans. *International Journal of Primatology*, 6(3), 289-322.

Hylander, W. L., Ravosa, M. J., Ross, C. F., Wall, C. E., & Johnson, K. R. (2000). Symphyseal fusion and jaw-adductor muscle force: An EMG study. *American Journal of Physical Anthropology*, 112(4), 469-492.

Ichim, I., Swain, M., & Kieser, J. A. (2006). Mandibular biomechanics and development of the human chin. *Journal of Dental Research*, 85(7), 638-642.

Isler, K., & Van Schaik, C. P. (2014). How humans evolved large brains: Comparative evidence. *Evolutionary Anthropology*, 23(2), 65-75.

Janis, C. M. (1990). Correlation of cranial and dental variables with dietary preferences in mammals: A comparison of macropodoids and ungulates. *Memoirs of the Queensland Museum*, 28(1), 349-366.

Jeffery, N., Davies, K., Köckenberger, W., & Williams, S. (2007). Craniofacial growth in fetal *Tarsius bancanus*: brains, eyes and nasal septa. *Journal of Anatomy*, 210(6), 703-722.

Jiménez-Arenas, J. M., Pérez-Claros, J. A., Aledo, J. C., Palmqvist, P. (2014). On the relationships of postcanine tooth size with dietary quality and brain volume in Primates: Implications for hominin evolution. *BioMed Research International*. doi: 10.1155/2014/406507.

Johnson, T. M. (2016). Let's get virtual: examination of best practices to provide public access to digital versions of three-dimensional objects*. Information Technology and Libraries (Online)*, 35(2), 39.

Jolly, C. J. (1970). The seed-eaters: A new model of hominid differentiation based on a baboon analogy. *Man*, 5(1), 5-26.

Jonckheere, A. R. (1954). A distribution-free k-sample test again ordered alternatives. *Biometrika*, 41, 133-145.

Jungers, W. (1978). On canine reduction in early hominids. *Current Anthropology*, 19(1), 155-156.

Kamilar, J. M., & Cooper, N. (2013). Phylogenetic signal in primate behaviour, ecology and life history. *Philosophical Transactions of the Royal Society B: Biological Sciences*, 368(1618), 20120341.

Kappeler, P. M. (1990). The evolution of sexual size dimorphism in prosimian primates. *American Journal of Primatology*, 21(3), 201-214.

Kay, R. F. (1975). The functional adaptations of primate molar teeth. *American Journal of Physical Anthropology*, 43(2), 195-215.

Kim, K. D., Ruprecht, A., Wang, G., Lee, J. B., Dawson, D. V., & Vannier, M. W. (2005). Accuracy of facial soft tissue thickness measurements in personal computer-based multiplanar reconstructed computed tomographic images. *Forensic Science International*, 155(1), 28-34.

King, W. (1864). The reputed fossil man of the Neanderthal. *Quarterly Journal of Science*, 1(1864), 88-97.

Kingston, J. D., Marino, B. D., & Hill, A. (1994). Isotopic evidence for Neogene hominid paleoenvironments in the Kenya Rift Valley. *Science*, 264(5161), 955-958.

Kirkpatrick R. C. (2007) The Asian colobines: Diversity among leafeating monkeys. In: Campbell, C. J., Fuentes, A., MacKinnon, C. K., Panger, M., & Bearder, S. K. (Eds.), *Primates in perspective*. Oxford University Press, Oxford.

Klingenberg, C. P. (2008). Morphological integration and developmental modularity. *Annual Review of Ecology, Evolution, and Systematics*, 39, 115-132.

Klingenberg, C. P., & McIntyre, G. S. (1998). Geometric morphometrics of developmental instability: analyzing patterns of fluctuating asymmetry with Procrustes methods. *Evolution*, 52(5), 1363-1375.

Klingenberg, C. P., Mebus, K., & Auffray, J. C. (2003). Developmental integration in a complex morphological structure: how distinct are the modules in the mouse mandible? *Evolution & Development*, 5(5), 522-531.

Koyabu, D. B., & Endo, H. (2009). Craniofacial variation and dietary adaptations of African colobines. *Journal of Human Evolution*, 56(6), 525-536.

Kubo, D., Kono, R. T., Saso, A., Mizushima, S., & Suwa, G. (2008). Accuracy and precision of CT-based endocranial capacity estimations: A comparison with the conventional millet seed method and application to the Minatogawa 1 skull. *Anthropological Science*, 116(1), 77-85.

Kutner, M. H., Nachtsheim, C. J., Neter, J., & Li., W. (2005). *Applied linear statistical models*, 5th edition. McGraw-Hill, Boston.

Kustaloglu, O. A. (1961). *Australopithecus* and *Paranthropus* dentitions. *Southwestern Journal of Anthropology*, 17(3), 226-238.

Laden, G., & Wrangham, R. (2005). The rise of the hominids as an adaptive shift in fallback foods: Plant underground storage organs (USOs) and australopith origins. *Journal of Human Evolution*, 49(4), 482-498.

Lague, M. R., Collard, N. J., Richmond, B. G., & Wood, B. A. (2008). Hominid mandibular corpus shape variation and its utility for recognizing species diversity within fossil *Homo*. *Journal of Anatomy*, 213(6), 670-685.

Lahr, M. M. (1996). *The evolution of modern human diversity: a study of cranial variation*. Cambridge University Press, New York.

Lam, Y. M., Pearson, O. M., Marean, C. W., & Chen, X. (2003). Bone density studies in zooarchaeology. *Journal of Archaeological Science*, 30(12), 1701-1708.

Lambert, J. E. (1998). Primate digestion: interactions among anatomy, physiology, and feeding ecology. *Evolutionary Anthropology*, 7(1), 8-20.

Lambert, J. E. (2009). Summary to the symposium issue: Primate fallback strategies as adaptive phenotypic plasticity—scale, pattern, and process. *American Journal of Physical Anthropology*, 140(4), 759-766.

Larsen, C. S. (1981). Skeletal and dental adaptations to the shift to agriculture on the Georgia coast. *Current Anthropology*, 22(4), 422-423.

Larsen, C. S. (1995). Biological changes in human populations with agriculture. *Annual Review of Anthropology*, 24(1), 185-213.

Latif, A. (1957). An electromyographic study of the temporalis muscle in normal persons during selected positions and movements of the mandible. *American Journal of Orthodontics*, 43(8), 577-591.

Lee-Thorp, J. (2011). The demise of "Nutcracker Man". P*roceedings of the National Academy of Sciences of the United States of America*, 108(23), 9319-9320.

Lee-Thorp, J. A., Sponheimer, M., Passey, B. H., De Ruiter, D. J., & Cerling, T. E. (2010). Stable isotopes in fossil hominin tooth enamel suggest a fundamental dietary shift in the Pliocene. *Philosophical Transactions of the Royal Society of London B: Biological Sciences*, 365(1556), 3389-3396.

Lefebvre, L. (2013). Brains, innovations, tools and cultural transmission in birds, non-human primates, and fossil hominins. *Frontiers in Human Neuroscience*, 7, 245.

Legendre, P., & Legendre, L. F. (2012). *Numerical ecology*. 3rd English ed. Elsevier, Amsterdam.

Lehmann, J., & Dunbar, R. I. M. (2009). Network cohesion, group size and neocortex size in female-bonded Old World primates. *Proceedings of the Royal Society of London B: Biological Sciences*, 276(1677), 4417-4422.

Leigh, S. R. (1992). Patterns of variation in the ontogeny of primate body size dimorphism. *Journal of Human Evolution*, 23(1), 27-50.

Leigh, S. R., & Shea, B. T. (1995). Ontogeny and the evolution of adult body size dimorphism in apes. *American Journal of Primatology*, 36(1), 37-60.

Leigh, S. R., & Shea, B. T. (1996). Ontogeny of body size variation in African apes. *American Journal of Physical Anthropology*, 99(1), 43-65.

Leonard, W. R., & Robertson, M. L. (1994). Evolutionary perspectives on human nutrition: The influence of brain and body size on diet and metabolism. *American Journal of Human Biology*, 6(1), 77-88.

Leonard, W. R., Robertson, M. L., Snodgrass, J. J., & Kuzawa, C. W. (2003). Metabolic correlates of hominid brain evolution. *Comparative Biochemistry and Physiology Part A: Molecular & Integrative Physiology*, 136(1), 5-15.

Leutenegger, W. (1982). Encephalization and obstetrics in primates with particular reference to human evolution. In Armstorong, E., & Falk, D. (Eds.), *Primate brain evolution: Methods and concepts*. Plenum Publishing, New York.

Leutenegger, W., & Kelly, J. T. (1977). Relationship of sexual dimorphism in canine size and body size to social, behavioral, and ecological correlates in anthropoid primates. *Primates*, 18(1), 117-136.

Leutenegger, W., & Shell, B. (1987). Variability and sexual dimorphism in canine size of *Australopithecus* and extant hominoids. *Journal of Human Evolution*, 16(4), 359-367.

Lieberman, D. E. (1995). Testing hypotheses about recent human evolution from skulls: Integrating morphology, function, development, and phylogeny. *Current Anthropology*, 36(2), 159-197.

Lieberman, D. E., McBratney, B. M., & Krovitz, G. (2002). The evolution and development of cranial form in *Homo* sapiens. *Proceedings of the National Academy of Sciences of the United States of America*, 99(3), 1134-1139.

Lieberman, D. E., Ross, C. F., & Ravosa, M. J. (2000). The primate cranial base: Ontogeny, function, and integration. *American Journal of Physical Anthropology*, 113(S31), 117-169.

Lieberman, P., (1992). Human speech and language. In Jones, S., Martin, R. D., & Pilbeam, D. R. (Eds.), *The Cambridge encyclopedia of human evolution*, 134-137. Cambridge University Press, New York.

Lucas, P. W., Prinz, J. F., Agrawal, K. R., & Bruce, I. C. (2004). Food texture and its effect on ingestion, mastication and swallowing. *Journal of Texture Studies*, 35(2), 159-170.

Lupo, K. D. (1998). Experimentally derived extraction rates for marrow: implications for body part exploitation strategies of Plio-Pleistocene hominid scavengers. *Journal of Archaeological Science*, 25(7), 657-675.

Macchiarelli, R., & Bondioli, L. (1986). Post-Pleistocene reductions in human dental structure: A reappraisal in terms of increasing population density. *Human Evolution*, 1(5), 405-417.

Macho, G.A., & Moggi-Cecchi, J., (1992). Reduction of maxillary molars in *Homo sapiens sapiens*: A different perspective. *American Journal of Physical Anthropology*. 87, 151-159.

Mafart, B., Guipert, G., De Lumley, M. A., & Subsol, G. (2004). Three-dimensional computer imaging of hominid fossils: a new step in human evolution studies. *Canadian Association of Radiologists Journal*, 55(4), 264.

Mah, P., Reeves, T. E., & McDavid, W. D. (2014). Deriving Hounsfield units using grey levels in cone beam computed tomography. *Dentomaxillofacial Radiology*, 39(6): 323e335.

Majid, Z., Chong, A. K., Ahmad, A., Setan, H., & Samsudin, A. R. (2005). Photogrammetry and 3D laser scanning as spatial data capture techniques for a national craniofacial database. *The Photogrammetric Record*, 20(109), 48-68.

Markovsky, I., & Van Huffel, S. (2007). Overview of total least-squares methods. *Signal processing*, 87(10), 2283-2302.

Martinón-Torres, M., de Castro, J. M. B., Gómez-Robles, A., Margvelashvili, A., Prado, L., Lordkipanidze, D., & Vekua, A. (2008). Dental remains from Dmanisi (Republic of Georgia): Morphological analysis and comparative study. *Journal of Human Evolution*, 55(2), 249-273.

McCollum, M. A. (1999). The robust australopithecine face: A morphogenetic perspective. *Science*, 284(5412), 301-305.

McHenry, H. M. (1982). The pattern of human evolution: studies on bipedalism, mastication, and encephalization. *Annual Review of Anthropology*, 11(1), 151-173.

McHenry, H. M. (1984). Relative cheek-tooth size in *Australopithecus*. *American Journal of Physical Anthropology*, 64(3), 297-306.

McHenry, H. M. (1994). Tempo and mode in human evolution. *Proceedings of the National Academy of Sciences of the United States of America*, 91(15), 6780-6786.

McHenry, H. M., Berger, L. R. (1998). Body proportions in *Australopithecus afarensis* and *A. africanus* and the origin of the genus *Homo*. *Journal of Human Evolution*. 35, 1-22.

McHenry, H. M., & Coffing, K. (2000). *Australopithecus* to *Homo*: Transformations in body and mind. *Annual Review of Anthropology*, 29(1), 125-146.

Meloro, C., Cáceres, N. C., Carotenuto, F., Sponchiado, J., Melo, G. L., Passaro, F., & Raia, P. (2015). Chewing on the trees: Constraints and adaptation in the evolution of the primate mandible. *Evolution*, 69(7), 1690-1700.

Milton, K., & May, M. L. (1976). Body weight, diet and home range area in primates. *Nature*, 259(5543), 459-462.

Mikkelsen, T. S., Hillier, L. W., Eichler, E. E., & Zody, M. C. (2005). Initial sequence of the chimpanzee genome and comparison with the human genome. Nature, 437(7055), 69.

Mioche, L., Bourdiol, P., Martin, J. F., & Noël, Y. (1999). Variations in human masseter and temporalis muscle activity related to food texture during free and side-imposed mastication. *Archives of Oral Biology*, 44(12), 1005-1012.

Mitteroecker, P., Gunz, P., Bernhard, M., Schaefer, K., & Bookstein, F. L. (2004). Comparison of cranial ontogenetic trajectories among great apes and humans. *Journal of Human Evolution*, 46(6), 679-698.

Mitteroecker, P., & Gunz, P. (2009). Advances in geometric morphometrics. *Evolutionary Biology*, 36(2), 235-247.

Mosimann, J. E. (1970). Size allometry: Size and shape variables with characterizations of the lognormal and generalized gamma distributions. *Journal of the American Statistical Association*, 65(330), 930-945.

National Research Council US. (2003). *Nutrient requirements of nonhuman primates*. The National Academies Press, Washington D. C.

Norconk, M. A., Wright, B. W., Conklin-Brittain, N. L., & Vinyard, C. J. (2009). Mechanical and nutritional properties of food as factors in platyrrhine dietary adaptations. In Garber, P. A., Estrada, A., Bicca-Marques, J. C., Heymann, E. W., & Strier, K. B. (Eds.), *South American Primates*. Springer Science & Business Media, New York.

Norton, G. W., Rhine, R. J., Wynn, G. W., & Wynn, R. D. (1987). Baboon diet: A five-year study of stability and variability in the plant feeding and habitat of the yellow baboons (*Papio cynocephalus*) of Mikumi National Park, Tanzania. *Folia Primatologica*, 48(1-2), 78-120.

Nunn, C. L., & Van Schaik, C. P. (2002). A comparative approach to reconstructing the socioecology of extinct primates. In Plavcan, M. J., Kay, R. F., Jungers, W. L., & Van Schaik, C. P. (Eds.), *Reconstructing behavior in the primate fossil record*. Springer Science & Business Media, New York.

Olejniczak, A. J., Smith, T. M., Skinner, M. M., Grine, F. E., Feeney, R. N., Thackeray, J. F., & Hublin, J. J. (2008). Three-dimensional molar enamel distribution and thickness in *Australopithecus* and *Paranthropus*. *Biology Letters*, 4(4), 406-410.

Olson, E. C., & Miller, R. L. (1999). *Morphological integration*. University of Chicago Press, Chicago.

Orme, D., Freckleton, R., Thomas, G., Petzoldt, T., Fritz, S., Isaac, N., & Pearse, W. (2013). caper: Comparative Analyses of Phylogenetics and Evolution in R. *R package version 0.5.2*. http://CRAN.R-project.org/package=caper

Pagel, M. (1999). Inferring the historical patterns of biological evolution. *Nature*, 401(6756), 877-884.

Palmer, M. W. (1993). Putting things in even better order: the advantages of canonical correspondence analysis. *Ecology*, 74(8), 2215-2230.

Paradis, E., Claude, J., & Strimmer, K. (2004). APE: analyses of phylogenetics and evolution in R language. *Bioinformatics*, 20(2), 289-290.

Parker, S. T., & Gibson, K. R. (1977). Object manipulation, tool use and sensorimotor intelligence as feeding adaptations in cebus monkeys and great apes. *Journal of Human Evolution*, 6(7), 623-641.

Pearson, O. M. (2008). Statistical and biological definitions of "anatomically modern" humans: Suggestions for a unified approach to modern morphology. *Evolutionary Anthropology*, 17(1), 38-48.

Pellegrin, P. (1986). *Aristotle's classification of animals: biology and the conceptual unity of the Aristotelian corpus*. University of California Press, Berkeley.

Peyron, M. A., Maskawi, K., Woda, A., Tanguay, R., & Lund, J. P. (1997). Effects of food texture and sample thickness on mandibular movement and hardness assessment during biting in man. *Journal of Dental Research*, 76(3), 789-795.

Pielou, E. C. (1969). *An introduction to mathematical ecology*. Wiley, New York.

Pilbeam, D., & Gould, S.J., (1974). Size and scaling in human evolution. *Science*, 186, 892-901.

Pinhasi, R., Eshed, V., & Shaw, P. (2008). Evolutionary changes in the masticatory complex following the transition to farming in the southern Levant. *American Journal of Physical Anthropology*, 135(2), 136-148.

Pinhasi, R., & Meiklejohn, C. (2011). Dental reduction and the transition to agriculture in Europe. In Pinhasi, R., & Stock, J. T. (Eds.), *Human Bioarchaeology of the Transition to Agriculture*, John Wiley & Sons, Hoboken.

Pinheiro, J., Bates, D., DebRoy, S., Sarkar, D., & Team, R. C. (2015). nlme: Linear and Nonlinear Mixed Effects Models. *R package version 3.1*, http://CRAN.R-project.org/package=nlme.

Plavcan, J. M. (2001). Sexual dimorphism in primate evolution. *American Journal of Physical Anthropology*, 116(S33), 25-53.

Plavcan, J. M. (2004). Sexual selection, measures of sexual selection, and sexual dimorphism in primates. In: Kappeler, P. M., Van Schaik, C. P., (Eds.). *Sexual selection in primates: New and comparative perspectives*. Cambridge University Press, New York.

Plavcan, J. M., & Daegling, D. J. (2006). Interspecific and intraspecific relationships between tooth size and jaw size in primates. *Journal of Human Evolution*, 51(2), 171-184.

Plavcan, J. M., & Van Schaik, C. P. (1997). Interpreting hominid behavior on the basis of sexual dimorphism. *Journal of Human Evolution*, 32(4), 345-374.

Porto, A., de Oliveira, F. B., Shirai, L. T., De Conto, V., & Marroig, G. (2009). The evolution of modularity in the mammalian skull I: Morphological integration patterns and magnitudes. *Evolutionary Biology*, 36(1), 118-135.

Potts, R. (2013). Hominin evolution in settings of strong environmental variability. *Quaternary Science Reviews*, 73, 1-13.

Pouydebat, E., Gorce, P., Coppens, Y., & Bels, V. (2009). Biomechanical study of grasping according to the volume of the object: Human versus non-human primates. *Journal of Biomechanics*, 42(3), 266-272.

Powell, A., Shennan, S., & Thomas, M. G. (2009). Late Pleistocene demography and the appearance of modern human behavior. *Science*, 324(5932), 1298-1301.

Prat, S., Brugal, J. P., Tiercelin, J. J., Barrat, J. A., Bohn, M., Delagnes, A., Harmand, S., Kimeu, K., Mzalendo, K., Texier, P. J., & Roche, H. (2005). First occurrence of early Homo in the Nachukui formation (West Turkana, Kenya) at 2.3-2.4 Myr. Journal of human evolution, 49(2), 230-240.

Price, T. D., Qvarnström, A., & Irwin, D. E. (2003). The role of phenotypic plasticity in driving genetic evolution. *Proceedings of the Royal Society of London B: Biological Sciences*, 270(1523), 1433-1440.

Quam, R., Bailey, S., & Wood, B. (2009). Evolution of M1 crown size and cusp proportions in the genus *Homo*. *Journal of Anatomy*, 214(5), 655-670.

R Core Team (2015). R: A language and environment for statistical computing. R Foundation for Statistical Computing, Vienna, Austria. URL http://www.R-project.org/.

Raadsheer, M. C., Van Eijden, T. M. G. J., Van Ginkel, F. C., & Prahl-Andersen, B. (1999). Contribution of jaw muscle size and craniofacial morphology to human bite force magnitude. *Journal of Dental Research*, 78(1), 31-42.

Rak, Y., & Hylander, W. L. (2008). What else is the tall mandibular ramus of the robust australopithecines good for? In Vinyard, C. J., Ravosa, M. J., & Wall, C. E. (Eds.), *Primate craniofacial function and biology*. Springer Science & Business Media, New York.

Raman, S., & Wenger, R. (2008). Quality isosurface mesh generation using an extended marching cubes lookup table. *Computer Graphics Forum* 27(3), 791-798

Ramsthaler, F., Kettner, M., Gehl, A., & Verhoff, M. A. (2010). Digital forensic osteology: Morphological sexing of skeletal remains using volume-rendered cranial CT scans. *Forensic Science International*, 195(1), 148-152.

Reader, S. M., Hager, Y., & Laland, K. N. (2011). The evolution of primate general and cultural intelligence. *Philosophical Transactions of the Royal Society B: Biological Sciences*, 366(1567), 1017-1027.

Rensch, B. (1950). Die Abhängigkeit der relativen Sexualdifferenz von der Körpergrösse. *Bonner Zoologische Beiträge*, 1, 58-69.

Revell, L. J. (2012). phytools: an R package for phylogenetic comparative biology (and other things). *Methods in Ecology and Evolution*, 3(2), 217-223.

Riesenfeld, A. (1969). The adaptive mandible: An experimental study. *Cells Tissues Organs*, 72(2), 246-262.

Rightmire, G. P. (2004). Brain size and encephalization in Early to Mid-Pleistocene *Homo*. *American Journal of Physical Anthropology*, 124(2), 109-123.

Rightmire, G. P. (2008). *Homo* in the Middle Pleistocene: Hypodigms, variation, and species recognition. *Evolutionary Anthropology*, 17(1), 8-21.

Robinson, J. T. (1954). Prehominid dentition and hominid evolution. *Evolution*, 8(4), 324-334.

Robinson, J. G., & Redford, K. H. (1986). Body size, diet, and population density of Neotropical forest mammals. *The American Naturalist*, 128(5), 665-680.

Roebroeks, W., & Villa, P. (2011). On the earliest evidence for habitual use of fire in Europe. *Proceedings of the National Academy of Sciences of the United States of America*, 108(13), 5209-5214.

Roff, D. A. (1996). The evolution of threshold traits in animals. *The Quarterly Review of Biology*, 71(1), 3-35.

Rolland, N. (2004). Was the emergence of home bases and domestic fire a punctuated event? A review of the Middle Pleistocene record in Eurasia. *Asian Perspectives*, 43(2), 248-280.

Rose, L. M. (1994). Sex differences in diet and foraging behavior in white-faced capuchins (*Cebus capucinus*). *International Journal of Primatology*, 15(1), 95-114.

Ross, C. F., Hall, M. I., & Heesy, C. P. (2007). Were basal primates nocturnal? Evidence from eye and orbit shape. In Ravosa, M. J., & Dagosto, M. (Eds.), *Primate origins: adaptations and evolution*. Springer Science & Business Media, New York.

Ross, C. F., Iriarte-Diaz, J., & Nunn, C. L. (2012). Innovative approaches to the relationship between diet and mandibular morphology in primates. *International Journal of Primatology*, 33(3), 632-660.

Ross, C. F., Reed, D. A., Washington, R. L., Eckhardt, A., Anapol, F., & Shahnoor, N. (2009a). Scaling of chew cycle duration in primates. *American Journal of Physical Anthropology*, 138(1), 30-44.

Ross, C. F., Washington, R. L., Eckhardt, A., Reed, D. A., Vogel, E. R., Dominy, N. J., & Machanda, Z. P. (2009b). Ecological consequences of scaling of chew cycle duration and daily feeding time in Primates. *Journal of Human Evolution*, 56(6), 570-585.

Roth, G., & Dicke, U. (2005). Evolution of the brain and intelligence. *Trends in Cognitive Sciences*, 9(5), 250-257.

Rowlett, R. M. (2000). Fire control by *Homo erectus* in East Africa and Asia. *Acta Anthropologica Sinica*, 19(Supplement), 198-208.

Rueffler, C., Van Dooren, T. J., Leimar, O., & Abrams, P. A. (2006). Disruptive selection and then what?. *Trends in Ecology & Evolution*, 21(5), 238-245.

Ruff, C. (2002). Variation in human body size and shape. *Annual Review of Anthropology*, 31(1), 211-232.

Ruff, C. B., Trinkaus, E., & Holliday, T. W. (1997). Body mass and encephalization in Pleistocene *Homo*. *Nature*, 387(6629), 173.

Russo, G. A., & Kirk, E. C. (2013). Foramen magnum position in bipedal mammals. *Journal of Human Evolution*, 65(5), 656-670.

Ruvolo, M. (1997). Molecular phylogeny of the hominoids: inferences from multiple independent DNA sequence data sets. *Molecular biology and evolution*, 14(3), 248-265.

Sailer, L. D., Gaulin, S. J., Boster, J. S., & Kurland, J. A. (1985). Measuring the relationship between dietary quality and body size in primates. *Primates*, 26(1), 14-27.

Sandgathe, D. M., Dibble, H. L., Goldberg, P., McPherron, S. P., Turq, A., Niven, L., & Hodgkins, J. (2011). Timing of the appearance of habitual fire use. *Proceedings of the National Academy of Sciences of the United States of America*, 108(29), 298-298.

Sasaki, K., Hannam, A. G., & Wood, W. W. (1989). Relationships between the size, position, and angulation of human jaw muscles and unilateral first molar bite force. *Journal of Dental Research*, 68(3), 499-503.

Scherjon, F., Bakels, C., MacDonald, K., & Roebroeks, W. (2015). Burning the land: an ethnographic study of off-site fire use by current and historically documented foragers and implications for the interpretation of past fire practices in the landscape. *Current Anthropology*, 56(3), 314-315.

Schick, K. D., & Toth, N. P. (1994). *Making silent stones speak: Human evolution and the dawn of technology*. Simon and Schuster, New York.

Shimelmitz, R., Kuhn, S. L., Jelinek, A. J., Ronen, A., Clark, A. E., & Weinstein-Evron, M. (2014). 'Fire at will': The emergence of habitual fire use 350,000 years ago. *Journal of Human Evolution*, 77, 196-203.

Schlager, S. (2013). Morpho: Calculations and visualizations related to Geometric Morphometrics. *R package version 0.17*. http://sourceforge.net/projects/morpho-rpackage/

Schrago, C. G., Menezes, A. N., Moreira, M. A., Pissinatti, A., & Seuánez, H. N. (2012). Chronology of deep nodes in the neotropical primate phylogeny: Insights from mitochondrial genomes. PloS one, 7(12), e51699.

Schroeder, L., Scott, J. E., Garvin, H. M., Laird, M. F., Dembo, M., Radovčić, D., Berger, L. R., de Ruiter, D. J., & Ackermann, R. R. (2017). Skull diversity in the *Homo* lineage and the relative position of *Homo naledi*. *Journal of Human Evolution*, 104, 124-135.

Schwartz, J. H., & Tattersall, I. (2000). The human chin revisited: What is it and who has it? *Journal of Human Evolution*, 38(3), 367-409.

Schwartz, J. H., & Tattersall, I. (2005). *The human fossil record, craniodental morphology of genus* Homo (Africa and Asia) (Vol. 2). John Wiley & Sons, Hoboken.

Sciulli, P. W. (1979). Size and morphology of the permanent dentition in prehistoric Ohio Valley Amerindians. *American Journal of Physical Anthropology*, 50(4), 615-628.

Scott, R. S., Teaford, M. F., & Ungar, P. S. (2012). Dental microwear texture and anthropoid diets. *American Journal of Physical Anthropology*, 147(4), 551-579.

Scott, R. S., Ungar, P. S., Bergstrom, T. S., Brown, C. A., Childs, B. E., Teaford, M. F., & Walker, A. (2006). Dental microwear texture analysis: Technical considerations. *Journal of Human Evolution*, 51(4), 339-349.

Scott, R. S., Ungar, P. S., Bergstrom, T. S., Brown, C. A., Grine, F. E., Teaford, M. F., & Walker, A. (2005). Dental microwear texture analysis shows within-species diet variability in fossil hominins. *Nature*, 436(7051), 693-695.

Shea, B. T. (1983). Allometry and heterochrony in the African apes. *American Journal of Physical Anthropology*, 62(3), 275-289.

Sholts, S. B., Wärmländer, S. K., Flores, L. M., Miller, K. W., & Walker, P. L. (2010). Variation in the measurement of cranial volume and surface area using 3D laser scanning technology. *Journal of Forensic Sciences*, 55(4), 871-876.

Shultz, S., & Dunbar, R. (2010). Encephalization is not a universal macroevolutionary phenomenon in mammals but is associated with sociality. *Proceedings of the National Academy of Sciences of the United States of America*, 107(50), 21582-21586.

Shultz, S., Nelson, E., & Dunbar, R. I. (2012). Hominin cognitive evolution: Identifying patterns and processes in the fossil and archaeological record. *Philosophical Transactions of the Royal Society B: Biological Sciences*, 367(1599), 2130-2140.

Silver, S. C., & Marsh, L. K. (2003). Dietary flexibility, behavioral plasticity, and survival in fragments: lessons from translocated howlers. In Marsh, L. K. (Ed.) *Primates in fragments: Ecology and conservation*. Springer Science & Business Media, New York.

Singh, N., Harvati, K., Hublin, J. J., & Klingenberg, C. P. (2012). Morphological evolution through integration: a quantitative study of cranial integration in Homo, Pan, Gorilla and Pongo. *Journal of Human Evolution*, 62(1), 155-164.

Smaers, J. B. (2014). evomap: R package for the evolutionary mapping of continuous traits. GitHub, https://github. com/JeroenSmaers/evomap.

Smaers, J. B., & Rohlf, F. J. (2016). Testing species' deviation from allometric predictions using the phylogenetic regression. *Evolution*, 70(5), 1145-1149.

Smith, A. L., Benazzi, S., Ledogar, J. A., Tamvada, K., Pryor Smith, L. C., Weber, G. W., Spencer, M. A., Lucas, P. W., Michael, S., Shekeban, A., Al-Fadhalah, K., Almusallam, A. S., Dechow, P. C., Grosse, I. R., Ross, C. F., Madden, R. H., Richmond, B. G., Wright, B. W., Wang, Q., Byron, C., Slice, D. E., Wood, S., Dzialo, C., Berthaume, M. A., van Casteren, A. and Strait, D. S. (2015), The feeding biomechanics and dietary ecology of *Paranthropus boisei*. *The Anatomical Record*, 298, 145–167.

Smith, J. M., Burian, R., Kauffman, S., Alberch, P., Campbell, J., Goodwin, B., Lande, R., Raup, D., & Wolpert, L. (1985). Developmental constraints and evolution: a perspective from the Mountain Lake conference on development and evolution. *The Quarterly Review of Biology*, 60(3), 265-287.

Smith, P. (1977). Regional variation in tooth size and pathology in fossil hominids. *American Journal of Physical Anthropology*, 47(3), 459-466.

Smith, R. J. (1978). Mandibular biomechanics and temporomandibular joint function in primates. *American Journal of Physical Anthropology*, 49(3), 341-349.

Smith, R. J. (1981). Interspecific scaling of maxillary canine size and shape in female primates: Relationships to social structure and diet. *Journal of Human Evolution*, 10(2), 165-173.

Smith, R. J. (1983). The mandibular corpus of female primates: Taxonomic, dietary, and allometric correlates of interspecific variations in size and shape. *American Journal of Physical Anthropology*, 61(3), 315-330.

Smith, R. J., Jungers, W. L. (1997). Body mass in comparative primatology. *Journal of Human Evolution*, 32, 523-559.

Snodgrass, J. J., Leonard, W. R., & Robertson, M. L. (2009). The energetics of encephalization in early hominids. In Hublin, J. J., & Richards, M. P. (Eds.), *The evolution of hominin diets*. Springer Science & Business Media, New York.

Sofaer, J. A., Bailit, H. L., MacLean, C. J., (1971). A developmental basis for differential tooth reduction during hominid evolution. *Evolution*. 25, 509-517.

Spencer, M. A. (1998). Force production in the primate masticatory system: Electromyographic tests of biomechanical hypotheses. *Journal of Human Evolution*, 34(1), 25-54.

Speth, J. D. (1989). Early hominid hunting and scavenging: The role of meat as an energy source. *Journal of Human Evolution*, 18(4), 329-343.

Spoor, F., Gunz, P., Neubauer, S., Stelzer, S., Scott, N., Kwekason, A., & Dean, M. C. (2015). Reconstructed *Homo habilis* type OH 7 suggests deep-rooted species diversity in early Homo. *Nature*, 519(7541), 83-86.

St. Hoyme, L. E., & Turner II, C. G. (1980). Australian tooth-size clines and the death of a stereotype [and Comments and Reply]. *Current Anthropology*, *21*(2), 141-164.

Standring, S., & Gray, H. (2008). *Gray's Anatomy: The Anatomical Basis of Clinical Practice*, 40th Edition. Elsevier, St. Louis.

Stanford, C. B., & Bunn, H. T. (2001). *Meat-eating and human evolution*. Oxford University Press, New York.

Steele, J., Clegg, M., & Martelli, S. (2013). Comparative morphology of the hominin and African ape hyoid bone, a possible marker of the evolution of speech. *Human Biology*, 85(5), 639-672.

Stringer, C. (2015). The many mysteries of *Homo naledi*. *eLife*, 4, e10627.

Stringer, C. B., & Barnes, I. (2015). Deciphering the Denisovans. *Proceedings of the National Academy of Sciences of the United States of America*, 112(51), 15542-15543.

Stull, K. E., Tise, M. L., Ali, Z., & Fowler, D. R. (2014). Accuracy and reliability of measurements obtained from computed tomography 3D volume rendered images. *Forensic Science International*, 238, 133-140.

Suwa, G., White, T. D., & Howell, F. C. (1996). Mandibular postcanine dentition from the Shungura Formation, Ethiopia: Crown morphology, taxonomic allocations, and Plio-Pleistocene hominid evolution. *American Journal of Physical Anthropology*, 101(2), 247-282.

Swindler, D. R. (2002). *Primate dentition: an introduction to the teeth of non-human primates*. Cambridge University Press, New York.

Tams, J., Van Loon, J. P., Otten, E., Rozema, F. R., & Bos, R. R. M. (1997). A three-dimensional study of bending and torsion moments for different fracture sites in the mandible: An in vitro study. *International Journal of Oral and Maxillofacial Surgery*, 26(5), 383-388.

Taylor, A. B. (2002). Masticatory form and function in the African apes. *American Journal of Physical Anthropology*, 117(2), 133-156.

Taylor, A. B. (2006a). Diet and mandibular morphology in African apes. *International Journal of Primatology*, 27(1), 181.

Taylor, A. B. (2006b). Feeding behavior, diet, and the functional consequences of jaw form in orangutans, with implications for the evolution of Pongo. *Journal of Human Evolution*, 50(4), 377-393.

Teaford, M. F., & Oyen, O. J. (1989). In vivo and in vitro turnover in dental microwear. *American Journal of Physical Anthropology*, 80(4), 447-460.

Teaford, M. F., & Ungar, P. S. (2000). Diet and the evolution of the earliest human ancestors. *Proceedings of the National Academy of Sciences of the United States of America*, 97(25), 13506-13511.

Teleki, G. (1974). Chimpanzee subsistence technology: materials and skills. *Journal of Human Evolution*, 3(6), 575IN13585-584IN16594.

Tennie, C., O'Malley, R. C., & Gilby, I. C. (2014). Why do chimpanzees hunt? Considering the benefits and costs of acquiring and consuming vertebrate versus invertebrate prey. *Journal of Human Evolution*, 71, 38-45.

Throckmorton, G. S., Finn, R. A., & Bell, W. H. (1980). Biomechanics of differences in lower facial height. *American journal of orthodontics*, 77(4), 410-420.

Trinkaus, E. (2003). Neandertal faces were not long; modern human faces are short. *Proceedings of the National Academy of Sciences of the United States of America*, 100(14), 8142-8145.

Ungar, P. (2004). Dental topography and diets of *Australopithecus afarensis* and early *Homo*. *Journal of Human Evolution*, 46(5), 605-622.

Ungar, P. S. (2012). Dental evidence for the reconstruction of diet in African early *Homo*. *Current Anthropology*, 53(6), S318-S329.

Ungar, P. S., Grine, F. E., Teaford, M. F., & El Zaatari, S. (2006). Dental microwear and diets of African early *Homo*. *Journal of Human Evolution*, 50(1), 78-95.

Ungar, P. S., Krueger, K. L., Blumenschine, R. J., Njau, J., & Scott, R. S. (2012). Dental microwear texture analysis of hominins recovered by the Olduvai Landscape Paleoanthropology Project, 1995–2007. *Journal of Human Evolution*, 63(2), 429-437.

Van Eijden, T. M. (2000). Biomechanics of the mandible. *Critical Reviews in Oral Biology & Medicine*, 11(1), 123-136.

Van Ruijven, L. J., Giesen, E. B. W., & Van Eijden, T. M. G. J. (2002). Mechanical significance of the trabecular microstructure of the human mandibular condyle. *Journal of Dental Research*, 81(10), 706-710.

Van Schaik, C. P., Deaner, R. O., & Merrill, M. Y. (1999). The conditions for tool use in primates: Implications for the evolution of material culture. *Journal of Human Evolution*, 36(6), 719-741.

Van Spronsen, P. H., Weijs, W. A., Valk, J., Prahl-Andersen, B., & Van Ginkel, F. C. (1989). Comparison of jaw-muscle bite-force cross-sections obtained by means of magnetic resonance imaging and high-resolution CT scanning. *Journal of Dental Research*, 68(12), 1765-1770.

Venables, W. N., & Ripley, B. D. (2013). *Modern applied statistics with S-PLUS*. Springer Science & Business Media, New York.

Voisin J. L., Condemi S., Wolpoff M. H., Frayer D. W. (2012). A new online database (http://anthropologicaldata.free.fr) and a short reflection about the productive use of internet compiling data. *PaleoAnthropology*, 2012, 241-244.

Vrba, E. S. (1996). Climate, heterochrony, and human evolution. *Journal of Anthropological Research*, 52(1), 1-28.

Wagner, G. P., & Zhang, J. (2011). The pleiotropic structure of the genotype-phenotype map: the evolvability of complex organisms. *Nature reviews*. 12(3), 204.

Wakat, D. K., Johnson, R. E., Krzywicki, H. J., & Gerber, L. I. (1971). Correlation between body volume and body mass in men. *The American Journal of Clinical Nutrition*, 24(11), 1308-1312.

Walker, A. C. & Leakey, R. E. (1988). The evolution of *Australopithecus boisei*. In Grine, F. E., (Ed.), *The Evolutionary History of the Robust Australopithecines*, Transaction Publishers, New Brunswick.

Walker, A., Leakey, R. E., Harris, J. M., & Brown, F. H. (1986). 2.5-myr *Australopithecus boisei* from west of Lake Turkana, Kenya. *Nature*, 322, 517-522.

Wang, G., Zhu, Z., Shi, P., & Zhang, Y. (2010). Comparative genomic analysis reveals more functional nasal chemoreceptors in nocturnal mammals than in diurnal mammals. *Chinese Science Bulletin*, 55(34), 3901-3910.

Weber, G. W. (2001). Virtual anthropology (VA): a call for glasnost in paleoanthropology. *The Anatomical Record*, 265(4), 193-201.

Weber, B. H. (2011). Extending and expanding the Darwinian synthesis: The role of complex systems dynamics. *Studies in History and Philosophy of Biological and Biomedical Sciences*, 42(1), 75-81.

Weidenreich, F. (1941). The brain and its role in the phylogenetic transformation of the human skull. *Transactions of the American Philosophical Society*, 31(5), 320-442.

Weijs, W. A. (1988). The functional significance of morphological variation of the human mandible and masticatory muscles. *Acta Morphologica Neerlando-Scandinavica*, 27(1-2), 149-162.

Weijs, W. A. (1994). Evolutionary approach of masticatory motor patterns in mammals. In Bels, L., Chardon, M., & Vandewalle, P. (Eds.), *Biomechanics of feeding in vertebrates*. Springer, Berlin.

Weinberg, S. M., Naidoo, S., Govier, D. P., Martin, R. A., Kane, A. A., & Marazita, M. L. (2006). Anthropometric precision and accuracy of digital three-dimensional photogrammetry: comparing the Genex and 3dMD imaging systems with one another and with direct anthropometry. *Journal of Craniofacial Surgery*, 17(3), 477-483.

Westneat, M. W. (2003). A biomechanical model for analysis of muscle force, power output and lower jaw motion in fishes. *Journal of Theoretical Biology*, 223(3), 269-281.

Whitcher, B., Schmid, V. J., & Thornton, A. (2011). Working with the DICOM and NIfTI Data Standards in R. *Journal of Statistical Software*, 44(6), 1-28.

White, T. D., Black, M. T., & Folkens, P. A. (2011). *Human osteology*. Academic press, New York.

Whitehead, P. F., & Jolly, C. J. (Eds.). (2000). *Old World monkeys*. Cambridge University Press, New York.

Wildman, D. E., Uddin, M., Liu, G., Grossman, L. I., & Goodman, M. (2003). Implications of natural selection in shaping 99.4% nonsynonymous DNA identity between humans and chimpanzees: enlarging genus *Homo*. *Proceedings of the national Academy of Sciences of the United States of America*, 100(12), 7181-7188.

Willis, M. S., & Swindler, D. R. (2004). Molar size and shape variations among Asian colobines. *American Journal of Physical Anthropology*, 125(1), 51-60.

Winterhalder, B., & Kennett, D. J. (2006). Behavioral ecology and the transition from hunting and gathering to agriculture. In Kennett, D. J., & Winterhalder, B. (Eds.), *Behavioral ecology and the transition to agriculture*, University of California Press, Berkeley.

Wittman, A. B., & Wall, L. L. (2007). The evolutionary origins of obstructed labor: Bipedalism, encephalization, and the human obstetric dilemma. *Obstetrical & Gynecological Survey*, 62(11), 739-748.

Wold, S., Esbensen, K., & Geladi, P. (1987). Principal component analysis. *Chemometrics and intelligent laboratory systems*, 2(1-3), 37-52.

WoldeGabriel, G., White, T. D., Suwa, G., Renne, P., de Heinzelin, J., Hart, W. K., & Heiken, G. (1994). Ecological and temporal placement of early Pliocene hominids at Aramis, Ethiopia. *Nature*, 371(6495), 330-333.

Wolpoff, M. H. (1971). *Metric Trends in Hominid Dental Evolution*. Case Western University Press: Cleveland.

Wolpoff M. H. (1979). The Krapina dental remains. *American Journal of Physical Anthropology*, 50 (1), 67-114.

Wood, B. (1979). An analysis of tooth and body size relationships in five primate taxa. *Folia primatologica*, 31(3), 187-211.

Wood, B. (1992). Origin and evolution of the genus *Homo*. *Nature*, 355, 783-790.

Wood, B. (2011). *Wiley-Blackwell Encyclopedia of Human Evolution*, John Wiley & Sons, Hoboken.

Wood, B., Aiello, L. C., (1998). Taxonomic and functional implications of mandibular scaling in early hominins. *American Journal of Physical Anthropology*. 105, 523-538.

Wood, B., & Brooks, A. (1999). Human evolution: We are what we ate. *Nature*, 400(6741), 219-220.

Wood, B., & Constantino, P. (2007). *Paranthropus boisei*: Fifty years of evidence and analysis. *American Journal of Physical Anthropology*, 134(45), 106-132.

Wood, B., & Stack, C. G. (1980). Does allometry explain the differences between "Gracile" and "Robust" australopithecines? *American Journal of Physical Anthropology*, 52(1), 55-62.

Wood, B., & Strait, D. (2004). Patterns of resource use in early *Homo* and *Paranthropus*. *Journal of Human Evolution*, 46(2), 119-162.

Wrangham, R., (2009). *Catching fire: How cooking made us human*. Basic Books. New York.

Wrangham, R., & Carmody, R. (2010). Human adaptation to the control of fire. *Evolutionary Anthropology*, 19(5), 187-199.

Wrangham, R., & Conklin-Brittain, N. (2003). Cooking as a biological trait. *Comparative Biochemistry and Physiology Part A: Molecular & Integrative Physiology*, 136(1), 35-46.

Wrangham, R. W., Conklin-Brittain, N. L., & Hunt, K. D. (1998). Dietary response of chimpanzees and cercopithecines to seasonal variation in fruit abundance. I. Antifeedants. *International Journal of Primatology*, 19(6), 949-970.

Y'Edynak, G. (1989). Yugoslav Mesolithic dental reduction. *American Journal of Physical Anthropology*, 78(1), 17-36.

Zehr, E. P., Hundza, S. R., & Vasudevan, E. V. (2009). The quadrupedal nature of human bipedal locomotion. *Exercise and Sport Sciences Reviews*, 37(2), 102-108.

Zelditch, M. L., Swiderski, D. L., & Sheets, H. D. (2012). *Geometric morphometrics for biologists: a primer*. Academic Press, New York.

Zink, K. D., & Lieberman, D. E. (2016). Impact of meat and Lower Palaeolithic food processing techniques on chewing in humans. *Nature*. 531, 500-503.

Zink, K. D., Lieberman, D. E., & Lucas, P. W. (2014). Food material properties and early hominin processing techniques. *Journal of Human Evolution*, 77, 155-166.

Appendix 1

Ap1.1 The catarrhine sample. The collection and sources of the CT scan models of each specimen in the sample are provided. (Continues to the next page). (**SMT**: Smithsonian Institution; **KUPRI**: Kyoto University Primate Institute; **MCZ**: Museum of Comparative Zoology at Harvard; **LIV**: University of Liverpool; **RMCA**: Royal Museum for Central Africa; **UCL**: University College London).

Species	Group	Collection	Code	Source
Allenopithecus nigroviridis	Cercopithecinae	SMT	USNM 395131	Smithsonian
Bunopithecus hoolock	Hylobatidae	SMT	USNM 257988	Smithsonian
Bunopithecus hoolock	Hylobatidae	SMT	USNM 545009	Smithsonian
Bunopithecus hoolock	Hylobatidae	SMT	USNM 257987	Smithsonian
Cercocebus agilis	Cercopithecinae	KUPRI	575	KUPRI database
Cercocebus atys	Cercopithecinae	KUPRI	604	KUPRI database
Cercocebus atys	Cercopithecinae	KUPRI	600	KUPRI database
Cercocebus atys	Cercopithecinae	KUPRI	602	KUPRI database
Cercocebus atys	Cercopithecinae	KUPRI	603	KUPRI database
Cercocebus galeritus	Cercopithecinae	KUPRI	588	KUPRI database
Cercocebus galeritus	Cercopithecinae	KUPRI	595	KUPRI database
Cercocebus torquatus	Cercopithecinae	MCZ	18612	MorphoSource
Cercocebus torquatus	Cercopithecinae	MCZ	32625	MorphoSource
Cercopithecus albogularis	Cercopithecinae	SMT	452581	Smithsonian
Cercopithecus albogularis	Cercopithecinae	SMT	452574	Smithsonian
Cercopithecus ascanius	Cercopithecinae	SMT	182355	Smithsonian
Cercopithecus ascanius	Cercopithecinae	SMT	452510	Smithsonian
Cercopithecus campbelli	Cercopithecinae	SMT	1071	Smithsonian
Cercopithecus campbelli	Cercopithecinae	SMT	1072	Smithsonian
Cercopithecus mitis	Cercopithecinae	SMT	452531	Smithsonian
Cercopithecus mitis	Cercopithecinae	SMT	182386	Smithsonian
Cercopithecus neglectus	Cercopithecinae	KUPRI	972	KUPRI database
Cercopithecus nictitans	Cercopithecinae	SMT	480838	Smithsonian
Cercopithecus nictitans	Cercopithecinae	SMT	537776	Smithsonian
Cercopithecus nictitans	Cercopithecinae	SMT	220377	Smithsonian
Cercopithecus nictitans	Cercopithecinae	SMT	481770	Smithsonian
Cercopithecus petaurista	Cercopithecinae	SMT	477317	Smithsonian
Cercopithecus petaurista	Cercopithecinae	SMT	481778	Smithsonian
Cercopithecus petaurista	Cercopithecinae	SMT	435021	Smithsonian

Ap1.1 (Continued)

Species	Group	Collection	Code	Source
Cercopithecus petaurista	Cercopithecinae	SMT	481779	Smithsonian
Chlorocebus aethiops	Cercopithecinae	KUPRI	860	KUPRI database
Chlorocebus aethiops	Cercopithecinae	KUPRI	861	KUPRI database
Chlorocebus sabaeus	Cercopithecinae	SMT	381449	Smithsonian
Chlorocebus sabaeus	Cercopithecinae	SMT	381445	Smithsonian
Colobus guereza	Colobinae	KUPRI	940	KUPRI database
Colobus polykomos	Colobinae	KUPRI	669	KUPRI database
Colobus polykomos	Colobinae	KUPRI	671	KUPRI database
Colobus polykomos	Colobinae	KUPRI	33	KUPRI database
Erythrocebus patas	Cercopithecinae	KUPRI	968	KUPRI database
Erythrocebus patas	Cercopithecinae	KUPRI	925	KUPRI database
Gorilla beringei	Hominidae	SMT	396935	Smithsonian
Gorilla beringei	Hominidae	SMT	396936	Smithsonian
Gorilla beringei	Hominidae	SMT	545026	Smithsonian
Gorilla beringei	Hominidae	SMT	545029	Smithsonian
Gorilla beringei	Hominidae	SMT	545030	Smithsonian
Gorilla beringei	Hominidae	SMT	545031	Smithsonian
Gorilla beringei	Hominidae	SMT	239883	Smithsonian
Gorilla beringei	Hominidae	SMT	395636	Smithsonian
Gorilla beringei	Hominidae	SMT	396934	Smithsonian
Gorilla beringei	Hominidae	SMT	397351	Smithsonian
Gorilla beringei	Hominidae	SMT	545028	Smithsonian
Gorilla beringei	Hominidae	SMT	545032	Smithsonian
Gorilla beringei	Hominidae	SMT	545034	Smithsonian
Gorilla gorilla	Hominidae	SMT	220380	Smithsonian
Gorilla gorilla	Hominidae	SMT	252575	Smithsonian
Gorilla gorilla	Hominidae	SMT	252576	Smithsonian
Gorilla gorilla	Hominidae	SMT	252577	Smithsonian
Gorilla gorilla	Hominidae	SMT	252579	Smithsonian
Gorilla gorilla	Hominidae	SMT	252580	Smithsonian
Gorilla gorilla	Hominidae	SMT	582726	Smithsonian
Gorilla gorilla	Hominidae	SMT	590947	Smithsonian

Ap1.1 (Continued)

Species	Group	Collection	Code	Source
Gorilla gorilla	Hominidae	SMT	590948	Smithsonian
Gorilla gorilla	Hominidae	KUPRI	25	KUPRI database
Gorilla gorilla	Hominidae	LIV	2086	NESPOS
Gorilla gorilla	Hominidae	LIV	2286	NESPOS
Gorilla gorilla	Hominidae	UCL	CA1g	NESPOS
Gorilla gorilla	Hominidae	SMT	154553	Smithsonian
Gorilla gorilla	Hominidae	SMT	154554	Smithsonian
Gorilla gorilla	Hominidae	SMT	174712	Smithsonian
Gorilla gorilla	Hominidae	SMT	174713	Smithsonian
Gorilla gorilla	Hominidae	SMT	174714	Smithsonian
Gorilla gorilla	Hominidae	SMT	174715	Smithsonian
Gorilla gorilla	Hominidae	SMT	174716	Smithsonian
Gorilla gorilla	Hominidae	SMT	174720	Smithsonian
Gorilla gorilla	Hominidae	SMT	176205	Smithsonian
Gorilla gorilla	Hominidae	SMT	176207	Smithsonian
Gorilla gorilla	Hominidae	SMT	176211	Smithsonian
Gorilla gorilla	Hominidae	SMT	176213	Smithsonian
Gorilla gorilla	Hominidae	SMT	297857	Smithsonian
Gorilla gorilla	Hominidae	SMT	574138	Smithsonian
Gorilla gorilla	Hominidae	SMT	585487	Smithsonian
Hylobates agilis	Hylobatidae	SMT	141157	Smithsonian
Hylobates agilis	Hylobatidae	KUPRI	275	KUPRI database
Hylobates agilis	Hylobatidae	SMT	141158	Smithsonian
Hylobates klossii	Hylobatidae	SMT	121678	Smithsonian
Hylobates lar	Hylobatidae	KUPRI	181	KUPRI database
Hylobates lar	Hylobatidae	KUPRI	809	KUPRI database
Hylobates lar	Hylobatidae	LIV	001	NESPOS
Hylobates lar	Hylobatidae	SMT	143570	Smithsonian
Hylobates lar	Hylobatidae	SMT	260590	Smithsonian
Hylobates lar	Hylobatidae	KUPRI	459	KUPRI database
Hylobates lar	Hylobatidae	SMT	143567	Smithsonian
Hylobates muelleri	Hylobatidae	SMT	154371	Smithsonian

Ap1.1 (Continued)

Species	Group	Collection	Code	Source
Hylobates muelleri	Hylobatidae	SMT	154370	Smithsonian
Lophocebus albigena	Cercopithecinae	KUPRI	599	KUPRI database
Lophocebus albigena	Cercopithecinae	SMT	452500	Smithsonian
Lophocebus aterrima	Cercopithecinae	SMT	503882	Smithsonian
Macaca arctoides	Cercopithecinae	KUPRI	674	KUPRI database
Macaca arctoides	Cercopithecinae	SMT	111966	Smithsonian
Macaca arctoides	Cercopithecinae	KUPRI	168	KUPRI database
Macaca arctoides	Cercopithecinae	KUPRI	171	KUPRI database
Macaca assamensis	Cercopithecinae	KUPRI	693	KUPRI database
Macaca assamensis	Cercopithecinae	KUPRI	695	KUPRI database
Macaca assamensis	Cercopithecinae	SMT	259725	Smithsonian
Macaca assamensis	Cercopithecinae	KUPRI	170	KUPRI database
Macaca cyclopis	Cercopithecinae	KUPRI	908	KUPRI database
Macaca cyclopis	Cercopithecinae	KUPRI	910	KUPRI database
Macaca cyclopis	Cercopithecinae	KUPRI	904	KUPRI database
Macaca cyclopis	Cercopithecinae	KUPRI	906	KUPRI database
Macaca fascicularis	Cercopithecinae	KUPRI	986	KUPRI database
Macaca fascicularis	Cercopithecinae	KUPRI	987	KUPRI database
Macaca fascicularis	Cercopithecinae	SMT	114162	Smithsonian
Macaca fascicularis	Cercopithecinae	KUPRI	914	KUPRI database
Macaca fascicularis	Cercopithecinae	KUPRI	985	KUPRI database
Macaca fascicularis	Cercopithecinae	SMT	121511	Smithsonian
Macaca fuscata	Cercopithecinae	KUPRI	1262	KUPRI database
Macaca fuscata	Cercopithecinae	KUPRI	1268	KUPRI database
Macaca fuscata	Cercopithecinae	KUPRI	1272	KUPRI database
Macaca fuscata	Cercopithecinae	KUPRI	1248	KUPRI database
Macaca fuscata	Cercopithecinae	KUPRI	1252	KUPRI database
Macaca fuscata	Cercopithecinae	KUPRI	1254	KUPRI database
Macaca leonina	Cercopithecinae	SMT	124022	Smithsonian
Macaca leonina	Cercopithecinae	SMT	241022	Smithsonian
Macaca maura	Cercopithecinae	KUPRI	916	KUPRI database
Macaca mulatta	Cercopithecinae	KUPRI	1167	KUPRI database

Ap1.1 (Continued)

Species	Group	Collection	Code	Source
Macaca mulatta	Cercopithecinae	KUPRI	852	KUPRI database
Macaca mulatta	Cercopithecinae	KUPRI	1177	KUPRI database
Macaca mulatta	Cercopithecinae	KUPRI	48	KUPRI database
Macaca nemestrina	Cercopithecinae	KUPRI	1168	KUPRI database
Macaca nemestrina	Cercopithecinae	KUPRI	850	KUPRI database
Macaca nemestrina	Cercopithecinae	SMT	114502	Smithsonian
Macaca nemestrina	Cercopithecinae	KUPRI	899	KUPRI database
Macaca nemestrina	Cercopithecinae	KUPRI	901	KUPRI database
Macaca nemestrina	Cercopithecinae	SMT	123144	Smithsonian
Macaca nigra	Cercopithecinae	KUPRI	1163	KUPRI database
Macaca nigra	Cercopithecinae	KUPRI	1164	KUPRI database
Macaca pagensis	Cercopithecinae	KUPRI	884	KUPRI database
Macaca pagensis	Cercopithecinae	KUPRI	892	KUPRI database
Macaca pagensis	Cercopithecinae	KUPRI	872	KUPRI database
Macaca pagensis	Cercopithecinae	KUPRI	873	KUPRI database
Macaca radiata	Cercopithecinae	KUPRI	918	KUPRI database
Macaca radiata	Cercopithecinae	KUPRI	922	KUPRI database
Macaca radiata	Cercopithecinae	SMT	398463	Smithsonian
Macaca radiata	Cercopithecinae	KUPRI	921	KUPRI database
Macaca silenus	Cercopithecinae	KUPRI	1147	KUPRI database
Macaca silenus	Cercopithecinae	KUPRI	1149	KUPRI database
Macaca silenus	Cercopithecinae	KUPRI	1131	KUPRI database
Macaca silenus	Cercopithecinae	SMT	574135	Smithsonian
Macaca sinica	Cercopithecinae	KUPRI	1127	KUPRI database
Macaca sinica	Cercopithecinae	SMT	271190	Smithsonian
Macaca sinica	Cercopithecinae	KUPRI	1129	KUPRI database
Macaca sinica	Cercopithecinae	SMT	15259	Smithsonian
Macaca sylvanus	Cercopithecinae	SMT	476782	Smithsonian
Macaca sylvanus	Cercopithecinae	SMT	255979	Smithsonian
Macaca thibetana	Cercopithecinae	SMT	241162	Smithsonian
Macaca thibetana	Cercopithecinae	SMT	241163	Smithsonian
Mandrillus leucophaeus	Cercopithecinae	MCZ	19986	MorphoSource

Ap1.1 (Continued)

Species	Group	Collection	Code	Source
Mandrillus leucophaeus	Cercopithecinae	SMT	395698	Smithsonian
Mandrillus sphinx	Cercopithecinae	MCZ	34272	MorphoSource
Mandrillus sphinx	Cercopithecinae	MCZ	34089	MorphoSource
Mandrillus sphinx	Cercopithecinae	SMT	283109	Smithsonian
Mandrillus sphinx	Cercopithecinae	SMT	598494	Smithsonian
Nasalis larvatus	Colobinae	SMT	142217	Smithsonian
Nomascus concolor	Hylobatidae	SMT	320787	Smithsonian
Nomascus concolor	Hylobatidae	SMT	464992	Smithsonian
Nomascus concolor	Hylobatidae	SMT	320786	Smithsonian
Nomascus concolor	Hylobatidae	SMT	320789	Smithsonian
Nomascus concolor	Hylobatidae	SMT	542282	Smithsonian
Nomascus gabriellae	Hylobatidae	SMT	257995	Smithsonian
Nomascus leucogenys	Hylobatidae	SMT	240490	Smithsonian
Nomascus leucogenys	Hylobatidae	SMT	240491	Smithsonian
Nomascus leucogenys	Hylobatidae	SMT	240492	Smithsonian
Pan paniscus	Hominidae	RMCA	rg9338	RMCA online
Pan troglodytes	Hominidae	KUPRI	505	KUPRI database
Pan troglodytes	Hominidae	KUPRI	856	KUPRI database
Pan troglodytes	Hominidae	KUPRI	13	KUPRI database
Pan troglodytes	Hominidae	KUPRI	1486	KUPRI database
Pan troglodytes	Hominidae	SMT	174699	Smithsonian
Pan troglodytes	Hominidae	SMT	174701	Smithsonian
Pan troglodytes	Hominidae	SMT	174710	Smithsonian
Pan troglodytes	Hominidae	SMT	220062	Smithsonian
Pan troglodytes	Hominidae	SMT	220063	Smithsonian
Pan troglodytes	Hominidae	SMT	220064	Smithsonian
Pan troglodytes	Hominidae	SMT	282763	Smithsonian
Pan troglodytes	Hominidae	SMT	477333	Smithsonian
Pan troglodytes	Hominidae	SMT	481803	Smithsonian
Pan troglodytes	Hominidae	SMT	599173	Smithsonian
Pan troglodytes	Hominidae	SMT	84655	Smithsonian
Pan troglodytes	Hominidae	KUPRI	1179	KUPRI database

Ap1.1 (Continued)

Species	Group	Collection	Code	Source
Pan troglodytes	Hominidae	KUPRI	1320	KUPRI database
Pan troglodytes	Hominidae	KUPRI	659	KUPRI database
Pan troglodytes	Hominidae	KUPRI	857	KUPRI database
Pan troglodytes	Hominidae	KUPRI	19	KUPRI database
Pan troglodytes	Hominidae	KUPRI	1280	KUPRI database
Pan troglodytes	Hominidae	KUPRI	838	KUPRI database
Pan troglodytes	Hominidae	SMT	174704	Smithsonian
Pan troglodytes	Hominidae	SMT	176228	Smithsonian
Pan troglodytes	Hominidae	SMT	176235	Smithsonian
Pan troglodytes	Hominidae	SMT	220065	Smithsonian
Pan troglodytes	Hominidae	SMT	220327	Smithsonian
Pan troglodytes	Hominidae	SMT	395820	Smithsonian
Pan troglodytes	Hominidae	SMT	481804	Smithsonian
Pan troglodytes	Hominidae	SMT	599172	Smithsonian
Papio anubis	Cercopithecinae	SMT	397476	Smithsonian
Papio anubis	Cercopithecinae	KUPRI	352	KUPRI database
Papio anubis	Cercopithecinae	SMT	162899	Smithsonian
Papio hamadryas	Cercopithecinae	KUPRI	1025	KUPRI database
Papio hamadryas	Cercopithecinae	KUPRI	1165	KUPRI database
Papio hamadryas	Cercopithecinae	KUPRI	802	KUPRI database
Papio hamadryas	Cercopithecinae	KUPRI	72	KUPRI database
Papio hamadryas	Cercopithecinae	SMT	258502	Smithsonian
Papio papio	Cercopithecinae	SMT	381430	Smithsonian
Papio papio	Cercopithecinae	SMT	378669	Smithsonian
Piliocolobus badius	Colobinae	KUPRI	942	KUPRI database
Piliocolobus badius	Colobinae	KUPRI	944	KUPRI database
Piliocolobus badius	Colobinae	KUPRI	945	KUPRI database
Pongo abelii	Hominidae	SMT	143596	Smithsonian
Pongo abelii	Hominidae	SMT	143597	Smithsonian
Pongo abelii	Hominidae	SMT	143598	Smithsonian
Pongo abelii	Hominidae	SMT	143601	Smithsonian
Pongo abelii	Hominidae	SMT	143602	Smithsonian

Ap1.1 (Continued)

Species	Group	Collection	Code	Source
Pongo abelii	Hominidae	KUPRI	513	KUPRI database
Pongo abelii	Hominidae	SMT	143587	Smithsonian
Pongo abelii	Hominidae	SMT	143588	Smithsonian
Pongo abelii	Hominidae	SMT	143590	Smithsonian
Pongo abelii	Hominidae	SMT	143593	Smithsonian
Pongo abelii	Hominidae	SMT	143594	Smithsonian
Pongo pygmaeus	Hominidae	SMT	142169	Smithsonian
Pongo pygmaeus	Hominidae	SMT	142170	Smithsonian
Pongo pygmaeus	Hominidae	SMT	142182	Smithsonian
Pongo pygmaeus	Hominidae	SMT	142190	Smithsonian
Pongo pygmaeus	Hominidae	SMT	142191	Smithsonian
Pongo pygmaeus	Hominidae	SMT	142202	Smithsonian
Pongo pygmaeus	Hominidae	SMT	145300	Smithsonian
Pongo pygmaeus	Hominidae	SMT	145302	Smithsonian
Pongo pygmaeus	Hominidae	SMT	145306	Smithsonian
Pongo pygmaeus	Hominidae	SMT	145308	Smithsonian
Pongo pygmaeus	Hominidae	KUPRI	601	KUPRI database
Pongo pygmaeus	Hominidae	SMT	142181	Smithsonian
Pongo pygmaeus	Hominidae	SMT	142188	Smithsonian
Pongo pygmaeus	Hominidae	SMT	142189	Smithsonian
Pongo pygmaeus	Hominidae	SMT	142194	Smithsonian
Pongo pygmaeus	Hominidae	SMT	142196	Smithsonian
Pongo pygmaeus	Hominidae	SMT	142198	Smithsonian
Pongo pygmaeus	Hominidae	SMT	142200	Smithsonian
Pongo pygmaeus	Hominidae	SMT	145304	Smithsonian
Pongo pygmaeus	Hominidae	SMT	145319	Smithsonian
Pongo pygmaeus	Hominidae	SMT	153807	Smithsonian
Pongo pygmaeus	Hominidae	SMT	153823	Smithsonian
Pongo pygmaeus	Hominidae	SMT	546840	Smithsonian
Presbytis melalophos	Colobinae	KUPRI	1054	KUPRI database
Presbytis melalophos	Colobinae	KUPRI	933	KUPRI database
Presbytis melalophos	Colobinae	KUPRI	1056	KUPRI database

Ap1.1 (Continued)

Species	Group	Collection	Code	Source
Presbytis melalophos	Colobinae	KUPRI	931	KUPRI database
Procolobus verus	Colobinae	KUPRI	853	KUPRI database
Procolobus verus	Colobinae	SMT	477327	Smithsonian
Procolobus verus	Colobinae	SMT	477331	Smithsonian
Pygathrix nemaeus	Colobinae	SMT	356577	Smithsonian
Symphalangus syndactylus	Hylobatidae	KUPRI	1082	KUPRI database
Symphalangus syndactylus	Hylobatidae	SMT	141161	Smithsonian
Symphalangus syndactylus	Hylobatidae	SMT	143580	Smithsonian
Symphalangus syndactylus	Hylobatidae	SMT	143581	Smithsonian
Symphalangus syndactylus	Hylobatidae	SMT	271048	Smithsonian
Symphalangus syndactylus	Hylobatidae	SMT	519573	Smithsonian
Symphalangus syndactylus	Hylobatidae	KUPRI	1011	KUPRI database
Symphalangus syndactylus	Hylobatidae	KUPRI	753	KUPRI database
Symphalangus syndactylus	Hylobatidae	SMT	171981	Smithsonian
Symphalangus syndactylus	Hylobatidae	SMT	283563	Smithsonian
Symphalangus syndactylus	Hylobatidae	SMT	395514	Smithsonian
Theropithecus gelada	Cercopithecinae	KUPRI	1029	KUPRI database
Theropithecus gelada	Cercopithecinae	SMT	319992	Smithsonian
Theropithecus gelada	Cercopithecinae	KUPRI	590	KUPRI database
Theropithecus gelada	Cercopithecinae	KUPRI	597	KUPRI database
Theropithecus gelada	Cercopithecinae	SMT	305107	Smithsonian
Trachypithecus cristatus	Colobinae	KUPRI	1047	KUPRI database
Trachypithecus cristatus	Colobinae	KUPRI	935	KUPRI database
Trachypithecus cristatus	Colobinae	KUPRI	937	KUPRI database
Trachypithecus cristatus	Colobinae	SMT	113174	Smithsonian
Trachypithecus cristatus	Colobinae	SMT	113170	Smithsonian
Trachypithecus cristatus	Colobinae	SMT	83949	Smithsonian
Trachypithecus obscurus	Colobinae	SMT	104446	Smithsonian
Trachypithecus obscurus	Colobinae	SMT	83259	Smithsonian
Trachypithecus obscurus	Colobinae	SMT	123993	Smithsonian

Ap1.2 The metric data sample from Pliocene australopithecines to upper Palaeolithic *Homo sapiens*. The species, individuals and sex information are reported. The type of data measured on each specimen is indicated as Dental Diameters (DD), Alveolar Lengths (AL) and Robusticity (RB). The data were measured on the actual specimens and were available from the "Human Origins Database" and the "Anthropological data free" database. For the medieval dental sample, an approximate number of individuals is indicated in the table. See Chapter 2 for further details. (Continues to the next page).

Species	Code	Sex	Data	Group
A. afarensis	A.L. 145-35	N	RB	australopithecines
	A.L. 188-1	N	RB	australopithecines
	A.L. 198-1	N	RB	australopithecines
	A.L. 207-13	N	RB	australopithecines
	A.L. 266-1	N	RB	australopithecines
	A.L. 277-1	N	RB	australopithecines
	A.L. 288-1	F	AL - RB	australopithecines
	A.L. 333w-12	N	RB	australopithecines
	A.L. 333w-1a+b	N	RB	australopithecines
	A.L. 333w-32+60	N	RB	australopithecines
	A.L. 400-1a	N	RB	australopithecines
	L.H. 4	N	RB	australopithecines
A. africanus	MLD 2	N	RB	australopithecines
	MLD 18	F	AL - RB	australopithecines
	MLD 34	N	RB	australopithecines
	MLD 40	F	AL - RB	australopithecines
	Sts 7	M	AL	australopithecines
	Sts 52	F	AL - RB	australopithecines
P. aethiopicus	OMO L860-2	N	RB	australopithecines
	OMO 18-18	N	RB	australopithecines
	OMO 57-41	N	RB	australopithecines
P. boisei	KNM-ER 403	N	AL - RB	australopithecines
	KNM-ER 404	N	AL - RB	australopithecines
	KNM-ER 725	N	AL - RB	australopithecines
	KNM-ER 726	N	AL - RB	australopithecines
	KNM-ER 727	N	RB	australopithecines
	KNM-ER 728	N	AL - RB	australopithecines
	KNM-ER 729	N	AL - RB	australopithecines
	KNM-ER 733	N	RB	australopithecines
	KNM-ER 801	N	AL - RB	australopithecines

Ap1.2 (Continued)

Species	Code	Sex	Data	Group
P. boisei	KNM-ER 805	N	AL - RB	australopithecines
	KNM-ER 810	N	AL - RB	australopithecines
	KNM-ER 818	N	AL - RB	australopithecines
	KNM-ER 1468	N	AL - RB	australopithecines
	KNM-ER 1469	N	AL - RB	australopithecines
	KNM-ER 1477	N	RB	australopithecines
	KNM-ER 1803	N	AL - RB	australopithecines
	KNM-ER 1806	N	AL - RB	australopithecines
	KNM-ER 1820	N	RB	australopithecines
	KNM-ER 3229	N	RB	australopithecines
	KNM-ER 3230	N	AL - RB	australopithecines
	KNM-ER 3729	N	RB	australopithecines
	KNM-ER 3731	N	RB	australopithecines
	KNM-ER 3889	N	AL - RB	australopithecines
	KNM-ER 5877	N	AL - RB	australopithecines
	KNM-ER 15930	N	RB	australopithecines
	KNM-ER 16841	N	RB	australopithecines
	OMO L74A-21	N	AL - RB	australopithecines
	OMO L7A-125	N	AL - RB	australopithecines
	Peninj 1	N	AL - RB	australopithecines
P. robustus	SK 6	N	RB	australopithecines
	SK 12	N	RB	australopithecines
	SK 23	F	AL - RB	australopithecines
	SK 34	F	AL - RB	australopithecines
H. erectus	Sangiran 1b	N	DD - RB	Early *Homo*
	Sangiran 5	N	DD - RB	Early *Homo*
	Sangiran 6	N	DD - RB	Early *Homo*
	Sangiran 8	N	DD - RB	Early *Homo*
	Sangiran 9	N	DD - RB	Early *Homo*
	Trinil 5	N	DD	Early *Homo*
	ZKD A1-1	N	DD	Early *Homo*

Ap1.2 (Continued)

Species	Code	Sex	Data	Group
H. erectus	ZKD A1-57	N	DD	Early *Homo*
	ZKD A2-2	N	DD	Early *Homo*
	ZKD A3-56	N	DD	Early *Homo*
	ZKD AN-517	N	DD	Early *Homo*
	ZKD AN-518	N	DD	Early *Homo*
	ZKD B1-3	N	DD	Early *Homo*
	ZKD B1-63	N	DD	Early *Homo*
	ZKD B2-64	N	DD	Early *Homo*
	ZKD B3-9	N	DD	Early *Homo*
	ZKD B4-75	N	DD	Early *Homo*
	ZKD B5-77	N	DD	Early *Homo*
	ZKD C1-4	N	DD	Early *Homo*
	ZKD C1-49	N	DD	Early *Homo*
	ZKD C3-45	N	DD	Early *Homo*
	ZKD C3-46	N	DD	Early *Homo*
	ZKD C3-47	N	DD	Early *Homo*
	ZKD C3-53	N	DD	Early *Homo*
	ZKD D1-40	N	DD	Early *Homo*
	ZKD D1-42	N	DD	Early *Homo*
	ZKD D1-43	N	DD	Early *Homo*
	ZKD D1-44	N	DD	Early *Homo*
	ZKD D1-61	N	DD	Early *Homo*
	ZKD F1-25	N	DD	Early *Homo*
	ZKD F1-5	N	DD	Early *Homo*
	ZKD F3-31	N	DD	Early *Homo*
	ZKD F3-37	N	DD	Early *Homo*
	ZKD G1-6	N	DD	Early *Homo*
	ZKD G1-60	N	DD	Early *Homo*
	ZKD G1-7	N	DD	Early *Homo*
	ZKD H1-12	N	DD	Early *Homo*
	ZKD H1-15	N	DD	Early *Homo*

Ap1.2 (Continued)

Species	Code	Sex	Data	Group
H. erectus	ZKD H2-13	N	DD	Early *Homo*
	ZKD H4-83	N	DD	Early *Homo*
	ZKD I1-PA87	N	DD	Early *Homo*
	ZKD K1-96	N	DD	Early *Homo*
	ZKD K2-97	N	DD	Early *Homo*
	ZKD L4-302	N	DD	Early *Homo*
	ZKD L4-307	N	DD	Early *Homo*
	ZKD L4-309	N	DD	Early *Homo*
	ZKD M1-301	N	DD	Early *Homo*
	ZKD M1-303	N	DD	Early *Homo*
	ZKD M1-308	N	DD	Early *Homo*
	ZKD M3-305	N	DD	Early *Homo*
H. ergaster	KNM-BK 67	N	DD - AL - RB	Early *Homo*
	KNM-BK 8518	N	DD - AL - RB	Early *Homo*
	KNM-ER 730	N	DD - AL - RB	Early *Homo*
	KNM-ER 731	N	DD - RB	Early *Homo*
	KNM-ER 820	N	DD - RB	Early *Homo*
	KNM-ER 992	N	DD - AL - RB	Early *Homo*
	KNM-ER 1507	N	DD - RB	Early *Homo*
	KNM-ER 1812	N	DD - AL - RB	Early *Homo*
	OH 22	N	DD - AL - RB	Early *Homo*
	OH 23	N	DD - AL - RB	Early *Homo*
	OH 51	N	DD	Early *Homo*
	SK 15	N	DD	Early *Homo*
H. habilis	KNM-ER 1501	N	DD - AL - RB	Early *Homo*
	KNM-ER 1502	N	DD - RB	Early *Homo*
	KNM-ER 1805	N	DD - AL - RB	Early *Homo*
	OH 13	N	DD - AL - RB	Early *Homo*
	OH 16	N	DD	Early *Homo*
	OH 37	N	DD - AL - RB	Early *Homo*

Ap1.2 (Continued)

Species	Code	Sex	Data	Group
H. rudolfensis	KNM-ER 819	N	DD - AL - RB	Early *Homo*
	KNM-ER 1482	N	DD - AL - RB	Early *Homo*
	KNM-ER 1483	N	DD - AL - RB	Early *Homo*
	KNM-ER 1590	N	DD	Early *Homo*
	KNM-ER 1801	N	DD - AL - RB	Early *Homo*
	KNM-ER 1802	N	DD - AL - RB	Early *Homo*
	KNM-ER 60000	N	DD - AL	Early *Homo*
H. heidelbergensis	Arago 2	F	DD - RB	Lower Palaeolithic
	Atapuerca AT-1	F	DD	Lower Palaeolithic
	AT-2	N	DD	Lower Palaeolithic
	AT-3	F	DD	Lower Palaeolithic
	AT-4	N	DD	Lower Palaeolithic
	AT-5	N	DD	Lower Palaeolithic
	AT-9	N	DD	Lower Palaeolithic
	AT-11	N	DD	Lower Palaeolithic
	AT-13	N	DD	Lower Palaeolithic
	AT-14	F	DD	Lower Palaeolithic
	AT-21	N	DD	Lower Palaeolithic
	AT-22	F	DD	Lower Palaeolithic
	AT-28	F	DD	Lower Palaeolithic
	AT-30	F	DD	Lower Palaeolithic
	AT-47	F	DD	Lower Palaeolithic
	AT-55	N	DD	Lower Palaeolithic
	AT-64	N	DD	Lower Palaeolithic
	AT-74	F	DD	Lower Palaeolithic
	AT-75	F	DD	Lower Palaeolithic
	AT-101	F	DD	Lower Palaeolithic
	AT-103	F	DD	Lower Palaeolithic
	AT-104	F	DD	Lower Palaeolithic
	AT-141	F	DD	Lower Palaeolithic

Ap1.2 (Continued)

Species	Code	Sex	Data	Group
H. heidelbergensis	AT-142	N	DD	Lower Palaeolithic
	AT-143	N	DD	Lower Palaeolithic
	AT-147	N	DD	Lower Palaeolithic
	AT-148	F	DD	Lower Palaeolithic
	AT-149	F	DD	Lower Palaeolithic
	AT-162	N	DD	Lower Palaeolithic
	AT-166	N	DD	Lower Palaeolithic
	AT-167	F	DD	Lower Palaeolithic
	AT-168	F	DD	Lower Palaeolithic
	AT-169	F	DD	Lower Palaeolithic
	AT-195	N	DD	Lower Palaeolithic
	AT-221	F	DD	Lower Palaeolithic
	AT-222	N	DD	Lower Palaeolithic
	AT-271	F	DD	Lower Palaeolithic
	AT-272	F	DD	Lower Palaeolithic
	AT-273	F	DD	Lower Palaeolithic
	AT-275	F	DD	Lower Palaeolithic
	AT-277	F	DD	Lower Palaeolithic
	AT-281	N	DD	Lower Palaeolithic
	AT-282	N	DD	Lower Palaeolithic
	AT-284	N	DD	Lower Palaeolithic
	AT-285	N	DD	Lower Palaeolithic
	AT-286	F	DD	Lower Palaeolithic
	AT-300	N	DD	Lower Palaeolithic
	AT-505 + AT-604	F	DD	Lower Palaeolithic
	AT-555	N	DD	Lower Palaeolithic
	AT-557	F	DD	Lower Palaeolithic
	AT-561	F	DD	Lower Palaeolithic
	AT-562	F	DD	Lower Palaeolithic
	AT-576	F	DD	Lower Palaeolithic

Ap1.2 (Continued)

Species	Code	Sex	Data	Group
H. heidelbergensis	AT-580	F	DD	Lower Palaeolithic
	AT-590	N	DD	Lower Palaeolithic
	AT-592	N	DD	Lower Palaeolithic
	AT-594	F	DD	Lower Palaeolithic
	AT-595	F	DD	Lower Palaeolithic
	AT-596	N	DD	Lower Palaeolithic
	AT-597	N	DD	Lower Palaeolithic
	AT-598	N	DD	Lower Palaeolithic
	AT-599	N	DD	Lower Palaeolithic
	AT-603	N	DD	Lower Palaeolithic
	AT-605	M	DD	Lower Palaeolithic
	AT-607	F	DD	Lower Palaeolithic
	AT-608	N	DD	Lower Palaeolithic
	AT-609	F	DD	Lower Palaeolithic
	AT-723	F	DD	Lower Palaeolithic
	AT-792	M	DD	Lower Palaeolithic
	AT-793 + AT-250	F	DD	Lower Palaeolithic
	AT-806	M	DD	Lower Palaeolithic
	AT-807	N	DD	Lower Palaeolithic
	AT-809	M	DD	Lower Palaeolithic
	AT-811	F	DD	Lower Palaeolithic
	AT-828	M	DD	Lower Palaeolithic
	AT-829	M	DD	Lower Palaeolithic
	AT-888	M	DD	Lower Palaeolithic
	AT-941	M	DD	Lower Palaeolithic
	AT-942	N	DD	Lower Palaeolithic
	AT-943	M	DD	Lower Palaeolithic
	AT-946	M	DD	Lower Palaeolithic
	AT-950	F	DD	Lower Palaeolithic
	AT-950	F	DD	Lower Palaeolithic

Ap1.2 (Continued)

Species	Code	Sex	Data	Group
H. heidelbergensis	AT-950	F	DD	Lower Palaeolithic
	AT-950	F	DD	Lower Palaeolithic
	AT-956	N	DD	Lower Palaeolithic
	AT-957	M	DD	Lower Palaeolithic
	AT-1123	M	DD	Lower Palaeolithic
	AT-1458	N	DD	Lower Palaeolithic
	AT-1460	F	DD	Lower Palaeolithic
	AT-1461	F	DD	Lower Palaeolithic
	AT-1464	F	DD	Lower Palaeolithic
	AT-1466	N	DD	Lower Palaeolithic
	AT-1467	N	DD	Lower Palaeolithic
	AT-1468	N	DD	Lower Palaeolithic
	AT-1469	N	DD	Lower Palaeolithic
	AT-1474	N	DD	Lower Palaeolithic
	AT-1726	F	DD	Lower Palaeolithic
	AT-1742	N	DD	Lower Palaeolithic
	AT-1751	F	DD	Lower Palaeolithic
	AT-1752	M	DD	Lower Palaeolithic
	AT-1753	F	DD	Lower Palaeolithic
	AT-1759	F	DD	Lower Palaeolithic
	AT-1760	F	DD	Lower Palaeolithic
	AT-1761	F	DD	Lower Palaeolithic
	AT-1762	F	DD	Lower Palaeolithic
	AT-1763	F	DD	Lower Palaeolithic
	AT-1775	F	DD	Lower Palaeolithic
	AT-1828	M	DD	Lower Palaeolithic
	AT-1919	F	DD	Lower Palaeolithic
	AT-1945	N	DD	Lower Palaeolithic
	AT-1957	N	DD	Lower Palaeolithic
	AT-1957	N	DD	Lower Palaeolithic

Ap1.2 (Continued)

Species	Code	Sex	Data	Group
H. heidelbergensis	AT-1959	N	DD	Lower Palaeolithic
	AT-1993	N	DD	Lower Palaeolithic
	AT-2027	N	DD	Lower Palaeolithic
	AT-2066	M	DD	Lower Palaeolithic
	AT-2193	F	DD	Lower Palaeolithic
	AT-2195	M	DD	Lower Palaeolithic
	AT-2270	F	DD	Lower Palaeolithic
	AT-2271	M	DD	Lower Palaeolithic
	AT-2273	N	DD	Lower Palaeolithic
	AT-2275	N	DD	Lower Palaeolithic
	AT-2276	N	DD	Lower Palaeolithic
	AT-2277	M	DD	Lower Palaeolithic
	AT-2278	N	DD	Lower Palaeolithic
	AT-2343	M	DD	Lower Palaeolithic
	AT-2384	N	DD	Lower Palaeolithic
	AT-2385	N	DD	Lower Palaeolithic
	AT-2386	M	DD	Lower Palaeolithic
	AT-2387	F	DD	Lower Palaeolithic
	AT-2390	M	DD	Lower Palaeolithic
	AT-2391	N	DD	Lower Palaeolithic
	AT-2396	N	DD	Lower Palaeolithic
	AT-2397	N	DD	Lower Palaeolithic
	AT-2438	N	DD	Lower Palaeolithic
	AT-2730	M	DD	Lower Palaeolithic
	AT-2753	M	DD	Lower Palaeolithic
	AT-2760	N	DD	Lower Palaeolithic
	AT-2761	N	DD	Lower Palaeolithic
	AT-2763	N	DD	Lower Palaeolithic
	AT-2767	M	DD	Lower Palaeolithic
	AT-2768	M	DD	Lower Palaeolithic

Ap1.2 (Continued)

Species	Code	Sex	Data	Group
H. heidelbergensis	AT-2775	F	DD	Lower Palaeolithic
	AT-2776	F	DD	Lower Palaeolithic
	AT-2779	N	DD	Lower Palaeolithic
	AT-2780	N	DD	Lower Palaeolithic
	AT-2781	N	DD	Lower Palaeolithic
	AT-2787	F	DD	Lower Palaeolithic
	AT-3045	M	DD	Lower Palaeolithic
	AT-3175	M	DD	Lower Palaeolithic
	AT-3176	M	DD	Lower Palaeolithic
	AT-3179	N	DD	Lower Palaeolithic
	AT-3182	N	DD	Lower Palaeolithic
	AT-3187	M	DD	Lower Palaeolithic
	AT-3188	M	DD	Lower Palaeolithic
	AT-3190	M	DD	Lower Palaeolithic
	AT-3198	M	DD	Lower Palaeolithic
	AT-3199	M	DD	Lower Palaeolithic
	AT-3241	N	DD	Lower Palaeolithic
	AT-3242	N	DD	Lower Palaeolithic
	AT-3243	N	DD	Lower Palaeolithic
	AT-3250	M	DD	Lower Palaeolithic
	AT-3252	N	DD	Lower Palaeolithic
	AT-3253	F	DD	Lower Palaeolithic
	AT-3256	N	DD	Lower Palaeolithic
	AT-3827	F	DD	Lower Palaeolithic
	AT-3880	N	DD	Lower Palaeolithic
	AT-3882	F	DD	Lower Palaeolithic
	AT-3883	F	DD	Lower Palaeolithic
	AT-3889	F	DD	Lower Palaeolithic
	AT-3890	M	DD	Lower Palaeolithic
	AT-3933	F	DD	Lower Palaeolithic

Ap1.2 (Continued)

Species	Code	Sex	Data	Group
H. heidelbergensis	AT-3934	F	DD	Lower Palaeolithic
	AT-3937	F	DD	Lower Palaeolithic
	AT-3939	F	DD	Lower Palaeolithic
	AT-3940	F	DD	Lower Palaeolithic
	AT-3941	F	DD	Lower Palaeolithic
	AT-3942	F	DD	Lower Palaeolithic
	AT-4100	N	DD	Lower Palaeolithic
	AT-4101	N	DD	Lower Palaeolithic
	AT-4147	N	DD	Lower Palaeolithic
	AT-4318	M	DD	Lower Palaeolithic
	AT-4328	F	DD	Lower Palaeolithic
	AT-4331	N	DD	Lower Palaeolithic
	Boxgrove 2	N	DD	Lower Palaeolithic
	Boxgrove 3	N	DD	Lower Palaeolithic
H. neanderthalensis	A. B. Delaunay 1	N	DD	Middle Palaeolithic
	A. B. Delaunay 21	N	DD	Middle Palaeolithic
	Amud 1	M	DD	Middle Palaeolithic
	Archi 1	M	DD	Middle Palaeolithic
	Bolomor Cave HCB-02	N	DD	Middle Palaeolithic
	Combe-Grenal I	N	DD	Middle Palaeolithic
	Combe-Grenal IV	N	DD	Middle Palaeolithic
	Combe-Grenal XII	N	DD	Middle Palaeolithic
	Combe-Grenal XXIX	N	DD	Middle Palaeolithic
	Dederiyeh-8902	N	DD	Middle Palaeolithic
	Fate F2	N	DD	Middle Palaeolithic
	Fate F3	N	DD	Middle Palaeolithic
	Fate F6	N	DD	Middle Palaeolithic
	Fate F12	N	DD	Middle Palaeolithic
	Fossellone 3	N	DD	Middle Palaeolithic
	Grotte Boccard GB78	N	DD	Middle Palaeolithic

Ap1.2 (Continued)

Species	Code	Sex	Data	Group
H. neanderthalensis	Grotte du Bison P7	N	DD	Middle Palaeolithic
	Gruta da Oliveira 9	N	DD	Middle Palaeolithic
	Hunas	N	DD	Middle Palaeolithic
	Kalamakia KAL6	N	DD	Middle Palaeolithic
	Kalamakia KAL9	N	DD	Middle Palaeolithic
	Kebara 2	N	DD	Middle Palaeolithic
	Krapina D/D	F	DD	Middle Palaeolithic
	Krapina F/H	M	DD	Middle Palaeolithic
	Krapina MND C	M	DD	Middle Palaeolithic
	Krapina MND E	F	DD	Middle Palaeolithic
	Krapina MND G	F	DD	Middle Palaeolithic
	Krapina MND J	M	DD	Middle Palaeolithic
	Krapina MND K	N	DD	Middle Palaeolithic
	Krapina MND M	N	DD	Middle Palaeolithic
	Krapina MND O	N	DD	Middle Palaeolithic
	Krapina MND P	N	DD	Middle Palaeolithic
	Krapina N/N	M	DD	Middle Palaeolithic
	Krapina R64	M	DD	Middle Palaeolithic
	Krapina 6	N	DD	Middle Palaeolithic
	Krapina 9	N	DD	Middle Palaeolithic
	Krapina 29	N	DD	Middle Palaeolithic
	Krapina 33	N	DD	Middle Palaeolithic
	Krapina 34	N	DD	Middle Palaeolithic
	Krapina 35	N	DD	Middle Palaeolithic
	Krapina 50	N	DD	Middle Palaeolithic
	Krapina 78	N	DD	Middle Palaeolithic
	Krapina 90	N	DD	Middle Palaeolithic
	Krapina 104	N	DD	Middle Palaeolithic
	Krapina 105	N	DD	Middle Palaeolithic
	Krapina 107	N	DD	Middle Palaeolithic

Ap1.2 (Continued)

Species	Code	Sex	Data	Group
H. neanderthalensis	Krapina 111	N	DD	Middle Palaeolithic
	Krapina 113	N	DD	Middle Palaeolithic
	Krapina 118	N	DD	Middle Palaeolithic
	Krapina 198	N	DD	Middle Palaeolithic
	Krapina 199	N	DD	Middle Palaeolithic
	La Quina 9	N	DD	Middle Palaeolithic
	Lakonis LKH 1	N	DD	Middle Palaeolithic
	Le Mànie 1	N	DD	Middle Palaeolithic
	Montgaudier	F	DD	Middle Palaeolithic
	Montmaurin C.G. 2D3	N	DD	Middle Palaeolithic
	Moula-Guercy M-D1	N	DD	Middle Palaeolithic
	Moula-Guercy M-G2	N	DD	Middle Palaeolithic
	Moula-Guercy M-L4	N	DD	Middle Palaeolithic
	Pontnewydd PN5	N	DD	Middle Palaeolithic
	Pontnewydd PN6	N	DD	Middle Palaeolithic
	Pontnewydd PN10	N	DD	Middle Palaeolithic
	Pontnewydd PN11	N	DD	Middle Palaeolithic
	Pontnewydd PN13	N	DD	Middle Palaeolithic
	Pontnewydd PN15	N	DD	Middle Palaeolithic
	Pontnewydd PN16	N	DD	Middle Palaeolithic
	Pontnewydd PN20	N	DD	Middle Palaeolithic
	Pontnewydd PN21	N	DD	Middle Palaeolithic
	Regourdou 1	M	DD	Middle Palaeolithic
	Scladina 4A-9	N	DD	Middle Palaeolithic
	Scladina 4A-15	N	DD	Middle Palaeolithic
	Scladina 4A-19	N	DD	Middle Palaeolithic
	Shanidar 1	N	DD	Middle Palaeolithic
	Shanidar 2	N	DD	Middle Palaeolithic
	Shanidar 4	N	DD	Middle Palaeolithic
	Shanidar 6	N	DD	Middle Palaeolithic

Ap1.2 (Continued)

Species	Code	Sex	Data	Group
H. neanderthalensis	Soulabé Las Maretas 1	N	DD	Middle Palaeolithic
	Soulabé Las Maretas 2	N	DD	Middle Palaeolithic
	Soulabé Las Maretas 4	N	DD	Middle Palaeolithic
	Subalyuk 1	N	DD	Middle Palaeolithic
	Taddeo 4	N	DD	Middle Palaeolithic
	Valdegoba 1	M	DD	Middle Palaeolithic
	Vaufrey 1	N	DD	Middle Palaeolithic
H. sapiens	Dederiyeh 9007	F	DD	Middle Paleolithic
	Dederiyeh 9008	N	DD	Middle Paleolithic
	Qafzeh 7	N	DD	Middle Paleolithic
	Qafzeh 8	M	DD	Middle Paleolithic
	Qafzeh 9	F	DD	Middle Paleolithic
	Qesem P3-QC9	N	DD	Middle Paleolithic
	Qesem P4-QC10	N	DD	Middle Paleolithic
	Abri Pataud 26.244	N	DD	Upper Paleolithic
	Abri Pataud P1	F	DD	Upper Paleolithic
	Arene Candide 1	M	DD	Upper Paleolithic
	Arene Candide 19.6725	M	DD	Upper Paleolithic
	Arene Candide 2	M	DD	Upper Paleolithic
	Arene Candide 20	M	DD	Upper Paleolithic
	Arene Candide 4	M	DD	Upper Paleolithic
	Arene Candide 5	M	DD	Upper Paleolithic
	Bacho Kiro 2641	N	DD	Upper Paleolithic
	Bacho Kiro 2823	N	DD	Upper Paleolithic
	Barma Grande 2	M	DD	Upper Paleolithic
	Barma Grande 4	F	DD	Upper Paleolithic
	Barma Grande 5	M	DD	Upper Paleolithic
	Brassempouy 2	N	DD	Upper Paleolithic
	Cap Blanc 1	F	DD	Upper Paleolithic
	Dolní Vestonice DV13	M	DD	Upper Paleolithic

Ap1.2 (Continued)

Species	Code	Sex	Data	Group
H. sapiens	Dolní Vestonice DV14	M	DD	Upper Paleolithic
	Dolní Vestonice DV15	M	DD	Upper Paleolithic
	Dolní Vestonice DV16	M	DD	Upper Paleolithic
	Dolní Vestonice DV3	F	DD	Upper Paleolithic
	Balauzière II	N	DD	Upper Paleolithic
	Balauzière III	N	DD	Upper Paleolithic
	Balauzière IV	N	DD	Upper Paleolithic
	Balauzière XII	N	DD	Upper Paleolithic
	Grotte des Enfants 4	M	DD	Upper Paleolithic
	Grotte des Enfants 6	F	DD	Upper Paleolithic
	Gruta do Caldeirão 3	N	DD	Upper Paleolithic
	Gruta do Caldeirão 5	N	DD	Upper Paleolithic
	Gruta do Caldeirão 6	N	DD	Upper Paleolithic
	Lachaud Mandible B	F	DD	Upper Paleolithic
	Lachaud Mandible A	F	DD	Upper Paleolithic
	Lachaud No number	N	DD	Upper Paleolithic
	Les Rois 55.148b	N	DD	Upper Paleolithic
	Les Rois 55.148g	N	DD	Upper Paleolithic
	Les Rois A	N	DD	Upper Paleolithic
	Les Rois BR51.10	N	DD	Upper Paleolithic
	Les Rois R50.24	N	DD	Upper Paleolithic
	Les Rois R50.27	N	DD	Upper Paleolithic
	Les Rois R50.31	N	DD	Upper Paleolithic
	Les Rois R51.12	N	DD	Upper Paleolithic
	Les Rois R51.14	N	DD	Upper Paleolithic
	Les Rois R51.16	N	DD	Upper Paleolithic
	Les Rois R51.17	N	DD	Upper Paleolithic
	Les Rois R51.22	N	DD	Upper Paleolithic
	Les Rois R51.23	N	DD	Upper Paleolithic
	Les Rois R51.31	N	DD	Upper Paleolithic

Ap1.2 (Continued)

Species	Code	Sex	Data	Group
H. sapiens	Les Rois R51.32	N	DD	Upper Paleolithic
	Les Rois R51.6	N	DD	Upper Paleolithic
	Les Vachons 1	N	DD	Upper Paleolithic
	Madeleine 24835	N	DD	Upper Paleolithic
	Mladeč 52	N	DD	Upper Paleolithic
	Mladeč 54	M	DD	Upper Paleolithic
	Neve David ND1	M	DD	Upper Paleolithic
	Paglicci 12	M	DD	Upper Paleolithic
	Paglicci C	N	DD	Upper Paleolithic
	Paglicci PA21N	F	DD	Upper Paleolithic
	Pavlov 1	M	DD	Upper Paleolithic
	Pavlov 519156	N	DD	Upper Paleolithic
	Pavlov 592256.84	N	DD	Upper Paleolithic
	Pavlov 641436	N	DD	Upper Paleolithic
	Peştera Muierii 1	F	DD	Upper Paleolithic
	Předmost 1	M	DD	Upper Paleolithic
	Předmost 10	F	DD	Upper Paleolithic
	Předmost 14	M	DD	Upper Paleolithic
	Předmost 18	M	DD	Upper Paleolithic
	Předmost 259	N	DD	Upper Paleolithic
	Předmost 26	N	DD	Upper Paleolithic
	Předmost 27	M	DD	Upper Paleolithic
	Předmost 3	M	DD	Upper Paleolithic
	Předmost 3070	N	DD	Upper Paleolithic
	Předmost 4	F	DD	Upper Paleolithic
	Předmost 476	N	DD	Upper Paleolithic
	Předmost 5	F	DD	Upper Paleolithic
	Předmost 7	M	DD	Upper Paleolithic
	Předmost 9	M	DD	Upper Paleolithic
	Romanelli R5	N	DD	Upper Paleolithic

Ap1.2 (Continued)

Species	Code	Sex	Data	Group
H. sapiens	Romanelli R7	N	DD	Upper Paleolithic
	Romanelli R8	N	DD	Upper Paleolithic
	Romito 1	F	DD	Upper Paleolithic
	Romito 2	M	DD	Upper Paleolithic
	Romito 3	M	DD	Upper Paleolithic
	Romito 4	F	DD	Upper Paleolithic
	Romito 5	F	DD	Upper Paleolithic
	Romito 6	M	DD	Upper Paleolithic
	Saint Germain 14	N	DD	Upper Paleolithic
	Saint Germain 4	F	DD	Upper Paleolithic
	Saint Germain B11	F	DD	Upper Paleolithic
	Saint Germain B31	N	DD	Upper Paleolithic
	Saint Germain B41	N	DD	Upper Paleolithic
	Šandalja II 14028	N	DD	Upper Paleolithic
	Šandalja II 14035	N	DD	Upper Paleolithic
	Taforalt XI C1	M	DD	Upper Paleolithic
	Taforalt XII C1	M	DD	Upper Paleolithic
	Taforalt XIV	M	DD	Upper Paleolithic
	Taforalt XV-C2	M	DD	Upper Paleolithic
	Taforalt XVII-C2	M	DD	Upper Paleolithic
	Taforalt XX-C1	M	DD	Upper Paleolithic
	Taforalt XX-C2	F	DD	Upper Paleolithic
	Taforalt XXV-C3	M	DD	Upper Paleolithic
	Taforalt XXVI-C1	M	DD	Upper Paleolithic
	Taforalt XXVII-C1	F	DD	Upper Paleolithic
	Taforalt XXVII-C2	M	DD	Upper Paleolithic
	Veyrier 3	M	DD	Upper Paleolithic
	Arudy 2	M	DD	Mesolithic
	Aveline's Hole 174	F	DD	Mesolithic
	Aveline's Hole 176	F	DD	Mesolithic

Ap1.2 (Continued)

Species	Code	Sex	Data	Group
H. sapiens	Aveline's Hole 178	F	DD	Mesolithic
	Aveline's Hole EM504	N	DD	Mesolithic
	Aveline's Hole 105	N	DD	Mesolithic
	Aveline's Hole 146	N	DD	Mesolithic
	Aveline's Hole 148	N	DD	Mesolithic
	Aveline's Hole 186	N	DD	Mesolithic
	Aveline's Hole 228	N	DD	Mesolithic
	Aveline's Hole 237	N	DD	Mesolithic
	Aveline's Hole 82	N	DD	Mesolithic
	Aveline's Hole 94	N	DD	Mesolithic
	Bäckaskog 1	F	DD	Mesolithic
	Badger Hole 1853	N	DD	Mesolithic
	Bergmandsdal 5085516	N	DD	Mesolithic
	Birsematten 1	F	DD	Mesolithic
	Bonafacio 2	F	DD	Mesolithic
	Bottendorf 1	M	DD	Mesolithic
	Cheix 1	F	DD	Mesolithic
	Cuatamentero 900	N	DD	Mesolithic
	Culoz 2	M	DD	Mesolithic
	Dragsholm B529.73	F	DD	Mesolithic
	El Cingle G3.T14	N	DD	Mesolithic
	El Cingle H9.T12	N	DD	Mesolithic
	El Cingle I9.T10	N	DD	Mesolithic
	El Cingle K7.1	N	DD	Mesolithic
	El Cingle K8.T8	N	DD	Mesolithic
	El Cingle M9.R3	N	DD	Mesolithic
	Falkensteiner Hohle 1	N	DD	Mesolithic
	Felsdach Inzigkofen 900	N	DD	Mesolithic
	Gough’s Cave 1	M	DD	Mesolithic
	Gramat 1	M	DD	Mesolithic

Ap1.2 (Continued)

Species	Code	Sex	Data	Group
H. sapiens	Gramat 2	M	DD	Mesolithic
	Gramat 900	N	DD	Mesolithic
	Gyzycko Perkunowo 1	N	DD	Mesolithic
	Henriksholm 1	N	DD	Mesolithic
	Henriksholm 12	F	DD	Mesolithic
	Henriksholm 14	M	DD	Mesolithic
	Henriksholm 15	M	DD	Mesolithic
	Henriksholm 19A	M	DD	Mesolithic
	Henriksholm 19C	M	DD	Mesolithic
	Henriksholm 2	M	DD	Mesolithic
	Henriksholm 3	F	DD	Mesolithic
	Henriksholm 5	M	DD	Mesolithic
	Henriksholm 6	F	DD	Mesolithic
	Henriksholm 7	N	DD	Mesolithic
	Henriksholm 8	F	DD	Mesolithic
	Hoëdic 1	F	DD	Mesolithic
	Hoëdic 10	F	DD	Mesolithic
	Hoëdic 2	M	DD	Mesolithic
	Hoëdic 4	M	DD	Mesolithic
	Hoëdic 5	M	DD	Mesolithic
	Hoëdic 6	M	DD	Mesolithic
	Hoëdic 7A	F	DD	Mesolithic
	Hoëdic 8	F	DD	Mesolithic
	Hoëdic 9	M	DD	Mesolithic
	Hoëdic 900s	N	DD	Mesolithic
	Hoëdic 902s	N	DD	Mesolithic
	Hohlenstein 1	M	DD	Mesolithic
	Hohlenstein 2	F	DD	Mesolithic
	Hohler Fels 7061/589	F	DD	Mesolithic
	Hohler Fels 7061a	M	DD	Mesolithic

Ap1.2 (Continued)

Species	Code	Sex	Data	Group
H. sapiens	Hohler Fels 7061b	M	DD	Mesolithic
	Hohler Fels 7229	M	DD	Mesolithic
	Holmegaard 900	N	DD	Mesolithic
	Holmegard 1532	M	DD	Mesolithic
	Hylliekroken 1	F	DD	Mesolithic
	Kams 1	M	DD	Mesolithic
	Kaufertsberg 1	F	DD	Mesolithic
	Koed II84644	M	DD	Mesolithic
	Koed IV82644	M	DD	Mesolithic
	Koelbjerg 1	F	DD	Mesolithic
	Korsør Glasvaerk 902	M	DD	Mesolithic
	Korsør Nor 1	M	DD	Mesolithic
	Korsør Nor 2 133375	F	DD	Mesolithic
	Le Peyrat 5	M	DD	Mesolithic
	Le Peyrat 900	N	DD	Mesolithic
	Le Peyrat 901	N	DD	Mesolithic
	Le Peyrat 902	N	DD	Mesolithic
	Le Peyrat 903	N	DD	Mesolithic
	Le Rastel 1	M	DD	Mesolithic
	Loschbour 20551943	M	DD	Mesolithic
	Mas d'Azil 901	N	DD	Mesolithic
	Mas d'Azil 902	N	DD	Mesolithic
	McArthur Cave IB215	F	DD	Mesolithic
	McArthur Cave IB216	M	DD	Mesolithic
	McKay Cave IB217a	N	DD	Mesolithic
	McKay Cave IB217b	N	DD	Mesolithic
	Melby 1	M	DD	Mesolithic
	Molara II.1	M	DD	Mesolithic
	Molara Y	N	DD	Mesolithic
	Mondeval de Sora 1	M	DD	Mesolithic

Ap1.2 (Continued)

Species	Code	Sex	Data	Group
H. sapiens	Montclus 1	F	DD	Mesolithic
	Muge Arruda 0.5.L	F	DD	Mesolithic
	Muge Arruda 173.L	F	DD	Mesolithic
	Muge Arruda 175.L	F	DD	Mesolithic
	Muge Arruda 177.L	N	DD	Mesolithic
	Muge Arruda 1A.1937.P	F	DD	Mesolithic
	Muge Arruda 3.1937.P	M	DD	Mesolithic
	Muge Arruda 3.L	F	DD	Mesolithic
	Muge Arruda 39.L	F	DD	Mesolithic
	Muge Arruda 50.P	N	DD	Mesolithic
	Muge Arruda 6.1937.P	F	DD	Mesolithic
	Muge Arruda 8.P	N	DD	Mesolithic
	Muge Arruda 9.1937.P	M	DD	Mesolithic
	Muge Arruda 900.P	F	DD	Mesolithic
	Muge Arruda 901.A1.L	F	DD	Mesolithic
	Muge Arruda 902.L	M	DD	Mesolithic
	Muge Arruda 903.L	F	DD	Mesolithic
	Muge Arruda 903.p	N	DD	Mesolithic
	Muge Arruda 904.L	N	DD	Mesolithic
	Muge Arruda 908.L	F	DD	Mesolithic
	Muge Arruda 909.L	F	DD	Mesolithic
	Muge Arruda 910.L	M	DD	Mesolithic
	Muge Arruda 914.L	N	DD	Mesolithic
	Muge Arruda 918.L	N	DD	Mesolithic
	Muge Arruda 919.L	N	DD	Mesolithic
	Muge Arruda 921.L	N	DD	Mesolithic
	Muge Arruda 922.L	F	DD	Mesolithic
	Muge Arruda 928.L	F	DD	Mesolithic
	Muge Arruda C1.L	F	DD	Mesolithic
	Muge Arruda IVA.L	F	DD	Mesolithic

Ap1.2 (Continued)

Species	Code	Sex	Data	Group
H. sapiens	Muge Arruda VI.L	M	DD	Mesolithic
	Muge Arruda XXV.E.L	M	DD	Mesolithic
	Muge Moita 1.L	F	DD	Mesolithic
	Muge Moita 1.P	F	DD	Mesolithic
	Muge Moita 11.P	F	DD	Mesolithic
	Muge Moita 12.L	F	DD	Mesolithic
	Muge Moita 13.P	M	DD	Mesolithic
	Muge Moita 14.P	M	DD	Mesolithic
	Muge Moita 15.P	M	DD	Mesolithic
	Muge Moita 16.P	F	DD	Mesolithic
	Muge Moita 17.P	M	DD	Mesolithic
	Muge Moita 18.P	M	DD	Mesolithic
	Muge Moita 19.L	F	DD	Mesolithic
	Muge Moita 20.L	M	DD	Mesolithic
	Muge Moita 3.L	M	DD	Mesolithic
	Muge Moita 30.P	M	DD	Mesolithic
	Muge Moita 31.P	M	DD	Mesolithic
	Muge Moita 32.P	M	DD	Mesolithic
	Muge Moita 33.P	F	DD	Mesolithic
	Muge Moita 5.L	M	DD	Mesolithic
	Muge Moita 9.P	M	DD	Mesolithic
	Muge Moita VII.L	F	DD	Mesolithic
	Muge Moita W.L	M	DD	Mesolithic
	Muge Moita XLI.L	M	DD	Mesolithic
	Muge Moita XVI.L	F	DD	Mesolithic
	Muge Moita XVII.L	F	DD	Mesolithic
	Muge Moita XXX.L	F	DD	Mesolithic
	Muge Moita XXXIIA.L	N	DD	Mesolithic
	Mullerup M1173	N	DD	Mesolithic
	Nivaa II28.9.1915	N	DD	Mesolithic

Ap1.2 (Continued)

Species	Code	Sex	Data	Group
H. sapiens	Obříství 1.55	N	DD	Mesolithic
	Obříství 3.5	N	DD	Mesolithic
	Obříství 4.5	N	DD	Mesolithic
	Ofnet 2475.2	M	DD	Mesolithic
	Ofnet 2476.3	F	DD	Mesolithic
	Ofnet 2477.4	F	DD	Mesolithic
	Ofnet 2481.8	F	DD	Mesolithic
	Ofnet 2483.1	N	DD	Mesolithic
	Ofnet 2484.11	M	DD	Mesolithic
	Ofnet 2486.13	F	DD	Mesolithic
	Ofnet 2487.14	F	DD	Mesolithic
	Ofnet 2488.15	F	DD	Mesolithic
	Ofnet 2490.18	F	DD	Mesolithic
	Ofnet 2492.2	N	DD	Mesolithic
	Ofnet 2493.21	M	DD	Mesolithic
	Ofnet 2496.24	M	DD	Mesolithic
	Ofnet 2497.25	F	DD	Mesolithic
	Ofnet 2501.29	F	DD	Mesolithic
	Ofnet 2504.32	M	DD	Mesolithic
	Ofnet 900	F	DD	Mesolithic
	Oronsay 10638B	N	DD	Mesolithic
	Oronsay 17124C	N	DD	Mesolithic
	Oronsay 8135A	N	DD	Mesolithic
	Parabita 10	M	DD	Mesolithic
	Rhunda 1	M	DD	Mesolithic
	Rochereil 1	F	DD	Mesolithic
	Saint Rabier 1	N	DD	Mesolithic
	Schellnecker Wand 1	F	DD	Mesolithic
	Sejrø 106956	M	DD	Mesolithic
	Skateholm 1 13	M	DD	Mesolithic

Ap1.2 (Continued)

Species	Code	Sex	Data	Group
H. sapiens	Skateholm 1 2	M	DD	Mesolithic
	Skateholm 1 22	M	DD	Mesolithic
	Skateholm 1 24	F	DD	Mesolithic
	Skateholm 1 26	F	DD	Mesolithic
	Skateholm 1 27	N	DD	Mesolithic
	Skateholm 1 28	M	DD	Mesolithic
	Skateholm 1 3	F	DD	Mesolithic
	Skateholm 1 31	N	DD	Mesolithic
	Skateholm 1 33	M	DD	Mesolithic
	Skateholm 1 34	N	DD	Mesolithic
	Skateholm 1 36	N	DD	Mesolithic
	Skateholm 1 37	F	DD	Mesolithic
	Skateholm 1 4	F	DD	Mesolithic
	Skateholm 1 43	F	DD	Mesolithic
	Skateholm 1 47a	F	DD	Mesolithic
	Skateholm 1 47b	M	DD	Mesolithic
	Skateholm 1 49	N	DD	Mesolithic
	Skateholm 1 5	M	DD	Mesolithic
	Skateholm 1 53	M	DD	Mesolithic
	Skateholm 1 57	N	DD	Mesolithic
	Skateholm 1 58	F	DD	Mesolithic
	Skateholm 1 59	N	DD	Mesolithic
	Skateholm 1 6	F	DD	Mesolithic
	Skateholm 1 63a	M	DD	Mesolithic
	Skateholm 1 63b	M	DD	Mesolithic
	Skateholm 1 7	M	DD	Mesolithic
	Skateholm 2 II	M	DD	Mesolithic
	Skateholm 2 III	M	DD	Mesolithic
	Skateholm 2 IV	M	DD	Mesolithic
	Skateholm 2 IX	F	DD	Mesolithic

Ap1.2 (Continued)

Species	Code	Sex	Data	Group
H. sapiens	Skateholm 2 V	M	DD	Mesolithic
	Skateholm 2 VI	F	DD	Mesolithic
	Skateholm 2 VII	F	DD	Mesolithic
	Skateholm 2 VIII	F	DD	Mesolithic
	Skateholm 2 XA	M	DD	Mesolithic
	Skateholm 2 Xb	M	DD	Mesolithic
	Skateholm 2 XI	N	DD	Mesolithic
	Skateholm 2 XIV	F	DD	Mesolithic
	Skateholm 2 XV	M	DD	Mesolithic
	Skateholm 2 XVI	F	DD	Mesolithic
	Skateholm 2 XVII	M	DD	Mesolithic
	Skateholm 2 XX	M	DD	Mesolithic
	Skateholm 2 XXII	F	DD	Mesolithic
	Sølager 30.12.1901	M	DD	Mesolithic
	St. Rabier 1	N	DD	Mesolithic
	Staré Mesto 1	F	DD	Mesolithic
	Stetten I.5829a	F	DD	Mesolithic
	Stora Bjers 1	M	DD	Mesolithic
	Téviec 1	F	DD	Mesolithic
	Téviec 10	M	DD	Mesolithic
	Téviec 11	M	DD	Mesolithic
	Téviec 13	M	DD	Mesolithic
	Téviec 14	F	DD	Mesolithic
	Téviec 15	F	DD	Mesolithic
	Téviec 16	M	DD	Mesolithic
	Téviec 3	F	DD	Mesolithic
	Téviec 4	M	DD	Mesolithic
	Téviec 8	M	DD	Mesolithic
	Téviec 9	F	DD	Mesolithic
	Tybrind Vig I 2033AAD	F	DD	Mesolithic

Ap1.2 (Continued)

Species	Code	Sex	Data	Group
H. sapiens	Tybrind Vig I 900A	F	DD	Mesolithic
	Uzzo 1a	F	DD	Mesolithic
	Uzzo 1b	M	DD	Mesolithic
	Uzzo 4A	M	DD	Mesolithic
	Uzzo 4B	F	DD	Mesolithic
	Uzzo 5	M	DD	Mesolithic
	Uzzo 7	M	DD	Mesolithic
	Vaengesø 1850BMY	M	DD	Mesolithic
	Vatte di Zambana 1	F	DD	Mesolithic
	Vedbaek 10544	M	DD	Mesolithic
	Vlasac (Ia + Ib) 31	M	DD	Mesolithic
	Vlasac (Ia + Ib) 32	F	DD	Mesolithic
	Vlasac (Ia + Ib) 34	M	DD	Mesolithic
	Vlasac (Ia + Ib) 38	F	DD	Mesolithic
	Vlasac (Ia + Ib) 51	N	DD	Mesolithic
	Vlasac (Ia + Ib) 51b	N	DD	Mesolithic
	Vlasac (Ia + Ib) 53	N	DD	Mesolithic
	Vlasac (Ia + Ib) 67	F	DD	Mesolithic
	Vlasac (Ia + Ib) 13	N	DD	Mesolithic
	Vlasac (Ia + Ib) 17	M	DD	Mesolithic
	Vlasac (Ia + Ib) 29	F	DD	Mesolithic
	Vlasac (Ia + Ib) 29A	N	DD	Mesolithic
	Vlasac (Ia + Ib) 45	M	DD	Mesolithic
	Vlasac (Ia + Ib) 47	M	DD	Mesolithic
	Vlasac (Ia + Ib) 48	F	DD	Mesolithic
	Vlasac (Ia + Ib) 55	F	DD	Mesolithic
	Vlasac (Ia + Ib) 56	M	DD	Mesolithic
	Vlasac (Ia + Ib) 60	M	DD	Mesolithic
	Vlasac (Ia + Ib) 69	M	DD	Mesolithic
	Vlasac (Ia + Ib) 70	F	DD	Mesolithic

Ap1.2 (Continued)

Species	Code	Sex	Data	Group
H. sapiens	Vlasac (Ia + Ib) 78	M	DD	Mesolithic
	Vlasac (Ia + Ib) 80A	F	DD	Mesolithic
	Vlasac II 25	M	DD	Mesolithic
	Vlasac II 27	F	DD	Mesolithic
	Vlasac II 43	M	DD	Mesolithic
	Vlasac II 79	M	DD	Mesolithic
	Vlasac II 82	M	DD	Mesolithic
	Vlasac II 82b	M	DD	Mesolithic
	Vlasac III 2	F	DD	Mesolithic
	Vlasac III 24	M	DD	Mesolithic
	Vlasac III 40	F	DD	Mesolithic
	Vlasac III 83	F	DD	Mesolithic
	Vlasac III 18A	M	DD	Mesolithic
	Vlasac III 18c	N	DD	Mesolithic
	Vlasac III 41	M	DD	Mesolithic
	Vlasac III 46	F	DD	Mesolithic
	Vlasac III 4a	M	DD	Mesolithic
	Vlasac III 6	M	DD	Mesolithic
	Vlasac III 74	M	DD	Mesolithic
	Vlasac III 77	F	DD	Mesolithic
	Vlasac III 78A	M	DD	Mesolithic
	Vlasac III 9	F	DD	Mesolithic
	Zlaty Kun 1	F	DD	Mesolithic
	Herpaly 12	M	DD	Neolithic
	Herpaly 13	F	DD	Neolithic
	Herpaly 14	F	DD	Neolithic
	Krskany 1.64	F	DD	Neolithic
	Krskany 13.64	N	DD	Neolithic
	Krskany 14.65	F	DD	Neolithic
	Krskany 15.65	N	DD	Neolithic

Ap1.2 (Continued)

Species	Code	Sex	Data	Group
H. sapiens	Krskany 16.65	N	DD	Neolithic
	Krskany 17.65	M	DD	Neolithic
	Krskany 18.65	F	DD	Neolithic
	Krskany 19.65	M	DD	Neolithic
	Krskany 2.64	M	DD	Neolithic
	Krskany 20.65	F	DD	Neolithic
	Krskany 21.65	M	DD	Neolithic
	Krskany 22.65	M	DD	Neolithic
	Krskany 23.65	N	DD	Neolithic
	Krskany 24.65	F	DD	Neolithic
	Krskany 25.65	M	DD	Neolithic
	Krskany 26.65	F	DD	Neolithic
	Krskany 27.65	M	DD	Neolithic
	Krskany 29.65	N	DD	Neolithic
	Krskany 3.64	M	DD	Neolithic
	Krskany 30.65	N	DD	Neolithic
	Krskany 32.65	F	DD	Neolithic
	Krskany 33.65	M	DD	Neolithic
	Krskany 35.65	F	DD	Neolithic
	Krskany 36.65	M	DD	Neolithic
	Krskany 38.65	N	DD	Neolithic
	Krskany 39.65	F	DD	Neolithic
	Krskany 4.264	F	DD	Neolithic
	Krskany 41.65	F	DD	Neolithic
	Krskany 42.65	N	DD	Neolithic
	Krskany 44.65	F	DD	Neolithic
	Krskany 48.65	F	DD	Neolithic
	Krskany 5.64	N	DD	Neolithic
	Krskany 52.65	F	DD	Neolithic
	Krskany 56.65	M	DD	Neolithic

Ap1.2 (Continued)

Species	Code	Sex	Data	Group
H. sapiens	Krskany 57.65	F	DD	Neolithic
	Krskany 58.65	M	DD	Neolithic
	Krskany 6.64	F	DD	Neolithic
	Krskany 62.65	M	DD	Neolithic
	Krskany 63.65	M	DD	Neolithic
	Krskany 64.65	F	DD	Neolithic
	Krskany 65.65	F	DD	Neolithic
	Krskany 68.65	N	DD	Neolithic
	Krskany 69.65	M	DD	Neolithic
	Krskany 71.65	N	DD	Neolithic
	Krskany 72.65	M	DD	Neolithic
	Krskany 75.65	F	DD	Neolithic
	Krskany 76.75	M	DD	Neolithic
	Krskany 77.65	M	DD	Neolithic
	Krskany 8.64	M	DD	Neolithic
	Krskany 9.64	M	DD	Neolithic
	Krskore - Gat 32	M	DD	Neolithic
	Krskore - Gat 68291 1	F	DD	Neolithic
	Krskore - Gat 682910.9	M	DD	Neolithic
	Krskore - Gat 682911.1	N	DD	Neolithic
	Krskore - Gat 682918.17	F	DD	Neolithic
	Krskore - Gat 682929	M	DD	Neolithic
	Krskore - Gat 682930.35	F	DD	Neolithic
	Krskore - Gat 682931.36	N	DD	Neolithic
	Krskore - Gat 682932.1	F	DD	Neolithic
	Krskore - Gat 682932.2	N	DD	Neolithic
	Krskore - Gat 68295.3	F	DD	Neolithic
	Muhlhausen 11	M	DD	Neolithic
	Muhlhausen 12	N	DD	Neolithic
	Muhlhausen 20	M	DD	Neolithic

Ap1.2 (Continued)

Species	Code	Sex	Data	Group
H. sapiens	Muhlhausen 21	F	DD	Neolithic
	Muhlhausen 23	F	DD	Neolithic
	Muhlhausen 25	M	DD	Neolithic
	Muhlhausen 26	M	DD	Neolithic
	Muhlhausen 27	F	DD	Neolithic
	Muhlhausen 31	F	DD	Neolithic
	Muhlhausen 32	M	DD	Neolithic
	Muhlhausen 33	F	DD	Neolithic
	Muhlhausen 34	M	DD	Neolithic
	Muhlhausen 36	M	DD	Neolithic
	Muhlhausen 37	F	DD	Neolithic
	Muhlhausen 41	N	DD	Neolithic
	Muhlhausen 42	N	DD	Neolithic
	Muhlhausen 43	M	DD	Neolithic
	Muhlhausen 44	M	DD	Neolithic
	Muhlhausen 45	F	DD	Neolithic
	Muhlhausen 47	M	DD	Neolithic
	Muhlhausen 48	M	DD	Neolithic
	Muhlhausen 49	N	DD	Neolithic
	Muhlhausen 54	M	DD	Neolithic
	Muhlhausen 55	F	DD	Neolithic
	Muhlhausen 56	M	DD	Neolithic
	Muhlhausen 57	M	DD	Neolithic
	Muhlhausen 59	F	DD	Neolithic
	Muhlhausen 6	M	DD	Neolithic
	Muhlhausen 61	M	DD	Neolithic
	Muhlhausen 64	M	DD	Neolithic
	Muhlhausen 65	F	DD	Neolithic
	Muhlhausen 66	M	DD	Neolithic
	Muhlhausen 67	M	DD	Neolithic

Ap1.2 (Continued)

Species	Code	Sex	Data	Group
H. sapiens	Muhlhausen 68	F	DD	Neolithic
	Muhlhausen 70	M	DD	Neolithic
	Muhlhausen 72	M	DD	Neolithic
	Muhlhausen 77	F	DD	Neolithic
	Muhlhausen 78	F	DD	Neolithic
	Muhlhausen 79	F	DD	Neolithic
	Muhlhausen 9	M	DD	Neolithic
	Szegvar 10152 3	F	DD	Neolithic
	Szegvar 10154 5	M	DD	Neolithic
	Szegvar 10158	M	DD	Neolithic
	Szegvar 26	F	DD	Neolithic
	Szegvar 29	F	DD	Neolithic
	Szegvar 30	M	DD	Neolithic
	Szegvar 31	M	DD	Neolithic
	Szegvar 44	M	DD	Neolithic
	Szegvar 51	M	DD	Neolithic
	Szegvar 54	F	DD	Neolithic
	Szegvar 67	M	DD	Neolithic
	Szegvar 69	M	DD	Neolithic
	Szegvar 71	F	DD	Neolithic
	Szegvar 712727	M	DD	Neolithic
	Vedrovice 1.85	F	DD	Neolithic
	Vedrovice 10.74	M	DD	Neolithic
	Vedrovice 10.89	M	DD	Neolithic
	Vedrovice 100.81	F	DD	Neolithic
	Vedrovice 101.81	F	DD	Neolithic
	Vedrovice 102.81	F	DD	Neolithic
	Vedrovice 104.81	F	DD	Neolithic
	Vedrovice 105.81	M	DD	Neolithic
	Vedrovice 107.82	F	DD	Neolithic

Ap1.2 (Continued)

Species	Code	Sex	Data	Group
H. sapiens	Vedrovice 109.84	N	DD	Neolithic
	Vedrovice 13.75	F	DD	Neolithic
	Vedrovice 14.75	F	DD	Neolithic
	Vedrovice 15.75	M	DD	Neolithic
	Vedrovice 16.75	N	DD	Neolithic
	Vedrovice 17.75	N	DD	Neolithic
	Vedrovice 18.75	N	DD	Neolithic
	Vedrovice 19.75	M	DD	Neolithic
	Vedrovice 2.63	N	DD	Neolithic
	Vedrovice 2.85	M	DD	Neolithic
	Vedrovice 21.75	F	DD	Neolithic
	Vedrovice 22.75	F	DD	Neolithic
	Vedrovice 23.75	M	DD	Neolithic
	Vedrovice 28.76	N	DD	Neolithic
	Vedrovice 29.76	F	DD	Neolithic
	Vedrovice 3.66	N	DD	Neolithic
	Vedrovice 3.85	N	DD	Neolithic
	Vedrovice 30.76	N	DD	Neolithic
	Vedrovice 32.76	N	DD	Neolithic
	Vedrovice 36.76	F	DD	Neolithic
	Vedrovice 37.76	N	DD	Neolithic
	Vedrovice 38.76	F	DD	Neolithic
	Vedrovice 39.76	N	DD	Neolithic
	Vedrovice 4.69	N	DD	Neolithic
	Vedrovice 40.76	N	DD	Neolithic
	Vedrovice 42.76	F	DD	Neolithic
	Vedrovice 43.77	F	DD	Neolithic
	Vedrovice 44.77	N	DD	Neolithic
	Vedrovice 45.77	F	DD	Neolithic
	Vedrovice 46.77	M	DD	Neolithic

Ap1.2 (Continued)

Species	Code	Sex	Data	Group
H. sapiens	Vedrovice 48.77	F	DD	Neolithic
	Vedrovice 5.171	N	DD	Neolithic
	Vedrovice 5.88	N	DD	Neolithic
	Vedrovice 51.77	N	DD	Neolithic
	Vedrovice 54.78	M	DD	Neolithic
	Vedrovice 57.78	M	DD	Neolithic
	Vedrovice 59.78	M	DD	Neolithic
	Vedrovice 6.88	F	DD	Neolithic
	Vedrovice 61.78	N	DD	Neolithic
	Vedrovice 62.78	F	DD	Neolithic
	Vedrovice 63.78	N	DD	Neolithic
	Vedrovice 64.78	F	DD	Neolithic
	Vedrovice 66.78	M	DD	Neolithic
	Vedrovice 67.78	F	DD	Neolithic
	Vedrovice 68.78	F	DD	Neolithic
	Vedrovice 69.78	M	DD	Neolithic
	Vedrovice 7.88	F	DD	Neolithic
	Vedrovice 70.79	F	DD	Neolithic
	Vedrovice 71.79	M	DD	Neolithic
	Vedrovice 72.79	F	DD	Neolithic
	Vedrovice 73.79	M	DD	Neolithic
	Vedrovice 75.79	F	DD	Neolithic
	Vedrovice 76.79	M	DD	Neolithic
	Vedrovice 77.79	M	DD	Neolithic
	Vedrovice 78.79	N	DD	Neolithic
	Vedrovice 79.79	M	DD	Neolithic
	Vedrovice 8.88	N	DD	Neolithic
	Vedrovice 80.79	F	DD	Neolithic
	Vedrovice 81.79	F	DD	Neolithic
	Vedrovice 82.8	M	DD	Neolithic

Ap1.2 (Continued)

Species	Code	Sex	Data	Group
H. sapiens	Vedrovice 84.8	N	DD	Neolithic
	Vedrovice 86.8	F	DD	Neolithic
	Vedrovice 88.8	M	DD	Neolithic
	Vedrovice 91.8	F	DD	Neolithic
	Vedrovice 93.8	F	DD	Neolithic
	Vedrovice 94.8	F	DD	Neolithic
	Vedrovice 97.8	F	DD	Neolithic
	Vedrovice 99.81	M	DD	Neolithic
	Halimba 1	M	DD	Middle Ages
	Halimba 45	F	DD	Middle Ages
	Halimba 46	M	DD	Middle Ages
	Halimba (na) x 11	F	DD	Middle Ages
	Halimba (na) x 11	M	DD	Middle Ages
	Halimba (na) x 11	N	DD	Middle Ages
	Kapolna (na) x 30	F	DD	Middle Ages
	Kapolna (na) x 30	M	DD	Middle Ages
	Temeto (na) x 3	F	DD	Middle Ages
	Temeto (na) x 3	M	DD	Middle Ages
	Var (na) x 35	F	DD	Middle Ages
	Var (na) x 35	M	DD	Middle Ages

Ap1.3 The hominin 3D models used in this work. The type of model and its source are indicated. (Continues to the next page). (**AFR**: Africanfossils.org; **DAFH**: the Digital Archive of Fossil Hominoids; **LJMU**: Liverpool John Moores University casts collection; **SAP**: Sapienza University of Rome Casts collection; **PB**: provided by Peter Brown; **MNHN**: Muséum National d'Histoire Naturelle, Paris; **NESPOS**: nespos.org; **MorphoSource**: morphosource.org; **NHM**: Natural History Museum, London; **SMT**: Smithsonian Institution).

Species	Code	Sex	Source	Type
A. afarensis	AL 288-1	F	LJMU	3D from cast
A. africanus	STS 52	F	DAFH	CT-scan
P. boisei	PENINJ 1	N	SAP	3D from cast
H. ergaster	KNM-ER 992	N	AFR	3D from cast
H. rudolfensis	KNM-ER 60000	N	AFR	3D from cast
H. floresiensis	Liang Bua LB 1	F	PB	CT-scan
H. heidelbergensis	Arago 13	N	SAP	3D from cast
	Mauer 1	M	SAP	3D from cast
H. neanderthalensis	BD 1	F	NESPOS	CT-scan
	Amud 1	M	MorphoSource	3D from cast
	Atapuerca AT-888	M	SAP	3D from cast
	Banolas 1	F	NESPOS	CT-scan
	Ehringsdorf G1	N	NESPOS	CT-scan
	Guattari 3	N	NESPOS	CT-scan
	Krapina 58	N	NESPOS	CT-scan
	La Ferrassie 1	M	MNHN	CT-scan
	La Quina 5	N	NESPOS	CT-scan
	La Quina 9	N	MNHN	CT-scan
	Le Moustier 1	M	NESPOS	CT-scan
	Montmaurin 1	F	NESPOS	CT-scan
	Regourdou 1	N	NESPOS	CT-scan
	Tabun 1	F	NHM	CT-scan
H. sapiens	Australia 226089	M	SMT	CT-scan
	Australia 331242	M	SMT	CT-scan
	Australia 329778	F	SMT	CT-scan
	Australia 344711	M	SMT	CT-scan
	Australia 344712	F	SMT	CT-scan
	Australia 344714	F	SMT	CT-scan
	Greenland 242709	M	SMT	CT-scan
	Greenland 242718	F	SMT	CT-scan

Ap1.3 (Continued)

Species	Code	Sex	Source	Type
H. sapiens	Greenland 242719	F	SMT	CT-scan
	Greenland 242760	M	SMT	CT-scan
	Ipiutak 103	M	SMT	CT-scan
	Ipiutak 161	F	SMT	CT-scan
	Ipiutak 168	F	SMT	CT-scan
	Ipiutak 192	M	SMT	CT-scan
	New Britain 226096	M	SMT	CT-scan
	New Britain 226099	F	SMT	CT-scan
	New Britain 226101	F	SMT	CT-scan
	New Britain 226102	F	SMT	CT-scan
	New Britain 226103	M	SMT	CT-scan
	New Britain 226107	M	SMT	CT-scan

Ap1.4 Definitions of the landmarks used in this study. The numbers corresponds to the ones shown in Figure 2.2, Chapter 2. The landmarks from 1 to 28 belong to the mandibular configuration, from 29 to 43 to the neurocranium. (Continues to the next page).

Landmark number	Landmark Definitions
1	The buccal point at the superior tip of the septum between the mandibular central incisors.
2	The lingual point at the superior tip of the septum between the mandibular central incisors.
3	The lingual point at the superior tip of the septum between the mandibular lateral incisor and the canine (I_2/C).
4	The buccal point at the superior tip of the septum between the mandibular lateral incisor and the canine (I_2/C).
5	The buccal point at the superior tip of the septum between the mandibular canine and the first premolar and closest to the premolar (C/P_3).
6	The lingual point at the superior tip of the septum between the mandibular canine and the first premolar and closest to the premolar (C/P_3).
7	The buccal point at the superior tip of the septum between the mandibular third premolar and the fourth premolar (P_3/P_4).
8	The lingual point at the superior tip of the septum between the mandibular third premolar and the fourth premolar (P_3/P_4).
9	The buccal point at the superior tip of the septum between the mandibular fourth premolar and the first molar (P_4/M_1).
10	The lingual point at the superior tip of the septum between the mandibular fourth premolar and the first molar (P_4/M_1).
11	The buccal point at the superior tip of the septum between the mandibular first molar and the second molar (M_1/M_2).
12	The lingual point at the superior tip of the septum between the mandibular first molar and the second molar (M_1/M_2).
13	The buccal point at the superior tip of the septum between the mandibular second molar and the third molar (M_2/M_3).
14	The lingual point at the superior tip of the septum between the mandibular second molar and the third molar (M_2/M_3).
15	The most posterior point of the tooth row between the mandibular third molar septum and the retro-molar sulcus.
16	The most inferior point of the mandibular symphysis on the mid-sagittal plane.
17	The mid-sagittal point on the mandibular inferior transverse torus projecting most posteriorly.
18	The mid-sagittal point on the mandibular superior transverse torus projecting most posteriorly.

Ap1.4 (Continued)

Landmark number	Landmark Definitions
19	The most anterior point on the rim of the mental foramen.
20	The most inferior point of the gonial region, at the inferior margin of the masseteric fossa.
21	The most superior point of the gonial region, at the most posterior margin of the masseteric fossa.
22	The point at which the minimum mandibular ramus breadth intersects the anterior border of the ramus.
23	The most superior point, or tip, of the coronoid process.
24	The point on the mandibular notch situated medially between the tip of the coronoid process and the line connecting the most external points on the mandibular condyle.
25	The most anterior point of the mandibular condyle.
26	The interior most lateral point of the mandibular condyle.
27	The exterior most lateral point of the mandibular condyle.
28	The most posterior point of the mandibular condyle.
29	Glabella, or the most anterior and prominent point on the frontal bone, situated on the sagittal plane, between the superciliary arches and above the root of the nasal bones.
30	Bregma, or the point where the coronal suture is intersected perpendicularly by the sagittal suture.
31	Lambda, or the point where the sagittal and lambdoid suture of the skull intersect each other.
32	Opisthocranion, the most posterior point on the occipital bone at the end of the maximum diameter of the skull measured from the glabella.
33	Opisthion, or the most posterior point on the margin of the foramen magnum, positioned along the sagittal plane.
34	The most inferior point on the suture between the maxilla and the zygomatic bone.
35	Jugale, or the point at the union of the frontal and temporal processes of the zygomatic bone.
36	The most posterior point of the zygomaticofrontal suture, where the frontal bone meets the process of the zygomatic, on the external margin of the orbit.

Ap1.4 (Continued)

Landmark number	Landmark Definitions
37	Frontotemporale, or the most anterior point of the temporal line on the frontal bone.
38	The point of intersection between the coronal suture and the inferior temporal line.
39	The most posterior point of the inferior temporal line, located onto the parietal bone.
40	Asterion, or the point where the parietal, occipital and temporal bones converge.
41	The most external point of the supramastoid crest.
42	Porion, or the uppermost point on the external auditory meatus.
43	On the temporal bone, the most posterior and concave point on the internal side of the zygomatic arch.

Ap1.5 Body weight in grams for the catarrhine species from National Research Council US (2003). Empty cells refer to cases not represented in the sample. For further details on source of data, refer to Chapter 2. (Continues to the next page).

	Species	Female Body Weight (g)	Male Body Weight (g)
Colobines	*Colobus guereza*	9200	-
	Colobus polykomos	7900	9890
	Nasalis larvatus	-	20400
	Piliocolobus badius	8210	8360
	Presbytis melalophos	6470	6590
	Procolobus verus	4200	4700
	Pygathrix nemaeus	-	11000
	Trachypithecus cristatus	5760	6610
	Trachypithecus obscurus	6260	7900
Cercopithecines	*Allenopithecus nigroviridis*	3180	-
	Cercocebus agilis	5660	-
	Cercocebus atys	6200	11000
	Cercocebus galeritus	5260	9610
	Cercocebus torquatus	5500	9470
	Cercopithecus albogularis	4210	7550
	Cercopithecus ascanius	2920	3700
	Cercopithecus campbelli	2700	4500
	Cercopithecus mitis	4250	7930
	Cercopithecus neglectus	-	7350
	Cercopithecus nictitans	4260	6670
	Cercopithecus petaurista	2900	4400
	Chlorocebus aethiops	-	4260
	Chlorocebus sabaeus	2980	4260
	Erythrocebus patas	6500	12400
	Lophocebus albigena	6020	8250
	Lophocebus aterrima	5760	-
	Macaca arctoides	8400	12200
	Macaca assamensis	6900	11300
	Macaca cyclopis	4940	6000
	Macaca fascicularis	3590	5360
	Macaca fuscata	8030	11000
	Macaca leonina	5550	11000
	Macaca maura	6050	-
	Macaca mulatta	8800	11000
	Macaca nemestrina	6500	11200
	Macaca nigra	-	9890
	Macaca pagensis	5500	7500

Ap1.5 (Continued)

	Species	Female Body Weight (g)	Male Body Weight (g)
Cercopithecines	*Macaca radiata*	3850	6670
	Macaca silenus	6100	8900
	Macaca sinica	3200	5680
	Macaca sylvanus	9800	12200
	Macaca thibetana	12800	18300
	Mandrillus leucophaeus	-	17500
	Mandrillus sphinx	12900	31600
	Papio anubis	13300	25100
	Papio hamadryas	9900	16900
	Papio papio	13000	25000
	Theropithecus gelada	11700	19000
Hylobatidae	*Bunopithecus hoolock*	6880	6870
	Hylobates agilis	5820	5880
	Hylobates klossii	5920	-
	Hylobates lar	5340	5900
	Hylobates muelleri	5350	5710
	Nomascus concolor	7620	7790
	Nomascus gabriellae	-	7000
	Nomascus leucogenys	7320	-
	Symphalangus syndactylus	10700	11900
Great apes	*Gorilla beringei*	97500	162500
	Gorilla gorilla	71500	170400
	Pan paniscus	33200	-
	Pan troglodytes	45800	59700
	Pongo abelii	35600	77900
	Pongo pygmaeus	35800	78500

Ap1.6 Body weight in grams for the hominin species, available from McHenry & Berger (1998), Jiménez-Arenas et al. (2014) and Grabowski et al. (2015). Empty cells refer to cases that where not represented in the sample. For further details on source of data, refer to Chapter 2.

Species	Female body weight (g)	Male body weight (g)
Australopithecus afarensis	31200	-
Australopithecus africanus	25800	38900
Paranthropus boisei	30900	45100
Paranthropus robustus	24000	-
Homo ergaster	46300	54300
Homo habilis	27300	38400
Homo rudolfensis	55500	55500
Homo floresiensis	27500	-
Homo heidelbergensis	62000	62000
Homo neanderthalensis	74400	74400
Homo sapiens	54700	61000

Ap1.7 Missing data in the sample. The amount of estimate landmarks is reported. The number of landmarks refer to the mandibular configuration of fossil hominins, since no missing data were present on the neurocranium and in the catarrhine sample. For further details on missing data estimation, refer to Chapter 2.

Species	Code	Missing landmarks
Australopithecus afarensis	AL 288-1 (Lucy)	4 of 28 (14.3%)
Australopithecus africanus	STS 52	4 of 28 (14.3%)
Paranthropus boisei	KNM-ER 729	4 of 28 (14.3%)
	PENINJ 1	3 of 28 (10.7%)
Homo ergaster	KNM-ER 992	4 of 28 (14.3%)
	KNM-ER 60000	3 of 28 (10.7%)
Homo neanderthalensis	Atapuerca AT-888	2 of 28 (7.1%)
	Guattari 3	3 of 28 (10.7%)
	Regourdou 1	1 of 28 (3.6%)
	Tabun 1	2 of 28 (7.1%)

Ap1.8 The primate phylogenetic tree used in the analyses. Colobines are shown in green, cercopithecines in blue, hylobatids in magenta and great apes in red. The complete hominin phylogeny is reported in Figure 2.8, Chapter 2.

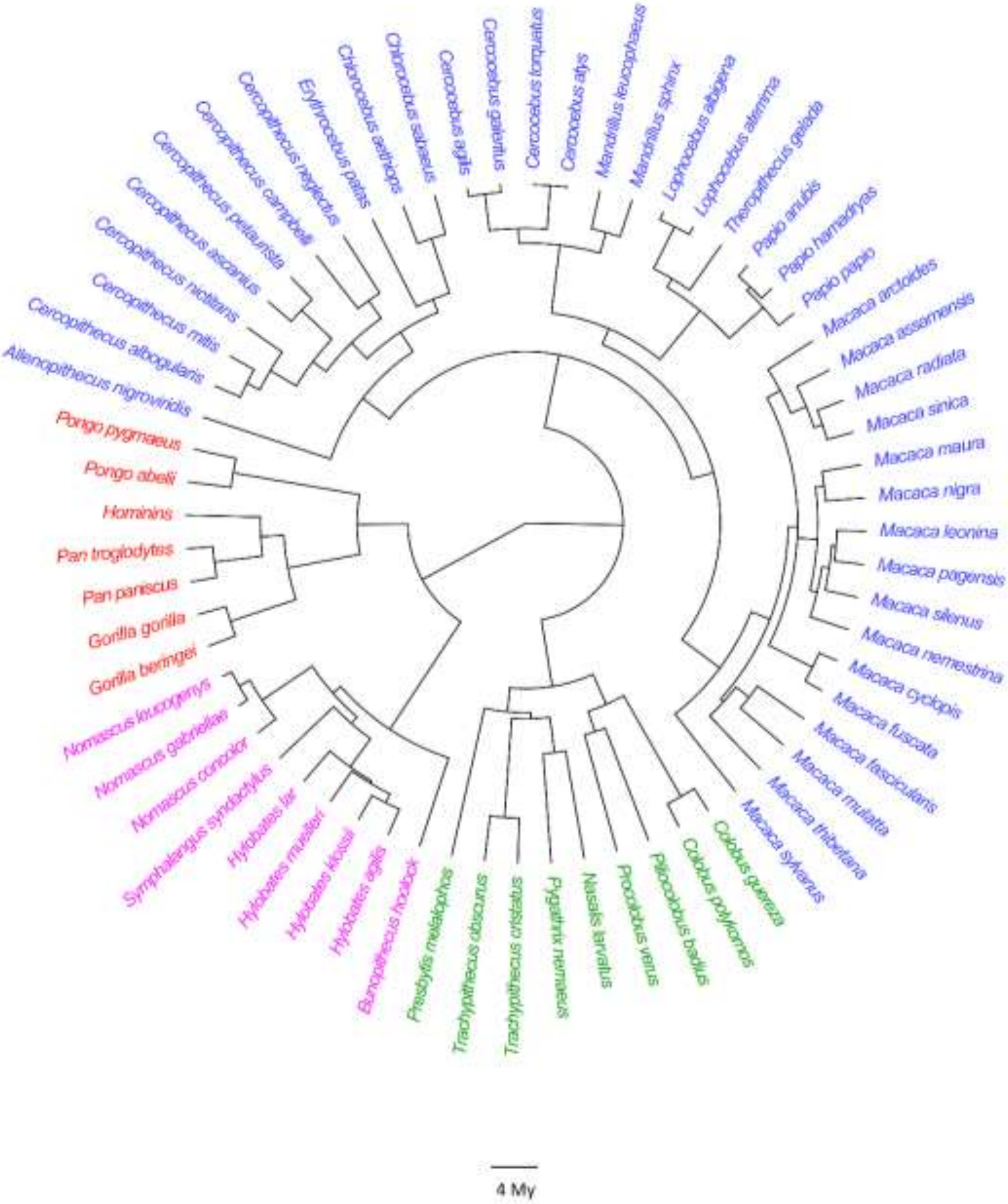

Appendix 2

Ap2.1 Complement to Table 4.3, Chapter 4. P-values of the regressions between dietary/tool use proxies and morphology, using the female sample. The significant p-values of the regressions showing positive adjusted R^2 are shown in bold. For further information, refer to Chapter 4.

		DQ	DH	Asfc	epLsar	Tfv	HAsfc9	CCL	FT	TU	EF
CS	**X**	0.644	0.771	0.984	0.674	0.165	0.659	0.188	0.679	0.884	0.714
	X²	0.864	0.757	0.272	0.221	0.384	0.522	0.657	0.757	0.583	0.644
	B	**<0.001**	**<0.001**	**<0.001**	**<0.001**	**<0.001**	**<0.001**	**0.023**	**<0.001**	**<0.001**	**<0.001**
I_1-I_2	**X**	**<0.001**	0.197	0.012	0.405	**0.025**	**<0.001**	0.165	0.2	0.059	0.74
	X²	0.96	0.937	0.128	0.731	0.799	0.53	0.789	0.253	0.762	0.244
	B	**<0.001**	**<0.001**	**0.021**	**<0.001**	**<0.001**	**<0.001**	**0.036**	**<0.001**	**<0.001**	**<0.001**
P_3-P_4	**X**	0.112	0.938	0.509	0.66	**<0.001**	0.304	0.675	0.686	0.834	0.217
	X²	0.549	0.704	0.159	0.561	0.896	**0.045**	0.663	0.19	0.121	0.713
	B	**<0.001**	**<0.001**	**<0.001**	**<0.001**	**<0.001**	**<0.001**	0.082	**<0.001**	**<0.001**	**<0.001**
M_1-M_3	**X**	0.986	0.544	0.443	0.494	0.092	0.339	0.283	0.847	0.425	0.114
	X²	0.887	0.59	**0.025**	**0.02**	0.068	0.454	0.468	0.1	0.575	0.703
	B	**<0.001**	**<0.001**	**<0.001**	**<0.001**	**<0.001**	**<0.001**	**0.038**	**<0.001**	**<0.001**	**<0.001**
Rob SY	**X**	0.569	0.62	0.656	0.856	0.087	0.192	0.862	0.828	0.489	0.017
	X²	0.951	0.978	0.578	0.4	0.893	0.717	0.839	0.605	0.984	0.864
	B	0.041	0.016	0.507	0.293	0.968	0.376	0.94	0.755	0.097	0.083
Rob M_1	**X**	0.024	0.358	0.249	**0.019**	0.713	0.945	0.347	0.784	0.627	0.887
	X²	0.421	0.337	0.079	0.064	0.001	0.161	0.527	0.789	0.762	0.858
	B	0.411	0.999	0.872	**0.018**	0.804	0.702	0.594	0.85	0.629	0.621
Rob M_2	**X**	0.603	0.155	0.978	0.633	0.565	0.307	0.546	0.295	0.423	0.08
	X²	0.194	0.937	0.551	0.931	0.743	0.026	0.216	0.629	0.821	0.209
	B	0.962	0.677	0.314	0.35	0.39	0.07	0.183	0.873	0.455	0.431
Rob M_3	**X**	0.389	0.497	0.823	0.502	0.174	0.361	0.615	0.793	0.454	0.228
	X²	0.574	0.624	0.273	0.677	0.41	0.074	0.517	0.669	0.352	0.48
	B	0.842	0.919	0.338	0.501	0.685	0.067	0.28	0.563	0.384	0.595

Ap2.2 Complement to Table 4.4, Chapter 4. P-values of the regressions between dietary/tool use proxies and morphology, using the male sample. The significant p-values of the regressions showing positive adjusted R^2 are shown in bold. For further information, refer to Chapter 4.

		DQ	DH	Asfc	epLsar	Tfv	HAsfc9	CCL	FT	TU	EF
CS	**X**	0.809	0.412	0.171	0.854	0.136	0.403	0.211	0.215	0.913	0.381
	X^2	0.827	0.083	0.1	0.291	**0.035**	0.81	0.356	0.371	0.053	0.991
	B	**<0.001**	**<0.001**	**<0.001**	**<0.001**	**<0.001**	**<0.001**	**0.041**	**<0.001**	**<0.001**	**<0.001**
I_1-I_2	**X**	0.209	0.658	**0.033**	**0.035**	0.225	0.098	0.055	0.079	0.188	0.609
	X^2	0.983	0.984	0.137	0.245	0.109	0.397	0.203	0.602	0.847	0.299
	B	**<0.001**	**<0.001**	**0.001**	**0.003**	**<0.001**	**0.003**	**0.037**	**0.001**	**<0.001**	**<0.001**
P_3-P_4	**X**	0.522	0.393	0.327	0.145	0.84	0.075	0.503	0.296	0.639	0.445
	X^2	0.453	0.343	0.837	0.894	0.394	**0.047**	0.529	0.073	**0.002**	0.393
	B	**<0.001**	**<0.001**	**0.001**	**0.003**	**0.002**	**0.001**	0.554	**<0.001**	**<0.001**	**<0.001**
M_1-M_3	**X**	0.11	0.909	0.187	0.174	0.209	**0.005**	0.467	0.634	0.794	0.265
	X^2	0.938	**0.03**	0.704	0.424	0.593	0.267	0.785	0.454	0.174	0.534
	B	**<0.001**	**<0.001**	**<0.001**	**<0.001**	**<0.001**	**<0.001**	**0.008**	**<0.001**	**<0.001**	**<0.001**
Rob SY	**X**	0.658	0.674	0.518	0.876	0.338	0.242	0.434	0.805	0.155	0.384
	X^2	0.444	0.952	0.399	0.381	0.666	0.923	0.026	0.404	0.911	0.824
	B	0.432	0.518	0.908	0.516	0.298	0.652	0.928	0.999	0.842	0.548
Rob M_1	**X**	0.985	0.297	0.033	0.402	0.3	0.463	0.392	0.449	0.861	0.786
	X^2	0.484	0.337	0.153	0.718	0.088	0.258	0.065	0.985	0.83	0.489
	B	0.729	0.574	0.355	**0.05**	0.726	0.526	0.214	0.697	0.93	0.874
Rob M_2	**X**	0.95	0.555	0.76	0.348	0.274	0.522	0.78	0.689	0.852	0.523
	X^2	0.696	0.871	0.118	0.627	0.295	0.299	0.3	0.181	0.16	0.484
	B	0.562	0.561	0.164	0.149	0.298	0.157	0.746	0.551	0.232	0.449
Rob M_3	**X**	0.032	0.274	0.709	0.329	**0.047**	0.77	**0.046**	0.253	0.686	0.374
	X^2	0.025	0.279	0.689	0.574	**0.012**	0.479	**0.014**	0.623	0.658	0.885
	B	0.837	0.369	0.489	0.469	0.061	0.206	**0.029**	0.317	0.275	0.363

Ap2.3 Complement to Table 4.5, Chapter 4. Results of the Phylogenetic Generalized Least Squares regressions between mandibular Centroid Size (CS), incisal (I_1-I_2), premolar (P_3-P_4) and molar (M_1-M_3) versus body weight, under Ornstein-Uhlenbeck model of evolution. All results were significant.

Females	**intercept**	**slope**	**R^2**	**λ**	**p-value**
CS	2.448	0.286	0.84	0.179	<0.001
I_1-I_2	-0.445	0.271	0.66	0.467	<0.001
P_3-P_4	0.5	0.226	0.65	0.745	<0.001
M_1-M_3	0.753	0.27	0.72	0.14	<0.001

Males	**intercept**	**slope**	**R^2**	**λ**	**p-value**
CS	2.564	0.275	0.75	0.085	<0.001
I_1-I_2	-0.379	0.27	0.55	0.154	<0.001
P_3-P_4	1.056	0.179	0.21	0.088	0.001
M_1-M_3	0.78	0.271	0.68	0.099	<0.001

Ap2.4 Complement to Table 4.6, Chapter 4. Results of the Phylogenetic ANCOVA for slope differences between the groups of hominins, *Homo* and catarrhines, assuming an Ornstein-Uhlenbeck model of evolution. Here "Catarrhines" refers to non-hominin extant catarrhines. Significant p-values are shown in bold.

	Catarrhines vs Hominins			**Catarrhines vs *Homo***		
Females	**DF**	**F**	**p-value**	**DF**	**F**	**p-value**
CS	61 62	5.323	**0.024**	58 59	0.164	0.687
I_1-I_2	62 63	30.937	**< 0.001**	58 59	43.551	**< 0.001**
P_3-P_4	62 63	1.313	0.256	58 59	14.434	**< 0.001**
M_1-M_3	62 63	12.428	**< 0.001**	58 59	6.653	**0.012**

	Catarrhines vs Hominins			**Catarrhines vs *Homo***		
Males	**DF**	**F**	**p-value**	**DF**	**F**	**p-value**
CS	57 58	10.81	**0.002**	56 57	4.333	**0.042**
I_1-I_2	59 60	25.641	**< 0.001**	57 58	23.682	**< 0.001**
P_3-P_4	59 60	6.676	**0.012**	57 58	5.286	**0.025**
M_1-M_3	59 60	23.606	**< 0.001**	57 58	19.5	**< 0.001**

Ap2.5 Complement to Table 4.7, Chapter 4. Results of the Phylogenetic ANCOVA for differences on intercepts between the groups *Homo*, australopithecines and catarrhines, under Ornstein-Uhlenbeck model of evolution. Significant p-values in bold. (**Aus**: australopithecines; **Cat**: non-hominin extant catarrhines).

	***Homo* vs Aus vs Cat**			***Homo* vs Aus | Cat**		
Females	**DF**	**F**	**p-value**	**DF**	**F**	**p-value**
CS	61 63	3.413	**0.039**	61 62	6.683	**0.012**
I_1-I_2	62 64	0.843	0.435	62 63	0.529	0.47
P_3-P_4	62 64	0.105	0.9	62 63	0.174	0.679
M_1-M_3	62 64	6.064	**0.004**	62 63	7.619	**0.008**

	***Homo* vs Cat | Aus**			**Aus vs Cat | *Homo***		
Females	**DF**	**F**	**p-value**	**DF**	**F**	**p-value**
CS	61 62	1.267	0.265	61 62	0.204	0.653
I_1-I_2	62 63	1.664	0.202	62 63	1.213	0.275
P_3-P_4	62 63	0.019	0.892	62 63	0.011	0.915
M_1-M_3	62 63	0.298	0.587	62 63	5.115	**0.027**

	***Homo* vs Aus vs Cat**			***Homo* vs Aus | Cat**		
Males	**DF**	**F**	**p-value**	**DF**	**F**	**p-value**
CS	57 59	4.123	**0.021**	57 58	8.081	**0.006**
I_1-I_2	59 61	1.457	0.241	59 60	2.136	0.149
P_3-P_4	59 61	4.708	**0.013**	59 60	8.847	**0.004**
M_1-M_3	59 61	8.056	**< 0.001**	59 60	12.088	**0.001**

	***Homo* vs Cat | Aus**			**Aus vs Cat | *Homo***		
Males	**DF**	**F**	**p-value**	**DF**	**F**	**p-value**
CS	57 58	0.292	0.591	57 58	2.029	0.16
I_1-I_2	59 60	2.051	0.157	59 60	0.466	0.497
P_3-P_4	59 60	0.146	0.703	59 60	1.36	0.248
M_1-M_3	59 60	0.294	0.59	59 60	6.082	**0.017**

Ap2.6 Complement to Table 4.8, Chapter 4. Results of the Phylogenetic ANCOVA performed on the female sample. Test for hominin species divergence from the scaling trajectory of catarrhines, assuming an Ornstein-Uhlenbeck model of evolution. Significant p-values are shown in bold.

	CS			**I_1-I_2**		
	DF	**F**	**p-value**	**DF**	**F**	**p-value**
A. afarensis	61 62	12.689	**< 0.001**	62 63	43.145	**< 0.001**
A. africanus	61 62	3.622	0.062	62 63	14.729	**< 0.001**
H. ergaster	61 62	0.014	0.906	62 63	< 0.001	0.985
H. floresiensis	61 62	3.211	0.078	62 63	0.024	0.877
H. habilis	-	-	-	62 63	7.679	**0.007**
H. heidelbergensis	61 62	5.737	**0.02**	62 63	0.253	0.617
H. neanderthalensis	61 62	7.356	**0.009**	62 63	0.164	0.687
H. rudolfensis	61 62	0.314	0.577	62 63	14.609	**< 0.001**
H. sapiens	61 62	2.482	0.12	62 63	0.133	0.717
P. boisei	61 62	22.446	**< 0.001**	62 63	0.275	0.602
P. robustus	-	-	-	62 63	1.923	0.17

	P_3-P_4			**M_1-M_3**		
	DF	**F**	**p-value**	**DF**	**F**	**p-value**
A. afarensis	62 63	32.795	**< 0.001**	62 63	6.599	**0.013**
A. africanus	62 63	0.051	0.822	62 63	0.57	0.453
H. ergaster	62 63	0.03	0.864	62 63	1.063	0.306
H. floresiensis	62 63	0.386	0.537	62 63	6.08	**0.016**
H. habilis	62 63	0.424	0.517	62 63	2.153	0.147
H. heidelbergensis	62 63	0.003	0.959	62 63	0.775	0.382
H. neanderthalensis	62 63	0.402	0.528	62 63	4.341	**0.041**
H. rudolfensis	62 63	0.169	0.683	62 63	0.059	0.809
H. sapiens	62 63	0.433	0.513	62 63	0.345	0.559
P. boisei	62 63	113.978	**< 0.001**	62 63	5.859	**0.018**
P. robustus	62 63	0.265	0.609	62 63	3.134	0.082

Ap2.6 Complement to Table 4.9, Chapter 4. Results of the Phylogenetic ANCOVA performed on the male sample. Test for hominin species divergence from the scaling trajectory of catarrhines, assuming an Ornstein-Uhlenbeck model of evolution. Significant p-values are shown in bold.

	CS			**I_1-I_2**		
	DF	**F**	**p-value**	**DF**	**F**	**p-value**
A. afarensis	-	-	-	-	-	-
A. africanus	-	-	-	59 60	1.735	0.193
H. ergaster	57 58	0.444	0.508	59 60	0.066	0.798
H. floresiensis	-	-	-	-	-	-
H. habilis	-	-	-	59 60	8.914	**0.004**
H. heidelbergensis	57 58	3.32	0.073	59 60	< 0.001	0.989
H. neanderthalensis	57 58	3.637	0.061	59 60	0.607	0.439
H. rudolfensis	57 58	0.008	0.93	59 60	23.243	**< 0.001**
H. sapiens	57 58	2.381	0.128	59 60	3.596	0.063
P. boisei	57 58	8.081	**0.006**	59 60	0.01	0.918
P. robustus	-	-	-	-	-	-

	P_3-P_4			**M_1-M_3**		
	DF	**F**	**p-value**	**DF**	**F**	**p-value**
A. afarensis	-	-	-	-	-	-
A. africanus	59 60	0.196	0.66	59 60	0.416	0.522
H. ergaster	59 60	0.005	0.944	59 60	2.178	0.145
H. floresiensis	-	-	-	-	-	-
H. habilis	59 60	0.011	0.917	59 60	1.251	0.268
H. heidelbergensis	59 60	1.707	0.196	59 60	2.042	0.158
H. neanderthalensis	59 60	3.125	0.082	59 60	7.616	**0.008**
H. rudolfensis	59 60	0.748	0.391	59 60	0.68	0.413
H. sapiens	59 60	3.465	0.068	59 60	0.693	0.408
P. boisei	59 60	22.812	**< 0.001**	59 60	11.825	**0.001**
P. robustus	-	-	-	-	-	-